# Estimation and Control of Plastic Temperature in Heating Phase of Thermoforming Process

by

Md. Muminul Islam Chy.

Electrical and Computer Engineering

McGill University

Montreal

Quebec, Canada

A thesis submitted in partial fulfilment of degree of Doctor of Philosophy

On

November, 2013

# Abstract

Increasing consumption of plastic products in packaging, automotive, refrigeration, aerospace and other industries makes thermoforming a vital manufacturing process. The vast production of thermoformed parts encourages researchers to develop cost-effective and accurate controllers for the process. Heating phase is the most important phase of the process as the following phases depend on its outcome. Thus, it is very important to control the heating phase to ensure the economic viability of the product according to specifications. These specifications may not be met without a sophisticated process control system providing accurate control of key process variables that are inherently nonlinear and time-varying. This thesis analyzes the control problems of the process one by one and investigates a solution step by step.

The first problem in controlling any process is to understand the system and develop a relationship between inputs and outputs. Having a well-developed mathematical model that represents the system's behavior is important in developing model based controller. An accurate mathematical model is also very important to get a good idea about the process and for the simulation of the developed control technique to guarantee the future prospects of the proposed technique before it is implemented in real-time. System modeling is a useful tool in efficient controller design to achieve the desired output temperature of the sheet at the end of the heating cycle in the thermoforming process. An improved model is presented in this thesis to define a better mathematical relationship between inputs and outputs.

Another problem for ill-posed system like heating phase of thermoforming process is to find the set-points of heater temperatures that will heat the plastic sheet to the desired temperature at the end of the heating cycle. In this thesis, a new method is presented using conjugate gradient method to solve this problem along with details analysis of the proposed method.

Sensing two dimensional space signals accurately using limited number of sensors is a big challenge in developing a close loop controller. This thesis presents a new method for the estimation of surface temperature and thereby modifies it in such a way that it can estimate sheet temperature independent of sensor positions on the sheet. The proposed method estimate the temperature profile over the entire sheet through its spatial harmonics and the controller can control the spatial harmonics to obtain the desired temperature profile.

Although control techniques have been developed for the heating phase of the thermoforming process, oven heater temperatures in the thermoforming industry are still largely adjusted by trial and error based on the experience of the operator. In next part of this thesis, controllers are developed step by step that will achieve desired sheet temperature at the end of the cycle. The first controller developed in this thesis to control the surface temperature of a plastic sheet uses model predictive control (MPC) as a first step. MPC is one of the advanced methods for process control that can handle a multivariable process with presence of non-periodic disturbance. To overcome the computation burden of MPC, Multi-parametric programming is used to compute the optimization problem.

On the other hand, the thermoforming process can be described in terms of two distinct time scales, namely, the finite period of continuous time within each repeating cycle, and the cycle index. If the control formulations do not explicitly incorporate or exploit this 2D representation of cyclic systems, it can have limited success in controlling repetitive systems. Two-dimensional learning controller results in advantages over the in-cycle or cycle to cycle feedback control techniques where only in-cycle information or cycle to cycle information was used. For this reason, a real-time feedback control combining in-cycle and cycle-to-cycle strategies is proposed to improve control performance. This approach utilizes not only incoming information from the ongoing cycle, but also the information stored from the past cycles. To deal with constraints as well as non-repetitive disturbances in the process, the MPC technique is incorporated to update the control law within the cycle. To exploit the repetitive nature of the heating phase of the process, a cycle-to-cycle iterative learning control technique direction is proposed. The iterative learning strategy is useful for achieving desired temperature despite model mismatch and disturbances.

# Abrégé

La croissance continue dans la consommation de produits en plastique dans les domaines de l'empaquetage, la réfrigération, l'aérospatiale et autres font du thermoformage un procédé manufacturier incontournable. La grande production de pièces thermoformées encourage donc les chercheurs à développer des contrôleurs précis et à coût raisonnable pour ce procédé. La phase de chauffage est la plus importante du procédé puisque les phases suivantes dépendent de sa réussite. Ainsi, il est très important de bien contrôler la phase de chauffage pour assurer la qualité et la viabilité du produit thermoformé selon les requis. Ces requis pourraient ne pas être remplis sans système de contrôle sophistiqué fournissant une bonne précision de contrôle des variables du procédé qui sont non-linéaires et varient avec le temps. Ce mémoire analyse les problèmes de contrôle du procédé un à un et propose des solutions étape par étape.

Le premier problème qui se pose dans la commande de tout procédé est de bien comprendre le système et de développer des relations entre les variables d'entrée et de sortie. Il est important d'avoir un modèle mathématique bien développé représentant le comportement du système pour la conception d'un contrôleur basé sur ce modèle. Un modèle mathématique est aussi très important pour avoir une bonne idée du procédé ainsi que pour simuler la technique de contrôle ayant été développée pour en garantir les avantages avant qu'elle ne soit implantée en temps réel. La modélisation de système est un outil utile pour la conception de lois de commande efficaces pour atteindre la cible de température à la fin du cycle de chauffe dans le procédé de thermoformage. Un modèle amélioré est présenté ici pour définir une meilleure relation mathématique entre les entrées et les sorties.

Un autre problème pour les systèmes mal conditionnés tels que le procédé de thermoformage est de trouver les consignes de température des éléments chauffants qui chaufferont la feuille de plastique à la température désirée à la fin du cycle. Dans cette dissertation, une nouvelle méthode est présentée en détail pour résoudre ce problème en utilisant la technique du gradient conjugué.

La mesure de signaux à deux dimensions en utilisant un nombre limité de capteurs est un grand défi dans le développement d'un contrôleur en boucle fermée. Cette thèse présente une

nouvelle méthode de mesure de températures de surface et la modifie ensuite d'une façon telle que l'estimation de température devient alors indépendante de la position des capteurs sur la feuille. La méthode proposée estime le profil de température sur toute la feuille par ses harmoniques spatiales et le contrôleur peut contrôler ces harmoniques pour obtenir le profil de température voulu.

Même si des algorithmes de commande ont déjà été développés pour la phase de chauffage du procédé de thermoformage, les températures des radiateurs sont encore largement ajustées à la main par une technique d'essai-erreur basée sur l'expérience de l'opérateur. Dans la partie suivante de cette thèse, des contrôleurs sont développés étape par étape pour arriver à la température désirée à la fin du cycle. Le premier contrôleur développé dans cette thèse est du type commande à modèle prédictif (CMP) dans un premier temps. La CMP est une des méthodes de commande parmi les plus évoluées et qui peut traiter des procédés multi-variables en présence de perturbations non-périodiques. Pour alléger la charge de calcul de la CMP, la programmation multi-paramétrique est utilisée pour résoudre le problème d'optimisation.

D'un autre point de vue, le procédé de thermoformage peut être décrit en termes de deux échelles de temps distinctes, soit la période de cycle en temps continu qui se répète à chaque cycle, ainsi que l'index du cycle. Si la formulation du problème de contrôle n'incorpore pas explicitement cette représentation 2D, la commande peut avoir un succès limité pour ce type de système répétitif. Les contrôleurs 2D à apprentissage offrent des avantages par rapport aux contrôleurs n'agissant qu'en cycle, ou de cycle en cycle ou l'information d'une seule de ces dimensions est utilisée. Pour cette raison, un algorithme de contrôle rétroactif en temps réel combinant des stratégies de commande en cycle, et cycle-en-cycle est proposé pour en améliorer la performance. Cette approche inclut non seulement l'information du cycle en cours, mais également des cycles précédents. La commande CMP est utilisée en-cycle afin de pouvoir traiter les contraintes et réduire l'effet des perturbations non-répétitives. Une approche de commande itérative à apprentissage est proposée pour s'occuper des variations de cycle en cycle. Cette commande est utile pour atteindre les températures désirées en dépit des erreurs du modèle et des perturbations.

# Acknowledgements

I would like to express my thankfulness and show appreciation those people who have supported in this research work and helped me by giving their valuable opinion for the preparation of this thesis. Dr. Benoit Boulet, my thesis supervisor, has been very important in the success of the thesis. He always endowed me with the strength to finish this work. This work might not be possible without his guidance and encouragement. His valuable and constructive suggestions during planning and writing this thesis have been very much appreciated.

I am also indebted to other members of my thesis committee, Ioannis Psaromiligkos and Hannah Michalska, through the numerous discussions. I want to give many thanks to other graduate students and staff of my department at McGill University. Numerous people and innumerable instances, which I cannot enumerate in a single page, have helped me to accomplish this project.

My parents and my beloved wife have always been patient and supportive to me, understanding and allowing me to be workaholic. I would like to appreciate all the circumstances around me, which have been so generous to this humble being.

# Table of Contents

# Abbreviations

| | |
|---|---|
| MPC | Model Predictive Control |
| FFT | Fast Fourier Transform |
| ILMPC | Iterative Learning Model Predictive Control |
| IHP | Inverse Heating Problem |
| IFFT | Inverse Fast Fourier Transform |
| ILC | Iterative Learning Control |
| TILC | Terminal Iterative Learning Control |
| PI | Proportional-integral |
| PI | Proportional-integral-derivative |
| MIMO | Multi-input-multi-output |
| PEMRG | Plastics Europe Market Research Group |
| RC | Repetitive Control |
| R2R | Run-to-run |
| EWMA | Exponential Weighting Moving Average |
| NUFFT | Non-Uniform Fast Fourier Transform |
| SVD | Singular Value Decomposition |

# List of figures

# List of tables

# Contributors

| | |
|---|---|
| Md Muminul Chy | Literature review<br>Problem identification<br>Development of ideas to solve the problem<br>Implementation of the idea<br>Originator of the thesis |
| Dr. Benoit Boulet | Thesis supervision |
| Dr. Hannah Michalska | Thesis committee member |
| Dr. Ioannis Psaromiligkos | Thesis committee member |
| McGill University/NSERC | Funder |

# Chapter 1

# Introduction

## 1.1 Thesis Objective

Among the growing manufacturing sectors, the plastic manufacturing industry occupies a strategic place because of the many advantages offered by plastic products. These products are gradually supplanting traditional materials such as aluminum, glass, wood and paper. The consumption of plastics around the world has increased throughout the last several decades along with the improvement of technology in this time period. Plastic products can be as diverse as yogurt jars, plastic packaging, bathtubs, boat hulls or automotive body parts. In fact, plastic consumption per capita also increases with the development of a country's economy such as is the case in China, India and other developing countries. Plastics are widely used in packing, electrical and electronics, building, medical, automotive, aeronautics, sports and leisure, fishing, agriculture, textile and toy applications because of its low density, thermal, electrical and acoustical insulation, low permeability to liquids and gases, good mechanical performances such as tensile and impact resistance, good aesthetical characteristics in terms of color, gloss and touch, as well as easy conversion into useful products.

Table.1.1 shows the rate of increase in annual consumption of plastic products throughout the past few decades and future plastics growth also projected for next decade using the consumption data over a fifty year time span, from 1960 to 2010 [Source: Plastics Europe Market Research Group (PEMRG)]. The annual rate of consumption growth 8.1% on average which increased the consumption of all solid polymers from 7 million tons in the world during the year of 1960 to 196 million tons during the year of

2005 [Source: Pardos Marketing: Industrial Market Research Consultancy specializing in plastic and applications]. It continues to increase and is estimated to achieve over 365 million tons during the year 2015 and it will continue to achieve over 540 million tons during 2020, using a more conservative annual rate of 6.5 %. Total world production and consumption of plastics from the beginning of the twentieth century has kept an average annual rate of growth of 15 %. It doubles the consumption of the products in every five years until 1975-1979. This high increase rate was never achieved again after the first oil shock; the average annual growth rate of plastics was 15% from 1960 to 1974, and 8% thereafter, from 1974 to 2000, and 2005. Plastics consumption is growing in the new vast and fast developing country markets. The growth rate is averaging more than 10-15 % a year, just like it was in the prime time of the plastics built-up in Europe, USA and Japan, in the 1960-1975 era.

The diversity and wide use of plastic encourage researchers to develop more sophisticated and cost-effective way for product manufacturing processes. The process of

*Table.1.1: Annual Consumption of Plastic Product in World (Thousands of Tons)*

| Types of Plastic Product | 1960 (1000 tons) | 1979 (1000 tons) | 2000 (1000 tons) | 2010 (1000 tons) | 2020 (projected) (1000 tons) |
|---|---|---|---|---|---|
| Commodity | 7000 | 60000 | 155000 | 287000 | 510000 |
| Engineering | 50 | 900 | 4500 | 12000 | 24500 |
| Specialty | 3 | 40 | 170 | 400 | 1100 |
| Advanced Composites | 0 | 1 | 80 | 200 | 500 |
| Total | 7100 | 62000 | 160000 | 300000 | 538000 |

Source: (a) Plastics Europe Market Research Group (PEMRG) in Plastics Europe, 2010

(b) Pardos Marketing: Industrial Market Research Consultancy specializing in plastic and applications.

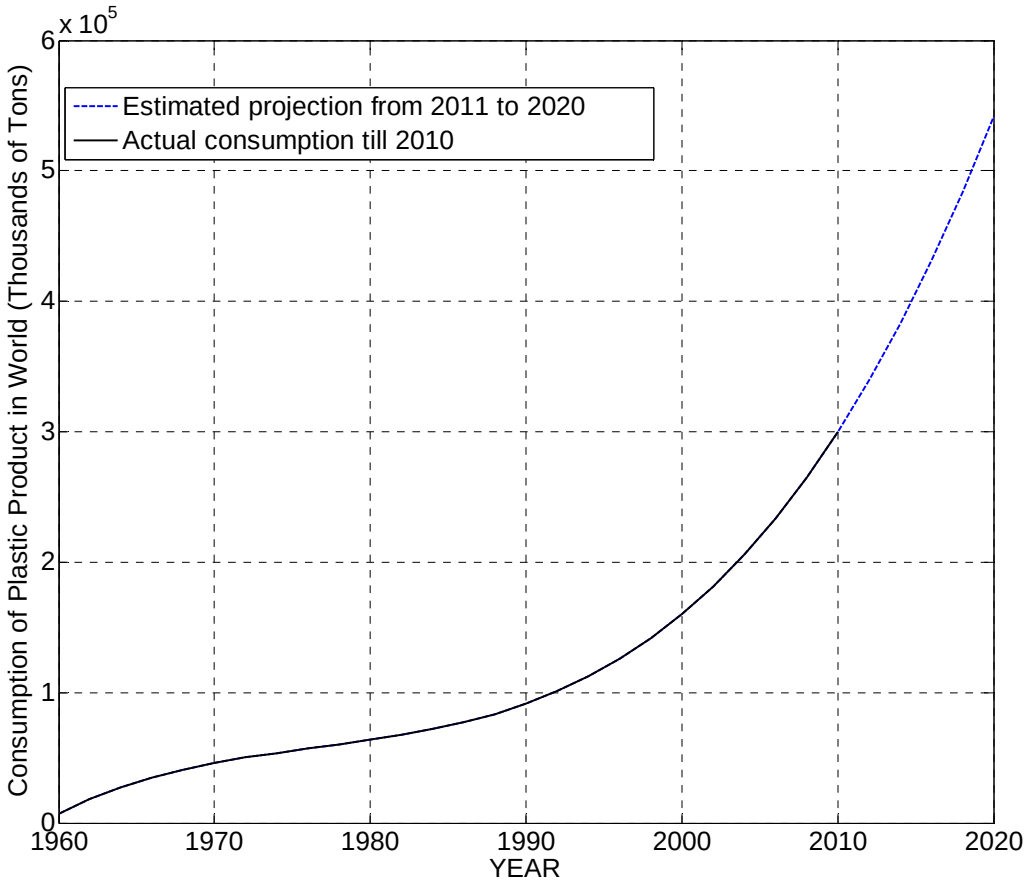


Fig.1.1: Consumption of Plastic Product in World (Thousands of Tons)

heating a plastic sheet to form it on an open mold is called thermoforming. The plastic sheet is heated by the oven heaters to its forming temperature and then formed by stretching it over, or into, an open single surface mold. The sheet is pushed against the mold surface unit until it is cooled. The formed part is then trimmed from the sheet. The thermoforming process consists of three phases, namely, the heating phase, forming phase and solidification phase. The first and most important part of the thermoforming process is bringing the sheet up to the softening temperature, i.e., the heating phase. The sheet is then formed to a mold using pressure in order to achieve the desired shape in forming phase. Finally, in solidification phase, the formed part is left to cool in the mold until the material solidifiers and rigid enough to be removed from the mold.

As heating is the first phase of the thermoforming process, the remaining phases of the process depend on the outcome of this phase. In this thesis, a detailed analysis of the heating phase is presented and effective control strategies to track the desired sheet temperature profiles throughout the heating cycle are developed. Proper control of sheet temperature results in an overall improvement of the thermoforming process. The main objective of the control system of the heating phase of the thermoforming process is to control the heater temperature of the oven such that the sheet gets heated at the specified temperature profile. The specification of the temperature profile over the whole sheet is a crucial step which should be achieved at the end of the heating phase, because the mechanical properties of the plastic largely depend on the temperature of the sheet [1-3]. A change in temperature of the sheet results in a change in mechanical properties such as the fluid behavior index and fluid viscosity of the plastic sheet [4,5]. In the forming phase, the plastic sheet is formed in the desired shape over the mold depending on these properties of the plastic. Moreover, different heat conduction boundary conditions exist within the part due to different parts of the plastic making contact with the multi-cavity mold boundary at different times. The quality of the plastic product can be improved through better control of material distribution before actual forming of the sheet by close control of sheet temperature distribution. Due to these reasons, uneven temperature profiles are often required to influence the mechanical formability of the plastic based on the shape of the object to be formed. Thus, the required temperature profile over the sheet at the end of the heating phase depends on the desired final part thickness at different locations and the intended application of the part.

Efficient temperature control and disturbance rejection helps to reduce the number of rejected parts and decrease the production cost. This is particularly important for producers of products manufactured from very expensive plastic materials. To increase production efficiency in terms of production rate, it is important to reduce the time it takes to make each individual part. This forces the controller to control the sheet surface temperature with a more aggressive trajectory for sheet temperature and shorter heating times for thermoforming operations. Heating a sheet at an aggressive rate will not give enough time for the heat to propagate across the sheet thickness through conduction as it

is a slow process compared to radiation. Another purpose of the controller could be to control the heater of the oven to decrease energy consumption by generating optimal control signals. Control of the heating temperature of the oven can be utilized in such a way that it can also potentially result in a decrease of machine maintenance cost. The performance of the heating elements in the oven can deteriorate with time which may affect heating quality. A controller can control the system to extend the life of the heating elements. These are some of the important motivations for the application of the heating phase control.

## 1.2 Literature Review

Most of the improved and recently developed control techniques depend on a mathematical model of the system. An accurate mathematical model is very important to get an idea about the system's behavior. It is also important for simulation of the developed control technique to gain confidence in the proposed technique before it is implemented in real-time. System modeling is a useful tool in efficient controller design to achieve the desired output temperature of the sheet at the end of the heating cycle in the thermoforming process. Some researchers have developed simple models of heat transfer in heating phase of the thermoforming process [5,6]. They are focused on various mechanisms of heat transfer for a variety of polymer processing techniques. In [5], Moore introduces the modeling of sheet reheat phase of the thermoforming process considering heat transfer by the combination of conduction, convection and radiation. He proposes the discretization of the plastic sheet across its thickness to consider heat propagation through its thickness only. In [6], Throne developed a model for heat transfer in semitransparent polymers for heating phase of the thermoforming process considering the wavelength dependency of sheet absorptivity and heater emissivity. In [7], the researcher analyzed the dependency of the absorbtivity and emissivity of the sheet on the wavelength of the transmitted heat that influence the development of the model of the heating phase. In [8], the researchers established the spectral properties of infrared heat emitters. In [9], the authors analyzed the uncertainty of the model parameters that are related to the input – output relationship of the heating phase. This work focuses on the treatment of parameter

uncertainty in the simulation of the sheet reheat phase of the thermoforming process. In [10], the researchers put emphasis on the importance of optimizing the reheating stage in blow moulding and thermoforming process. For that analysis, they come up with a model to predict the transient temperature distributions over both thin and thick-gauge polypropylene thermoformed sheets using an effective radiative heat transfer coefficient and the effective bulk temperature. Ajersch [11] improves on that modeling by incorporating the absorption of heat within the sheet as it heated. Gauthier [12] proposed certain improvements of the heating phase of a thermoforming machine by considering the transmission factor of incident heat over the plastic surface based on the previous model developed by Ajersch . He used the Beer Lambert Law to evaluate the part of heat energy that is transmitted through the plastic sheet layer and the part that is absorbed by the same plastic sheet. Although these researchers developed a good model for the heating phase of the thermoforming process, there are still some discrepancies between the simulation and experimental results. In this thesis, an improved model is developed for the heating phase of the thermoforming process through some development of the existing model developed by Ajersch resulting into superior quality of predictions through more accurate evaluation of input parameters of convection heat transfer, investigation of some other heating sources and development of a model for air temperature inside the oven.

One of the problems that researchers face in controlling sheet temperature in heating phase is sensing the whole sheet temperature using a fixed number of sensors. To control the temperature profile at every point of the sheet to the specified profile, an infinite number of heater units in the oven and an infinite number of sensors to feedback the temperature would be required, which is not feasible. Thus, it becomes a challenge for researchers to estimate the sheet temperature and hence control the temperature profile of the sheet using a minimum number of sensors by a fixed number of heaters in the oven [13]. Estimation of a complete temperature profile over the whole sheet is necessary for an accurate and efficient control of the temperature, although the number of sensors should be kept low to minimize their cost. The effectiveness of the controller depends on the accuracy of the estimation of the complete temperature profile and the incorporation

of the estimation into the design of the controller. Some researchers use the signal from the sensor directly as the feedback signal to compare with the desired temperature at the point of the sheet [14,15]. The controller design based on these error signals works to minimize the difference between the actual temperature and desired temperature of the sheet zone. But the differences between the actual temperature and desired temperature at locations between any two sensors cannot be optimized using that control technique. If the sensor output can be used to estimate or interpolate the whole temperature profile over the sheet and this information is incorporated in the design of the controller in such a way that it will control whole sheet temperature instead of the temperature at some particular points of the sheet, then the sheet temperature can be achieved to the specified profile required for the forming phase. The approach in [11] uses virtual sensors (that uses information available from other real sensor to estimate temperature at other points to reduce sensor cost) in addition to real sensors so that some more temperature points can be incorporated into the design of the controller. The temperatures at these virtual sensors are estimated from the real sensor temperatures using a weighted average based on distance. Although more points can be incorporated in the design of the controller using the virtual sensors to optimize the difference between desired and actual temperatures, the difference between the desired and actual sheet temperature profiles still cannot be optimized by this method across the entire sheet as the controller only minimize temperature difference at certain points.

Another challenge for research is to obtain heater temperature set-points for the desired temperature profile over the sheet at the end of the heating phase because of weak actuators (ceramic heaters) and high nonlinearity of the system. Excessive heating can cause the plastic material to degrade and may result in a change of color or premature failure when exposed to the outdoors. This not only affects the physical and mechanical properties of the part, but also endangers the economic viability of the product. It therefore becomes very important to control the temperature profile over the sheet to the desired temperature profile. Complex thermal couplings between large numbers of heaters and sheet zones and very low sensitivity make it more difficult to calculate the heater temperature set-points. Researchers have developed nonlinear models of heat

transfer between the heaters and the sheet by considering all three kinds of heat transfer in the oven: conduction, convection and radiation. The standard direct heat transfer problem is well-posed because the solution exists, is unique and stable under small changes of input data. But the inverse heating problem (IHP) is not well-posed [16, 17, 18, 19]. Some analytical methods like the exact method [20], polynomial method [21, 22] and integral method [23,24,25,26,27] are used to solve the IHP. But they are limited to one-dimensional linear problems with particular initial and boundary conditions. Lots of complications come out when the analytical methods are applied for solving the IHP in nonlinear and three-dimensional systems. Sometimes, the results do not converge or oscillate for a nonlinear system. So these methods are not suitable for the solution of the IHP in the heating phase of thermoforming. Some heuristic methods of solution are based on pure intuition rather than mathematical formality. Even if they are not accurate, some of them are still used to solve IHP in different processes because of their ability to treat ill-posed unstable problems. These methods are based on the idea of reformulating the inverse problem in terms of approximate well-posed problem by utilizing some kind of regularization technique that work only in limited applications. But the error increases abruptly with the increase of complexity of the system. The performance of such methods is not satisfactory for most complex nonlinear systems like the thermoforming process. In most others methods, the solution is obtained by least-squares minimization. Tikhonov's regularization procedure modifies the least-squares equation by adding a smoothing term in order to reduce the unstable effect of the measurement error [28]. Because of computational cost and ill-posedness of the thermoforming process, most of the works use the pseudo-inverse of the view factor matrix, which is basically the ratio of energy leaving each surface that reaches the other surface. It is one of the simplest methods. Although the computational cost is low in this method, the solution is often erroneous and it does not take into consideration the cycle time in calculating set-points of the heater temperature of the cyclic process. In another work, a neural network is used to solve the IHP [29]. Kudo et al. [30] and França et al. [31, 32, 33, 34] solved the IHP for radiating systems. There are also adaptive filtering algorithms that are used to solve the IHP based on a probabilistic approach [35,36]. These adaptive filtering algorithms do not converge to real setpoints for the thermoforming process as it is high sensitive to change in input

and the solution behavior changes continuously with the initial conditions. Although discrete methods [37, 38, 39, 40, 41, 42, 43] have the advantage of being applicable to any problem, they may experience some oscillation due to the unstable nature of the inverse problem. Discrete methods are very computationally costly and require a large memory for real-time implementation. As in the case of combined heat transfer problems, discretization leads to a system of nonlinear, ill-conditioned equations, so the result may not unique and stable. Ajersch tried to use the sensitivity matrix for solving the IHP for the thermoforming oven [11]. But the process is nonlinear, such that the sensitivity matrix changes quickly with its operating point. This method gives erroneous results even if the operating point is close to the linearization point. In [18], Duarte and Covas proposed a method for IHP based on multistage heating where the same sheet will be heated in different stages of the oven. This delays the whole process and makes it more costly. The method in [18] is based on intuition rather than mathematical formality that give approximate results. Moreover, the performance of the method degrades for uneven temperature profiles. Most of the methods used for solving IHP do not take into consideration the cycle time which has a role to play in deciding the set-points of the heaters. An iterative method may represent a good choice for solving such systems. In the iterative regularization principle, a sequential improvement of the solution takes place. A solution to the IHP is found at the end of the iterative procedure. There are many such algorithms based on the conjugate gradient used to produce robust and stable estimation of the solution of IHP which are frequently used in metallurgy, chemical industry, aerospace and electronics [44, 45, 46, 47, 48, 49, 50].

Two types of control techniques are used for the heating phase of the thermoforming process: cycle-to-cycle control and in-cycle control. A cycle-to-cycle control technique updates the control input for the heater temperature set-points at the end of each cycle such that the next part is improved upon iteratively via better sheet temperature distribution and to correct for gradual drift of machine operating parameters. On the other hand, the in-cycle technique calculates control input of the heater temperature during the heating phase. In the process of thermoforming, the temperature profile over the plastic sheet at the end of the cycle and the rate at which the sheet is

heated depend on the efficiency of the controller, the number and locations of heater units and the number and locations of sensors.

The control of the heating phase of the thermoforming process is a challenging problem because of the difficulty arising from the nonlinear and time-varying nature of the process. Moreover, a high level of uncertainty surrounding the process and in different material parameters, as well as the multi-input multi-output nature of the problem, with a high degree of coupling between inputs and outputs, make the control even harder. Finally, there are a number of hard constraints due to the heaters and the polymer material that must be taken into consideration such as maximum allowable sheet and heater temperatures. At present, in some cases standard proportional-integral-derivative (PID) controllers are used, even though the process is difficult to control using conventional PID controller due to the long time constant of the process [51,52,53,54]. The long time constant is caused by low heating and cooling rates of the heaters and plastic sheet, and the sheet temperature has a tendency to overshoot on set point changes and is slow to correct itself on disturbances. Moreover, the PID controller cannot handle process constraints such as the maximum and minimum heater temperatures, as well as limited heating and cooling rates of the heaters. Because of the limited heating and cooling rates, it is typically observed that the heaters fail to track the control inputs from the controller. Moreover, PID controllers typically take little model information into consideration to calculate the control input. Because of strong nonlinearities in the heating phase, they cannot achieve the specified performance level at different operating conditions. This poor control performance by PID controllers may lead to part quality variation problems that cannot meet industry's strictest quality standards. PID controllers also have a drawback in controlling an MIMO system as the IHP has to be solved in real time to decouple the system [16].

With the continuous growth of the thermoforming industry and ever-expanding applications of plastic parts, the demand for rapid production of complex parts with tighter tolerances, superior finish and lower cost is increasing rapidly. These requirements cannot be met without a sophisticated process control system providing accurate control

of key process variables that are inherently nonlinear and time-varying. Different control strategies, such as adaptive control and model predictive control (MPC) have therefore been adopted to handle the control problems [52,55,57,58,59,60,61,62,63]. Adaptive control can not give good performance for nonlinear systems with parameter uncertainty and it is sensitive to unmodelled dynamics and disturbances [57]. It may have poor transient that affects the heating rate throughout the thickness of the sheet as well as the performance of the thermoforming process. It also requires a lot of computation for a large and complex system such as the thermoforming process. Most of robust controllers use *a priori* knowledge of the upper bound on the uncertainties in developing the control actions, ignoring the fact that some characteristics of an uncertain system can be learned during the control process. The inability to learn results in a conservative design and stability of the system is achieved at the cost of performance.

MPC has some nice features. For example, it can automatically compensate for process interaction and disturbances as well as handle difficult process dynamic. Another important advantage of this type of control is its ability to cope with constraints on controls and states. So MPC can optimize the performance by allowing for operation close to the system constraints. MPC is also able to handle structural changes and it may be easy to tune. However, the computation of MPC to solve the optimization problem between every sampling instant may require complex calculations demanding a high speed processor [61]. In some other industrial applications that work with repetitive batch processes and where each process has to follow a trajectory corresponding to the desired performance, the use of a cycle-to cycle control technique is typical. In case of a repetitive process, sometimes ‘in-cycle’ control approaches are not perfect and trajectory tracking errors remain as the controller does not use information from the previous cycles [51,52,53,54,55,56,57,58]. As a result, the same error is repeated at each cycle due to repetitive disturbances. With the information obtained from previous cycles, it becomes possible to change the control input applied to the process in order to reduce the trajectory error.

Among cycle-to-cycle control approaches, Iterative Learning Control (ILC), Terminal Iterative Learning Control (TILC), Repetitive Control (RC) and Run-to-Run (R2R) control are mostly used. TILC computes the control input at the end of the cycle and it keeps the same control input over the next cycle. Process control using these techniques is also complicated by the fact that there is a high level of uncertainty surrounding the process, particularly with the material properties. Moreover, environmental conditions may change between cycles. Heater nonlinearity may make the controller delay in achieving the correct input signal. Sometimes a cycle-to-cycle controller converges very slowly resulting in lots of discarded parts. Moreover, the time varying nature of the process makes this technique insufficient to achieve the desired performance. RC is a control technique that is similar to ILC. The major difference between these two approaches is that ILC requires the return of the process to a specific initial state vector, always the same for all cycles, while in RC, the initial state vector of cycle $k$+1 corresponds to the final state vector of the process at the end of cycle $k$ [64,65,66, 67,68,69,70,71]. Thus, ILC is used for intermittent processes whose final states are different from their initial states. The same applies to TILC and R2R. Between two successive cycles, the process returns to its initial conditions (or state vector) [66]. To illustrate, if we use ILC to control the heating of a plastic sheet, then the initial state of the process corresponds to the plastic sheet's temperature before entering the thermoforming oven. The final state at the end of the cycle corresponds to the sheet temperature just before it goes to the forming phase of the thermoforming process. These initial and final sheet temperatures can be very different. RC is used for processes for which there is no wait between two successive cycles and the final state of a cycle will become the initial state of the next cycle. In some applications, R2R is used to eliminate the effect of periodic disturbances. It is also considered to be an Intelligent Control approach [66]. This cycle-to-cycle control method, like TILC, is based on measurements of the controlled outputs taken at the end of the cycle [64,65,66]. The R2R approach is composed of various control algorithms for cycle-to-cycle control to correct for gradual drift of the process operating parameters[64,68,69,70], and one of the algorithm, which is the most used, is the "Exponential Weighed Moving Average" (EWMA) [64,65,66, 67,68,69,70,71]. These R2R algorithms are analyzed from a stochastic point of view,

whereas the analysis of TILC algorithm approaches rely more on the deterministic analysis used in ILC.

## 1.3 Major contributions of this thesis

The major contributions of this thesis are listed below:

1) In this thesis, at first, the existing model of sheet heating is improved to give a better mathematical relationship between inputs and outputs. That is, an improved model is developed for the heating phase of the thermoforming process through some development of the existing model developed by Ajersch resulting into superior quality of predictions through more accurate evaluation of input parameters. The existing model of the heating phase is first presented along with the discrepancy between the existing model and the experimental results. This thesis presents an improved mathematical model as compared to the existing model to represent a more accurate relationship between inputs and outputs of the heating phase of the thermoforming process. The proposed state-space model of this process can present and explain some behaviors that are impossible to explain using the existing model. The development of this new model helps to improve the quality of predictions of the system's output and state through more accurate evaluation of the inputs and system properties. First, the modeling is developed based on the heat transfer method and the system's behaviour. Then, a series of specialized experimental data are compared with the simulation data obtained from the developed model to validate it. All three kind of heat transfer methods (conduction, convection and radiation) are considered in the development of the model of the heating process. The proposed state space model is simulated using Simulink to compare with real time results. The input output relationship of the proposed model closely follows the real time relationship of the inputs and outputs at different operating conditions. The proposed model gives improved results as compared to the existing model.

2) In this thesis, a conjugate gradient method is used to calculate the heating set-points of the heaters to heat the plastic sheet to the desired temperature. To calculate the

set-points of heater temperatures that will heat the plastic sheet to the desired temperature at the end of the heating cycle is a challenge for thermoforming process. Although radiation heat transfer plays a big role in a thermoforming oven, conduction and convection also have a significant contribution in sheet heating. The combination of all three forms of heat transfer makes the problem harder to solve. In addition, the IHP is often not well-posed in a thermoforming process, making the solution numerically unstable. In this thesis, a conjugate gradient based method is proposed while taking into consideration computational cost such that it can be implemented as a real-time algorithm in the controller. The performance of the proposed method for solving IHP, and thereby the corresponding sheet temperature controller, are tested at different operating conditions and compared with the conventional method of solving IHP based on the pseudo-inverse of the view factor matrix.

3) This thesis presents a new method for the estimation of sheet temperature using temperature sensors at different positions of the sheet. The proposed method is different from the conventional method in estimating sheet temperature through the prediction of spatial harmonics. This proposed estimation technique does not need the interpolated points' locations prior to estimation like other conventional techniques. Therefore, it can estimate temperature at every point over the sheet from its spatial harmonics and a major part of the computation can be done offline as soon as we know the sensor location. This reduces the computational cost of the proposed method. Two-dimensional FFT technique was used in the proposed estimation method of the temperature profile.

4) This thesis proposes a new control technique that controls sheet temperature by controlling the spatial temperature harmonics to reach the desired temperature profile. In conventional technique, the temperatures at certain points are controlled and the control of temperature at one point definitely affects other location. But this proposed harmonic controller controls the spatial harmonics of the sheet temperature. Using this technique, spatial temperature harmonics can be controlled independently as they are orthogonal to each other. Control of one harmonic will not affect the control of other harmonics which is not possible in the conventional technique. A simple PI controller is used to control

each spatial harmonic to achieve the desired temperature profile over the sheet. Each component of the two-dimensional space temperature harmonics is controlled by adjusting the heater temperatures. Thereafter, the performance of the proposed temperature control technique based on the spatial harmonics is compared with the conventional control technique in simulation.

5) Fourier transform technique is an effective tool that is used for the estimation of the spatial harmonics of temperature profile over the sheet. But one of the drawbacks of this method is that its use for the estimation of the temperature profile of the sheet requires that the sensors have to be placed at equidistant positions over the sheet. This placement may not be optimal for the prediction of the temperature profile of the sheet. The location of sensors should depend on the expected temperature profile variations. More sensors should be placed around the areas where the largest gradients of temperature are expected to capture all harmonics correctly. So the temperature sensors are usually placed at the optimal positions of the sheet for the best estimation of surface temperature of a sheet with the least number of sensors. An estimation technique of missing sensor point temperatures is proposed to transform a non-equidistant sensor data into equidistant sensor data. The Lagrange interpolation technique is used in this proposed technique. It was found in the simulation results that, the estimation of temperature using Lagrange interpolation bring more oscillation. But this technique may be more suitable in case of a temperature profile with high oscillation.

6) In Chapter 5 in this thesis, another estimation technique is proposed to predict harmonics using QR factorization method to avoid the drawback of Lagrange interpolation technique. The proposed method for the estimation of temperature can be used for any arrangement of sensors even for sensors with non-equidistant location. The proposed method is developed in such a way that it can do a high-quality estimation of the temperature profile over the entire sheet through its harmonics and the spatial harmonic controller can control the harmonics to obtain the desired temperature profile. The computational cost of computing Non-Uniform Fast Fourier Transform (NUFFT) to estimate the temperature profile can be reduced by computing the NUFFT matrix offline

to make the technique more computational efficient. The NUFFT matrix can be computed offline as soon as the locations of the sensors are known. The performance of the proposed estimator and controller is tested in simulation at different operating conditions to compare with the Lagrange interpolation technique and the conventional method of the estimation of temperature profile which is based on the weighted average of the temperature of the sensors surrounding the point.

7) This thesis presents a method to control the surface temperature of a plastic sheet using MPC. Even though the MPC controller can handle a multivariable process, the large number of computations makes it difficult to apply to large systems such as multi-zone temperature control in a thermoforming machine. This drawback is handled in this thesis using Multi-parametric quadratic programming that helps in solving the model predictive optimization problem offline which reduces the real-time computational burden of the controller. In this thesis, the design of a model predictive controller is reported and simulated on a complex thermoforming oven with a large number of inputs and outputs for precise control of sheet temperatures under hard constraints on heater temperature and their rates.

8) Properties of the thermoforming process, such as its nonlinear, time-varying dynamics and actuator constraints, make its control challenging. An iterative control technique along with model predictive control is presented in this thesis on 2D control of the thermoforming process. This approach utilizes not only incoming information from the ongoing cycle, but also the information stored from the past cycles. To deal with constraints as well as non-repetitive disturbances in the process, the MPC technique is incorporated to update the control law within the cycle. To exploit the repetitive nature of the heating phase of the process, a cycle-to-cycle iterative learning control technique direction is proposed. The iterative learning strategy is useful for achieving desired temperature despite model mismatch and disturbances. Even though the proposed multi-zone temperature controller can handle a multivariable process, the large number of computations makes it difficult to apply to large systems such as a thermoforming

machine. To reduce the computational burden, the control laws are computed offline using multi-parametric programming.

9) This thesis ends in Chapter 8 by drawing some conclusions and by providing some ideas for future research work.

# Chapter 2

# Modeling of the Heating Phase of a Thermoforming Machine

## 2.1 Introduction

The first step in gaining knowledge about a system and controlling it is to build a mathematical model that represents the behavior of the system. In the case of the thermoforming process, the model represents the relationship between the input current to the heating elements and the plastic sheet temperature. Generally, there are two basic methodologies that are available for process modeling. The first approach is known as the "black-box" modeling approach. This approach uses system identification techniques to obtain mathematical models from experimental input-output data. A model is developed to fit the input-output data to represent the behavior of the system. The second approach is direct: it utilizes in-depth knowledge of the system and various laws of physics to obtain mathematical equations which describe the system's behavior.

The first-principles approach and the black-box approach, have their own distinct advantages and disadvantages. One advantage is that a black-box model, depending on its structure, can often better describe the behavior of the system within a certain operating range, even though the modeling equations hold no physical meaning. Another advantage is the fact that this same approach is very versatile and can be applied to a wide range of systems. This accounts for the method's popularity. It does not need any kind of information about the system prior to the development of the model. However, some reasonable assumptions are often made about the system, such as linearity, time

invariance, operating range of the process etc. So, an in depth understanding of the system dynamics is not necessarily required for this kind of approach. As a result, the black box approach is often a practical, less labor intensive modeling strategy. One of the disadvantages of black box modeling is the fact that "plant friendly" inputs are not always possible. This means that some systems may not be suitable for the application of system identification techniques that require relatively large input perturbations, which can subsequently bring the system out of its normal operating range and cause a defective product or even damage equipment. Sometimes small signal PRBS (Pseudo Random Binary Signal) analysis is used to extract process models from processes that are sensitive to large perturbations [72, 73, 74]. Unfortunately, this technique is not directly applicable to thermoforming due to the slow response of the heating elements. As the thermoforming process is time-varying, most black box models will not be capable of capturing the time-varying dynamics of the process. Finally, the black box approach can sometimes require many identification experiments, which can be time consuming and costly depending on the process. In this thesis, we will consider the second approach, i.e., the first-principles approach for modeling.

The second approach has some distinct advantages as compared to first approach. To start, the mathematical equations that are derived have physical meaning. At first, it will identify the entire physical phenomena that take place in the process and use various laws of physics to represent the relationships. Each of the terms in the equations relates to a specific physical phenomenon which yields greater insight into system behavior. As a result, it is possible to tune the parameters in the model so that the model better represents the actual physical system. This also leads to a more flexible design since it is possible to simplify or expand upon the model as required. Another advantage is the fact this approach generally does not require as many model validation and identification experiments. Finally, the first-principles approach usually results in better extrapolation performance. This means that the model will often describe, quite well, the behavior of the system in operating ranges that are outside of the range in which the identification and validation experiments were performed. There are also drawbacks to the first principles approach. One important drawback, which is of major concern, is the fact that a lot of

time and effort is usually required to develop a suitable model. The model parameters can sometimes be difficult to obtain, particularly when there are many uncertain parameters within the model. This will also increase the controller design time. Inaccurate models are also a major disadvantage. Modeling errors can occur when unmodeled, higher order dynamics are left out, or when very complex physical phenomena are described by over-simplified mathematical relationships.

Researchers developed a full-order finite-element simulation model of the reheat phase of the thermoforming process [75, 76]. But this large and very complex model is not suitable for the design of an implementable controller. Another mathematical model for the reheat phase of the thermoforming process was developed by some researchers based on the combination of the three mechanism of heat transfer such as conduction, convection and radiation [5, 11, 12]. Some of the discrepancies of this model are investigated in this chapter. This chapter presents an improved mathematical model to represent a more accurate relationship among inputs and outputs of the heating phase of the thermoforming process. The proposed state-space model of the heating phase of the thermoforming process can present and explain some phenomena that are impossible to explain using the existing model. The main purpose of this chapter is to improve the quality of predictions of the system's output and state through more accurate evaluation of the inputs and system properties. We discuss the model developed and improved by Moore, Ajersch and Gauthier [5, 11, 12]. Then, some points in the model will be checked to get an improved and more accurate model.

## 2.2 Thermoforming oven

At first, we discuss different parts of thermoforming oven briefly before discussing the model of the system. The thermoforming oven is composed of different parts such as heater banks, plastic sheet, temperature sensor, oven walls etc. A mathematical model represents the physical interactions between different elements within the process to develop a relation between input, output and other disturbances related in the process. Before moving on to the modeling of the reheat phase of the

thermoforming process, let us provide some discussion about different elements of the system.

### 2.2.1 Heater Bank

The thermoforming oven heats the plastic sheet to the desired temperature that allows the forming of the sheet on a mold. The oven has two sets of heater banks at top and bottom of the oven. Each heater bank is composed of smaller heating elements. Although the heater banks have higher temperature at their center compared to its peripheral temperature, it could be assumed that the heater banks have uniform temperature all over their surface to make the model simple. These heating elements are usually made of ceramic, or quartz. The heat transferred by radiation depends on the emissivity of the heater. The heating elements are heated using electrical currents. The use of Pulse Width Modulation (PWM) of the current controls the power delivered by the heater. The AAA thermoforming oven, on which tests are conducted, has 12 heater banks with 6 at the top and 6 at the bottom of the oven, each composed of 3 heating elements.

### 2.2.2 Infrared sensor

The temperature measurements of the plastic sheet surface are important to control the temperature of the sheet. Without proper measurement of the process output signals, it is impossible to accurately control the process as desired. Infrared temperature sensors are used to sense the sheet temperature without physical contact with the sheet. For the AAA thermoforming machine the IR temperature sensors are located in top and bottom layer of the thermoforming oven and installed in such a way that it will scan the temperature of a certain point on the sheet over the whole temperature range. It also has sensor to sense the heater temperature that are embedded into the ceramic heater by manufacturer. It is also possible to incorporate sensor to sense the air temperature of the oven. But the problem is that the air temperature varies widely at different positions in the oven.

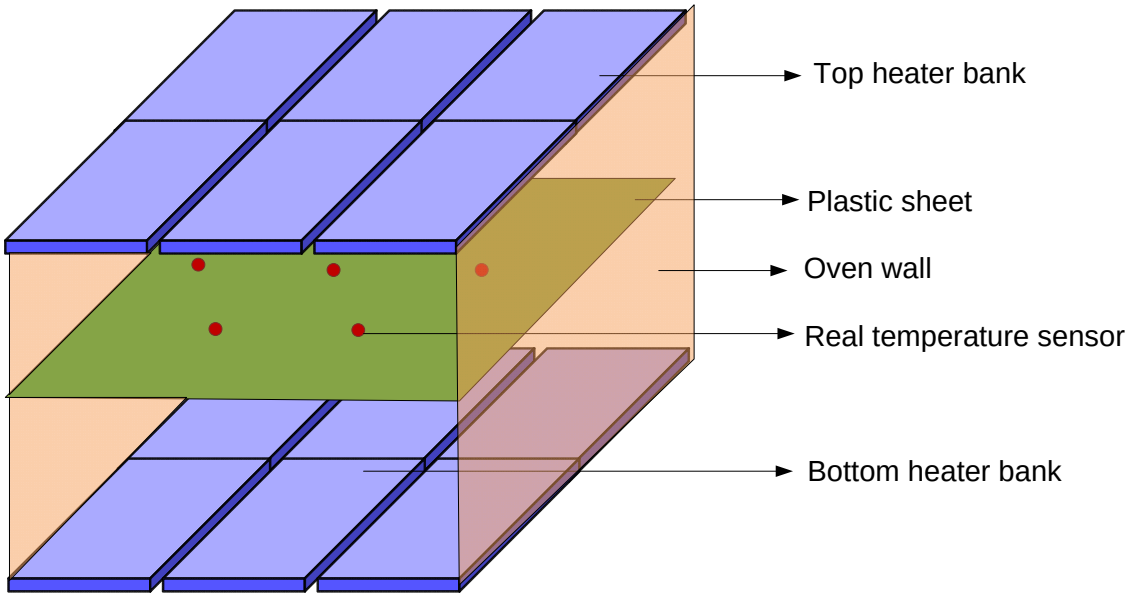


Fig.2.1: Thermoforming oven

### 2.2.3 Oven wall

The thermoforming oven can be open, semi closed or closed. The open oven has no side wall whereas in semi closed oven it has wall in two sides. The closed oven has four walls around it. In some cases, the oven has a wall that is partially closed. Depending on the type of the thermoforming machine, heating process is affected by the wall. The wall works as a good reflector of heat flux. In the AAA thermoforming oven, it has two walls on both sides made of asbestos.

### 2.2.4 Plastic Sheet

The plastic sheet is the most important part to be considered in developing the mathematical model. Heat transfer through the plastic is the vital phenomenon that should

be considered to develop the modeling of the process. Some of the plastic materials, known as Thermoplastics, do not change in their composition even if it is heated and can be molded again and again; while thermoset plastic can be heated and molded once only. Plastic could be referring to a wide range of natural, synthetic and semi-synthetic polymer material. It can also be classified based on some qualities such as elasticity, transparency, biodegradability, density, tensile strength and electric conductivity. Polymer plastic consists of high molecular mass that can vary in different properties like molecular composition, heat transfer property etc. The composite structures of the side hydrocarbon chains influence the properties of the polymer plastic. A plastic product can be modified in such a way that heat transfer properties through the material can be controlled. This ability to modify the properties of the plastic by repeating unit's molecular composition structure made plastics to become an essential part of the today's world. In this thesis, we will focus on mathematical heat transfer properties rather than molding properties. The heating process in the plastic sheet depends on the various properties of sheet like density of the material, heat capacity, thermal diffusivity, thermal conductivity, and emissivity. The plastic sheet is placed in the middle of the oven with the help of a clamping mechanism. Depending on the location and number of temperature sensors, the plastic sheet is divided into a number of zones, as shown in Fig. 2.2. The purpose of this zoning is to ensure control over the temperatures at certain locations on the sheet surface. Some parts require temperature uniformity across the surface, while others might require hotter spots at certain locations to ensure that the final part thickness at that spot is as desired.

## 2.3 Review of the existing model

The model used in this thesis is developed in [11]. Interested readers are encouraged to get details of the model from that reference. The developed model is briefly discussed here.

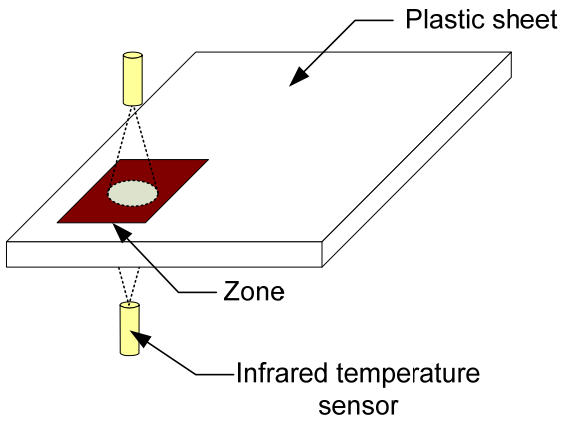


Fig.2.2: Zone and IR temperature sensors

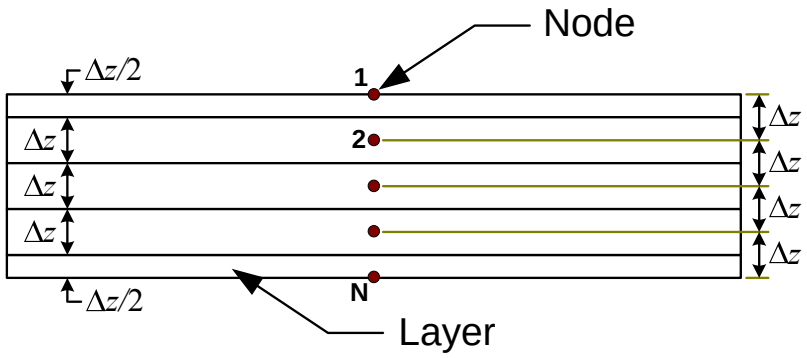


Fig. 2.3: Layers and nodes

To analyze the propagation of the heat inside the plastic sheet, heat transfer equations must be defined for some points throughout the thickness of the sheet. To do so, each zone is divided into layers throughout the thickness of the sheet (Fig.2.3). The layers have the same thickness, and at the middle of each layer there is a point referred to as a node. For each node, a differential equation describes the heat exchange of the corresponding layer. Since the surface of the plastic sheet is an important boundary of energy exchange, a node is located directly at the surface, see Fig.2.3. This forces the layer containing this point to have only half of the volume inside the plastic sheet, and hence, its thickness is only half of that of internal layers. The layers having their node at

the surface are identified as “surface layers” and the other layers are designated as the “internal layers”. Each IR temperature sensor looks at an area on the plastic sheet to perform the temperature measurement. Each area where the sensors are pointing is designated as a “zone”. To facilitate modeling, we assume that there are two IR sensors for each zone of the plastic sheet, one looking at the sheet from above and the other from below (Fig.2.2). For each node, a differential equation describes the heat exchange of the corresponding layer. There are three ways (conduction, convection and radiation) to exchange energy between heaters, ambient air and nodes. Neglecting the lateral conduction of heat between two zones as the thickness of the sheet is much smaller than its width and length, the conduction type of heat can be only transferred between two adjacent nodes through the thickness of the plastic sheet. The conduction heat transfer between surface node and its adjacent node can be expressed as,

$$\frac{dT_{su}}{dt} = \frac{2}{\rho V C_p}\left[\frac{kA}{\Delta z}\left(T_{in} - T_{su}\right)\right] \tag{2.1}$$

where, $\rho$ is density of the plastic sheet, $C_p$ is the specific heat of the sheet, $k$ is the heat conduction constant, $\Delta z$ is the layer thickness, $A$ is the zone area, $V$ is the volume of the layer, $T_{su}$ is the surface node temperature and $T_{in}$ is the temperature of the adjacent node of the surface.

In the case of an interior node of the sheet, nodes exist on both sides of that interior node and conduction heat transfer is present on both sides of the node. The conduction heat transfer equation can be written down as,

$$\frac{dT_i}{dt} = \frac{1}{\rho V C_p}\frac{kA}{\Delta z}\left(T_{i-1} - 2T_i + T_{i+1}\right)$$

Where, the subscript $i$ indicates the node number.

Convection has an effect only on the nodes of surface layers and expresses heat

exchange between the ambient air and the sheet. The convection heat transfer can be expressed as,

$$\frac{dT_{su}}{dt} = \frac{2}{\rho V C_p} hA\left(T_\infty - T_{su}\right) \tag{2.2}$$

Where; $h$ is the convection coefficient, $T_{su}$ is the surface node temperature and $T_\infty$ is the ambient air temperature.

The radiant energy exchange transmits energy from the heaters to the surface node of the plastic sheet which can be expressed as,

$$\frac{dT_i}{dt} = \left(\frac{2}{\rho V C_p}\right)\sigma \varepsilon_{eff} A_h \left[\sum_{j=1}^{M}\left(\theta_j^4 - T_i^4\right) F_{k,j}\right] \tag{2.3}$$

where σ is the Stefan Boltzmann constant, $\varepsilon_{eff}$ is the effective emissivity, $A_h$ is the area of the heater bank, $M$ is the total number of heaters, $F_{k,j}$ is the view factor between the $j_{\text{th}}$ heater bank and the $k_{\text{th}}$ zone,$\theta_j$ is the $j_{\text{th}}$ heater bank temperature. Details of the method for calculating effective emissivity and view factors can be found in [11].

**View factor:** In the case of radiant energy transfer, the fraction of the emitted energy by one surface reaching the second surface depends on the distance, position, and area of both surfaces. The ratio of the received energy by the second surface to the energy emitted by the first surface is called view factor. Researchers already developed the mathematical equations for the view factor according to the relative positions of the surfaces. Ehlert and Smith provide a calculation of the view factor for two different horizontal planes that are separated by a distance N as shown in Fig.2.4(a) in [77]. It is found by using view factor algebra that the view factor expression from one plane to the other plane is

$$F_{par} = \frac{1}{(x_2 - x_1)(y_2 - y_1)} \sum_{l=1}^{2}\sum_{k=1}^{2}\sum_{j=1}^{2}\sum_{i=1}^{2}(-1)^{(i+j+k+l)} G(x_i, y_j, \eta_k, \zeta_l) \tag{2.4}$$

where

$$G(x_i, y_j, \eta_k, \zeta_l) = \frac{1}{2\pi}\{(y_j - \eta_k)\sqrt{(x_i - \zeta_l)^2 + z^2}\,\tan^{-1}(\frac{y_j - \eta_k}{\sqrt{(x_i - \zeta_l)^2 + z^2}})\}$$

$$+\frac{1}{2\pi}\{(x_i - \zeta_l)\sqrt{(y_j - \eta_k)^2 + z^2}\,\tan^{-1}(\frac{x_i - \zeta_l}{\sqrt{(y_j - \eta_k)^2 + z^2}})\} - \frac{z^2}{4\pi}\ln\{(x_i - \zeta_l)^2 + (y_j - \eta_k)^2 + z^2\} \tag{2.5}$$

where $F_{par}$ is the view factor between two parallel planes.

View factor between perpendicular oven wall and sheet can be calculated using the equation in [77].

$$F_{per} = \frac{1}{(x_2 - x_1)(y_2 - y_1)} \sum_{l=1}^{2}\sum_{k=1}^{2}\sum_{j=1}^{2}\sum_{i=1}^{2}(-1)^{(i+j+k+l)} G_{per}(x_i, y_j, \eta_k, \zeta_l)$$

$$G_{per} = \frac{1}{2\pi}\left\{(y-\eta)(x^2+\zeta^2)^{1/2}\tan^{-1}\left[\frac{(y-\eta)}{(x^2+\zeta^2)^{1/2}}\right] - \frac{1}{4}\left[(x^2+\zeta^2) - (y-\eta)^2\right]\ln\left[(x^2+\zeta^2) - (y-\eta)^2\right]\right\} \tag{2.6}$$

where $F_{per}$ is the view factor between two perpendicular planes. Gauthier [12] considers the transmissivity of the plastic instead of considering that all the radiated heat is absorbed at the surface of the sheet. If the infrared radiation is able to penetrate inside the plastic sheet, the surface node will not absorb all the heat from the received incident radiant energy, and if it penetrates through the thickness of the sheet, then it heats up every node on its way, and a part of the incident radiant energy gets transmitted through the sheet depending on the transmissivity factor.

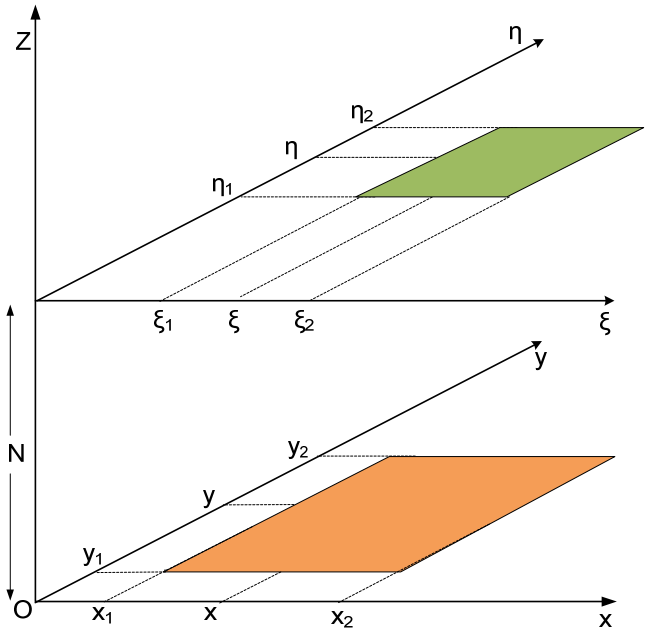


(a)

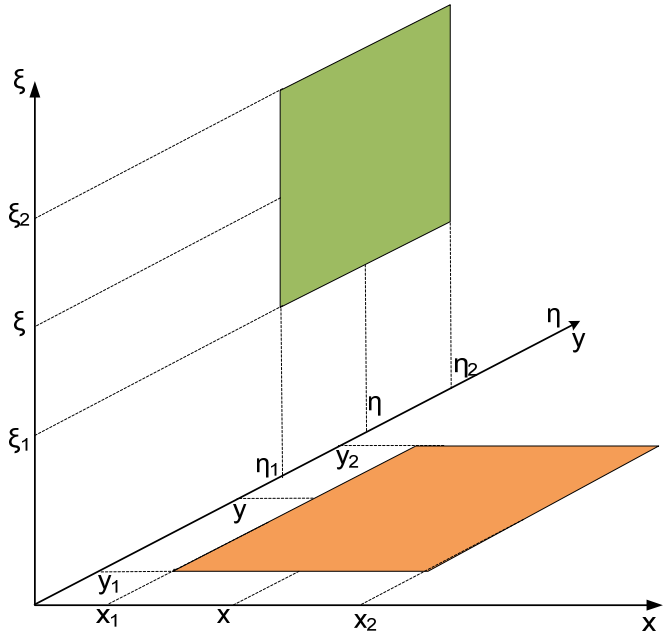


(b)

Fig. 2.4: Calculation of view factor for (a) parallel planes and (b) perpendicular planes

Using the Beer Lambert law (82), the absorbed fraction of transmitted energy in surface and inner nodes can be calculated as,

For surface nodes, $\beta_1 := 1 - e^{-A\Delta z/2}$

For inner nodes, $\beta_2 := 1 - e^{-A\Delta z}$

Combining all three forms of heat transfer into the equation for $2M$ heaters, $Z$ zones and 2 nodes for each zone, and taking the transmissivity into account in the energy transfer from the radiant heaters to the plastic sheet, the model for the $j^{th}$ zone in the heating phase becomes,

$$\begin{aligned}\frac{dT_{j,top}}{dt} &= \frac{2}{\rho V C_p}\left\{\left(\frac{kA}{\Delta z}(T_{j2} - T_{j,top})\right) + hA\left(T_{\infty_{top}} - T_{j,top}\right) + \beta_1 Q_{RT_j} + \beta_1(1-\beta_1)(1-\beta_2)^{N-2} Q_{RB_j}\right\} \\ \frac{dT_{j,bottom}}{dt} &= \frac{2}{\rho V C_p}\left\{\left(\frac{kA}{\Delta z}(T_{j,N-1} - T_{j,bottom})\right) + hA\left(T_{\infty bottom} - T_{j,bottom}\right) + \beta_1(1-\beta_1)(1-\beta_2)^{N-2} Q_{RT_j} + \beta_1 Q_{RB_j}\right\}\end{aligned} \tag{2.7}$$

the model for internal node $i$ of the $j^{th}$ zone the heating phase becomes,

$$\frac{dT_{j,i}}{dt} = \frac{1}{\rho V C_p}\left\{\left(\frac{kA}{\Delta z}(T_{j,i-1} - 2T_{j,i} + T_{j,i+1})\right) + \beta_2(1-\beta_1)\{(1-\beta_2)^{i-2} Q_{RT_j} + (1-\beta_2)^{N-2-i} Q_{RB_j}\}\right\} \tag{2.8}$$

where,

$$Q_{RT_j} = \sigma \varepsilon_{eff} A_h \left[\sum_{m=1}^{M}\left(\theta_m^4 - T_{j,top}^4\right) F_{mj}\right]$$

$$Q_{RB_j} = \sigma \varepsilon_{eff} A_h \left[\sum_{m=M+1}^{2M}\left(\theta_j^4 - T_{j,bottom}^4\right) F_{mj}\right]$$

## 2.4 Shortcomings of the existing model

The prediction of the output of the system for certain inputs, and hence the design of a controller, depends on the accuracy of the plant model. As heating phase is the first phase of the thermoforming process among all three different phases, an error in the prediction of the output temperature of the sheet will be followed by erroneous predictions of the subsequent phases of molding and cooling. If the controller is dependent on the model, such as a model reference adaptive controller or a model predictive controller, it becomes even more important to get an accurate model. The existing model has some shortcomings in defining oven air temperature as well as convection type of heat transfer. Moreover, it does not take into consideration other ways of heat transfer between heater and sheet.

### 2.4.1 Shortcomings in consideration of the heat source to heat the plastic sheet

According to the model developed by Moore, Ajersch and Gauthier [5, 11, 12], the way the sheet gets heated is as follows as shown in Fig. 2.5:

1. Heat radiation from the heater banks to the surface of the plastic sheet.
2. Heat conduction from the surface of the plastic sheet through its thickness.
3. Heat convection at the surface of the plastic sheet by oven air.
4. Absorption of the radiated heat throughout the plastic sheet thickness from the heater bank depending on the absorption coefficient of the plastic sheet.

This model is not complete as certain behaviors of the heating phase in the thermoforming machine cannot be explained by the model. It is observed that the sheet gets heated faster than is expected from the model [9, 11, 12]. Thus, there are some other forms of heat transfer happening in the sheet. As the increase in temperature occurs immediately after the sheet enters the oven and there is no delay in the transfer of heat, the extra heat gained is by radiation. So there must be some other heat source working as

a radiator to heat the sheet.

Walls are good reflectors of the heat waves generated from oven heaters. The heat emitted from the heaters is reflected by the oven wall towards the plastic sheet and it thus works as a heat source to heat the plastic sheet. Moreover, when a wall of the oven gets heated by the heaters, it works as another emitting source that heats the sheet. The walls get heated by the heaters and when a new sheet is placed in the oven, it gets heated not only by heaters, but also by the oven walls and hot air inside the oven, see Fig.2.6.

### 2.4.2 Shortcoming in convection heat transfer

Convection heat transfer is different from conduction as it happens between a surface and a fluid (stationary or moving) due to the difference in temperatures. In the developed model, the convection heat transfer coefficient is considered to be constant at the top and bottom surfaces of the plastic sheet, which cannot be true as it changes with roughness, geometric orientation, geometric area, fluid temperature, fluid density, fluid velocity etc. As convection heat transfer is due to cumulative motion of the fluid molecules that are moving across the surface of the solid, it largely depends on the geometric orientation of the heater which means a face up heater surface to the air passing above the surface should be different as compared to the convection heat transfer from a face down heater surface to the air passing below the surface. In the same way, the heat transferring from the sheet to the air at the top surface is higher than the heat transferring from the sheet at the bottom surface (when sheet temperature is higher than the air temperature and vice versa when sheet temperature is lower than the air temperature). Heat convection coefficient highly depends on the geometrical arrangement of the heater surface (face up, face down, perpendicular) and the heating medium as convection type heat transfer depends on the geometrical arrangement of the heater surface. Some researchers worked to calculate convection heat transfer coefficients for different geometrical areas and orientations of the heater surface [78,79,80]. So convection heat transfer coefficients for face up heaters, face down heaters, face up plastic sheet surface, face down plastic sheet surface, perpendicular oven walls will be different. They can be

calculated from different heat transfer research works that are already well established. There are also different kinds of convection heat transfer according to the nature of the flow: free or natural convection and forced convection.

### 2.4.3 Shortcoming in modeling of oven air temperature

Oven air temperature plays an important role in convection type of heating with both plastic sheet and heater. But this existing model excludes the modeling of the oven air temperature and it has no explanation about the heating process of the air. It cannot explain the relationship of the air temperature with the heaters and sheet temperature.

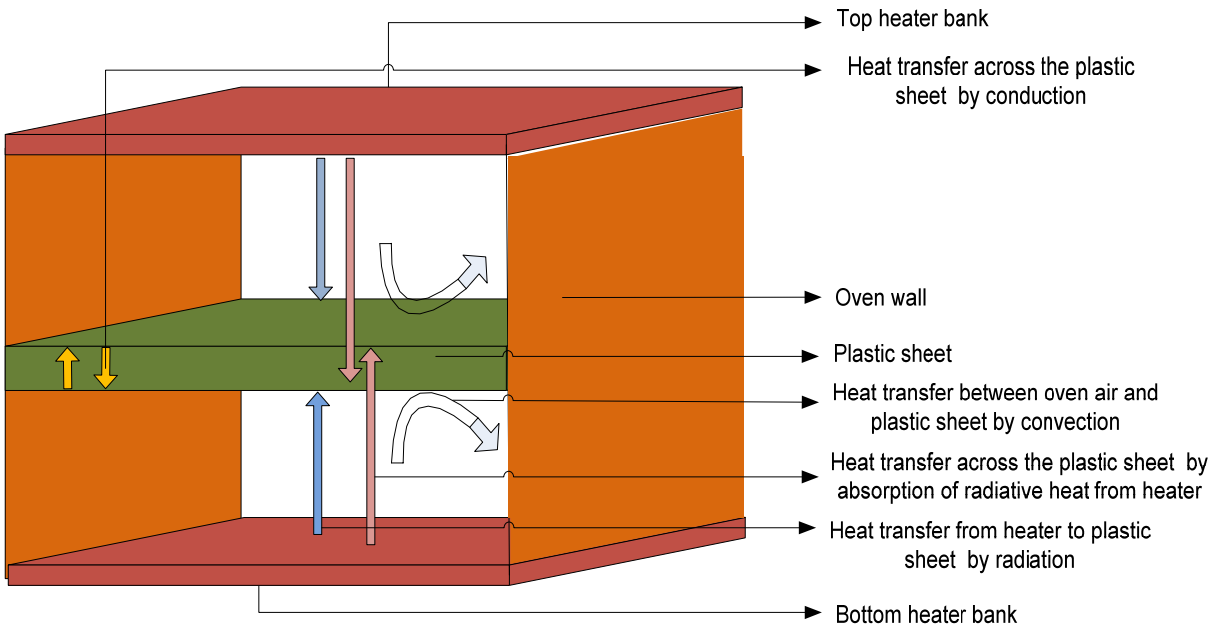


Fig. 2.5: Heat transfer in existing model of heating phase in thermoforming process

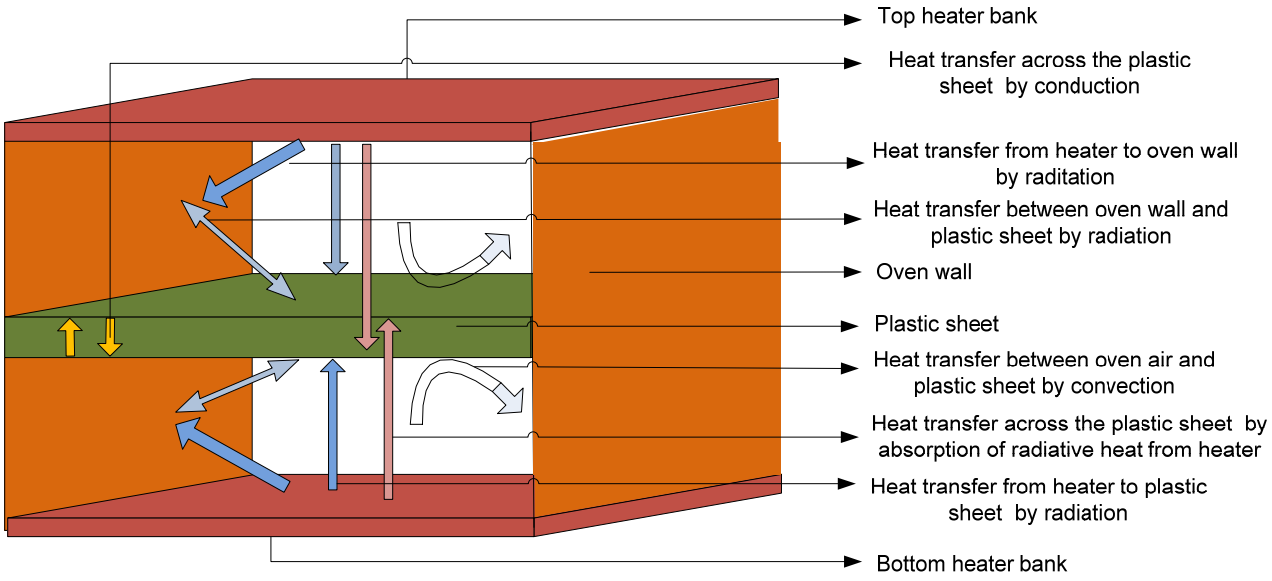


Fig. 2.6: Heat transfer in new model of heating phase in thermoforming process

### 2.4.4 Other shortcomings in the existing modeling

Certain parameters of heat transfer equations such as conduction coefficient, sheet density, sheet specific heat constant, heater emissivity, and sheet absorbtivity depend on process conditions and wavelength of the transmitted heat. In the present model, all those parameters are considered constant. A more accurate evaluation of the heat transfer parameters should be made to get a more accurate model. Another fact that cannot be explained using the present model is the experimental observation that the air and plastic sheet temperatures at the top surface of the sheet are higher than the air and sheet temperature at the bottom surface of the sheet [11]. One of the reasons behind this is the internal heat transfer due to air and heat flow between above the sheet and under the sheet.

## 2.5 Improvement of the modeling of sheet reheat phase

To predict the output of the heating process more accurately, the shortcomings

should be investigated and eliminated.

### 2.5.1 Improvement in heating process of the plastic sheet

Firstly, the radiative heat transfer from heater to the oven wall and oven wall to sheet surface are included in the model as shown in Fig. 2.6. The increase in oven wall temperature due to the radiative heat transfer between heater and oven wall can be expressed in the same way as discussed before as,

$$\frac{dT_{wall}}{dt} = \frac{2}{\rho_{wall} V_{wall} C_{p_{wall}}} \sigma \varepsilon_{eff_{wall}} A_h \left[ \sum_{m=1}^{M} \left( \theta_m^4 - T_{j,su}^4 \right) F_{mj} \right] \tag{2.9}$$

Where the view factor between each heater and each perpendicular oven wall can be calculated using the equation in (2.6). These walls will work as additional heating sources to heat the plastic sheet. The heat transfer between oven wall and sheet depends on the corresponding temperature. At the beginning of the cycle, when the entering sheet is at room temperature, it is heated by the hot oven wall and at the end of the cycle, when the sheet is already heated to a temperature that is higher than the oven wall, the heat energy will transfer from the sheet to the oven wall. So, depending on the temperature of the sheet and the oven wall, the corresponding radiative heat transfer equation will be included in the model. In this case, it is important to consider that the heat energy transmitted through the oven walls depends on the view factors of the oven walls with respect to the heaters as well as the view factors of the corresponding sheet zone with respect to the oven walls. The same relation can also be interpreted by considering the oven wall as the reflector of the emitted energy from the heater. The effect of the wall can be considered using a virtual heater in the opposite side of the wall as shown in Fig. 2.7. So we can apply the same relationship for heat radiation in equation (2.3) considering the reflection coefficient of the wall. As the wall is reflecting a portion of the heat energy it receives from the heater, the original equation should be multiplied by a reflection coefficient.

For a surface node,

$$\frac{dT_{j,top}}{dt} = \frac{2r_{coff}}{\rho V C_p}\left\{\beta_1 Q_{RT_j} + \beta_1(1-\beta_1)(1-\beta_2)^{N-2} Q_{RB_j}\right\}$$
$$\frac{dT_{j,bottom}}{dt} = \frac{2r_{coff}}{\rho V C_p}\left\{\beta_1(1-\beta_1)(1-\beta_2)^{N-2} Q_{RT_j} + \beta_1 Q_{RB_j}\right\}$$

For an internal node,

$$\frac{dT_{j,i}}{dt} = \frac{r_{coff}}{\rho V C_p}\left\{\beta_2(1-\beta_1)\{(1-\beta_2)^{i-2} Q_{RT_j} + (1-\beta_2)^{N-2-i} Q_{RB_j}\}\right\} \tag{2.10}$$

where,

$$Q_{RT_j} = \sigma \varepsilon_{eff} A_h \left[\sum_{m=1}^{M}\left(\theta_m^4 - T_{j,top}^4\right) F_{mj}'\right]$$
$$Q_{RB_j} = \sigma \varepsilon_{eff} A_h \left[\sum_{m=M+1}^{2M}\left(\theta_j^4 - T_{j,bottom}^4\right) F_{mj}'\right]$$

$F_{mj}'$ is the new view factor matrix with respect to the corresponding virtual heater and $r_{coff}$ is a reflection coefficient that can be determined using previous experimental data. Fresnel's equation describes the reflection and transmission of heat wave at an interface. It gives the reflection and transmission coefficient for wave parallel and perpendicular to the plane of incidence. It depends on the color and surface property of the wall. This method is considered for the rest of this chapter.

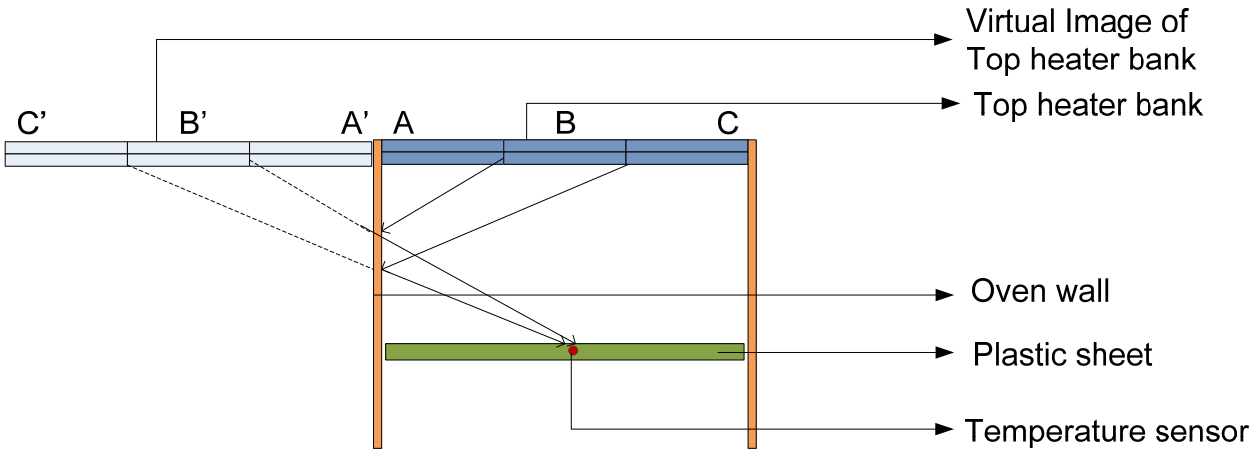


Fig.2.7: Radiated heat reflected through oven wall

### 2.5.2 Improvement in convection heating process

To theoretically evaluate the natural convective heat transfer coefficients, empirical equations are developed by the researcher [78,79,80]. These well-established equations can be used as follows:

$$Nu_L = \frac{hL}{k} = CRa_L^n \tag{2.11}$$

where $Nu_L$ is the average Nusselt number, $h$ is the heat transfer coefficient for convection, $k$ is the thermal conductivity of air**,** and $C$ and $n$ are constants. The Rayleigh number, defined as the product of Grashof number and Prandtl number, is based on the characteristic length $L$ of the geometry defined as follows:

$$Gr_L = \frac{g\beta(T_s - T_\infty)L^3}{v^2} \qquad \Pr = \frac{v}{\alpha} \qquad Ra_L = Gr_L \Pr = \frac{g\beta(T_s - T_\infty)L^3}{v\alpha}$$

Where $g$ is the local acceleration due to gravity, β is the thermal expansion coefficient, $T$ is the plate surface temperature, $T_\infty$ is the air temperature, $v$ is the kinematic viscosity and

$\alpha$ is the thermal diffusivity of air. To calculate the heat transfer coefficient for convection in case of a horizontal plate heater/cooler, the characteristic length $L$ can be defined as the ratio of the surface area to the perimeter [79],

$$L = \frac{A_s}{P}$$

As some physical properties are dependent on the temperature, it is recommended that all those parameters should be calculated in the arithmetic average temperature of plate and air. The following equations give the heat transfer coefficients for the facing down of a heated plate or the facing up of a cooled plate as proposed by McAdams [79]:

$$Nu_L = 0.27 Ra_L^{1/4} \qquad \text{for } 3\times10^5 \le Ra_L \le 3\times10^{10} \tag{2.12}$$

The heat transfer coefficient for the face up lower surface of a heated plate or the face down upper surface of a cooled plate is:

$$Nu_L = 0.54 Ra_L^{1/4} \qquad \text{for } 10^5 \le Ra_L \le 2\times10^7 \tag{2.13a}$$

$$Nu_L = 0.14 Ra_L^{1/3} \qquad \text{for } 2\times10^7 \le Ra_L \le 3\times10^{10} \tag{2.13b}$$

Churchill and Chu [80] proposed two relations as stated below to calculate the heat transfer coefficient for a vertical surface of a heated plate. To calculate the heat transfer coefficient with both laminar and turbulent flow:

$$Nu_m^{1/2} = 0.825 + \frac{0.387 Ra_L^{1/6}}{[1+(0.492/\mathrm{Pr})^{9/16}]^{8/27}} \quad \text{for } 10^{-1} < Ra_L < 10^{12} \tag{2.14}$$

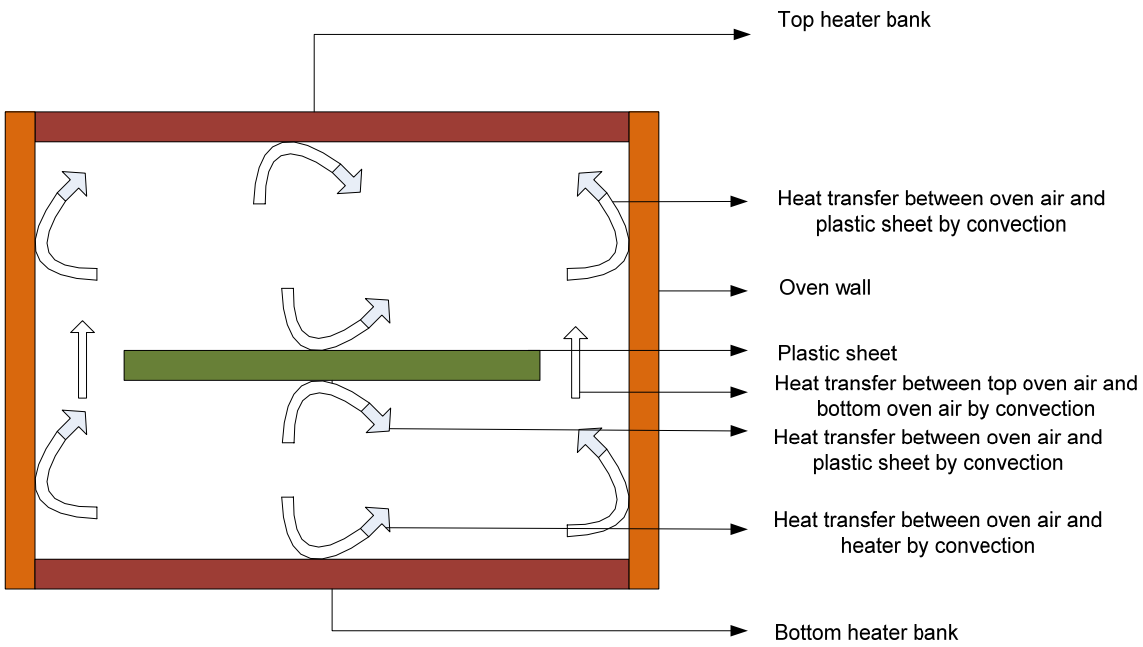


Fig. 2.8(a): Heat transfer to top and bottom oven air of heating phase in thermoforming process (front view)

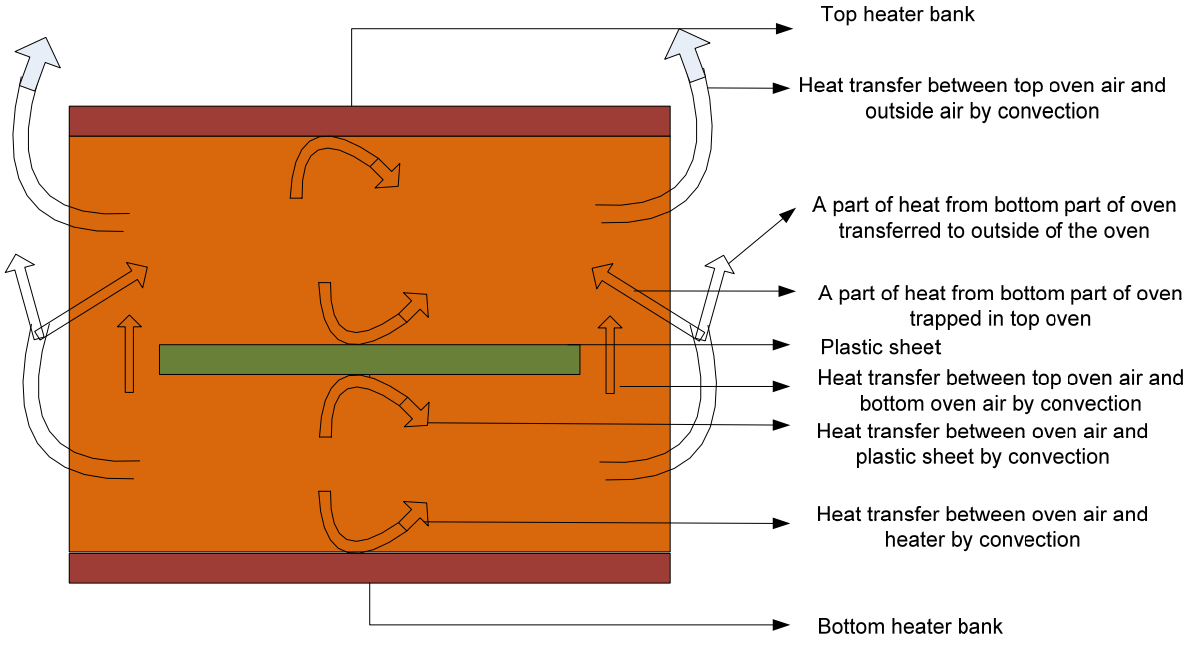


Fig. 2.8(b): Heat transfer to top and bottom oven air of heating phase in thermoforming process (cross sectional side view)

To calculate the heat transfer coefficient with only laminar flow:

$$Nu_m = 0.68 + \frac{0.67 Ra_L^{1/4}}{[1+(0.492/\mathrm{Pr})^{9/16}]^{4/9}} \qquad \text{for } 10^{-1} < Ra_L < 10^9 \tag{2.15}$$

Where Nusselt number, $Nu_m = \frac{h_m L}{k}$, $h_m$ is the mean heat transfer coefficient for convection and in case of vertical plate heater/cooler, the characteristic length $L$ can be defined as the height of the plate.

### 2.5.3 Modeling of oven air temperature in heating process

The heat transfer with the air inside the oven is of the following types as shown in Fig. 2.8 (a) and 2.8 (b):

1. Convection heat transfer between the air above the plastic sheet and face down heater at the top of the oven.
2. Convection heat transfer between the air below the plastic sheet and face up heater at the bottom of the oven.
3. Convection heat transfer between the air above the plastic sheet and face up top surface of the plastic sheet.
4. Convection heat transfer between the air below the plastic sheet and face down bottom surface of the plastic sheet.
5. Convection heat transfer between the air and the perpendicular wall surface in case of semi closed and closed oven.
6. Convection heat transfer between the air of the oven and the air temperature outside the oven.

The internal heat transfer within the oven if the sheet is smaller than the oven size can also be taken into consideration using convection heat transfer between the air above the sheet and the air below the sheet. If the sheet size is smaller than the size of the oven, hot air from the bottom part of the oven will pass to the top part of the oven due to a lower

density and gets trapped at the top surface of the oven. This increases the temperature of the air at the top and hence increases the sheet temperature at the top surface. In the case of semi-closed or open ovens, a percentage of the heat comes out due to convection heat transfer between the air of the oven and the air outside the oven. A part of the heat comes out from the bottom part of the oven, trapped again on its way to the top part of the oven and increases its temperature. The parameters of heat transfer equations like conduction coefficient of the sheet, sheet density, and sheet specific heat constant are dependent on the sheet temperature. These parameters for different sheet temperatures are usually available from the manufacturer and can be used by a least square method to establish a relationship between the sheet temperature and sheet conduction coefficient, sheet density, sheet specific heat constant.

## 2.6 Modeling of the actuator/heating element

The modeling of the actuator is important in order to completely know the behavior of the system. As the controller controls the process through actuators, control of a process becomes easier with a quick and powerful actuator. The actuator of the thermoforming process is weak and slow, therefore modeling of the actuator is necessary to get the relationship between control input and actuator output. Ajersch and Yang did some experiment to determine the maximum rate of heating and cooling to develop a model of the heater bank [11,81]. Although it can give some primary idea about the maximum heating and cooling rates, the heating and cooling rates that also depend on the operating condition of the system like the input power, the heat consumed by the sheet, the heat consumed by oven air and oven wall (that largely depends on sheet, oven air and oven wall temperature). The total energy transfer model of the heater, which relates electric energy input to the heater and temperature output of the heater, is shown in Fig.2.9. Since the maximum electrical power input to the heater is bounded, it is quite understandable that the maximum heating rate is bounded too. The boundaries of the maximum heating and cooling rates of the heater depend on the amount of heat transfer to the plastic sheet, oven wall by radiation and to oven air by convection. The heat energy emitted from the heater depends on the emissivity of the heater and the heat absorbing

material. The emissivity of a material is the ratio of energy radiated by the material to energy radiated by a black body at the same temperature. It is a measure of a material's ability to radiate absorbed energy. On the other hand, the energy radiated by the heater hitting at a material may be absorbed or reflected and depends on another crucial parameter which has a significant role in the material and is known as absorptivity of the material. The emissivity and absorptivity are properties of the material that depend on the wavelength of the radiated energy and temperature of the body [9]. So, the radiated energy from the heater as well as the absorbed energy by the sheet, air and the oven walls depend on the sheet temperature. In most of the cases, either these properties of the polymer material are not available from the manufacturer of the material, or consideration of these properties makes the model too complex to handle. However, Yousefi and al. did an experiment to measure effective emissivity using a thermoforming oven that consist of six ceramic heaters in [9]. They heated ABS sheet to measure emissivity within the operating range of the heater. They showed that the effective emissivity varied with the temperature within 0.765 to 0.79 and the relationship between them is linear. On the other hand, V. Kumar [7] and Howell, Siegel, Menguc [82] neglected the effect of sheet temperature and spectrum of the radiated heat on transmission, absorption and reflection of the radiated heat if the range of temperature variation is low (~150C). However, a constant value of emissivity and absorptivity is considered in the proposed model to keep it simple.

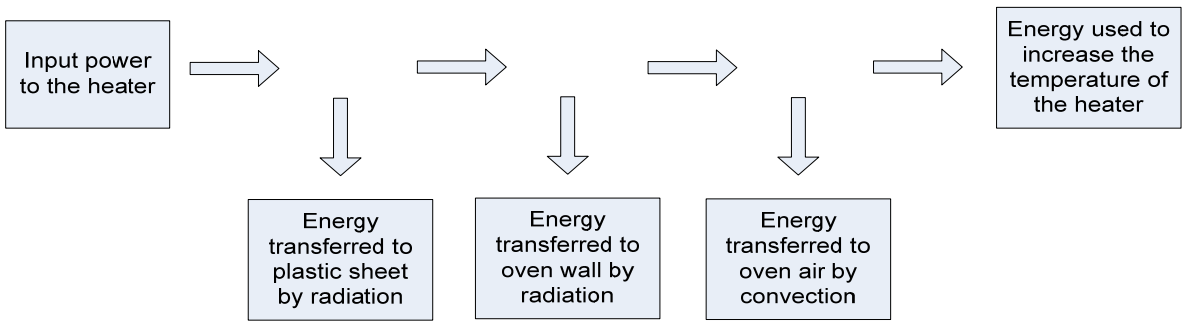


Fig. 2.9: energy transfer model in heater of thermoforming process

## 2.7 Experimental Set-up

The developed model of the heating phase of thermoforming machine is compared with real time data obtained using the AAA thermoforming machine, the same as in reference [9]. Both top and bottom heater banks are composed of 6 heating zones each. Each zone consists of 3 heating elements connected in parallel. A thermocouple is embedded in the central heating element of each heating zone to sense the temperature of the heater. In order to sense the surface temperature of the sheet, 7 infrared sensors (the Raytek thermalert MIC$^{tm}$) at the top and 5 infrared sensors at the bottom are installed in the machine. These sensors can measure the sheet temperature very quickly and accurately without direct contact. This type of infrared sensor must be operated within a certain ambient temperature range which is ensured by using an air cooled jacket around the sensor. The OPAL-RT RT-LAB software package is used in the real-time implementation. The software runs on a hardware package with command station, compilation node, target nodes, communication links and I/O boards. Two different PC workstations work as command station and target node. The command station uses windows 2000 as operating system to run the original software, generate code and control the parameters of the RT-LAB simulation whereas the target node uses QNX as its operating system for real-time implementation. The target node is used as the real-time processing computer for real-time execution of the simulation and communication with I/O devices. The target node first debugs the user's source code then compiles it in C code and finally loads it onto the target node. The I/O board is used to receive the IR sensors' outputs, thermocouple outputs and sends the set points of the heaters. The embedded thermocouples output is very low (in the range of milliVolts) and nonlinear which requires some signal conditioning before they are processed by the A/D. The controller outputs from the RT-LAB pass through the output board and go to solid-state relays for each zone. The solid-state relays will be on or off depending on the signal. When the relay switch is on it will allow the ac current to pass current through the heating element to heat it. On the other hand, if the switch is off, it will block the current. The total experimental set-up is shown in Fig.2.10.

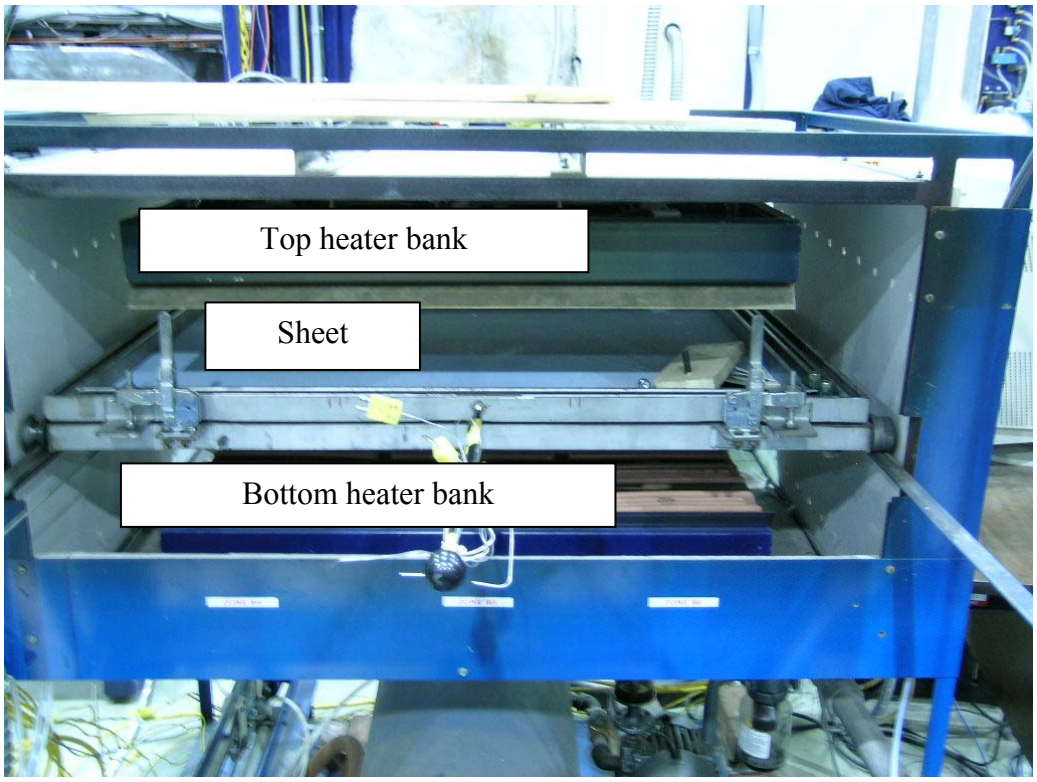


Fig.2.10: Experimental set-up of a Thermoforming oven

## 2.8 Comparison with experimental data

In this section, a comparison is made between the simulation results of the developed model for the AAA thermoforming machine and real-time data that was obtained with the same thermoforming machine used in reference [9]. All the real-time data used in this paper to compare the real-time data with simulation results were for only one cycle of the process with 500 seconds duration (from 9000 seconds to 9500 seconds). The oven is turned on a long time before the data is considered so that the data will be more reliable due to more uniform air temperature. In Fig. 2.11, real-time data of the upper and lower heater temperatures are compared with the corresponding simulation results for the heater set point of 180˚C in a single cycle of the process. The same inputs were provided for all the heaters in the top and bottom parts of the oven. The existing

model shows that the temperature of the heaters will be the same for both upper and lower heater for same input. But in the experimental data, it is found that the upper heaters attained a higher temperature than the lower heaters even for the same input. It is observed that the simulation results (solid lines) give values similar to the real-time data (points). In the following two figures the sheet temperature predicted at different points by the developed model are compared with the real-time values of the oven. The location of different points on the sheet that are used to compare the simulation and real time data is shown in Fig. 2.12. Shown in Fig. 2.13 and Fig. 2.14 are the sheet surface temperatures measured at these two different locations in the top surface and bottom surface within a cycle. The sheet is heated in open loop with all top and bottom heaters heated at 160C. The measured data are taken after a certain number of cycles. As expected, the sheet temperature at the center is higher than the temperature at corners. The temperature is decreasing towards the periphery of the sheet. This can be explained by the concept of view factor which are diminishing towards the corners. In Fig. 2.14, it is observed that the temperature at the bottom surface of the sheet is higher than the temperature at top surface of the sheet as the convection heating process is more active in the lower surface because of higher convection coefficient. It is observed that the developed model can predict experimental data satisfactorily, although there is a discrepancy in the case of the corner point of the sheet. The point is located closer to the outer part of the oven that can be cooled by the environment temperature. In the simulation model, it is assumed that the air inside the oven attained the same temperature which may be an inaccurate assumption in the case of a corner point. In Fig. 2.15, the predicted data for average air temperature between top heater and sheet as well as average air temperature between bottom heater and sheet is shown. As the air temperatures inside the oven were different at different point, the overall average temperature could not be computed using a real-time temperature sensor. So the real-time data could not be compared with this predicted data. The air temperature between sheet and bottom heater is higher than the air temperature between sheet and top heater. This can be explained by using convection heat transfer concept because convection heat transfer co-efficient is higher between bottom heater and air than top heater and air.

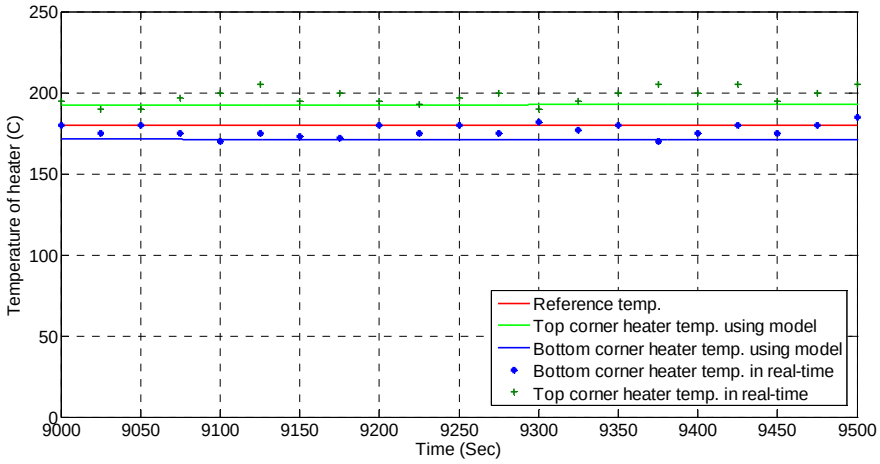


Fig.2.11: comparison of real-time top and bottom heater temperature with the corresponding simulated results.

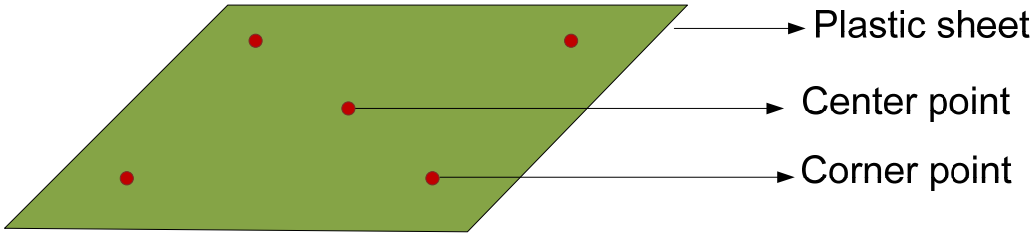


Fig.2.12: Corner and center point of the sheet

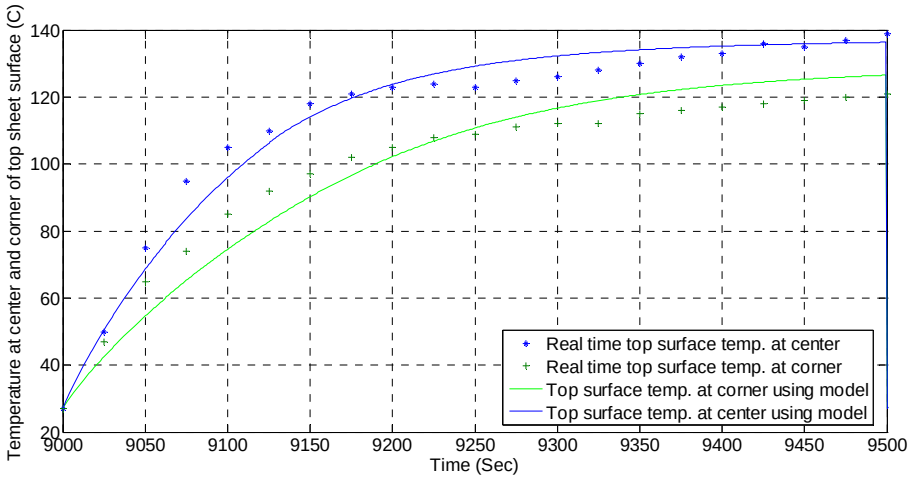


Fig.2.13: comparison of real-time sheet temperature at center and corner point of top surface of the sheet with the corresponding simulated results.

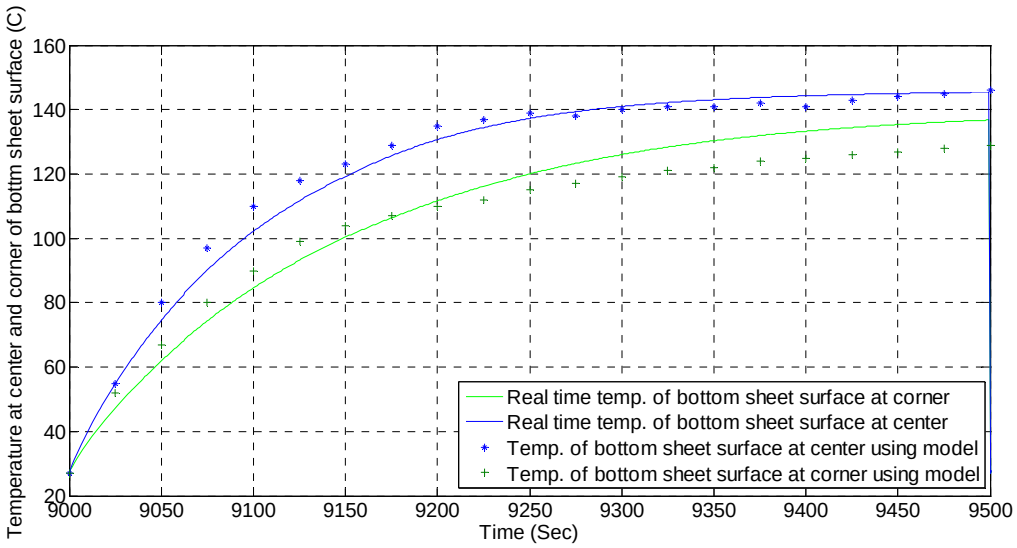


Fig.2.14: comparison of real-time temperature at center and corner point of bottom surface of the sheet with the corresponding simulated results.

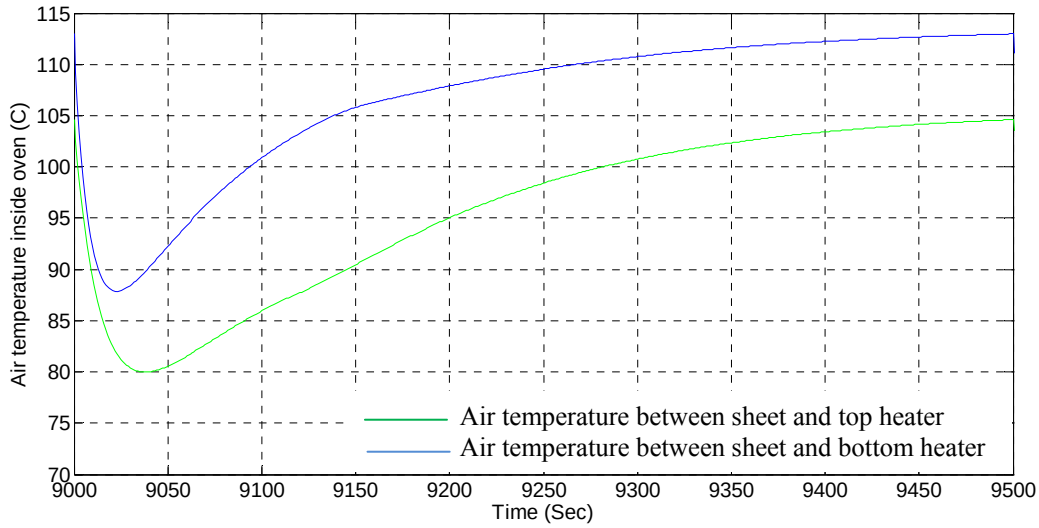


Fig.2.15: Average air temperature between sheet and top heater, average air temperature between sheet and bottom heater predicted from the model.

## 2.9 Conclusion

An experimental set-up has been developed in order to compare the simulation results of the developed model with experimental data. The comparisons of the result of the experiment show that the developed model can predict the experimental results reasonably well. These preliminary models can be extended considering the rapid deformation of the sheet during the heating process using finite element methods.

# Chapter 3

# Inverse Heating Problem in Thermoforming

## 3.1 Introduction

Finding the set-points of heater temperatures such that the sheet will achieve the desired temperature at the end of the heating cycle is known as the inverse heating problem (IHP) in thermoforming. Although the major part (50% to 80%) of the heat is transferred from the oven to the sheet by radiation, convection also has a significant (20% to 40%) contribution in sheet surface heating whereas conduction plays a significance role (10% to 50%) to heat the sheet through its thickness. This makes the inverse heating problem complex. In this chapter, a conjugate gradient method is used to solve the IHP in the control of sheet temperature. In the Conjugate Gradient method, all residual is orthogonal to every previous residuals as well as search direction and all new search direction is constructed to be orthogonal to every previous residual and search direction to ensure fastest convergence to the solution. Another major advantage of the conjugate gradient method is, it reduces space complexity and time complexity per iteration. So it is a good tool to solve linear and nonlinear equations [83, 84, 85, 86, 87, 88, 89, 90, 91, 92, 93]. This makes us to investigate the possibility of applying conjugate gradient methods in solving the IHP for thermoforming process. Thus, in this chapter, a method based on the conjugate gradient method is presented such that it can provide set-points temperature values for the heaters resulting in a specific temperature distribution in the plastic sheet after a predefined cycle time. In developing the method, computational cost is considered such that it can be implemented as a real-time algorithm in the controller.

## 3.2 Solving the direct heating problem

In this section, the direct heating problem is discussed and an algorithm is proposed to solve it. The main goal though is to solve the IHP, i.e., finding the correct heating element temperatures that, in a noise-free, perfect open-loop case, would produce the correct sheet temperature distribution. In such an inverse problem, one seeks to determine the appropriate input to obtain a predetermined result, whereas in the direct problem, one calculates the output resulting from the application of a certain input, which is typically easier. But in an iterative method for solving the IHP, the direct problem has to be solved at every iteration. The detailed algorithm solving the direct heating problem is presented in Fig. 3.1. The solution of the direct heating problem depends on the initial temperature of the sheet, the cycle time, and the boundary conditions. Using the geometric configuration of the sheet and heaters and the physical and mechanical properties of the plastic, all parameters of the model equation can be calculated. Then, the differential equations can be solved using a finite difference method with forward difference approximation considering the final temperature of each step as the initial temperature for the next step. The effect of changing the geometric configuration of the sheet and heating elements due to changes in temperature may be neglected, unless the processor is fast enough to take into account such changes. For example, sheet sag could be modeled. However, a consequence of changes in the geometry of the heating problem due to sheet sag is that the view factor matrix has to be updated at every sampling time. To incorporate the physical change into the direct problem solution, one can use the model equation from [11]. The geometric shape of the heater is also changed with heating element temperature.

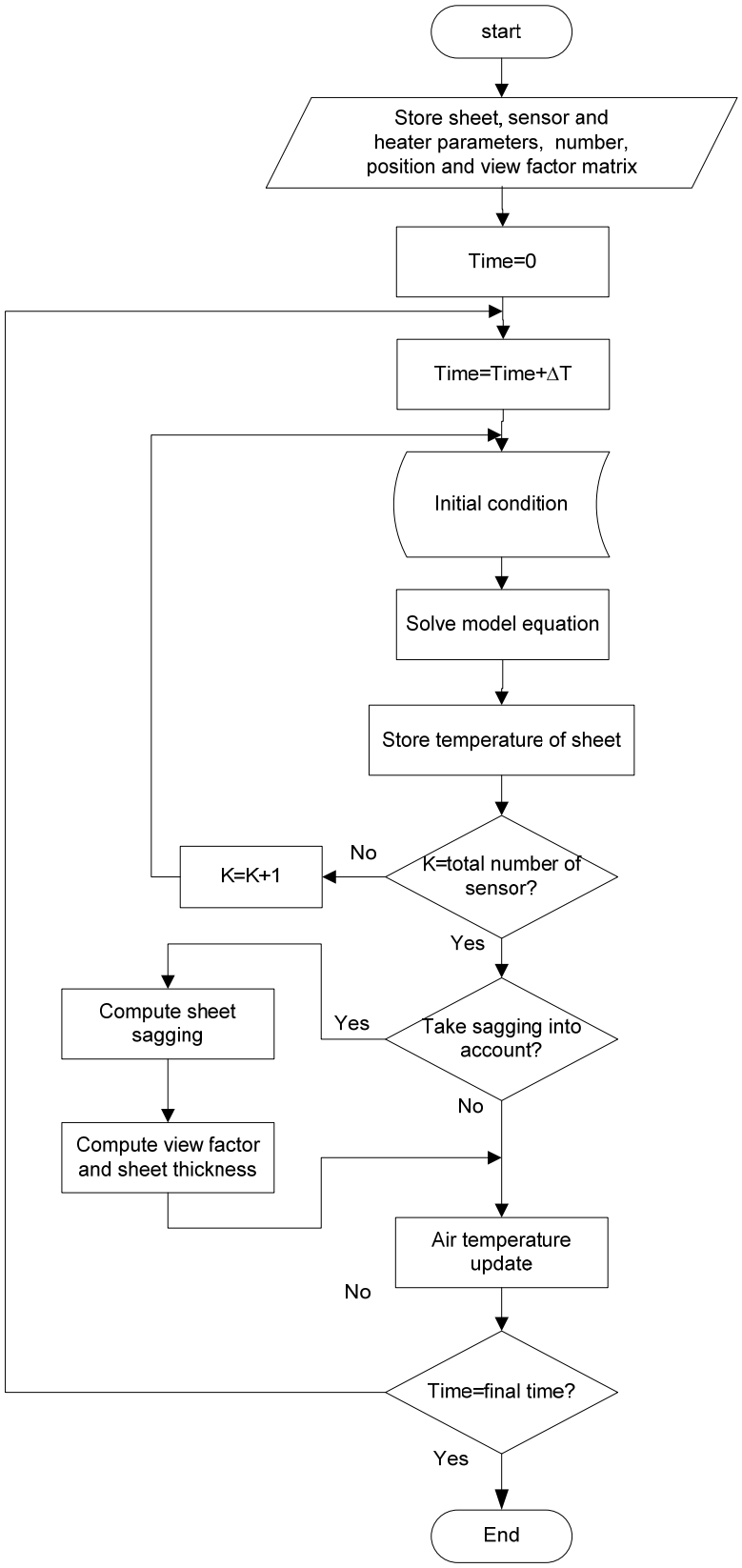


Fig.3.1: Algorithm for solving direct heating problem

## 3.3 Solution of inverse heating problem

The pseudo-inverse approach is a computationally efficient technique that can be used to solve the underdetermined IHP, namely to determine the heater set points that will heat the plastic sheet to the specified temperature at the end of the heating cycle. As radiation is the fastest and dominant way of heating the sheet, the pseudo-inverse of the view factor matrix has been proposed for solving the IHP [11]. The view factor matrix is the matrix whose entries represent view factors from the heaters to a point on the sheet.

As the behavior of the solution of inverse heating problem changes with change of initial condition and the system very low sensitive to input, it cannot be solved as easily as a direct heating problem. As the sensitivity of a sheet zone temperature to each individual heater is very low, a large change in heater temperature causes a small change in sheet temperature. Because of this “weakness” of the actuator, the control of the heating phase, hence the solution of IHP is difficult. It may be numerically unstable (even though it is not unstable physically) which means that the behavior of the solution changes so much that the error in the solution can be magnified and can grow exponentially instead of damped.

Since the IHP is difficult to solve as compared to the direct heating problem, a promising approach is developed to solve the IHP based on iteratively solving the direct heating problem to get more accurate results in every iteration. In the proposed technique, a conjugate gradient method of optimization is used which is a straightforward and powerful iterative technique for solving linear and nonlinear inverse problems. In this iterative method, a suitable step size is taken along a direction of descent to minimize the difference between the model output and desired temperatures as defined by objective function. The direction is obtained as a linear combination of the negative gradient direction at the current iteration and the previous direction of descent. Hence, the method not only minimizes the objective function along a negative gradient, it also minimizes the

objective function along all previous directions. The proposed algorithm for solving the IHP of the heating phase in thermoforming is described below.

Let us consider the desired temperature distribution at sensor points on the sheet after $t_1$ seconds to be $T_s = [T_{s1} \quad T_{s2} \quad \cdots \quad T_{sZ}]^T$. The temperatures obtained according to the model after $t_1$ seconds at the same sensor points on the sheet are $T_i = [T_{i1} \quad T_{i2} \quad \cdots \quad T_{iZ}]^T$ and an initial guess of the temperatures $T_{s(initial)}$ is taken as the current temperature of the sheet at different point. The heater temperatures are denoted as, $\theta = [\theta_1 \quad \theta_2 \quad ..... \quad \theta_M]^T$. The heater temperature is considered as the current temperature for the first iteration. The superscript $k$ used in this algorithm indicates the $k^{\text{th}}$ iteration. Starting with $\theta_0 = [\theta_{01} \quad \theta_{02} \quad ..... \quad \theta_{0M}]^T$ we search for the solution and in each iteration we need a function to tell us whether we are closer to the solution that is unknown to us. So if the function becomes smaller in an iteration it means that we are closer to solution considering that the objective function and the constraints in $\theta$ are convex. This function is called here objective function. The objective function for minimizing the difference between the model output and desired temperatures is selected as,

$$R = \left(T_s - T_i\right)^T \left(T_s - T_i\right) \tag{3.1}$$

*Step 1:* As a first step, the direct heat transfer problem of the model is computed for $t_1$ seconds to obtain $T_i$ by using the initial guess of the sensor temperatures and heater temperatures obtained in the previous iteration to estimate the sheet. Plastic sheet temperature can be calculated easily for known heater temperature using the model equation. The algorithm for solving the direct heating problem has already been discussed in the previous section. Some simplifications on the model equations can be considered to reduce the burden of computation.

*Step 2:* Calculate the objective function in (3.1) with the solution that was obtained from Step 1. Conjugate gradient method will actually try to compute heater temperature to

minimize this objective function. The magnitude of the objective function is compared to the prescribed error margin $\varepsilon$ and the iterative procedure is stopped when

$$R^{k+1} = \left(T_s - T_i^{k+1}\right)^T \left(T_s - T_i^{k+1}\right) < \varepsilon \tag{3.2}$$

Where $\varepsilon$ is the error margin. The error margin should be selected such that it will be achievable for that particular thermoforming oven.

*Step 3:* Compute the sensitivity matrix. The sensitivity matrix is a matrix whose entry $(i, j)$ represents the sensitivity of the temperature of sensor $i$ to heating element $j$. Each entry of the sensitivity matrix can thus be expressed as

$$S_{ij} = \frac{\partial T_i}{\partial \theta_j}.$$

$$S = \begin{bmatrix} \frac{\partial T_{i1}}{\partial \theta_1} & \frac{\partial T_{i1}}{\partial \theta_2} & .... & \frac{\partial T_{i1}}{\partial \theta_M} \\ \frac{\partial T_{i2}}{\partial \theta_1} & \frac{\partial T_{i2}}{\partial \theta_2} & .... & \frac{\partial T_{i2}}{\partial \theta_M} \\ : & : & & : \\ \frac{\partial T_{iZ}}{\partial \theta_1} & \frac{\partial T_{iZ}}{\partial \theta_2} & .... & \frac{\partial T_{iZ}}{\partial \theta_M} \end{bmatrix} \tag{3.3}$$

The sensitivity matrix plays a significant role in the convergence to a stable solution. If the change of temperature in a particular sensor is very low following a change in a heater's temperature, then the corresponding entry of the sensitivity matrix must be small. The computation of the sensitivity matrix is also complex and costly. As the conjugate gradient method will converge with the inexact search direction with some conditions (these conditions will be discussed in Section 3.5), a compromise can be made between computational burden for sensitivity matrix and exact search direction. Thus, a simplified procedure of calculating the sensitivity matrix will be presented in the next section.

*Step 4:* The gradient direction of the objective function is a vector pointing in the direction of the steepest slope of the function at that point. The gradient direction of the objective function can be calculated by differentiating equation (3.1) with respect to heater temperatures,

$$\nabla R^k = -2(S^k)^T \left(T_s - T_i^k\right) \tag{3.4}$$

*Step 5:* Conjugate gradient method combines the advantages of steepest descent method and conjugate direction method. Its search directions combine both gradient and conjugate part. The coefficient of conjugate part of search directions is known as conjugate coefficient. Conjugate coefficient $\gamma^k$ can be calculated in a few ways. Researchers worked on developing different ways to calculate the conjugate coefficient considering the convergence, number of iteration for solution and computational burden. The Fletcher-Reeves technique suggests the following expression for the method in [86,87],

$$\gamma^k(FR) = \frac{\sum_{j=1}^{M} \left[\nabla R^k\right]_j^2}{\sum_{j=1}^{M} \left[\nabla R^{k-1}\right]_j^2} \qquad \text{for } k = 1,2,3,...$$

$$\gamma^0(FR) = 0 \tag{3.5}$$

The Polak-Ribiere expression proposes another value for the conjugate gradient method [94],

$$\gamma^k(PR) = \frac{\sum_{j=1}^{M} \left\{ \left[ \nabla R^k \right]_j \left[ \nabla R^k - \nabla R^{k-1} \right]_j \right\}}{\sum_{j=1}^{M} \left[ \nabla R^{k-1} \right]_j^{\,2}} \qquad \text{for } k = 1,2,3,...$$

$$\gamma^0(PR) = 0 \tag{3.6}$$

The Hestenes-Stiefel expression to calculate conjugate coefficient is [89],

$$\gamma^k(HS) = \frac{\sum_{j=1}^{M} \left\{ \left[ \nabla R^k \right]_j \left[ \nabla R^k - \nabla R^{k-1} \right]_j \right\}}{\sum_{j=1}^{M} \left\{ \left[ \nabla R^{k-1} \right]_j \left[ \nabla R^k - \nabla R^{k-1} \right]_j \right\}} \qquad \text{for } k = 1,2,3,.....$$

$$\gamma^0(HS) = 0 \tag{3.7}$$

In the proposed method, we will use a modified Polak-Ribiere expression as it does not only give an accurate line search due its efficiency; it also tends to reset the search direction when needed to speed up the convergence. The modified Polak-Ribiere expression is:

$$\gamma^k = \gamma^k(PR) \qquad if\ \gamma^k(PR) > 0$$

$$\gamma^k = 0 \qquad if\ \gamma^k(PR) < 0 \tag{3.8}$$

*Step 6:* The direction of descent is computed in this step. The direction of descent is the linear combination of the gradient direction of the objective function and the direction of descent of the previous iteration which can be expressed as,

$$d^k = -\nabla R^k + \gamma^k d^{k-1} \tag{3.9}$$

*Step 7:* The step size $\beta^k$ along this direction can be computed in such a way that the new estimated values of the heating element temperatures will minimize the objective function in the direction of descent.

$$\min_{\beta^k} R^{k+1} = \min_{\beta^k} \left(T_s - T_i^{k+1}\right)^T \left(T_s - T_i^{k+1}\right) \tag{3.10}$$

By expanding $T_i^{k+1}$ with a Taylor series expansion,

$$T_i^{k+1} = T_i^k + \frac{\partial T_i^k}{\partial \theta^k}\left[\theta^{k+1} - \theta^k\right] + \frac{1}{2}\frac{\partial^2 T_i^k}{\partial^2 \theta^k}\left[\theta^{k+1} - \theta^k\right]^2 + \ldots$$

Neglecting the higher order terms and replacing the value of $\left[\theta^{k+1} - \theta^k\right]$ that we will get in the next step,

$$T_i^{k+1} = T_i^k + S^k \beta^k d^k$$

Substituting the value into equation (3.10),

$$\min_{\beta^k} R^{k+1} = \min_{\beta^k} \left(T_s - T_i^k - S^k \beta^k d^k\right)^T \left(T_s - T_i^k - S^k \beta^k d^k\right)$$

To solve the optimization problem with respect to $\beta^k$, we differentiate the equation with respect to $\beta^k$ and equate it to zero,

$$\left(T_s - T_i^k - S^k \beta^k d^k\right)^T \left(-S^k d^k\right) + \left(-S^k d^k\right)^T \left(T_s - T_i^k - S^k \beta^k d^k\right) = 0$$

With algebraic calculation, the following expression for step size can be obtained:

$$\beta^k = \frac{\left[S^k d^k\right]^T \left[T_i^k - T_s\right]}{\left[S^k d^k\right]^T \left[S^k d^k\right]} \tag{3.11}$$

*Step 8:* Compute the new estimate of heating element temperature by,

$$\theta^{k+1} = \theta^k + \beta^k d^k \tag{3.12}$$

*Step 9:* Increase the iteration index by 1 and return to Step 1 for the next iteration.
The whole algorithm is shown in Fig.3.2.

## 3.4 Sensitivity matrix calculation

There are some problems that could arise in the convergence of the proposed gradient method of the inverse heating problem. The proposed technique requires computing a sensitivity matrix at every iteration to calculate the set points of the heaters. It is unreasonable to calculate a sensitivity matrix for a nonlinear system at every operating point. The sensitivity matrix plays an important role in computing a solution of the inverse heating problem. It measures the sensitivity of the sheet temperature at a certain point with respect to a change of heater temperature. For the heating phase of the thermoforming process, entries of the sensitivity matrix are very small so that the convergence rate to a solution becomes very slow. In other words, the sensitivity matrix for the heating phase is ill-conditioned. Generally speaking, large entries in the sensitivity matrix are desirable for estimation of the heater temperature, which can be done by properly locating the sensors. The sensitivity changes dramatically with the change of the operating point of the system because of the nonlinearity of the process. If the sensitivity matrix is inaccurate, the proposed method may take a longer time to converge or may not even converge at all.

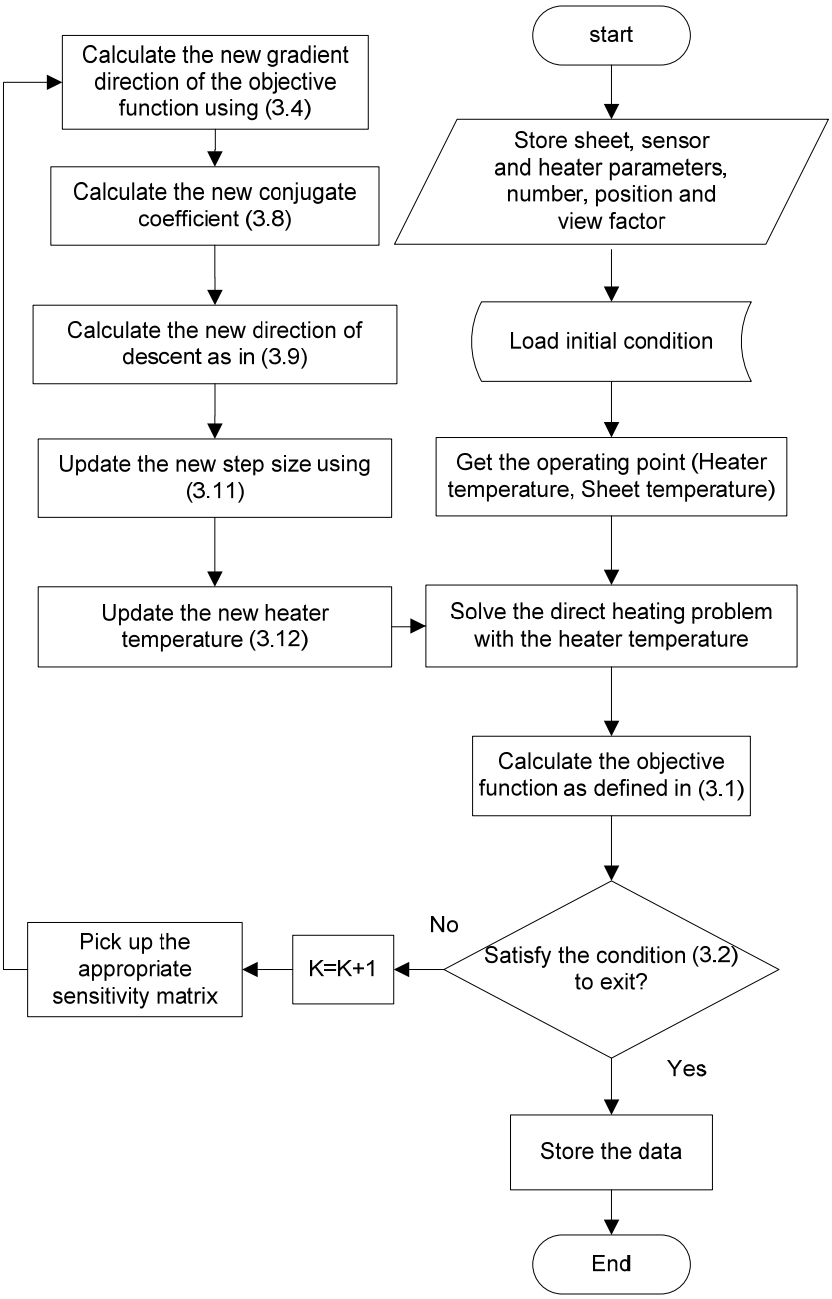


Fig.3.2: Algorithm for solving inverse heating problem.

The actuators and the system are very slow and the rate of change of heating temperature is bounded by its maximum and minimum limits [9]. Moreover, these limits are as low as a few degrees Celsius per second. Therefore, the system states change slowly with a change of system inputs, and the system can be considered to be linear if the sampling period is short enough. So, the linearized model that is nearest to the current operating point can be used for solving the inverse heating problem (instead of computing sensitivity matrix at each operating point) to reduce the computational burden significantly. Considering only one layer over the width of the sheet, the linearized model for k-th zone of the nonlinear model around the operating point $(U^*, X_k^*) = (\theta^*, T_k^*)$ can be expressed as:

$$\Delta \dot{X}_k = A_k \Delta X_k + B_k \Delta U$$

$$\Delta Y_k = C_k \Delta X_k$$

Where, $A_k \in \mathbb{R}^{n_k \times n_k}$, $B_k \in \mathbb{R}^{n_k \times m}$, $C_k \in \mathbb{R}^{p_k \times n_k}$. As we consider only one layer, the value of $n_k$ is 2. But the plant has $Z$ number of zones and the linear system equations for all those zones are strongly coupled with each other. Considering all the zone equations together, the process linear equation becomes,

$$\Delta \dot{X} = A\Delta X + B\Delta U$$

$$\Delta Y = C\Delta X \tag{3.13}$$

Where, $A \in \mathbb{R}^{n \times n}$, $B \in \mathbb{R}^{n \times m}$, $C \in \mathbb{R}^{p \times n}$,

and $n = Zn_k$, $p = Zp_k$

Based on the developed linearized model the proposed method can be modified to overcome the drawbacks already specified at the beginning of the section. The first drawback concerning computation will be significantly reduced due to the use of a linearized system model and the number of iterations needed to converge to a solution will be reduced. The output of a linear system can be obtained using the following equation:

$$y(t) = \int_0^t Ce^{A(t-\tau)} Bu(\tau) d\tau + Du(t) \tag{3.14}$$

Where $y(t) = \begin{bmatrix} y_1(t) & y_2(t) & y_3(t) & \dots & y_p(t) \end{bmatrix}^T$,

$$u(t) = \begin{bmatrix} u_1(t) & u_2(t) & u_3(t) & \dots & u_m(t) \end{bmatrix}^T$$

To calculate the sensitivity matrix, we give a unit step input at each input node and measure the change in output due to that unit change in input. Let us consider a unit step change in the input $u_1(t)$ to the system while other inputs remain the same. The difference between system output with a unit step increase in the input $(u_1(t)+1)$ and system output with same input $u_1(t)$ after time $t$ is,

$$\Delta y(t)\,|_{u_1(t)} = \int_0^t Ce^{A(t-\tau)}B \begin{bmatrix} u_1(\tau)+1 \\ u_2(\tau) \\ \cdot \\ \cdot \\ \cdot \\ u_m(\tau) \end{bmatrix} d\tau + D \begin{bmatrix} u_1(\tau)+1 \\ u_2(\tau) \\ \cdot \\ \cdot \\ \cdot \\ u_m(\tau) \end{bmatrix} - \int_0^t Ce^{A(t-\tau)}B \begin{bmatrix} u_1(\tau) \\ u_2(\tau) \\ \cdot \\ \cdot \\ \cdot \\ u_m(\tau) \end{bmatrix} d\tau - D \begin{bmatrix} u_1(\tau) \\ u_2(\tau) \\ \cdot \\ \cdot \\ \cdot \\ u_m(\tau) \end{bmatrix}$$

$$\Delta y(t)\,|_{u_1(t)} = \int_0^t Ce^{A(t-\tau)}B \begin{bmatrix} 1 \\ 0 \\ \cdot \\ \cdot \\ \cdot \\ 0 \end{bmatrix} d\tau + D \begin{bmatrix} 1 \\ 0 \\ \cdot \\ \cdot \\ \cdot \\ 0 \end{bmatrix} \qquad (3.15)$$

In the same way, for a unit step change in the input $u_2(t)$ to the system with other inputs staying at same, the difference between system output after time $t$ is,

$$\Delta y(t)\,|_{u_2(t)} = \int_0^t Ce^{A(t-\tau)}B\begin{bmatrix} u_1(\tau) \\ u_2(\tau)+1 \\ \cdot \\ \cdot \\ \cdot \\ u_m(\tau) \end{bmatrix} d\tau + D\begin{bmatrix} u_1(\tau) \\ u_2(\tau)+1 \\ \cdot \\ \cdot \\ \cdot \\ u_m(\tau) \end{bmatrix} - \int_0^t Ce^{A(t-\tau)}B\begin{bmatrix} u_1(\tau) \\ u_2(\tau) \\ \cdot \\ \cdot \\ \cdot \\ u_m(\tau) \end{bmatrix} d\tau - D\begin{bmatrix} u_1(\tau) \\ u_2(\tau) \\ \cdot \\ \cdot \\ \cdot \\ u_m(\tau) \end{bmatrix}$$

$$\Delta y(t)\,|_{u_2(t)} = \int_0^t Ce^{A(t-\tau)}B\begin{bmatrix} 0 \\ 1 \\ \cdot \\ \cdot \\ \cdot \\ 0 \end{bmatrix} d\tau + D\begin{bmatrix} 0 \\ 1 \\ \cdot \\ \cdot \\ \cdot \\ 0 \end{bmatrix},$$

…

$$\Delta y(t)\,|_{u_m(t)} = \int_0^t Ce^{A(t-\tau)}B\begin{bmatrix} 0 \\ 0 \\ \cdot \\ \cdot \\ \cdot \\ 1 \end{bmatrix} d\tau + D\begin{bmatrix} 0 \\ 0 \\ \cdot \\ \cdot \\ \cdot \\ 1 \end{bmatrix}$$

According to the definition of sensitivity matrix,

$$S = \begin{bmatrix} \frac{\partial y_1}{\partial u_1} & \frac{\partial y_1}{\partial u_2} & \cdots & \frac{\partial y_1}{\partial u_M} \\ \frac{\partial y_2}{\partial u_1} & \frac{\partial y_2}{\partial u_2} & \cdots & \frac{\partial y_2}{\partial u_M} \\ \vdots & \vdots & & \vdots \\ \frac{\partial y_p}{\partial u_1} & \frac{\partial y_p}{\partial u_2} & \cdots & \frac{\partial y_p}{\partial u_M} \end{bmatrix} \approx \begin{bmatrix} \Delta y(t)\,|_{u_1(t)} & \Delta y(t)\,|_{u_2(t)} & \cdots & \Delta y(t)\,|_{u_m(t)} \end{bmatrix}$$

$$S \approx \int_0^t Ce^{A(t-\tau)}B \begin{bmatrix} 1 & 0 & \dots & 0 \\ 0 & 1 & \dots & 0 \\ . & . & \dots & . \\ . & . & \dots & . \\ . & . & \dots & . \\ 0 & 0 & \dots & 1 \end{bmatrix} d\tau + D \begin{bmatrix} 1 & 0 & \dots & 0 \\ 0 & 1 & \dots & 0 \\ . & . & \dots & . \\ . & . & \dots & . \\ . & . & \dots & . \\ 0 & 0 & \dots & 1 \end{bmatrix} = \int_0^t (Ce^{A(t-\tau)}B)d\tau + D$$

Hence, the sensitivity matrix is:

$$S \approx Ce^{At} \int_0^t e^{-A\tau} B d\tau + D$$

$$S \approx Ce^{At}[A^{-1}B - A^{-1}e^{-At}B] + D$$

$$S \approx Ce^{At}A^{-1}B - CA^{-1}B + D \tag{3.16}$$

From equation (3.16), it can be concluded that the sensitivity matrix is time dependent and it is changing with time along the cycle time. This matrix needs to be computed at every sampling time. Since this sensitivity matrix will be computed based on the linear system at the current operating point, it is accurate as long as the linear system equation is accurate for the concerned nonlinear system.

The value of the sensitivity matrix has to be computed at every operating point online using equation (3.16) in order to compute a solution to the inverse heating problem. It could be computationally expensive for a slow processor. Thus, the sensitivity matrix can be computed offline at certain operating points, which can later be used online depending on the operating points of the heaters. There are different methods available for the computation of the sensitivity matrix but a popular method is based on the forward difference approximation. Thus, the forward difference equation can be used instead of the derivative in (3.16).

$$S_{ij} = \frac{T_{i(cycle\_time\_t)} - T_{i(ss\_temp)}}{\Delta\theta_j} \tag{3.17}$$

where $S_{ij}$ is the entry in the $i^{\text{th}}$ row and $j^{\text{th}}$ column, $T_{i(cycle\_time\_t)}$ is the temperature of the $i^{\text{th}}$ sensor after cycle time $t$, $T_{i(ss\_temp)}$ is the steady-state temperature of the $i^{\text{th}}$ sensor before applying the step change of temperature at heater $j$ and $\Delta\theta_j$ is the magnitude of the step change in temperature of the $j^{\text{th}}$ heater.

## 3.5 Convergence of the proposed method

Some researchers [85,89,91,93,95,96,97,99] worked to prove the convergence of the conjugate gradient method. Polak and Ribiere, Powell, Zoutendijk, Al-Baali, Gilbert and Nocedal gave some global convergence results. The purpose of this section is to review the condition of convergence in the case of exact and inexact sensitivity matrix for the thermoforming process. We analyze convergence using the results of [99] for this particular thermoforming process mainly when the sensitivity matrix is not accurate. Interested readers can see the detailed proofs and analysis in [91,93,95,96,97,99].

Let us denote the starting point by $\theta_1$ and define change in inputs as $\Delta\theta_k := \theta_{k+1} - \theta_k = \beta^k d^k$. We also define a function that will be the gradient of objective function i.e. $gr^k = \nabla R^k$. The direction of descent is defined as $d_k$ when $\langle gr^k, d_k \rangle < 0$. Let $\alpha_k$ be defined as the angle between $-\nabla R^k$ and $d_k$. So the angle $\alpha_k$ can be easily calculated by using vector laws:

$$\cos\alpha_k = \frac{\langle \nabla R^k, d_k \rangle}{\| \nabla R^k \| \| d_k \|} = -\frac{\langle gr^k, d_k \rangle}{\| gr^k \| \| d_k \|} \tag{3.18}$$

Interested readers can find detailed derivation for conjugate coefficient of the conjugate gradient methods as given in equation (3.5)-(3.7) and discussion of some of their properties in Gill, Murray, and Wright [90] and Fletcher [87].

*Assumptions 3.1:*

*(i) The level set* $L := \{\Theta: f(\Theta) \leq f(\Theta_1)\}$ *is bounded.*

*(ii) In some neighborhood* $N$ *of* $L$*, the objective function* $f: R^m \to R$ *is continuously differentiable, and its gradient is Lipschitz continuous, i.e., there exists a constant* $C > 0$ *such that*

$$\| gr^k(\theta) - gr^k(\tilde{\theta}) \| \leq C \| \theta - \tilde{\theta} \|, \text{ for all } \theta, \tilde{\theta} \in N \quad . \tag{3.19}$$

Note that these statements imply that there is a constant $\overline{p}$, such that

$$\| gr^k(\theta) \| \leq \overline{p}, \text{ for all } \Theta \in L . \tag{3.20}$$

At first, we will turn our attention to the line search. As studied by Wolfe [91,93], one efficient way consists in accepting a positive step-length $\beta^k$ if it satisfies the two conditions known as Wolfe conditions:

$$f(\theta_k + \beta^k d^k) \leq f(\theta_k) + \sigma_1 \beta^k \langle gr^k, d^k \rangle \tag{3.21}$$

$$\langle gr(\theta_k + \beta^k d^k), d^k \rangle \geq \sigma_2 \langle gr^k, d^k \rangle \tag{3.22}$$

where $0 < \sigma_1 < \sigma_2 < 1$. We now introduce the so-called ideal line search condition. A positive step-length $\beta^k$ is accepted if

$$f(\theta_k + \beta^k d^k) \leq f(\theta_k + \hat{\beta}^k d^k) \tag{3.23}$$

$$f(\theta_k + \beta^k d^k) \leq f(\theta_k + \hat{\beta}^k d^k) \tag{3.23}$$

where $\hat{\beta}^k$ is the smallest positive stationary point of the function $\xi_k(\beta) := f(\theta_k + \beta d^k)$ . Assumption 3.1 confirms that $\hat{\beta}^k$ exists. Note that both the first local minimizer and the global minimizer of $f$ along the search direction satisfy (3.23).

Any of the line search strategies is sufficient to establish the following very useful result.

*THEOREM 3.1*

*Suppose that Assumption 3.1 holds, and consider any iteration of the form (3.12). where $d^k$ is a descent direction and $\beta^k$ satisfies one of the following line search conditions:*
*(i) the Wolfe conditions (3.21)-(3.22), or*
*(ii) the ideal line search condition (3.23).*
*Then,*

$$\sum_{k \geq 1} \cos^2 \alpha_k \, \| gr^k \|^2 < \infty \tag{3.24}$$

This result was essentially proved by Zoutendijk [92] and Wolfe [91,93]. We can call (3.24) the *Zoutendijk condition* as mentioned in literature [92].

The term exact line search can be uncertain for the thermoforming process due to difficulty in calculating correct sensitivity matrix. It simply tries to indicate that the orthogonality condition is satisfied. That means,

$$\langle gr^k, d^{k-1} \rangle = 0 \tag{3.25}$$

if $d^{k-1}$ is a descent direction and that the line search satisfies Zoutendijk's condition and condition (3.25). From (3.9) and (3.25) we can show that

$$\cos\alpha_k = \frac{\| gr^k \|}{\| d^k \|} \tag{3.26}$$

This shows that $d^k$ is a descent direction. Now, we can find from Zoutendijk's condition (3.24) by substituting (3.26).

$$\sum_{k\geq 1} \frac{\| gr^k \|^4}{\| d^k \|^2} < \infty \tag{3.27}$$

If we can prove that $\frac{\| d^k \|}{\| gr^k \|}$ is bounded, which means that $\cos\alpha_k$ is bounded away from zero, then (3.27) immediately gives

$$\lim_{k\to\infty} \| gr^k \| = 0 \tag{3.28}$$

This is done by Polak and Ribiere for their method, assuming that *f* is strongly convex, i.e., $\langle gr(\theta) - gr(\tilde{\theta}), \theta - \tilde{\theta} \rangle \geq c \| \theta - \tilde{\theta} \|^2$ for some positive constant c and for all $\theta, \tilde{\theta}$ in $L$.

For general functions, however, it is usually impossible to bound $\frac{\| d^k \|}{\| gr^k \|}$ a priori, and only a weaker result than (3.28) can be obtained, namely,

$$\liminf_{k\to\infty} \| gr^k \| = 0 \tag{3.29}$$

We can use contradiction to get this result. Let us assume that the equation (3.29) does not hold, which means that the gradients remain bounded away from zero: there exists $p > 0$ such that

$$\| gr^k \| \geq p \tag{3.30}$$

for all k higher than or equal to 1. Then (3.27) implies that

$$\sum_{k\geq 1} \frac{1}{\| d^k \|^2} < \infty \tag{3.31}$$

We conclude that the iteration can fail only if $\| d^k \|^2 \to \infty$ sufficiently rapidly. The method of proof used by Zoutendijk for the Fletcher-Reeves method consists in showing that, if equation (3.30) holds, then $\| d^k \|^2$ can grow at most linearly, i.e., $\| d^k \|^2 \leq ck$ for some constant $c$. This opposes (3.31), and supports (3.29).

The analysis for inexact line searches that satisfy Zoutendijk's condition can proceed along the same lines if one can show that the iteration satisfies

$$\cos\alpha_k \geq c \frac{\| gr^k \|}{\| d^k \|} \tag{3.32}$$

for some positive constant c. Then, this relation can be used instead of (3.26) to give (3.27), and the rest of the analysis is as in the case of exact line searches.

A1-Baali [95] shows that the Fletcher-Reeves method gives (3.32) if the step-length satisfies the strong Wolfe conditions:

$$f(\theta_k + \beta^k d^k) \leq f(\theta_k) + \sigma_1 \beta^k \langle gr^k, d^k \rangle \tag{3.33}$$

$$|\langle gr(\theta_k + \beta^k d^k), d^k \rangle| \leq -\sigma_2 \langle gr^k, d^k \rangle \tag{3.34}$$

where $0 < \sigma_1 < \sigma_2 < 1$. In fact, it is necessary to require that $\sigma_2 < 0.5$ for the result to hold. He thus shows that (3.29) holds for the Fletcher-Reeves method.

A1-Baali's result is also remarkable in another respect. By establishing (3.32), which by (3.18) is equivalent to

$$\langle gr^k, d^k \rangle \leq -c \,||\, gr^k \,||^2 \tag{3.35}$$

They showed that the Fletcher-Reeves method always generates descent directions using the strong Wolfe conditions (with $\sigma_2 < 0.5$). Before this result it was believed that it was essential to impose the descent condition while doing the line search.

Researchers in [99] came up with the following condition that allows the conjugate gradient method to converge in case of inexact line search.

Condition: For a conjugate gradient method, we can suppose that

$$0 < p \leq ||\, gr^k \,|| \leq \bar{p} \qquad \text{for} \quad k \geq 1 \tag{3.37a}$$

If this statement is satisfied, then the method will be considered to have the property (it may have it or not) if there exist constants $b > 1$ and $\lambda > 0$ such that for all $k$,

$$|\gamma^k| \leq b \tag{3.37b}$$

And

$$\begin{aligned} &|| \theta^k - \theta^{k-1} || \leq \lambda \\ &| \gamma^k | \leq \frac{1}{2b} \end{aligned} \tag{3.37c}$$

Using the convergence analysis, we can modify the proposed method in case of inexact line search such that the convergence of the method is ensured even with the inaccurate sensitivity matrix that results from nonlinearity of the system. The flow chart of the new algorithm method is shown in Fig.3.4. The new method is modified based on the condition of convergence. At first, the sensitivity matrices are computed offline at different operating points using (3.17) to reduce the computational burden. An approximate sensitivity matrix will be picked up based on the operating points as long as the condition (3.37) is satisfied. If the condition fails at any point, an accurate sensitivity matrix will be computed using (3.16).

## 3.6 Performance Investigation

The effectiveness of the proposed method is investigated extensively in simulation. First, a simulation model based on the previous chapter is developed using Matlab/Simulink. Then, the performance of the proposed method and conventional method that is based on the pseudo inverse of the view factor matrix is compared using the developed model. The oven consists of top and bottom heater trays. Each tray consists of 6 (3x2) heaters. The proposed IHP solver is programmed in such a way that it will give the setpoints of the heaters to reach the desired sheet temperatures at the 9 sensor (4 real and 5 virtual sensors) locations within the desired time. Physical location of thermoforming oven heaters and sensors that was used for the simulation result of this chapter is shown in Fig. 3.5.

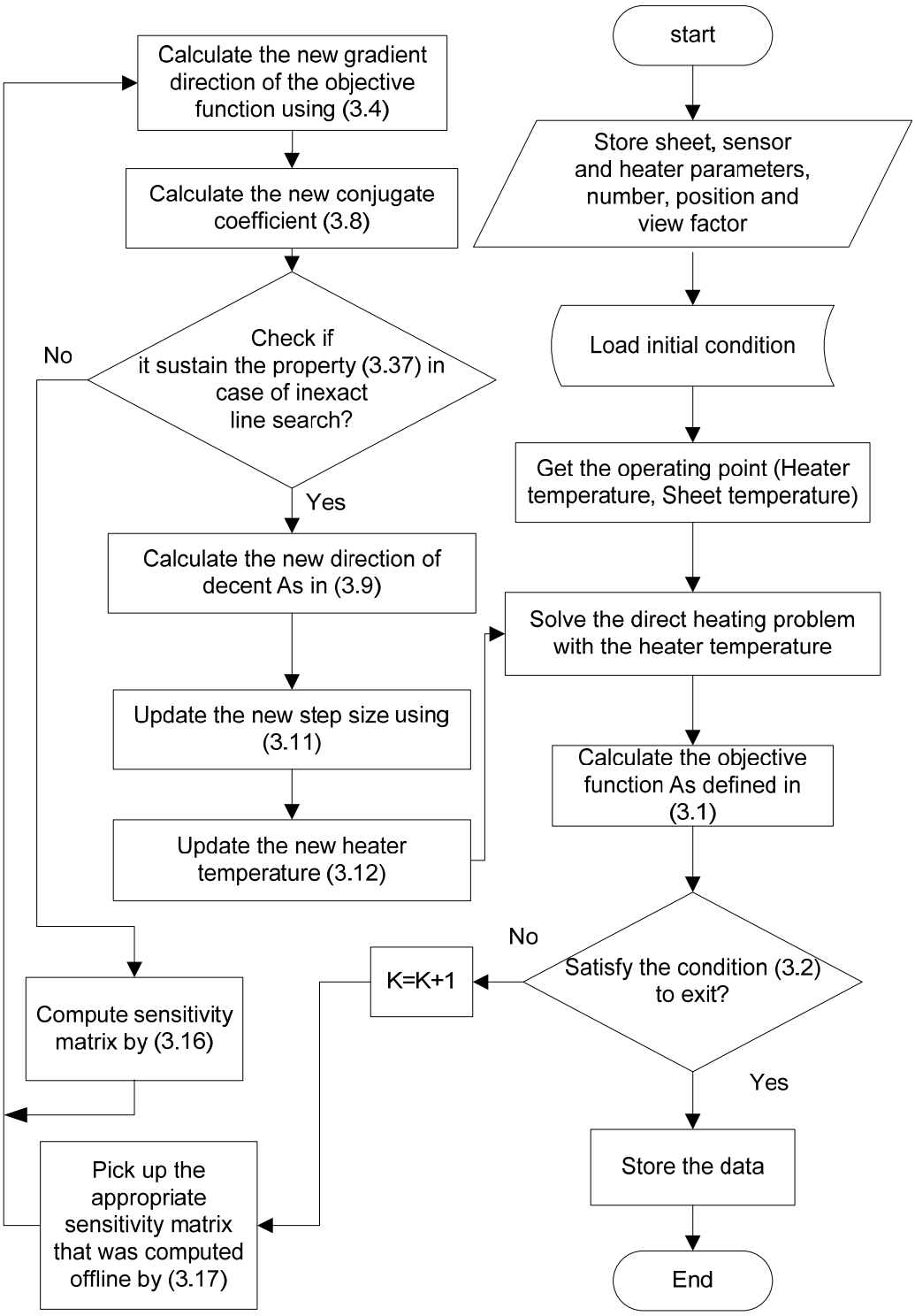


Fig.3.4: Algorithm for solving inverse heating problem.

The conventional and proposed methods are used to find out the exact value of the setpoints of heater temperatures such that the sheet will achieve the desired uniform sheet temperature of 80°C as shown in Fig.3.6 at the end of 50s considering the initial sheet and air temperature is 50°C. The set points for 6 heaters using the conventional method are

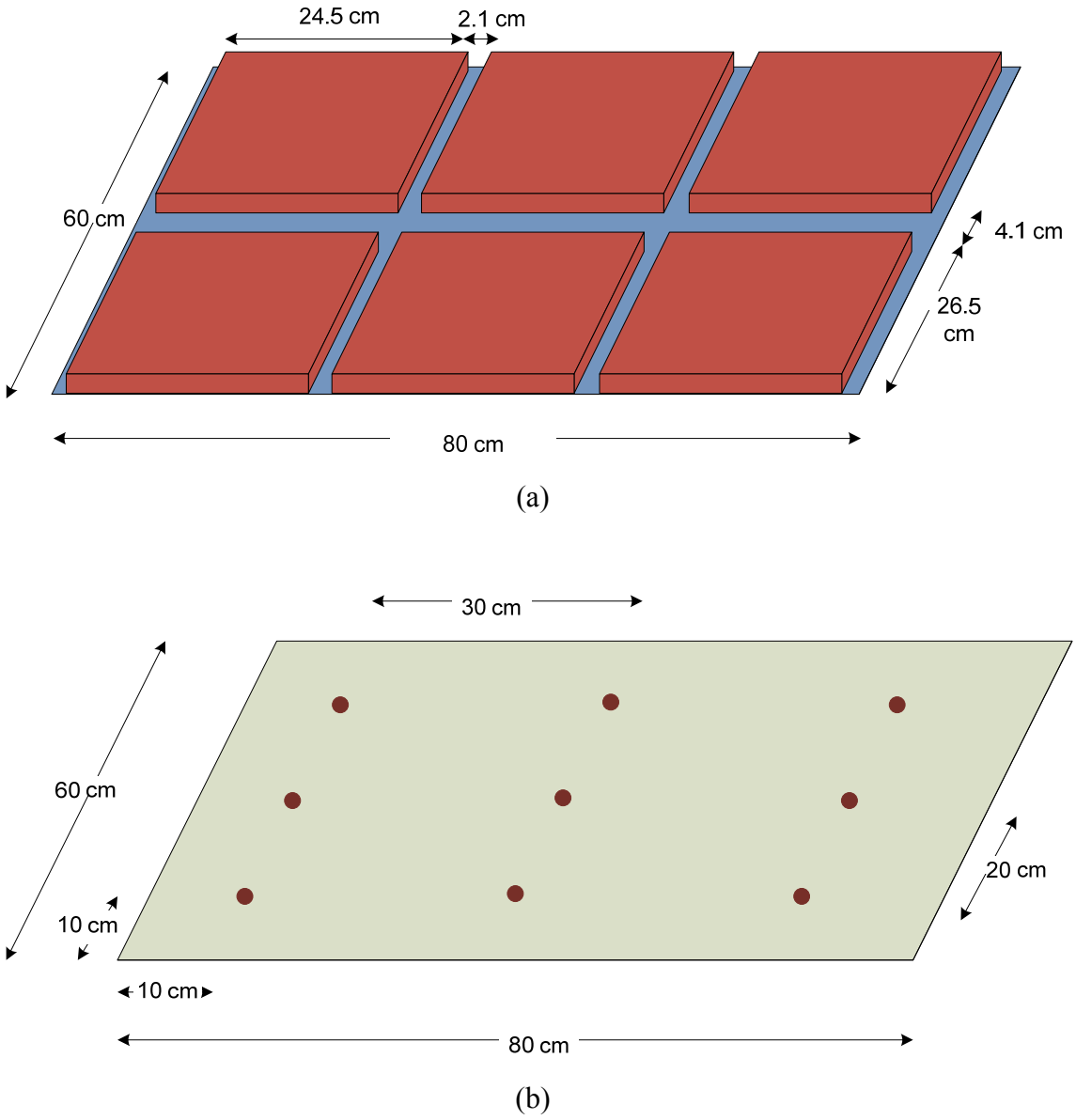


Fig.3.5: Physical location of (a) the thermoforming oven heaters (B) sensors

shown in Fig.3.7 (a). Then the simulink model was used to get the sheet temperature with these set points, the result after 50s and corresponding error are shown in Fig.3.7(b) and Fig.3.7(c). It is observed that there are large errors as the conventional method considers the system as a linear system, and furthermore the cycle time and the current operating point of the system were not incorporated in solving the IHP. The same result for the proposed method is presented in Fig.3.8. The errors are significantly reduced in this method. As the proposed method considers the temperature at the sensor points, the error at these points is very small. Although the proposed method increases the computations as compared to the conventional method, it gives more accurate results. It is observed that the proposed method converges to the solution in less than 20 iterations. As the heating phase is a slow process, the sampling period in a real-time application is as long as 1 or 2 seconds. Hence, the increase in computations due to the proposed IHP solver should not cause any problem to the processor. The performance between the conventional and proposed method is compared for different operating points as shown in Tables 3.1, 3.2, and 3.3. In Table 3.1, the setpoints of the heater temperatures are resolved for a desired sheet temperature of 120°C and the heaters are set to these temperatures. The corresponding sheet temperatures at the sensor points are measured after 50s. The solution of the proposed method gives accurate results as compared to the conventional method. The same results for desired sheet temperatures of 170°C and 220°C are presented in Tables 3.2 and 3.3, respectively. The performance of a PI controller incorporating the proposed method for the IHP for cycle to cycle operation solver is shown in Fig.3.9. The cycle duration is 600 second. At the beginning of each cycle the plastic sheet is entered into the oven and the setpoints of the heater is calculated using the proposed method. The temperature for the sheet is desired to be 150C at the end of the cycle. The sheet is heated to the desired temperature profile by the heaters of the oven during the cycle. At the end of the cycle the sheet transferred to the forming phase and a new sheet will enter into the oven to get heated for the new cycle. The proposed conjugate gradient method is used again based on air temperature and current heater temperature. The simulation results are presented for 10 consecutive cycles. It is observed that the sheet temperature at sensor points almost attain the desired temperature.

Even though the sheet temperature was a bit higher than desired at the end of the cycle for the first couple of cycles, it was getting better with each cycle.

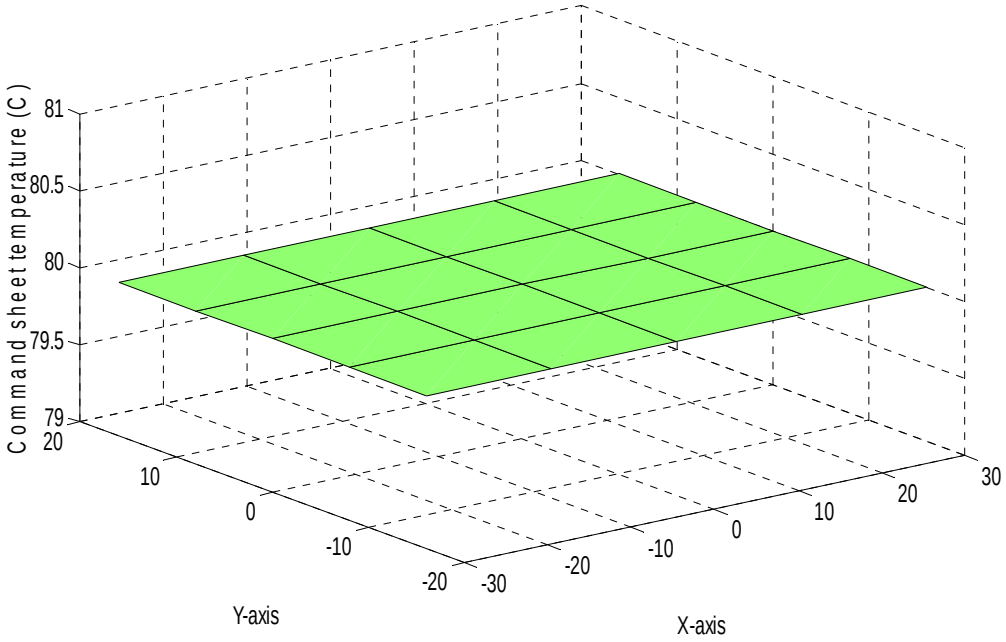


Fig.3.6: Desired temperature profile of the sheet.

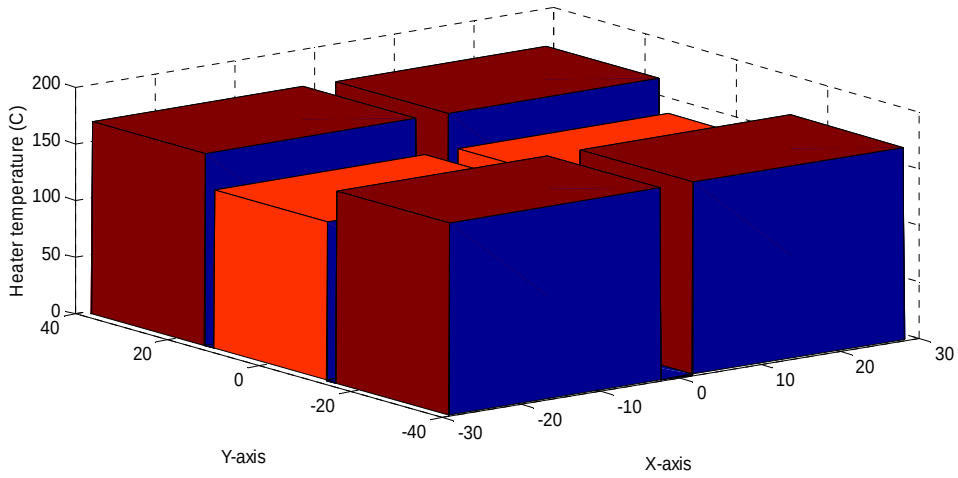


Fig.3.7 (a): the set point of the heater temperature calculated by conventional IHP solver using Pseudo-Inverse of sensitivity matrix to obtain desired sheet temperature of Fig.3.6.

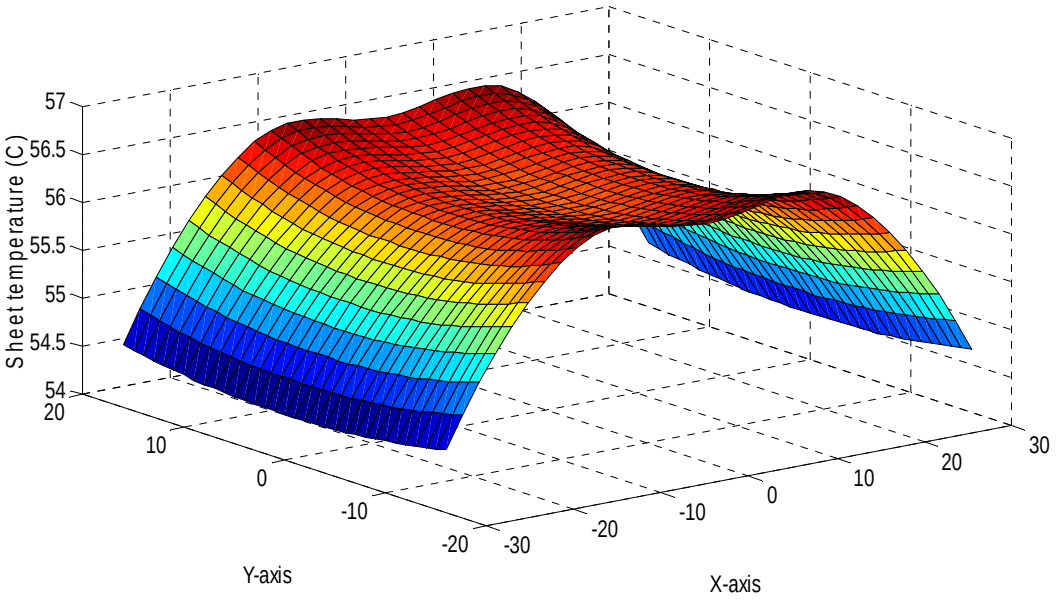


Fig.3.7 (b): Sheet temperature obtained with the heater temperature of Fig.3.7(a)

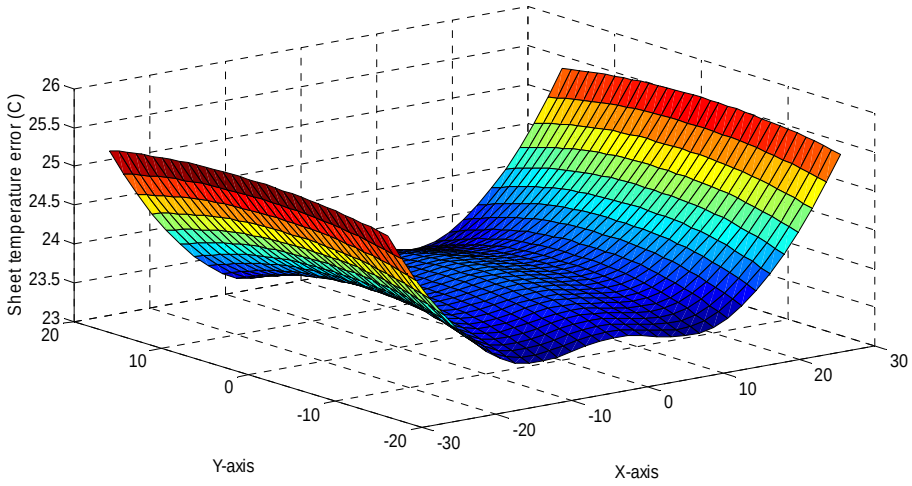


Fig.3.7(c): Error between desired and obtained sheet temperature

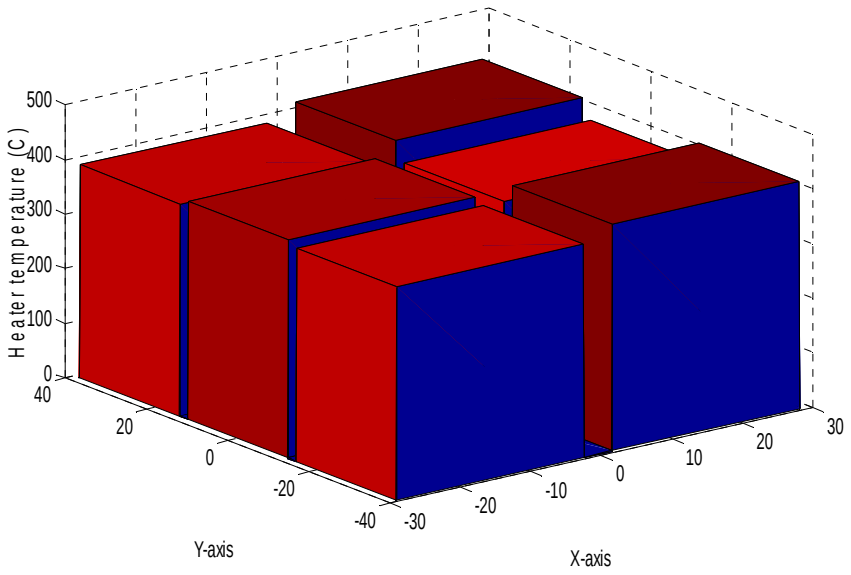


Fig.3.8 (a): Set point of the heater temperature calculated by proposed IHP solver to obtain desired sheet temperature of Fig.3.6.

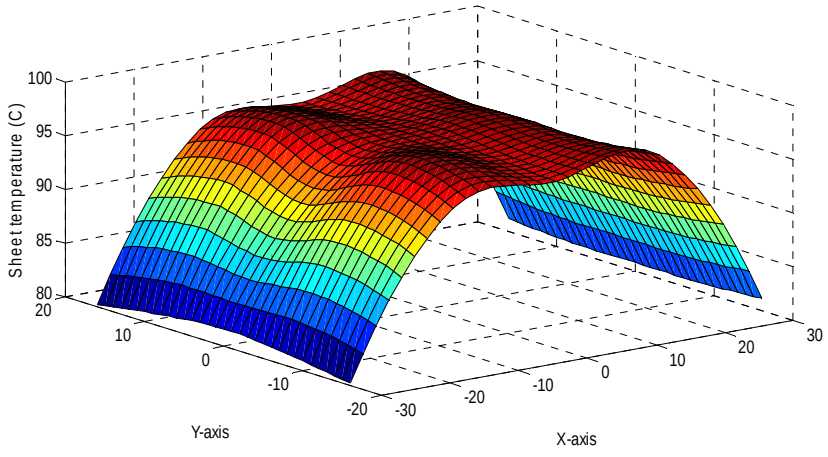


Fig.3.8 (b): Sheet temperature obtained with the heater temperature of Fig.3.8(a).

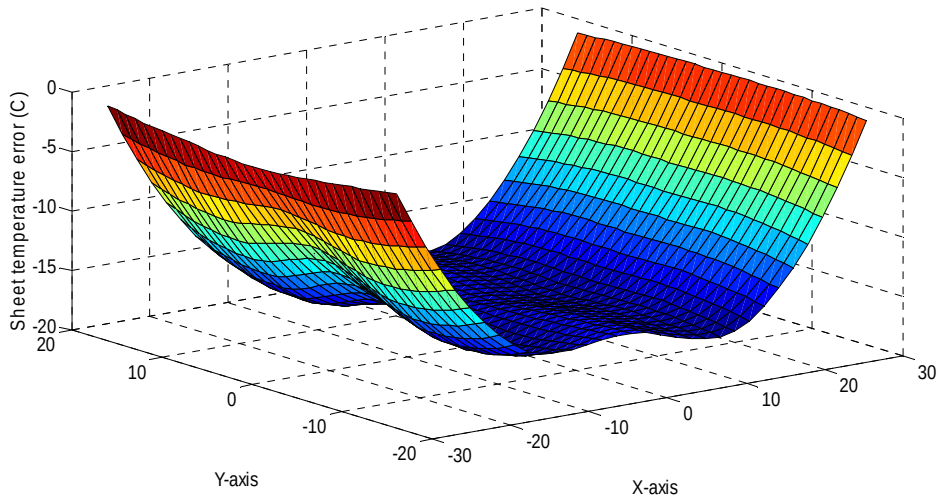


Fig.3.8(c): Error between desired and obtained sheet temperature

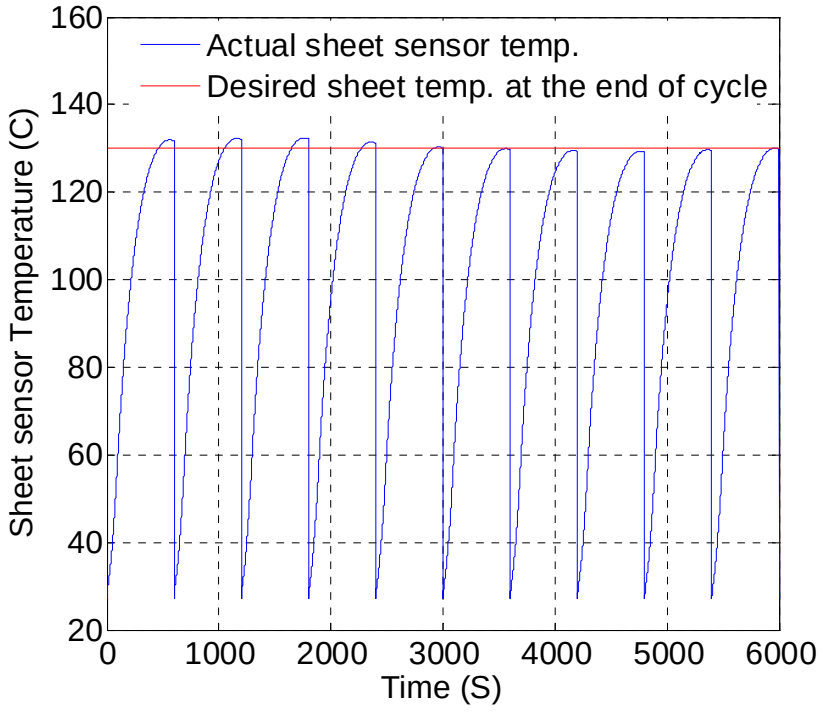


Fig.3.9: The actual temperature and desired temperature at the point of the real sensor (x-axis: Time in Second and y-axis: Temperature in °C)

*Table 3.1: Comparison between proposed and conventional method*

Solution of IHP with Initial sheet temperature =100°C, air temperature =100°C, Command sheet temperature =120°C and corresponding sheet temperature at real sensor position with the IHP solution after 50s.

| **Heater Zone temperature (°C)** | | | **Sensor temperature (°C)** | | |
|---|---|---|---|---|---|
| | ***Proposed method*** | ***Conventional method*** | | ***Proposed method*** | ***Conventional method*** |
| Zone 1 | 372.6504 | 254.2 | Sensor 1 | 120.8 | 107.3 |
| Zone 2 | 339.1641 | 209.8 | Sensor 2 | 120.8 | 107.3 |
| Zone 3 | 372.7453 | 254.2 | Sensor 3 | 120.9 | 107.3 |
| Zone 4 | 371.9607 | 254.2 | Sensor 4 | 120.9 | 107.3 |
| Zone 5 | 335.2856 | 209.8 | | | |
| Zone 6 | 371.9459 | 254.2 | | | |

*Table 3.2: Comparison between proposed and conventional method*

Solution of IHP with Initial sheet temperature =150°C, air temperature =150°C, Command sheet temperature =170°C and corresponding sheet temperature at real sensor position with the IHP solution after 50s.

| **Heater Zone temperature (°C)** | | | **Sensor temperature (°C)** | | |
|---|---|---|---|---|---|
| | ***Proposed method*** | ***Conventional method*** | | ***Proposed method*** | ***Conventional method*** |
| Zone 1 | 398.7254 | 360.1 | Sensor 1 | 171.3 | 164.3 |
| Zone 2 | 361.6055 | 297.2 | Sensor 2 | 171.3 | 164.3 |
| Zone 3 | 398.8696 | 360.1 | Sensor 3 | 171 | 164.3 |
| Zone 4 | 402.8696 | 360.1 | Sensor 4 | 171 | 164.3 |
| Zone 5 | 360.8435 | 297.2 | | | |
| Zone 6 | 402.8544 | 360.1 | | | |

*Table 3.3: Comparison between proposed and conventional method*

Solution of IHP with Initial sheet temperature =200°C, air temperature =200°C, Command sheet temperature =220°C and corresponding sheet temperature at real sensor position with the IHP solution after 50s.

| **Heater Zone temperature (°C)** | | | **Sensor temperature (°C)** | | |
|---|---|---|---|---|---|
| | ***Proposed method*** | ***Conventional method*** | | ***Proposed method*** | ***Conventional method*** |
| Zone 1 | 443.0235 | 466 | Sensor 1 | 221.8 | 225.3 |
| Zone 2 | 372.0556 | 384.6 | Sensor 2 | 221.8 | 225.3 |
| Zone 3 | 443.1497 | 466 | Sensor 3 | 221.8 | 225.3 |
| Zone 4 | 445.3795 | 466 | Sensor 4 | 221.8 | 225.3 |
| Zone 5 | 365.7297 | 384.6 | | | |
| Zone 6 | 445.4239 | 466 | | | |

## 3.7 Conclusion

A new technique based on the conjugate gradient method is proposed for solving the inverse heating problem for the heating phase of the thermoforming process. A method for solving the direct heating problem is presented which is then used in the iterative solution of the inverse heating problem. Although it increases the computational cost, the proposed method gives better setpoints for the heater temperatures to achieve a particular temperature distribution over the sheet. The complete method is tested in simulation. The effectiveness of the proposed algorithm is shown by simulation.

# Chapter 4

# Estimation of Sheet Temperature Profile

## 4.1 Introduction

This chapter presents a new method for the estimation of surface temperature of a sheet using temperature sensors pointing at different positions over the sheet. In the thermoforming process, the temperature profile over the plastic sheet at the end of the cycle depends on the efficiency of the controller, the number and locations of heater units and the number and locations of sensors. To control the temperature profile at every point of the sheet to the specified profile, an infinite number of heater units in the oven and an infinite number of sensors to feedback the temperature would be required, which is not feasible. Therefore, this problem is approached by estimating or interpolating the spatial temperature profile using the output from a minimum number of sensors. Although the number of sensors should be kept low to minimize their cost, estimation of a complete temperature profile over the whole sheet is necessary for an accurate and efficient control of the temperature. Thus, the effectiveness of the controller depends on the accuracy of the estimation of the complete temperature profile and the incorporation of the estimation into the design of the controller. Some researchers use the signal from the sensor directly as the feedback signal to compare with the desired temperature at the point of the sheet [11,12]. The controller design based on these error signals works to minimize the difference between the actual temperature and desired temperature of the sheet zone. But the differences between the actual temperature and desired temperature at locations between any two sensors cannot be optimized using that control technique. If the sensor output can be used to estimate or interpolate the whole temperature profile over the sheet

and this information is incorporated in the design of the controller in such a way that it will control whole sheet temperature instead of the temperature of some particular points of the sheet, then the sheet temperature can be achieved to the specified profile, within a prespecified tolerance, as required for the forming phase.

The approach in [11] uses virtual sensors in addition to real sensors so that some more temperature points can be incorporated into the design of the controller. The temperatures at these virtual sensors are estimated from the real sensor temperatures using a weighted average based on distance. Although more points can be incorporated in the design of the controller using the virtual sensors to optimize the difference between desired and actual temperatures, the difference between the desired and actual sheet temperature profiles still cannot be optimized by this method across the entire sheet. In this chapter, a new method is proposed for the estimation of the whole sheet temperature profile based on spatial harmonics. Then, a new controller is designed to control these spatial harmonics, which has the effect of controlling the temperature over the whole sheet instead of just controlling temperatures at certain locations. The proposed method is developed and designed in such a way that it can estimate the temperature profile over the entire sheet through its spatial harmonics and control the spatial harmonics to obtain the desired temperature profile. **C**omputational cost is also considered during the development of the proposed method. A PI controller is used to control each spatial harmonic to achieve the desired temperature profile over the sheet. The proposed estimation method of the temperature profile is based on the two-dimensional Fast Fourier Transform (FFT). Each component of the two-dimensional space temperature harmonics is controlled by adjusting the heater temperatures. For the sake of simplicity, we will consider that the sensors are located at equidistant points over the sheet. The reason behind this is that, we can apply the FFT to calculate spatial harmonics only for equidistant data points that will be obtained from temperature sensors. The performance of the proposed temperature estimation technique is tested in simulation for different desired temperature profiles to compare with a simple method of temperature estimation based on the weighted average temperature of the sensors surrounding the location of interest. Thereafter, the performance of the proposed temperature control technique based

on the spatial harmonics is compared with the conventional control technique in simulation. In the next chapter, we will expand the same idea in those cases where the sensors are located at different non-equidistant points.

## 4.2 Estimation of sheet temperature

In the heating phase in thermoforming, the temperature of the sheet is fed back to be compared with the temperature setpoint. In the proposed work, the temperature map of the whole sheet is estimated, instead of estimating temperatures at certain points only. Thereafter, the whole temperature sheet profile information will be fed back to the controller. The temperature profile over the sheet is a band-limited temperature map in terms of its spatial frequency contents [104,105,106,107,108,109]. Therefore, it can be expressed as a combination of components at harmonic spatial frequencies. The Fourier transform is an important signal processing tool which can be used to decompose the sheet temperature profile into its harmonic spatial frequencies. The output of the Fourier transformation denotes the temperature distribution on the sheet in the spatial frequency domain or Fourier space domain, while the input is the temperature distribution over the plastic sheet. In the Fourier domain, each coefficient represents a particular spatial frequency contained in the temperature distribution. The Fourier transform is used in a wide range of applications, such as image analysis, image filtering and image reconstruction [105,110,111]. Therefore, Fourier transform can be used to reconstruct the temperature profile of the sheet. The real sensor output can be used as a sampled value of the temperature distribution over the sheet. Thus, the number of sensors required to estimate the sheet temperature will depend on the spatial bandwidth of the temperature distribution and the accuracy specified for the controller. For a rectangular sensor array of size $N \times M$, the two-dimensional Discrete Fourier Transform (DFT) is given by [105]:

$$F(m,n) = \sum_{k=0}^{N-1} \sum_{l=0}^{M-1} f(k,l) \exp(-i2\pi(\frac{km}{N} + \frac{ln}{M})) \tag{4.1}$$

where $f(k,l)$ is the sample temperature output at the sensor point indexed by *(k,l)* on the sheet in the spatial domain, $F(m,n)$ is the spatial frequency representation of the temperature profile and the exponential term is the basis function corresponding to each point $F(m,n)$ in the Fourier space. The significance of the equation can be interpreted as follows: the value of each point $F(m,n)$ is obtained by multiplying the spatial temperature profile over the sheet with the corresponding basis function and summing the result. The complex exponential basis functions represent sine and cosine waves with increasing frequencies, i.e., $F(0,0)$ represents the DC-component of the temperature which corresponds to the average temperature of the sheet and $F(N-1,M-1)$ represents the highest frequency component. In a similar way, the Fourier harmonic frequencies can be transformed back to the spatial domain.The inverse Fourier transform is given by [105]:

$$f(k,l) = \frac{1}{NM}\sum_{m=0}^{N-1}\sum_{n=0}^{M-1} F(m,n)\exp(i2\pi(\frac{km}{N}+\frac{ln}{M})) \tag{4.2}$$

The DFT is the sampled Fourier transform and therefore it does not contain all frequencies forming the temperature profile, but only a set of samples which is large enough to fully describe the spatial domain temperature distribution. The number of frequencies corresponds to the number of sensors on the sheet, i.e., the temperature distributions in the spatial and Fourier domains are of the same dimensions. If the sensor arrangement on the sheet is not sufficiently dense to sample the temperature map according to the Nyquist criterion [105], then the exact temperature distribution cannot be estimated as a result of this under-sampling. If the number of sensors used to estimate temperature is not sufficient, then some of the higher spatial frequencies become aliased to lower spatial frequency representations in the sampled temperature profile. This creates undesirable artifacts that decrease the accuracy of the estimation. Fortunately, as the plastic sheet is heated by a finite number of heaters located at the top and bottom of the oven and considering lateral heat flow within the sheet, the temperatures between two adjacent points of the sheet do not differ much and the temperature map on the sheet has

no discontinuity. It makes the temperature profile a spatially band-limited signal, which means that its frequency spectrum contains components at low spatial frequencies while its magnitude gets insignificant at higher spatial frequencies. The two-dimensional Fourier transform indicates spatial frequency content in two orthogonal directions of the temperature distribution in the sheet. The maximum spatial frequency in any direction that can be recovered from the sensor samples can be determined by the Nyquist theorem as:

$$f_{\max(x)} = \frac{2}{d_x} \tag{4.3}$$

where $f_{\max(x)}$ is the maximum spatial frequency in the x direction that can be recovered, and $d_x$ is the distance between two nearest real sensors in the x direction. If the arrangement of the sensors satisfies the Nyquist criterion, the temperature profile can be exactly reconstructed from the real sensor outputs [107,108]. Now, we discuss the interpolation technique to estimate the temperature profile.

**Interpolation by zero-padding technique**

A signal can be exactly reconstructed using samples of the signal if the sampling rate satisfies the Nyquist criterion. This technique can be best described graphically with a one dimensional example through Fig.4.1. The discrete Fourier transform of the samples (as computed by the FFT algorithm) is used to get the frequency content of the signal. When the discrete Fourier transform of the samples is compressed, meaning that zeros are padded from the high-frequency side of the Fourier transform, no information is lost in the frequency spectrum of the original signal. Because the magnitude and phase at frequencies lower than the maximum detectable frequency remain unchanged and new high-frequency components with zero magnitude are added, zero padding has an interpolation effect in the spatial domain. Thus, the inverse Fourier transform will recover the signal with the same number of extra samples as the number of zeros added. This

means that, to interpolate the function by a factor *N*, {(*N-1*)*number of samples} zeros have to be added.

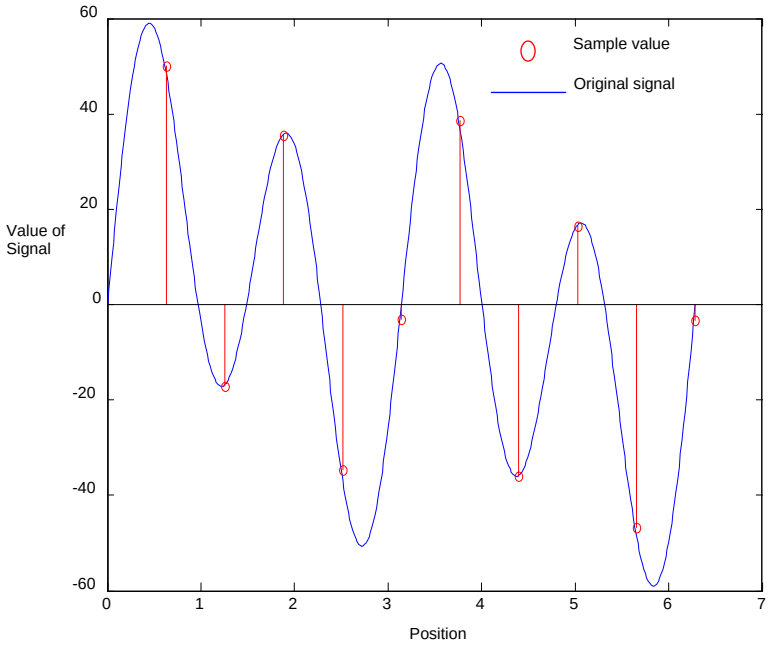


Fig.4.1 (a): Original analog signal is sampled at uniform sampling rate.

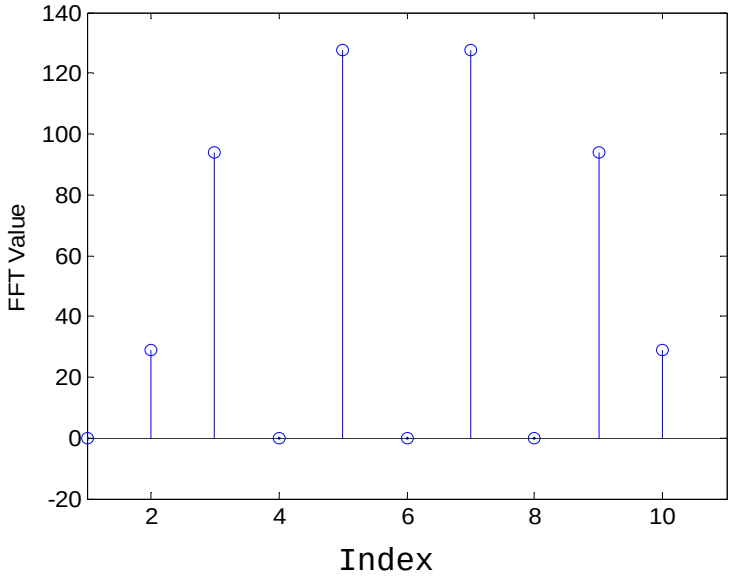


Fig.4.1 (b): FFT of the samples of fig.4.1 (a)

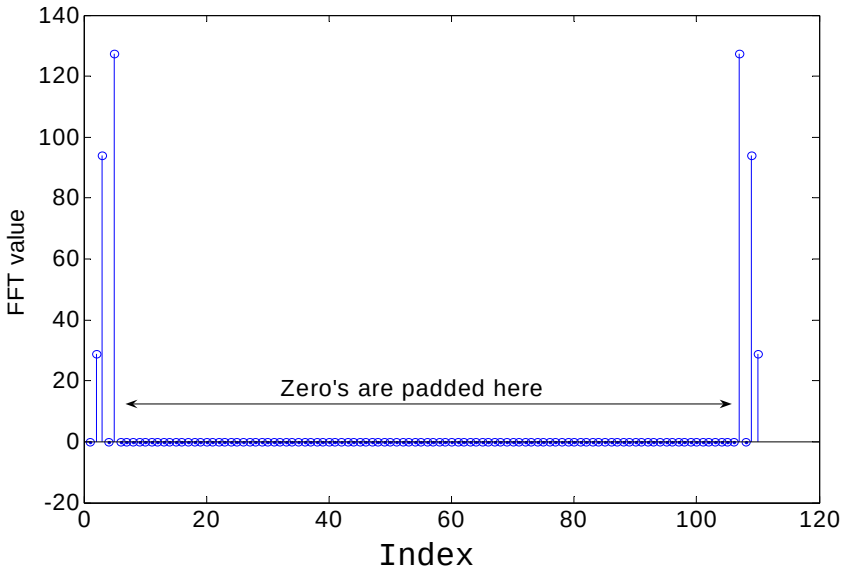


Fig.4.1 (c): FFT value after padding zero.

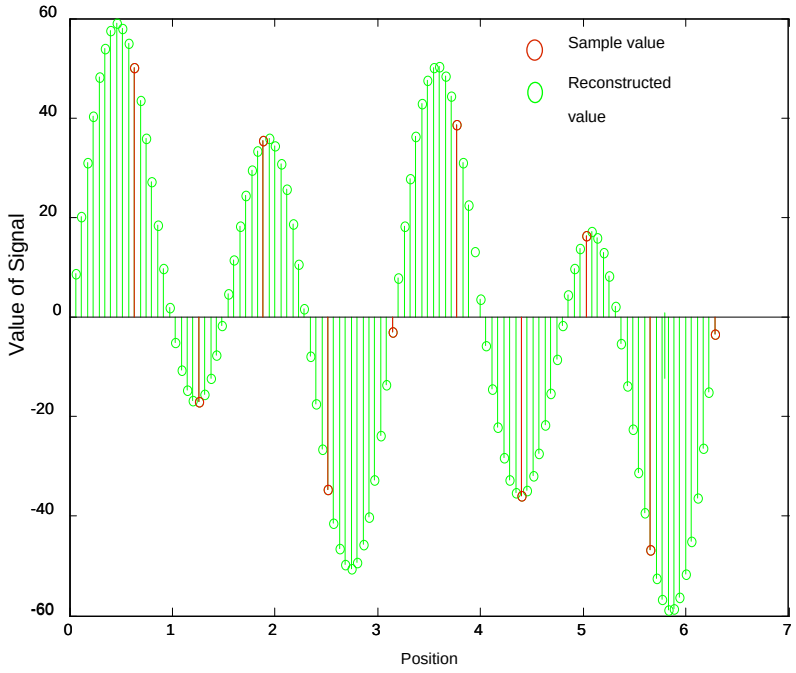


Fig.4.1 (d): The original signal is reconstructed by IFFT of the signal in Fig.4.1(c)

**Computational Complexity**

It is well established that the Fourier and inverse Fourier transform in equation (4.1) and (4.2) can be easily calculated by multiplying the real sensor output with a matrix that depends on the position of the sensors. The matrices are constant because the positions of the real sensors are constant for a particular thermoforming process. Therefore, the matrices can be computed offline. So the transformation from one domain to the other can be done by a simple matrix multiplication. The dimension of the matrices depends on the number of sensors. This will not cause a significant computational burden especially for a slow system such as the heating phase of the thermoforming process.

## 4.3 Design of the controller

One problem of the conventional controller design for the heating phase is the coupling among the outputs of the controller [11]. The conventional controller generates the control input based on the error signal between the output of the sensor and the setpoint temperature at that sensor point. However, the temperature at one real sensor point cannot be controlled independently due to the coupling among the heaters and all the different points of the sheet. Due to this well-known issue, the conventional proportional integral (PI) controller or proportional integral derivative (PID) controller that works on the output of a sensor cannot be used efficiently to control the heater bank to obtain the specified temperatures at the respective sensor points of the sheet. Some researchers, e.g., [12], looked into the possibility of incorporating a decoupling technique like the singular value decomposition (SVD) into the controller to decouple the control input based on the model which makes the controller more dependent on the model of the system. However, the model changes a lot at different operating conditions and is influenced by the disturbances.

On the other side, the spatial frequency domain of the Fourier transform is a method of expressing the spatial distribution of temperature that represents a point in some infinite dimensional vector space of functions in terms of the sum of its projections

onto a set of orthonormal basis functions with different frequencies. If the controller is designed in such a way that it will control the spatial harmonics instead of the conventional way of controlling the output of the sensors, two major problems can be solved. First, as orthogonal basis functions, the spatial harmonics are decoupled from each other, and they can be controlled independently. Second, by controlling the spatial harmonics, the controller can control the temperature over the whole sheet instead of controlling the temperature at certain points. The complete architecture of the proposed spatial harmonic controller is explained in Fig.4.2. The output temperature of the sheet is measured by real sensors. The number of sensors depends on the maximum temperature gradient. So the number of the sensors (hence Nyquist sampling rate) should be chosen in such a way that all the spatial harmonics recovered to control the temperature profile can be recovered efficiently. The outputs of the real sensors are processed through the 2D FFT to get the spatial frequency spectrum of the temperature profile. The desired temperature profile is also processed through a 2D FFT transformation. This 2D FFT transformation is basically a matrix multiplication, as given in equation (4.1). Thus, the computational cost for this transformation is not high. In the proposed controller, the desired spatial harmonics are compared with the actual temperature profile harmonics, and the error between them is passed to the PI controller. The output of the PI controller is processed by the 2D IFFT to convert it into a temperature map in the spatial domain.

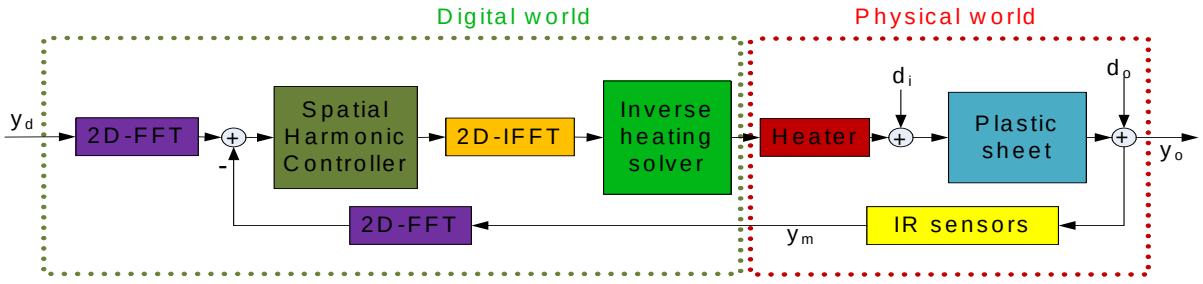


Fig.4.2: Block diagram of the proposed spatial

Note that the 2D IFFT transformation is also a matrix multiplication, like the 2D FFT. As 2D IFFT is a linear transformation, the IFFT for all spatial harmonics can be computed together in a single block in the figure. The next block is the inverse heating problem solver which computes the corresponding heater temperature set-points of the heater bank.

## 4.4 Performance Investigation

The effectiveness of the proposed method of estimation of temperature profile and the new spatial harmonic control technique of the heater banks of the thermoforming process are investigated extensively in simulation in this section. The simulation results are presented in two steps. First, the results for the estimation of the temperature are presented for certain temperature distribution over the sheet. Second, the simulation results are presented for cycle to cycle operation of the heating phase that is controlled by the proposed controller incorporated with the proposed estimation technique.

### 4.4.1 Simulation results for the estimation of temperature by 2D FFT

A spatial temperature distribution on the sheet as plotted in Fig.4.3 to be estimated using a particular number of sensors with the help of proposed technique can be described by the following equation:

$$T(x, y) = 150 - 50e^{-(x^2 + y^2)} \quad . \tag{4.4}$$

Where $x$ and $y$ are the Cartesian coordinates of the point of the sheet. Now, the proposed estimation technique will be used to predict this temperature profile distributed over the sheet to evaluate the performance of the 2D FFT technique. The resulting estimated temperatures with different combinations of sensors are shown in Fig.4.4. The corresponding error in the estimation of the temperature profile over the sheet is shown in

Fig.4.5. It is observed from the simulation results that the estimation error is decreasing with an increase in the number of sensors which is obvious. Using only one sensor, the estimated value of the temperature is equal to a dc value, which is the same as the value of the sensor temperature reading. FFT technique cannot detect higher order spatial harmonics from a single point value since the sampling of the temperature profile does not meet the Nyquist criterion. Thus, it is impossible to recontruct the temperature profile from that sensor output. The estimated temperature is fairly accurate with 4 sensors arranged as a 2X2 sensor array. The error in the reconstructed signal is decreased from 40°C to 2°C when we use 4 sensors instead of a single sensor. However, with further increase of the number of sensors, the 2D FFT technique can reconstruct the signal more accurately. This can be explained using the Nyquist theorem. A higher number of sensors indicates a higher sampling rate that allows the proposed technique to recover a higher number of spatial harmonics of the temperature profile which leads to a more accurate estimation. It can be observed that the magnitude of the error is very low between the sensors as compared to the outside of the area surrounded by sensors. Thus, the error is going to be larger at the periphery of the sheet. As expected, the error is zero at the sensor locations. From the performance investigation, it can be concluded that the whole temperature distribution over the sheet can be predicted accurately using the proposed FFT technique if a sufficient number of sensors is used based on the Nyquist criterion.

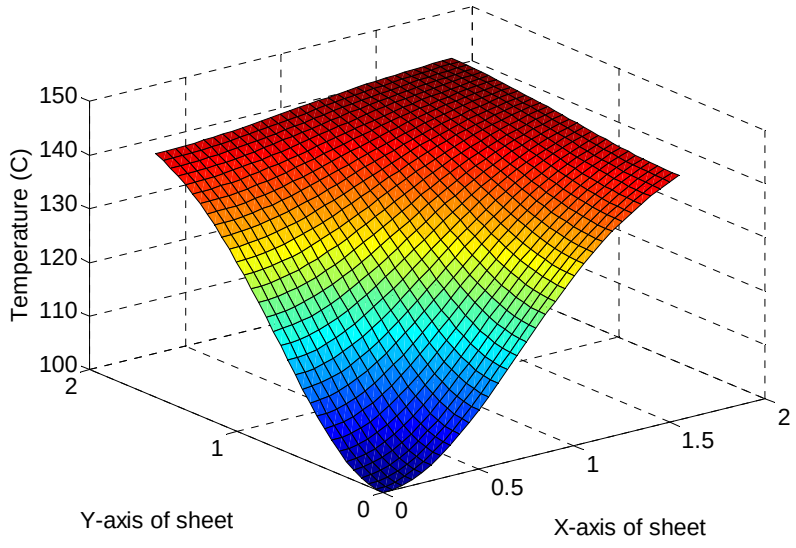

Fig.4.3: The actual temperature profile considered over the sheet to check accuracy of the proposed technique

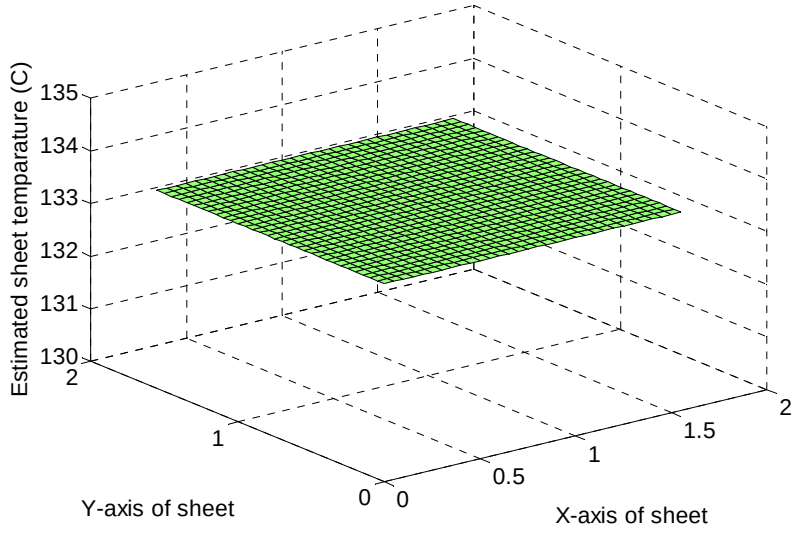


Fig.4.4(a): The estimated temperature profile over the sheet using 1 sensor located at (1,1)

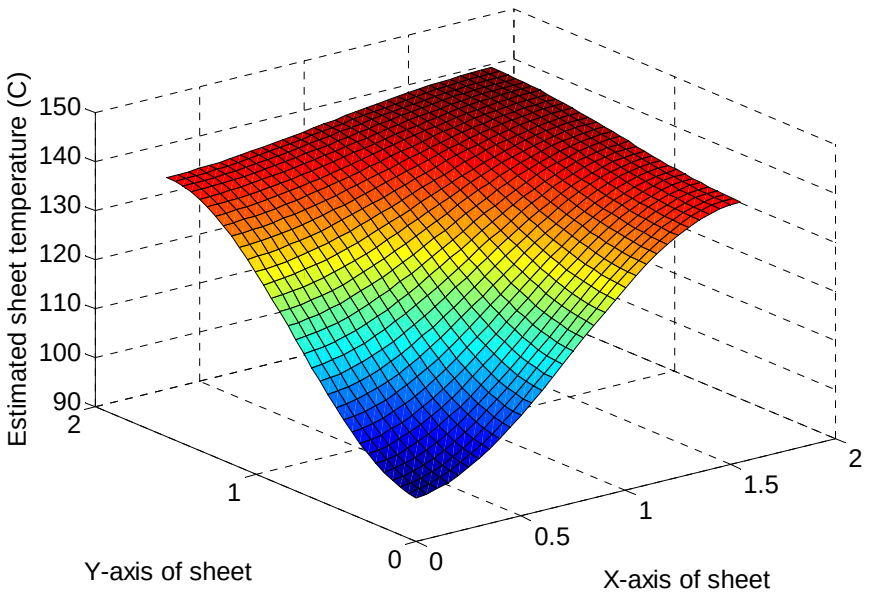


Fig.4.4(b): The estimated temperature profile over the sheet using 4 sensors (2 arrays with 2 sensors in each array) located at (0.5,0.5);(0.5,1.5);(1.5,0.5);(1.5,1.5)

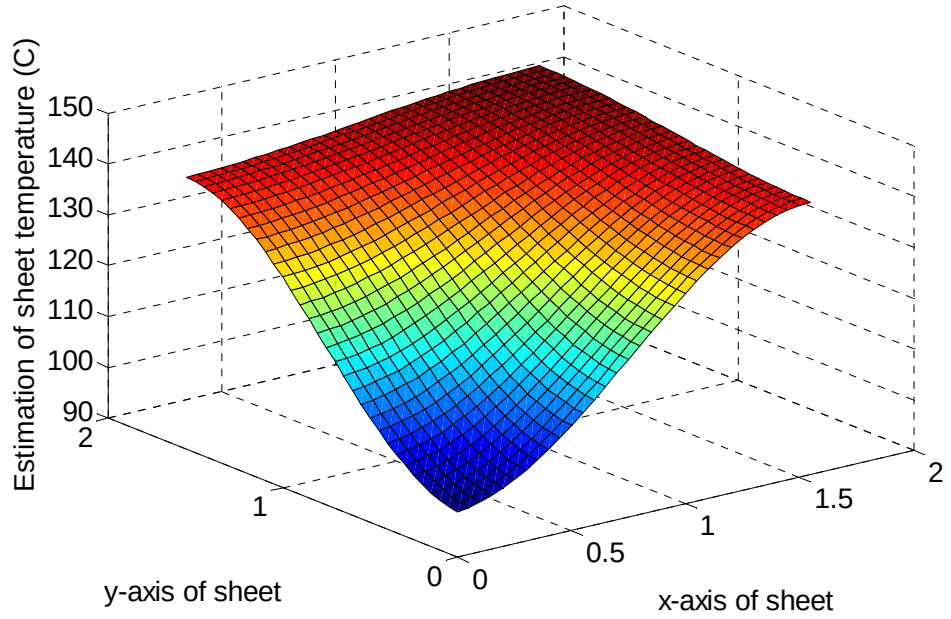


Fig.4.4(c): The predicted temperature profile over the sheet using 9 sensors (3 arrays with 3 sensors in each array) located at (0.5,0.5), (0.5,1.0), (0.5,1.5), (1.0,0.5), (1.0,1.0), (1.0,1.5), (1.5,0.5), (1.5,1.0), (1.5,1.5).

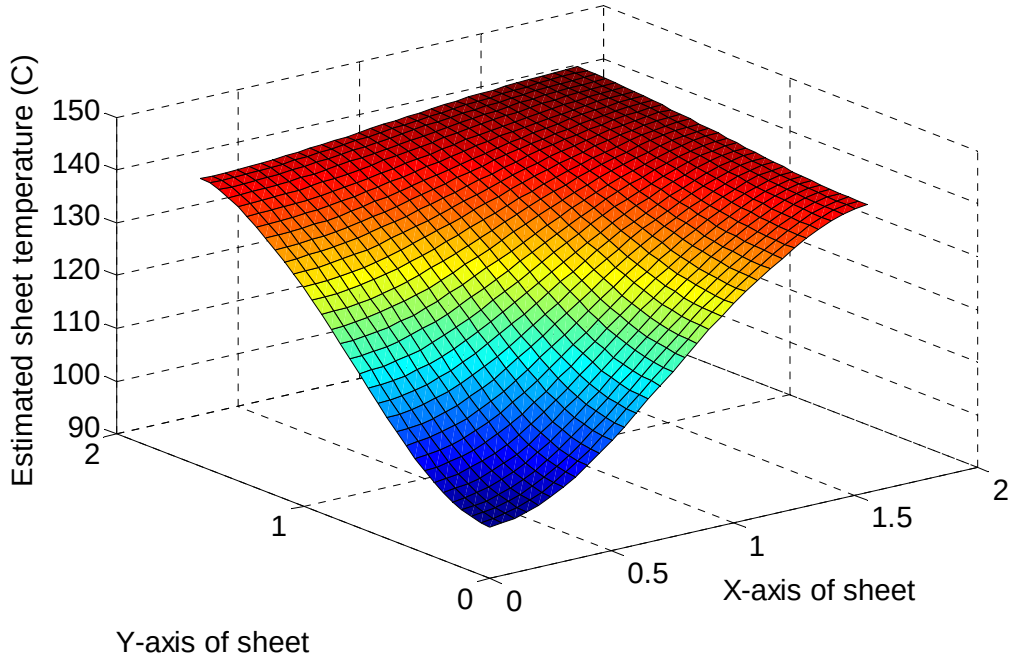


Fig.4.4(d): The predicted temperature profile over the sheet using 16 sensors (4 arrays with 4 sensors in each array) located at (0.4,0.4), (0.4,0.8), (0.4,1.2), (0.4,1.6), (0.8,0.4), (0.8,0.8), (0.8,1.2), (0.8,1.6), (1.2,0.4), (1.2,0.8), (1.2,1.2), (1.2,1.6), (1.6,0.4), (1.6,0.8), (1.6,1.2), (1.6,1.6)..

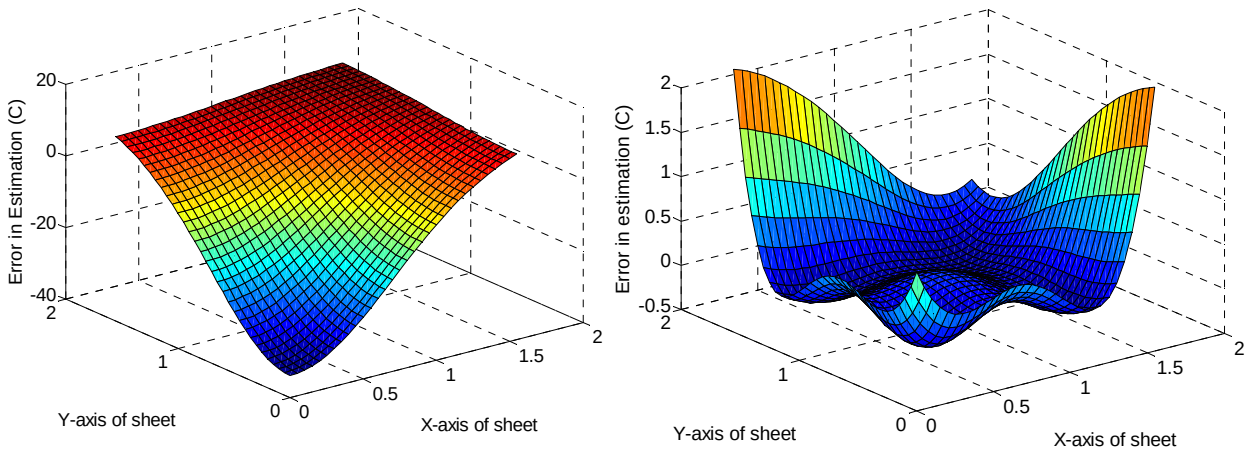


(a) (b)

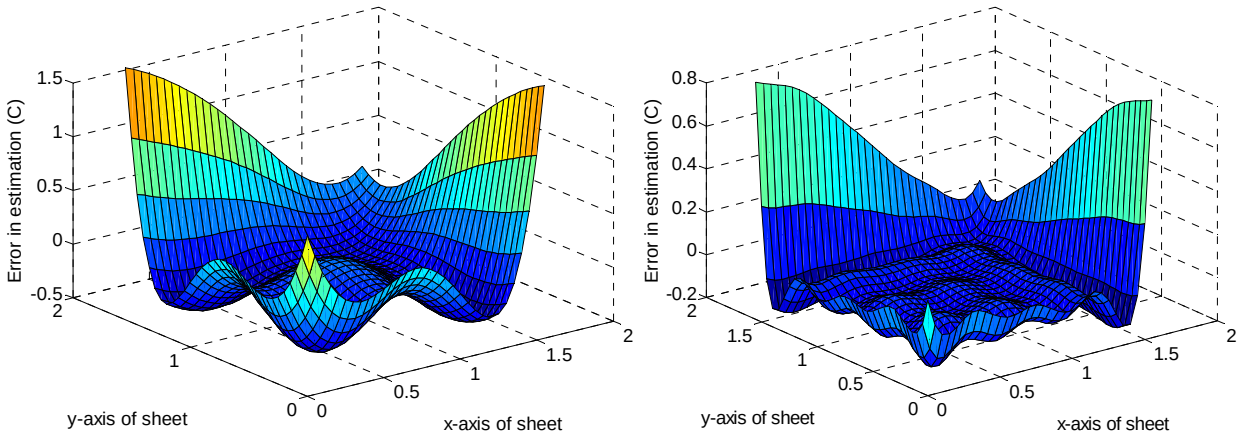


(C) (d)

Fig.4.5: The error between the actual temperature profile and predicted temperature profile over the sheet using (a) 1 sensor (b) 4 sensors (2x2) (c) 9 sensors (3x3) (d) 16 sensors (4x4)

### 4.4.2 Simulation results of the proposed harmonic controller

A simulation model of the heating phase of the thermoforming process was developed using Matlab / Simulink. The model of the thermoforming heating process as developed in Chapter 2 was used for the simulation. The physical structure of the thermoforming oven and the sensor positions that were used in the simulation are shown in Fig.4.6. The heater bank used in this simulation is composed of 6 heaters at the top and 6 at the bottom of the thermoforming oven. The 6 heaters are arranged in two arrays with 3 heaters in each array as shown in the figure. Four real sensors (2 arrays with 2 sensors in each array) at equidistant positions are used in the sheet to sense the temperature at the top of the sheet. In addition with these 4 sensors, 21 additional virtual sensors were used as shown in Fig.4.6. The same number and arrangement of sensors are used at the bottom of the sheet. The performance of the proposed spatial harmonic controller is compared with that of the conventional controller of the heating phase for cycle to cycle operation. The cycle duration is 600s. At the beginning of each cycle the plastic sheet is entered into the oven and is heated to the desired temperature profile by the heaters of the oven during the cycle. At the end of the cycle, the sheet is transferred to the forming station to form it in the desired shape over the mould as a new sheet enters into the oven to get heated for the new cycle. The conventional controller that is used for comparison with the proposed controller is as described in [11]. Same numbers of real and virtual sensors are used in the conventional controller to make a fair comparison with the proposed controller. The performance of the proposed controller is presented in Fig.4.7. The temperature set-point at the end of the cycle for the sheet is 150C. The desired temperature profile is a uniform temperature all over the sheet as shown in Fig.4.7(a). The obtained temperature profile of the sheet and corresponding error after a 600 second cycle duration are shown in Fig.4.7(b) and Fig.4.7(c). We choose the seventh cycle instead of the first cycle to show the control behavior of the controller because we want to evaluate the performance when the setpoints of the heater achieve a periodical pattern after a few cycles. The temperature of the air and oven elements will achieve the same cyclic pattern after some cycle in the process whereas in the first cycle the pattern mostly depends on the initial air and oven element temperature. Moreover, the plastic sheet roughly follows the same pattern of

temperature in the subsequent cycles. This fact will be clear looking at 10 cycles in some of the figures later in this section. The outputs of the sensors are used to calculate the spatial frequency and a PI controller is used to control the heater such that the sheet spatial harmonics converge to the desired spatial frequency. It is observed that the temperature at the middle of the sheet is higher than the two sides because the center is getting heated by more heaters. But the controller controls the heater temperature to minimize the error. The simulation results of the temperatures at the locations of the real sensors are shown in Fig.4.8 for the first 10 cycles of heating phase. We can see that for the first couple of cycles the sheet attains different temperatures at the end of the cycle and it achieves a particular pattern after several cycles. Fig. 4.9 shows the temperature at some points of the plastic sheet where the error between the actual temperature and desired temperature is highest within the sheet. It is observed that the temperatures at sensor points can reach the desired temperatures at the end of the cycle period whereas the temperatures at some other points cannot reach the setpoint temperatures as shown in Fig.4.9. As it was mentioned before, the temperature at every point of the sheet could be controlled to the desired temperature if an infinite number of heaters and sensors were

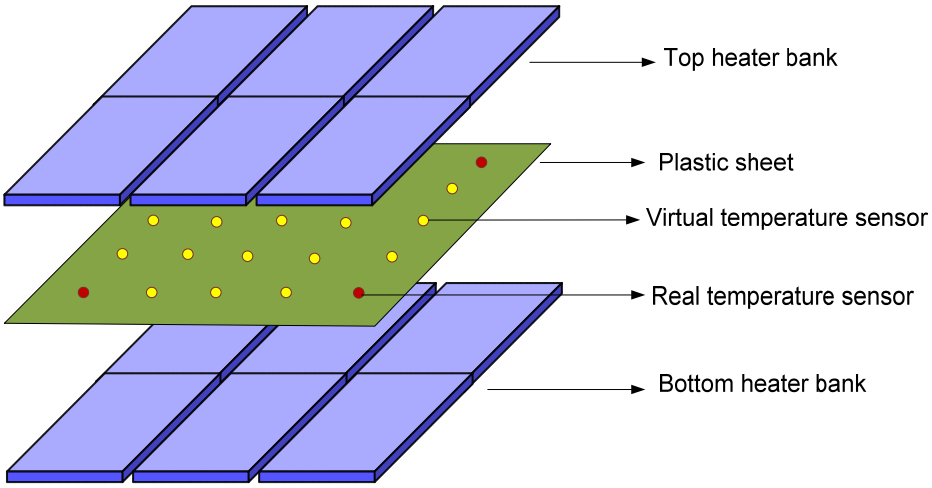


Fig.4.6: The physical configuration of the oven and real and virtual sensor positions on the plastic sheet

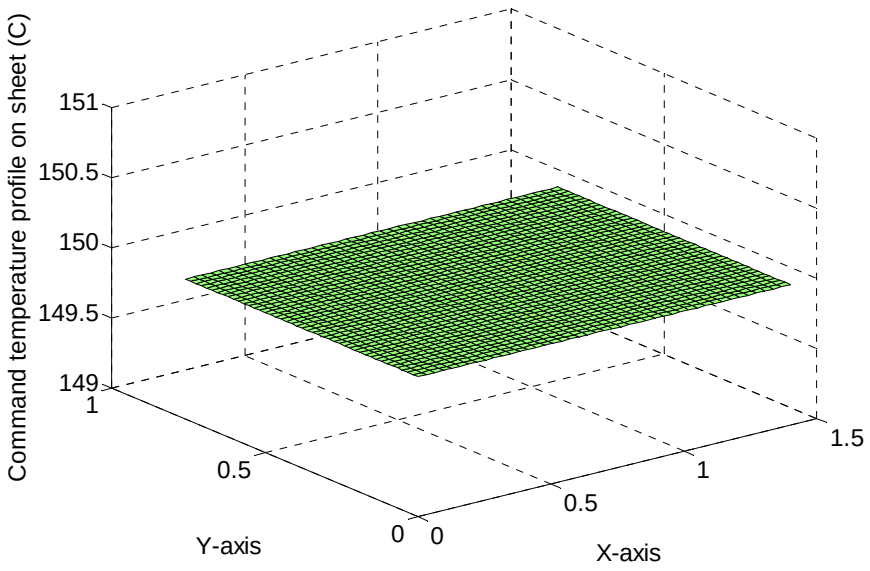
Command temperature profile on sheet (C)
151
150.5
150
149.5
149
1
0.5
0
Y-axis
0
0.5
1
1.5
X-axis

(a)

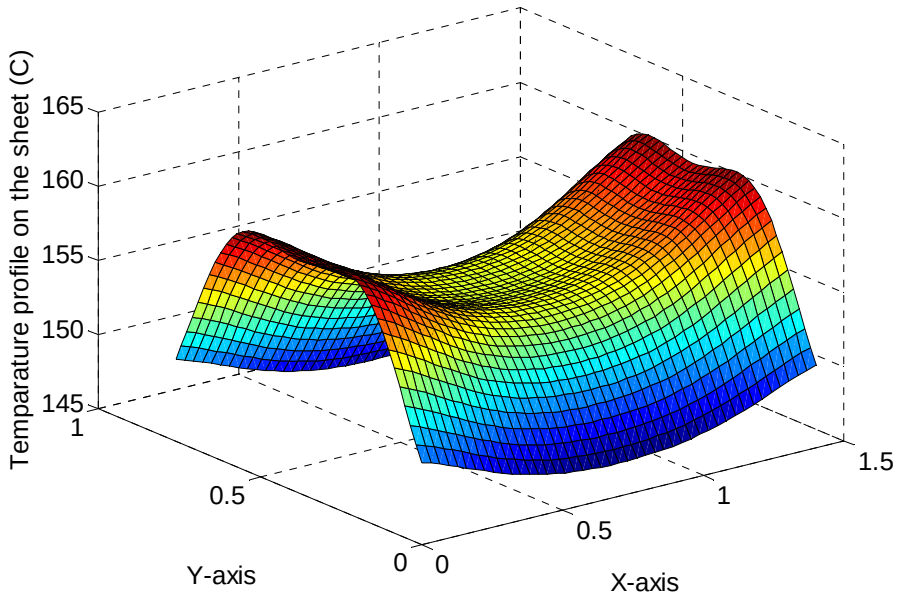
Temparature profile on the sheet (C)
165
160
155
150
145
1
0.5
0
Y-axis
0
0.5
1
1.5
X-axis

(b)

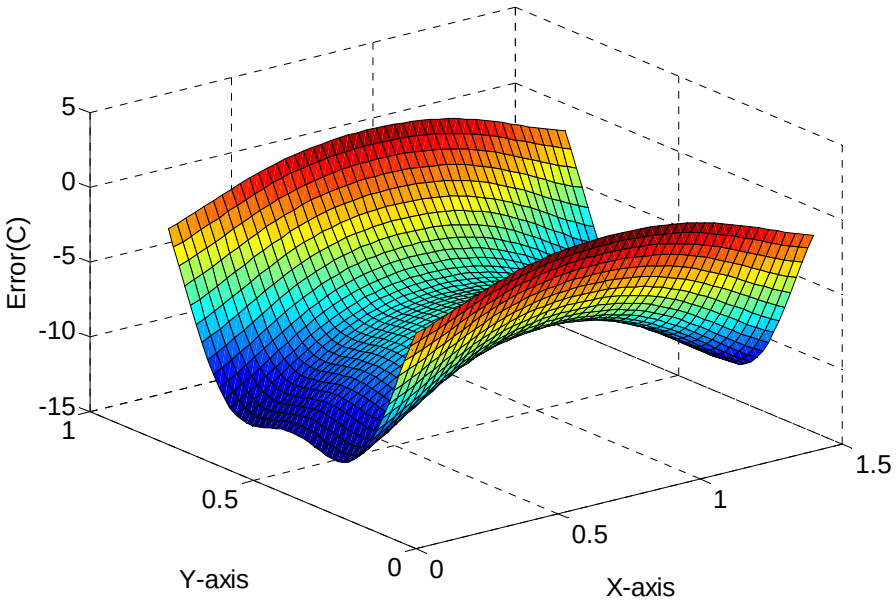


(c)

Fig.4.7: (a) Desired temperature profile (b) Obtained temperature profile after 7th cycle (c) Error between desired and obtained temperature profile using proposed controller

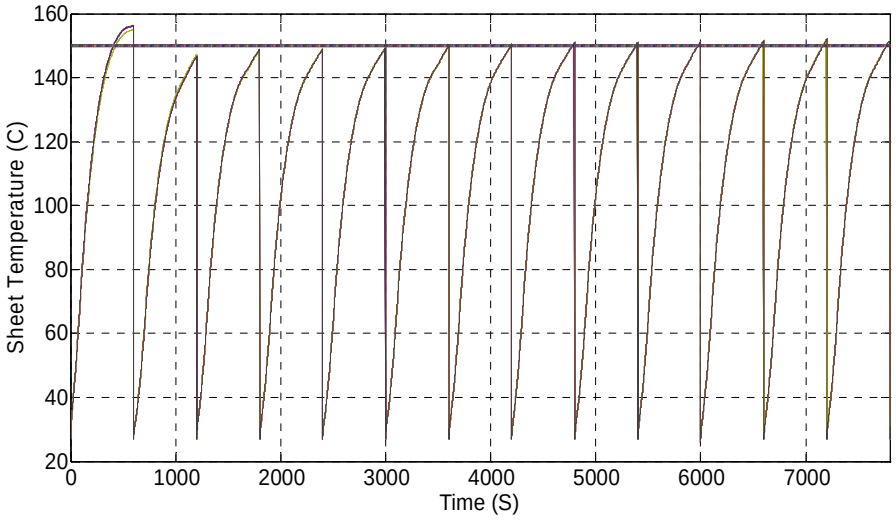


Fig.4.8: The actual temperature and desired temperature at the point of the real sensor for a desired temperature profile of Fig.4.7 (a) using the proposed technique.

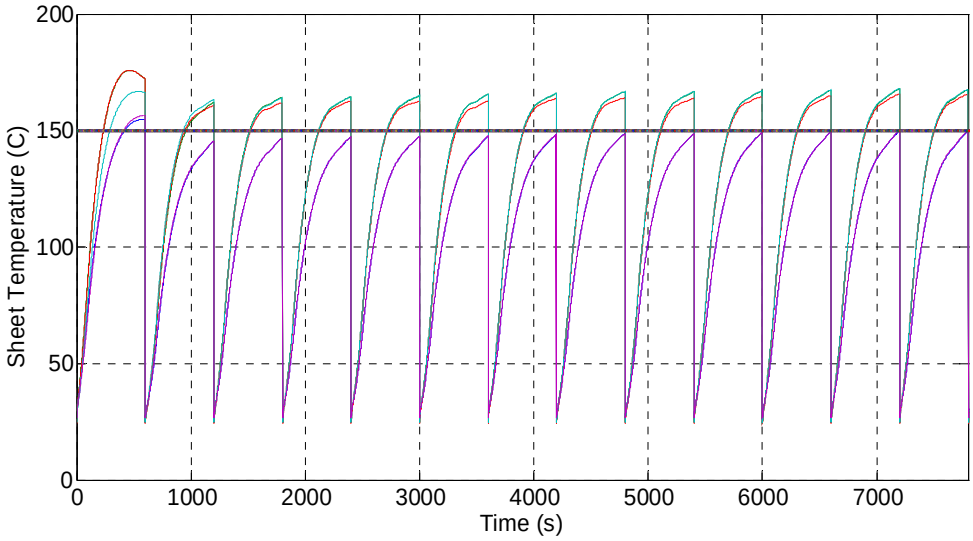


Fig.4.9: The actual temperature and desired temperature at some extreme point of the sheet for a desired temperature profile of Fig.4.7 (a) using the proposed technique.

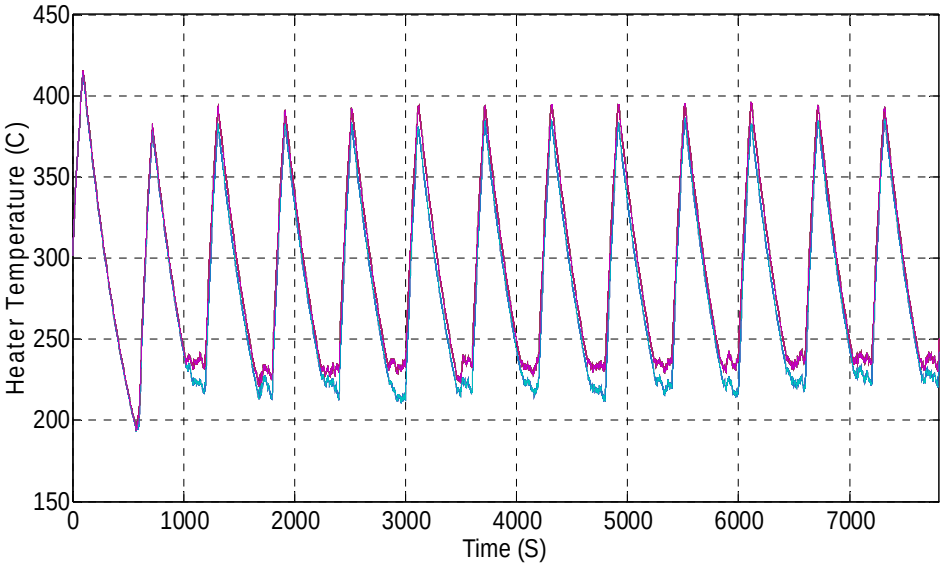


Fig.4.10: The heater temperature for a desired temperature profile of Fig.4.7 (a) for the proposed technique

used, which is impossible in practice. But the proposed controller controls the heater bank temperatures as shown in Fig.4.10 to minimize the error in the sheet temperature. The temperatures of the heaters follow a periodic shape for every cycle of the heating phase. In Fig.4.11 and Fig.4.12, the performance of the proposed controller is compared with the conventional controller for a different desired temperature profile on the sheet, as shown in Fig.4.11 (a). It is clearly observed that the error in the temperature of the sheet after $7^{th}$ cycle is much less in the proposed controller as compared to the conventional controller. In the case of the conventional controller, the temperature at the real sensor points cannot track the desired temperature because of inaccurate estimation of the temperature at the virtual sensor points. If virtual sensors are not used in the conventional controller, then the temperatures at the real sensor locations may track the desired temperature, but temperatures between the real sensors will be off. In Fig.4.13, the desired temperature at different sensor points after a cycle is shown by straight line whereas the actual temperature for the corresponding points is represented in the same color. It is observed that the sheet temperatures at some points can track desired temperatures more accurately with the proposed controller than with the conventional controller. The performance of the harmonic controller is superior to conventional controller because of its better estimation technique as well as improved controllability over the sheet points. At the end, the heater temperature of the thermoforming oven using the proposed controller is shown in Fig.4.14 to obtain the desired sheet temperature of Fig.4.11(a).

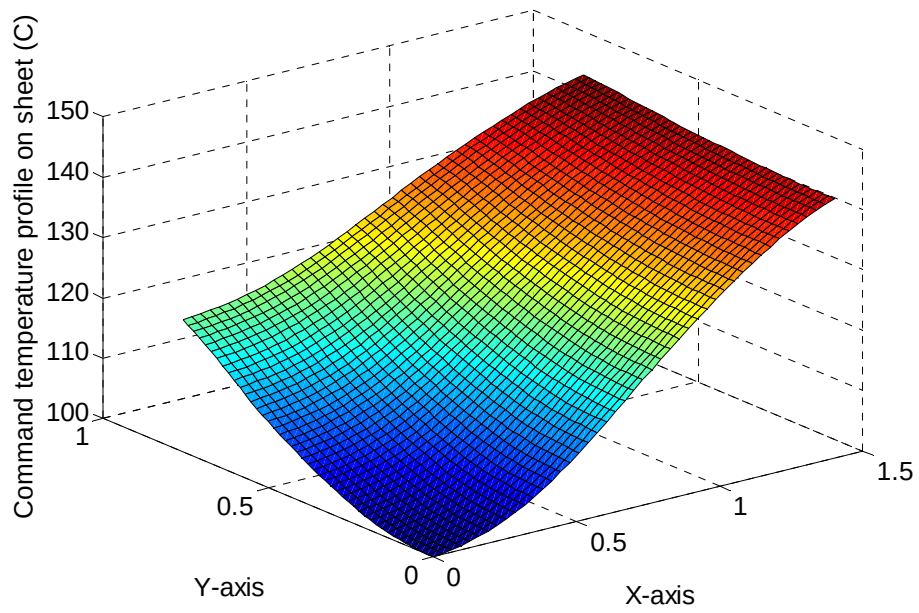
Command temperature profile on sheet (C)
150
140
130
120
110
100
1
0.5
0
Y-axis
0
0.5
1
1.5
X-axis

(a)

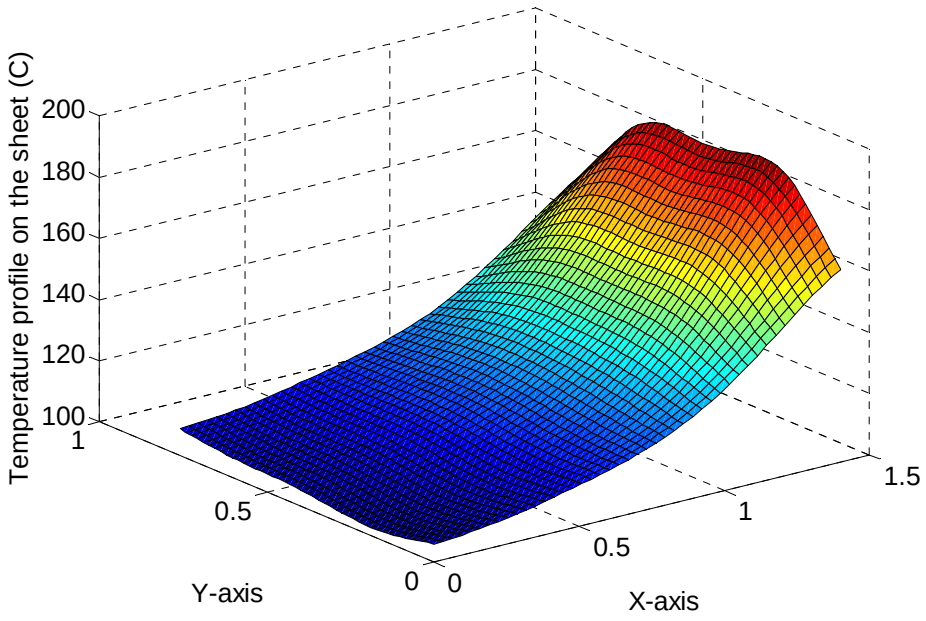
Temperature profile on the sheet (C)
200
180
160
140
120
100
1
0.5
0
Y-axis
0
0.5
1
1.5
X-axis

(b)

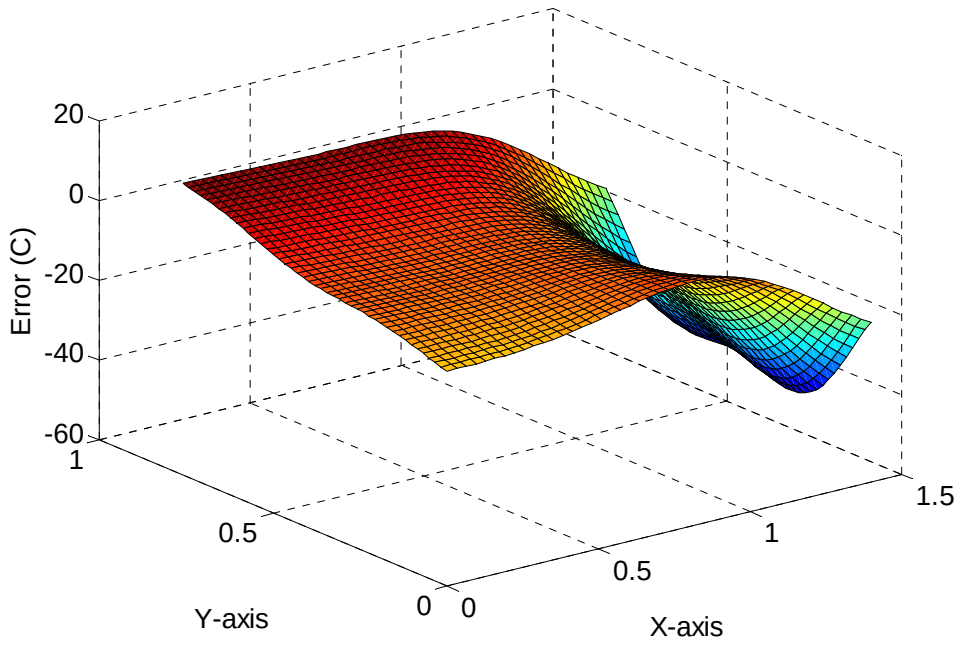


(c)

Fig.4.11: (a) Desired temperature profile (b) Obtained temperature profile after 7th cycle (c) Error between desired and obtained temperature profile using the conventional controller

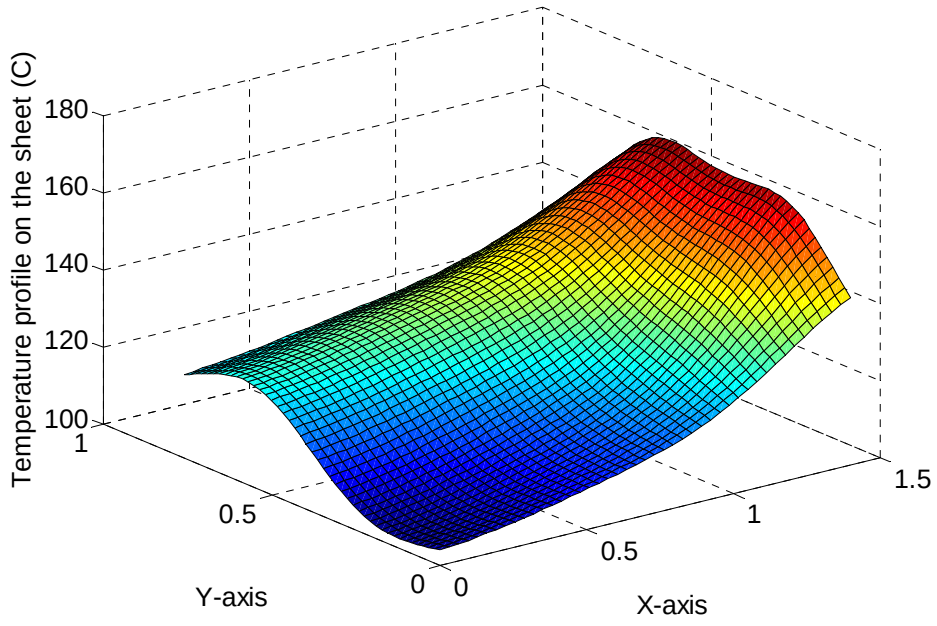


(a)

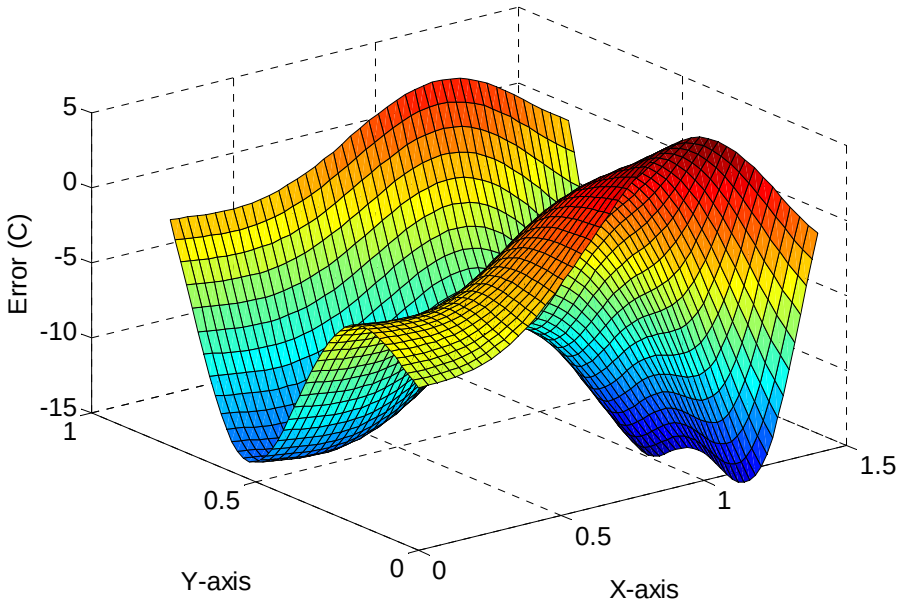


(b)

Fig.4.12: (a) Obtained temperature profile after 7th cycle (b) Error between desired and obtained temperature profile using the proposed controller for a desired temperature profile shown in fig.4.11 (a).

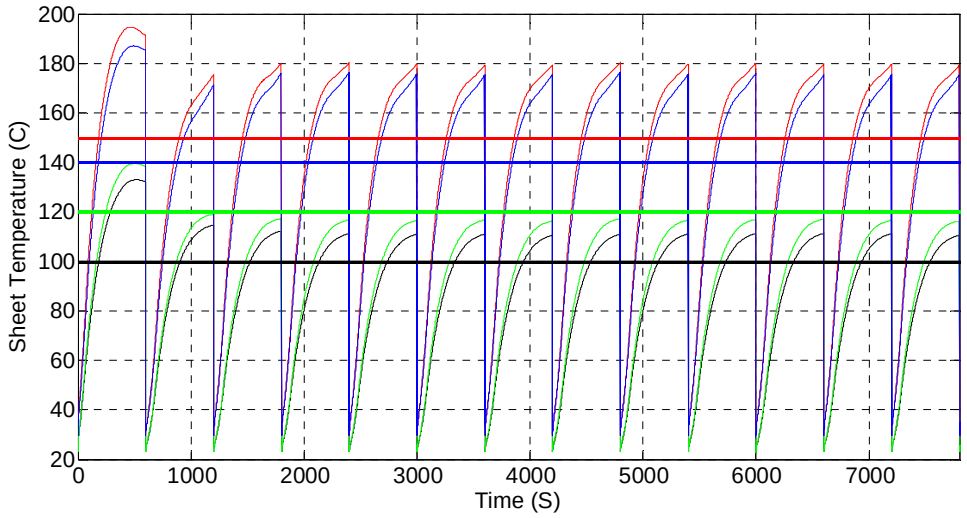


(a)

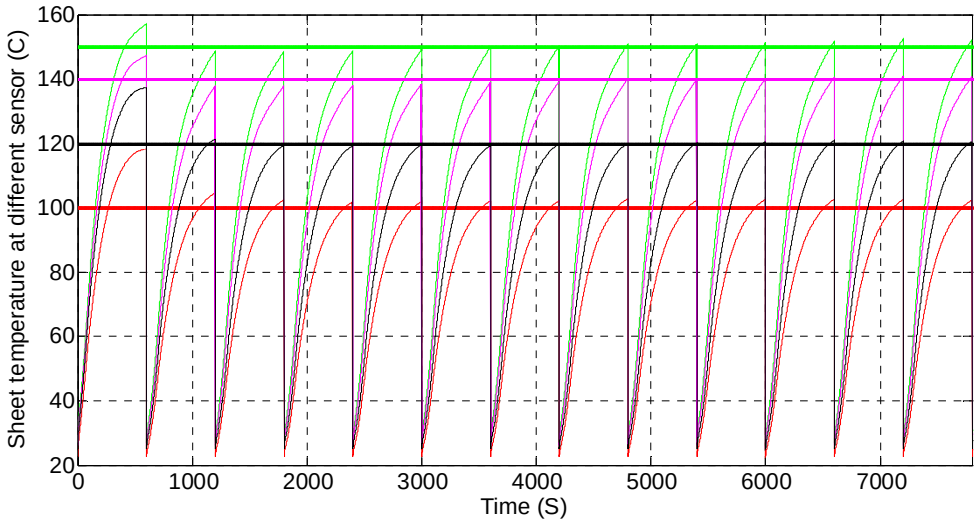


(b)

Fig.4.13: The actual temperature and desired temperature at the point of the real sensor for a desired temperature profile of Fig.4.10 (a). (a) Conventional controller (b) proposed controller.

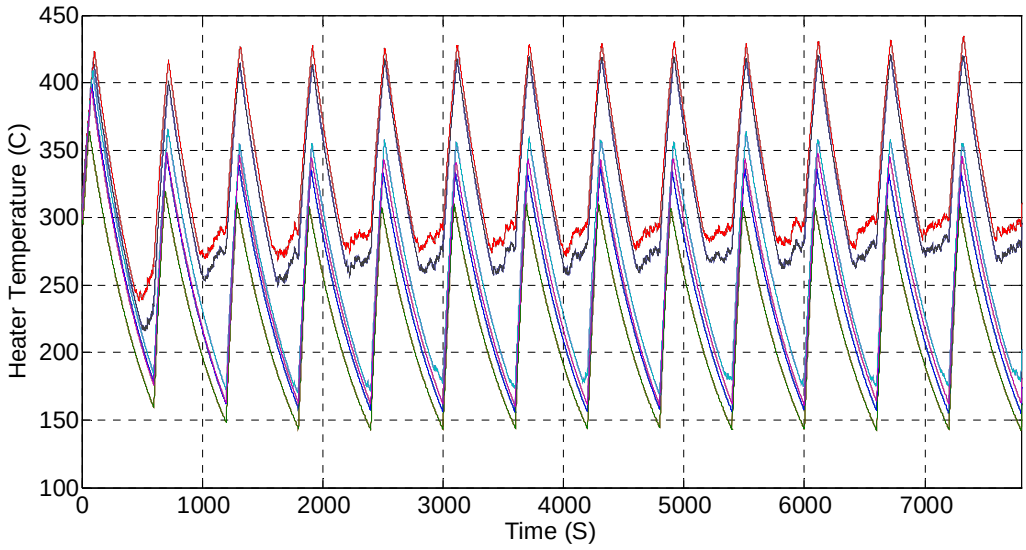


Fig.4.14: The heater temperature for a desired temperature profile of Fig.4.11(a)

## 4.5 Conclusion

A new technique for the estimation of the temperature of a sheet has been developed and a new spatial harmonic controller for the heater bank of the thermoforming process has been presented in this chapter. In the proposed estimation technique, the use of the spatial domain FFT leads to a better control of the sheet temperature. The superiority of the proposed estimation technique and proposed controller is shown through simulation. A performance comparison of the proposed sheet temperature spatial harmonic controller with the conventional controller has also been provided. With the accuracy of the proposed estimation technique evidenced by the results, the prospects of real-time industrial applications of the proposed spatial harmonic controller for sheet temperature in thermoforming are promising. One of the drawbacks of this method is that the sensors have to be placed at equidistant positions. This problem will be addressed in the next chapter.

# Chapter 5

# Estimation and control of temperature profile for non-equidistant temperature sensors

## 5.1 Introduction

The Fourier transform is a popular technique for the estimation of signals and images. This technique can be used for the estimation of the temperature profile over the sheet. In the last chapter, we used the Fast Fourier Transform (FFT) on equidistant sensor data to estimate the temperature profile and control the whole sheet temperature instead of only some points of the sheet. But the positions of the sensors are important to estimate the temperature accurately using an optimal number of sensors. The optimal positions of the sensors to estimate sheet temperature depends on the nature of the temperature profile. Therefore, it is not necessarily the case that optimal sensor positions will be at equidistant positions [13, 112]. As the FFT technique can only be used for equidistant sensor positions, it cannot handle the estimation and control of temperatures in non-equidistant locations of the sensors even though it is used in a wide range of applications, such as image reconstruction and image analysis from its samples. The purpose of this chapter is not to develop algorithms to determine the optimal position of the sensors over the sheet. It is rather to expand the application of the estimation and control method that was developed in the last chapter to those cases where sensors may not be placed at equidistant locations. The proposed method for the estimation of temperature in this chapter can be used for such sensor arrangements. The proposed method is developed in such a way that it can do a high-quality estimation of the temperature profile over the entire sheet through its harmonics. The spatial harmonic controller can then control the harmonics to obtain the desired temperature profile. Computational cost is also considered during the development of the proposed method. The computational cost of

computing Non-Uniform Fast Fourier Transform (NUFFT) to estimate the temperature profile is reduced to make the technique more computationally efficient. The chapter is organized as follows: Section 5.2 presents a modification of the FFT method using Lagrange interpolation in order to use the technique for non-uniform sensor data. In Section 5.3, another method is proposed to predict spatial harmonics directly from the non-equidistant sensor outputs. In section 5.4, a harmonic controller is designed to control these spatial harmonics, which has the effect of controlling the temperature over the whole sheet instead of just controlling temperatures at certain locations. That section is followed by sections comprising simulation results and conclusion. In simulation, the performance of the proposed estimator and controller is tested at different operating conditions to compare with the conventional method of temperature profile estimation based on the weighted average of the surrounding temperature sensors.

## 5.2 Modification of FFT using Lagrange interpolation

The FFT estimation technique for equidistant sensor positions cannot be used for non-equidistant sensor positions. But the temperature profile with non-equidistant sensors can be transformed to an equivalent temperature estimation problem with equidistant sensors using an interpolation technique. The non-equidistant temperature samples can be treated as equidistant temperature samples with a missing data problem. After interpolation, the FFT technique can be applied for estimation and control of the temperature profile of the sheet. There are a lot of interpolation techniques that were developed for interpolation of equidistant and 1-D samples. Some authors expanded those techniques for 2-D samples that can be used even for non-uniform data for image reconstruction [113,114,115,116,117,118]. Although they are good tools that can be used for image reconstruction efficiently, they impose a huge computational burden which makes them impractical to implement for sheet temperature estimation for the purpose of control. We will now discuss one of the most popular interpolation techniques to interpolate the non-equidistant sample data into the equidistant temperature sample data.

*Using Lagrange Interpolation:*

Lagrange interpolation is a useful technique that can be used to estimate the missing data from a non-equidistant temperature sample data to predict the equidistant sample. If the estimated one dimensional function $f(z)$ is a polynomial of degree $n$, then the polynomial function of degree *n* can be completely determined or predicted by its values at $n+1$ points (presuming that the samples satisfy the Kadec condition) using the relation [115],

$$f(z)=\sum_{k=0}^{n} f(z_k)\frac{G_n(z)}{(z-z_k)G_n^{/}(z_k)} \tag{5.1}$$

where

$$G_n^{/}(z_k)=\left.\frac{dG_n(z)}{dz}\right|_{z=z_k} \tag{5.2}$$

$$G_n(z)=(z-z_0)(z-z_1).....(z-z_{n-1})(z-z_n) \tag{5.3}$$

This 1-D Lagrange interpolation formula can be extended to a 2-D signal as shown in Fig.5.1, where a set of non-uniform samples on parallel lines are considered. The parallel lines are symbolized by $\{x_n\}$ and the samples on the lines are symbolized by $\{y_{nm}\}$ where $n$ and $m$ are integers. If $x_n$ is a set of samples satisfying 1-D Lagrange interpolation, then for each real number $y\in R$, $f(x,y)$ is a band limited function in terms of $x$. Since the samples $\{x_n\}$ satisfy the sufficiency condition for Lagrange interpolation, the function can be written as,

$$f(x,y)=\sum_{n=0}^{N} f(x_n,y)\frac{G_N(x)}{(x-x_n)G_N^{/}(x_n)} \tag{5.4}$$

where, $G_N^{/}(x_n)=\left.\frac{dG_N(x)}{dx}\right|_{x=x_n}$ and $N$ is the total number of lines.

Let us consider $y_{nm}$ as a sample data set with number of member $M_n$ for each specific $n$, then the set of 2-D non-uniform samples can be reconstructed by 2-D Lagrange interpolation formula. Now, for each $n$, $f(x_n, y)$ is a band limited 1-D function in terms of $y$ (because the temperature in the plastic sheet cannot change very fast with respect to the change of location). Likewise, the 1-D Lagrange interpolation is

$$f(x_n, y) = \sum_{m=0}^{M_n} f(x_n, y_{nm}) \frac{G_{M_n}(y)}{(y - y_{nm}) G_{M_n}{}'(y_{nm})} \tag{5.5}$$

where, $M_n$ is the number of temperature sample of $n^{th}$ line and $G_{M_n}{}'(y_{nm}) = \left. \frac{dG_{M_n}(x)}{dx} \right|_{x=y_{nm}}$.

Substituting equation (5.5) into equation (5.4),

$$f(x, y) = \sum_{n=0}^{N} \sum_{m=0}^{M_n} f(x_n, y_{nm}) \pi_{nm} \tag{5.6}$$

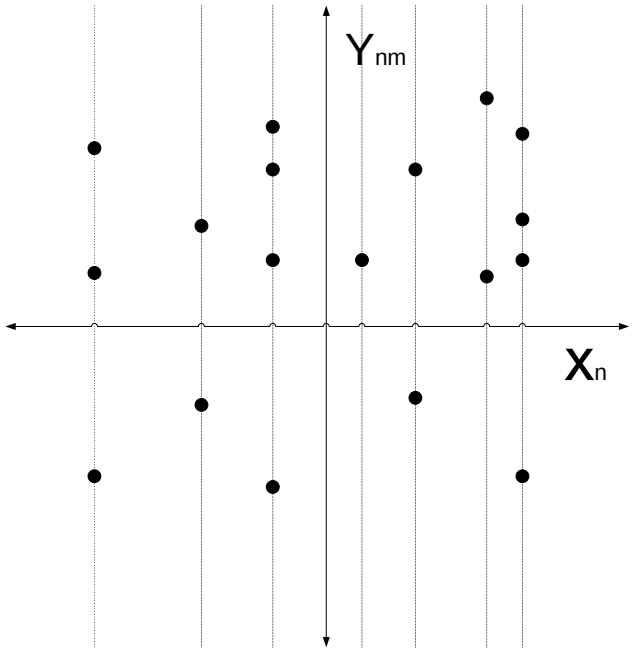


Fig.5.1: Lagrange interpolation for non-uniform data

where,

$$\pi_{nm} = \frac{G_{M_n}(y)}{(y - y_{nm})G_{M_n}{}'(y_{nm})} \frac{G_N(x)}{(x - x_n)G_N{}'(x_n)} \tag{5.7}$$

Up to this point, we only considered the reconstruction of a polynomial. The exponential term is the basis function corresponding to each point $F(m,n)$ in the Fourier space. Therefore, we would like to get the Lagrange interpolation for a 2-D signal in terms of exponentials. As temperature data samples are a set of $N$ number $\{f(z): f(z_k), k = 0,1.....,N-1\} \in R$ of a band limited low frequency function in the sense of spatial frequency content, it can be concluded that its DFT of these sample data $F$ has Hermitian symmetry. Considering the first $K$ samples and last $K-1$ samples of DFT domain has non-zero values, $2K-1$uniform or non-uniform samples of the signal will be sufficient to recover the set. $f(z)$ can be written with its DFT as,

$$f(z_k) = \sum_{i=0}^{K-1} F_i w_k^i + \sum_{i=1}^{K-1} F_{N-i} w_k^{N-i} \tag{5.8}$$

where $w_m{}^j = \exp(\frac{2\pi mj}{N}), m = 0,1,...N-1$

Using Hermitian symmetry,

$$f(z_k) = F_0 + \sum_{i=1}^{K-1} (F_i w_k^i + F_i^* w_k^{-i}) \tag{5.9}$$

The Lagrange interpolation for the exponential polynomial in (5.9) is

$$f(z_k) = \frac{1}{w_k^{K-1}} \sum_{i=0}^{2K-1} f(z_i)(w_{z_i})^{K-1} \pi_{i,k} \tag{5.10}$$

Where , $f(z_i)$ is considered to be symmetric around $z_k$ , and

$$\pi_{i,k} = \frac{\prod_{j} w_k - w_{z_j}}{\prod_{j \neq i} (w_{z_i} - w_{z_j})(w_k - w_{z_i})} \tag{5.11}$$

for 2-D signal this interpolation can also be implemented as already done before,

$$f(x_n, y_{nm}) = \frac{1}{w_n^{K_n - 1}} \frac{1}{w_{nm}^{K_{nm} - 1}} \sum_{i=0}^{2K_n - 1} \sum_{j=0}^{2K_{nm} - 1} f(x_i, y_{ij}) (w_i)^{K_n - 1} (w_{ij})^{K_{nm} - 1} \pi_{ij,k} \tag{5.12}$$

where

$$\pi_{ij,k} = \frac{\prod_{l} w_{k_{im}} - w_{y_{il}}}{\prod_{l \neq j} (w_{y_{ij}} - w_{y_{il}})(w_{k_{im}} - w_{y_{ij}})} \frac{\prod_{l} w_{k_n} - w_{x_l}}{\prod_{l \neq i} (w_{x_i} - w_{x_l})(w_{k_n} - w_{x_i})} \tag{5.13}$$

here, $\pi_{ij,k}, w_y, w_k, w_x$ can be computed offline so it will not represent a huge computational burden.

## 5.3 Spatial harmonic prediction from non-equidistant data

In the last section, a Lagrange interpolation of data obtained from non- equidistant sensors allows the estimation of missing data in a virtual equidistant sensors pattern. That equidistant data can be used in FFT to estimate spatial harmonics of the temperature distribution over the plastic sheet. So the number of harmonics in that case will be the same as the number of the estimated equidistant data points that is higher than the number of actual data points. Sometimes the sensors are positioned in such a non-equidistant pattern that the number of missing sample data obtained using interpolation becomes very high. With the increase of the number of estimated sensor data points as compared to the total reconstructed equidistant data, the probability of erroneous prediction increases. Lots of oscillations could occur in the estimated pattern of equidistant data because of the Lagrange interpolation. These oscillations increase the number of spatial harmonics to be controlled. In this section, a new method is proposed to predict the spatial harmonics directly from non-equidistant data. So the number of the harmonics in this method will be the same as the number of sensor data points.

Consider $T_{NM}$ the vector space that contains all trigonometric polynomials of order $N$ in $x$ and order $M$ in $y$ with the coefficient $a(n,m) \in \mathbb{C}$. So $f(x,y) \in T_{NM}$

$$f(x,y) = \sum_{n=0}^{N-1} \sum_{m=0}^{M-1} a(n,m) \exp(j2\pi(\frac{nx}{N} + \frac{my}{M})) \tag{5.14}$$

Let us consider this trigonometric polynomial in normalized way as,

$$f(x,y) = \sum_{n=0}^{N-1} \sum_{m=0}^{M-1} a(n,m) \exp(j2\pi(nx + my)) \tag{5.15}$$

The equation (5.14) can be compared with equation (4.2) of the previous chapter that was used as the transformation function from the spatial domain of the temperature profile to the sample temperature output at the sensor point of the sheet. In this section, the linear equation (5.14) will be solved based on a least-squares method to find the unknown coefficient $a(n,m)$, which will be used as Fourier coefficient in the spatial harmonic controller of the sheet temperature. Suppose that the samples of the trigonometric polynomial of equation (5.15) are given at the *r* non-uniform sampling points $(x_i, y_i)$. Let us consider $s_i := f(x_i, y_i)$ and $s = \{s_i\}_{i=1 \text{ to } r}$. So we can develop a technique to predict $f(x,y)$ by solving a series of $r$ linear equations for the unknown coefficient $a(n,m)$ with *NM* unknown coefficients. We can write down the $r$ equations as follows:

$$f(x_i, y_i) = \sum_{n=0}^{N-1} \sum_{m=0}^{M-1} a(n,m) \exp(j2\pi(nx_i + my_i)) \tag{5.16}$$

But trigonometric polynomial $f(x,y) \in T_{NM}$ can be uniquely reconstructed from its samples $s_i := f(x_i, y_i)$ only if the system matrix has full rank which means $r \geq MN$. Otherwise there are a few trigonometric polynomial solutions for these equations and system matrix will not have full rank for corresponding linear equations. To avoid this problem, we would chose the number of spatial harmonics $MN$ equal to or less than the number of linear equations which is the same as the number of non-uniform sensor point

temperature data. The linear equation (5.16) resembles a double Vandermonde matrix. It is not easy to solve a system with a Vandermonde matrix directly as it usually has high condition number which implies how sensitive that function is to small changes (or small errors) in its arguments even though some researchers [118] proposed a few numerical methods to solve this kind of system of linear equations in 1-D. The equations in (5.16) can be written as,

$$CA = G \tag{5.17}$$

Where the values of $C$, $A$ and $G$ are given in equation (5.18).

$$C = \begin{bmatrix} 1 & e^{j2\pi y_1} & e^{j2\pi 2y_1} & \dots & e^{j2\pi(M-1)y_1} & e^{j2\pi(x_1+y_1)} & \dots & e^{j2\pi(x_1+(M-1)y_1)} & \dots & e^{j2\pi((N-1)x_1+(M-1)y_1)} \\ 1 & e^{j2\pi y_2} & e^{j2\pi 2y_2} & \dots & e^{j2\pi(M-1)y_2} & e^{j2\pi(x_2+y_2)} & \dots & e^{j2\pi(x_2+(M-1)y_2)} & \dots & e^{j2\pi((N-1)x_2+(M-1)y_2)} \\ : & : & : & : & : & : & : & : & : & : \\ : & : & : & : & : & : & : & : & : & : \\ : & : & : & : & : & : & : & : & : & : \\ 1 & e^{j2\pi y_r} & e^{j2\pi 2y_r} & \dots & e^{j2\pi(M-1)y_r} & e^{j2\pi(x_r+y_r)} & \dots & e^{j2\pi(x_r+(M-1)y_r)} & \dots & e^{j2\pi((N-1)x_r+(M-1)y_r)} \end{bmatrix}$$

$$A = \begin{bmatrix} a(0,0) & a(0,1) & a(0,2) & \dots & a(0,(M-1)) & a(1,1) & \dots & a(1,(M-1)) & \dots & a((N-1),(M-1)) \end{bmatrix}^T$$

$$G = \begin{bmatrix} s_1 & s_2 & s_3 & \dots & \dots & \dots & \dots & \dots & \dots & s_r \end{bmatrix}^T$$

(5.18)

By multiplying by a weight matrix $D$ to compensate for varying density in the sampling geometry or to fine-tune the condition number of the matrix,

$$D\,C\,A \;=\; D\,G \tag{5.19}$$

Where,

$$D = diag\begin{bmatrix} wg_1 & wg_2 & wg_3 & \dots & \dots & \dots & \dots & \dots & \dots & wg_r \end{bmatrix}$$

Here $C$ is a double Vandermonde matrix; QR factorization can be used to solve this system of equations. So $\hat{A} = RA$ is computed first using QR decomposition of $DC$

.Since $DC$ has full rank, there is a unique matrix $Q \in C^{rxMN}$ with orthonormal columns and a unique $NM$ X $NM$ right triangular matrix $R$ with positive diagonal elements such that $DC = QR$. The solution of (5.17) is computed by first evaluating $\hat{A} = Q^* DG$ and then computing $A = R^{-1}(Q^* DG)$.

Sometimes (as an example if the entries of matrix $R$ is very low or if the matrix $C$ is ill-conditioned) based on the position of the temperature sensors, this algorithm has shown to be rather inefficient because of the double Vandermonde matrix. In that case, a new technique is developed in the next part of this section. This method is also based on a least squares method.

From equation (5.16), the total energy of the samples can be expressed as,

$$\sum_{i=1}^{r} | f(x_i, y_i) |^2 w_i$$

$$= \sum_{k=0}^{N-1} \sum_{n=0}^{N-1} \sum_{l=0}^{M-1} \sum_{m=0}^{M-1} a(k,l)\overline{a(n,m)} \sum_{i=1}^{r} \exp(j2\pi((k-n)x_i + (l-m)y_i))w_i$$

$$=< A, ZA > \qquad (5.19)$$

where, $A$ is a vector with coefficients $a(k,l)$ and $Z$ is the matrix with entries,

$$Z_{kl,nm} = \sum_{i=1}^{r} \exp(j2\pi((k-n)x_i + (l-m)y_i))w_i$$

The coefficients $a(n,m)$ have to be determined in such a way that the value of $\sum_{i=1}^{r} | f(x_i, y_i) - s_i |^2 w_i$ is minimum and $f(x,y) \in T_{NM}$.

Consider a new vector, $B=[b(0,0)\ ..\ b(0,M-1)\ b(1,0)\ ..\ b(1,M-1)\ ...\ b(N-1,M-1)]^T$ with the coefficient $b(k,l)=\sum_{i=1}^{r} w_i s_i \exp(-j2\pi(kx_i+ly_i))$.

Hence,

$$\sum_{i=1}^{r}|\ f(x_i,y_i)-s_i\ |^2 w_i=\sum_{i=1}^{r}|\ f(x_i,y_i)\ |^2 w_i-\sum_{i=1}^{r}(s_i\ \overline{f(x_i,y_i)}+\overline{s_i}\ f(x_i,y_i))w_i+\sum_{i=1}^{r}|\ s_i\ |^2 w_i$$

$$=<A,ZA>-<A,B>-<B,A>+\sum_{i=1}^{r}|\ s_i\ |^2\ w_i$$

if $A_{opt}$ is a vector such that $ZA_{opt}=B$ and trigonometric polynomial with $A_{opt}$ coefficient vector is $f(x,y)$, then

$$\sum_{i=1}^{r}(|\ f(x_i,y_i)-s_i\ |^2-|\ s_i\ |^2)w_i+\langle A_{opt},ZA_{opt}\rangle=\langle(A-A_{opt}),Z(A-A_{opt})\rangle>0$$

As Z is invertible (because of full rank), if $A\neq A_{opt}$, the last expression is strictly positive. So the least square is $A_{opt}$. Therefore, $A_{opt}=Z^{-1}B$

$Z^{-1}$ can be computed offline and hence this least squares solution can be obtained by multiplying the $B$ vector with $Z^{-1}$. This least squares solution can be used in the controller directly as the value of the spatial harmonic contents of the sheet temperature.

## 5.4 Incorporating the interpolation into the spatial harmonic controller

The spatial frequency domain transformation is simply a method of expressing the spatial distribution of temperature over the sheet in terms of the sum of its projections onto a set of orthonormal basis functions with different frequencies. In this context, the functions form an orthonormal basis in the space of spatial frequency of temperature distributions and the Fourier transform can be thought of as a transformation of

coordinate basis in this space. As we discussed in the last chapter, the spatial harmonic controller is designed in such a way that it can control the spatial frequency of the temperature distribution instead of conventional way of controlling the temperature at certain sensor points in order to solve two major problems. They are: (1) Spatial harmonic can be controlled independently as they are orthogonal to each other. Control of one harmonic does not affect the control of other harmonics that was not possible in conventional technique. In conventional technique, the temperature at certain points were controlled and control of temperature at one point definitely affect other points in the plastic; (2) This proposed harmonic controller controls the temperature profile over the whole sheet whereas the conventional controller controls temperature only at certain points. The Lagrange interpolation is used in the proposed method to alleviate the drawback of getting equidistant data as shown in Fig.5.2 (a). Then these data will be used to construct the FFT to obtain spatial harmonics. The output temperature of the sheet is measured by some real sensors which are positioned to capture a sufficiently accurate estimation of the temperature profile. The number of sensors depends on how rapidly the expected sheet temperature changes with distance. Therefore, the number of sensors must be high enough as per Nyquist criterion to recover all the spatial harmonics required to control the temperature profile efficiently. The outputs of the real sensors are passed to the interpolator to get the missing data point and estimate the temperature at every equidistant point of the sheet. Thereafter, 2-D FFT tool is used to get the spatial harmonic components of the temperature distribution. The command input for the desired temperature profile is obtained in spatial frequency domain through a 2-D FFT transformation. These spatial harmonics are compared with the actual temperature profile harmonics obtained from real sensors and the error spatial harmonic signal passed to the PI controller. The output of the PI controller is passed through the 2-D Inverse Fourier Transform (IFFT) to convert it into spatial temperature domain on the sheet. So the outputs of the controller are the spatial frequency corresponding to the error of each spatial frequency and the 2D IFFT will compute the 2D signal for every frequency. The next block inverse heating solver will compute the corresponding command heating temperature of the heater bank. Solving the Inverse heating problem with a computationally efficient method is a big challenge. Pseudo-inverse matrix of the view

factor matrix is used in this controller because of its short computational time. In the feedback path of the controller, the outputs of the sensors are used in the interpolation block to get the missing data of the $N \text{ X } M$ rectangular matrix and then the matrix is used for the prediction of spatial harmonics. However, if the number of sensor data is low as compared to the interpolated data, then the prediction of the spatial harmonics becomes erroneous. In that case, the estimation of the spatial harmonics can be done directly from the non-equidistant sensor using least square method as described in previous section. The block diagram for the corresponding method is shown in Fig.5.2 (b).

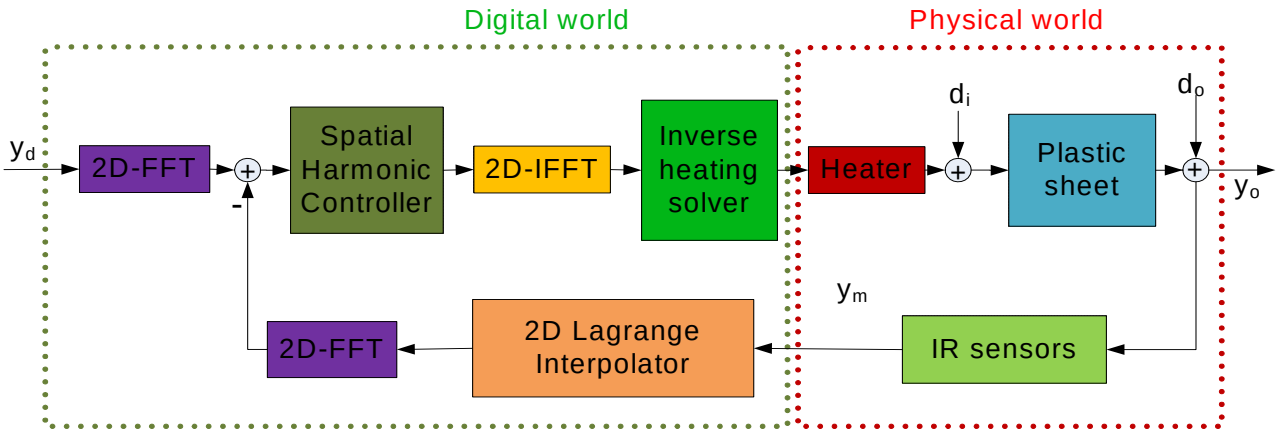


(a)

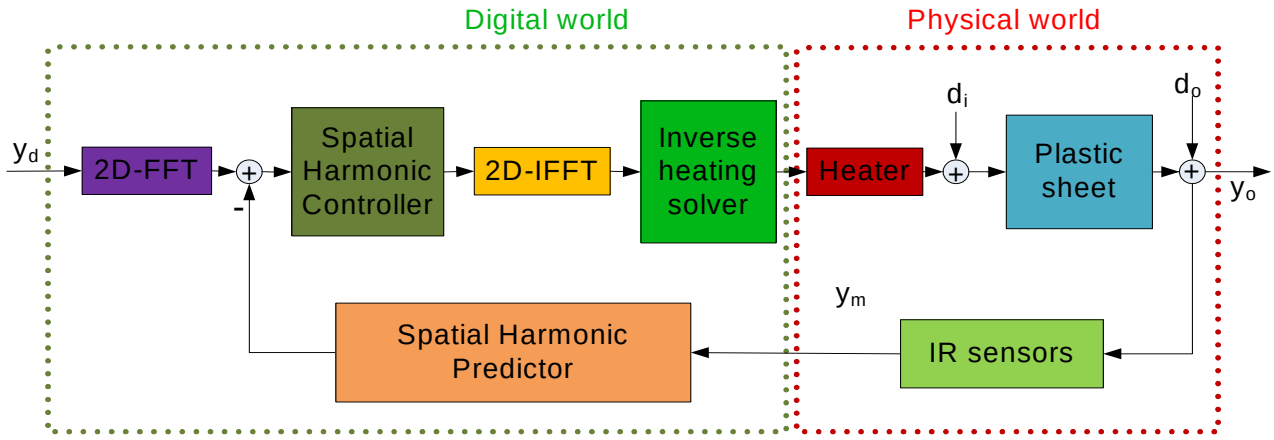


(b)

Fig.5.2: Block diagrams of the proposed spatial harmonic controller of heater bank for thermoforming process (a) Using Lagrange interpolator (b) Using harmonic predictor.

## 5.5 Performance Investigation

In order to verify the effectiveness of the proposed estimation method of temperature profile over the sheet and implementation of the spatial harmonic controller, a computer simulation model is developed in Matlab/Simulink software. The effectiveness of the proposed method of estimation of temperature profile and the new spatial harmonic control technique of the heater bank of the thermoforming process are investigated extensively in simulation in this section. Let us start with a spatial temperature distribution in sheet as shown in Fig.5.3:

$$T(x, y) = 150 - 50e^{-(x^2+y^2)}$$

Now, the proposed estimation technique is used to predict this temperature profile distributed over the sheet. Two types of sensor arrangement are used for the estimation of the sheet temperature to make a comparison of the performance. These sensor locations are shown in Fig. 5.4. At first, temperature of the sheet is estimated using the proposed method in Chapter 4 with 9 real sensors (three rows of sensors with three sensors in each row) at equidistant position over the sheet. The estimated result is shown in Fig.5.5 (a). Thereafter, the temperature is estimated using the proposed technique with Lagrange interpolation in Fig.5.5 (b). In the case of this method only 5 sensors were used and those are located in the positions as shown in Fig.5.4 (a). For this sensor arrangement, the sheet temperature cannot be estimated using the proposed method of Chapter 4 as the location of the sensors is not at equidistance. The Lagrange method is used to interpolate the temperature at the four interpolated points as shown in Fig.5.4 (a). Then FFT is used to estimate whole sheet temperature. In Fig.5.5(c), the non-uniform sensor temperature is used to estimate harmonics using least squares method from the 5 sensor points output with the same position in the sheet. As expected, the FFT method with 9 real sensors gives most accurate estimation as actual temperatures at all those nine points are used to estimate temperature over the whole sheet. It is also found that the proposed two methods are also giving reasonable estimation as compared to the FFT method with 9 sensors. In

case of Lagrange interpolation, the estimation is less accurate because Lagrange interpolation incorporates oscillation in the estimation. But this technique may be more suitable in case of a temperature profile with high oscillation. In the case of the harmonic predictor, the error in estimation of the temperature is low as 1%. Then, the same temperature profile is estimated with the same number of sensors with different locations as shown in Fig. 5.4 (b). In this arrangement, the proposed method with Lagrange interpolation is required to interpolate the sheet temperature at eleven new points to apply the FFT technique in the estimation of the temperature. With an increased number of interpolated-points, the error in estimation increases and eventually propagates through the proposed FFT-based estimation of temperature as shown in Fig. 5.5 (d). This drawback can be eliminated using the proposed spatial harmonics prediction technique. The estimation result for the spatial harmonics prediction technique with the same sensor locations (as in Fig. 5.4 (b)) is shown in Fig. 5.5(e). The errors for all these cases are shown in Fig.5.6. It is observed that the prediction of missing sensor point temperatures using Lagrange interpolation for this particular profile were reasonably accurate as the number of missing points is lower than the number of real sensor temperatures. That helps the proposed estimation to give lower error in 5.6 (b). But if the number of missing data points increases as compared to real sensor data, the error of estimation in the proposed technique increases as shown in 5.6(d) because of the wrong prediction of the missing data by Lagrange interpolation. On the other hand, the spatial harmonics prediction technique gives very reasonable error as shown in in Fig. 5.6 (c) and Fig. 5.6 (e) for both arrangements of the sensors.

In the next step, a simulation model is developed using Matlab/Simulink. The simulation model of the thermoforming heating oven (Fig. 4.1) was used for the simulation. Five real sensors are used in the sheet to sense the temperature. The performance of the proposed spatial harmonic predictive controller is compared with a conventional PI controller that is based on the error at the sensor points (5 real sensors and 20 virtual sensors). The cycle duration is 600 sec. At the beginning of each cycle, the plastic sheet is entered into the oven and it is heated until the end of the cycle to obtain the desired temperature profile by the heaters of the oven. Thereafter, the sheet is transferred to the forming phase at the end of the cycle and a new sheet enters the oven to

get heated for the new cycle. As we did in Chapter 4, we choose the seventh cycle instead of the first cycle to show the control behavior of the controller. The reference temperature profile is shown in Fig.5.7 (a). The outputs of the sensors are used to calculate the spatial frequency and a PI controller is used to control the heaters such that the sheet spatial harmonics converge at the desired spatial frequencies. The sheet temperature errors at the end of the cycle for the proposed harmonic predictive controller and the conventional controller are shown in Fig.5.7 (b) and Fig.5.7(c), respectively. It is observed that the proposed method gives better results than the conventional method. As the harmonic controller controls the temperature over the whole sheet rather than certain points only, it results in much less error with the reference temperature profile. We can conclude that the performance of the proposed controller has the same performance as in Chapter 4 even though the estimation of temperature was more accurate. Because of the weakness of the actuator (heaters of the thermoforming oven), the performance of the controller cannot be improved even with better estimation of the temperature.

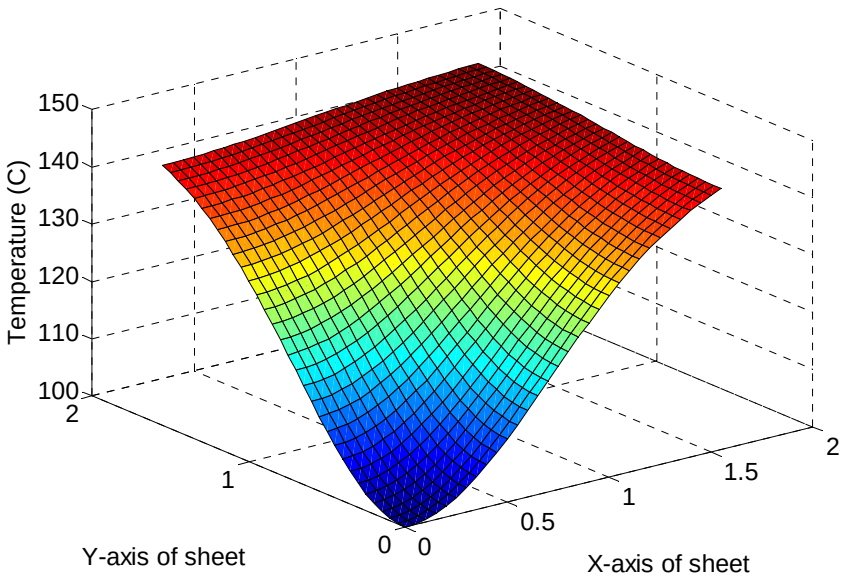


Fig.5.3: Assumed temperature over the sheet

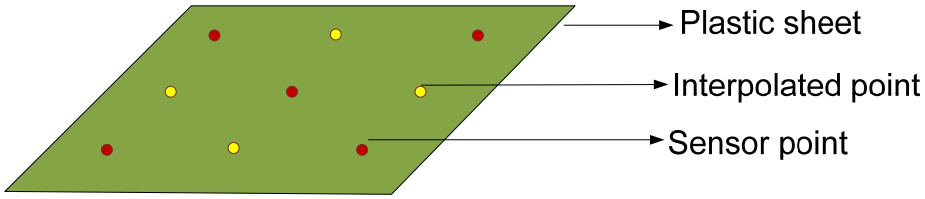


(a)

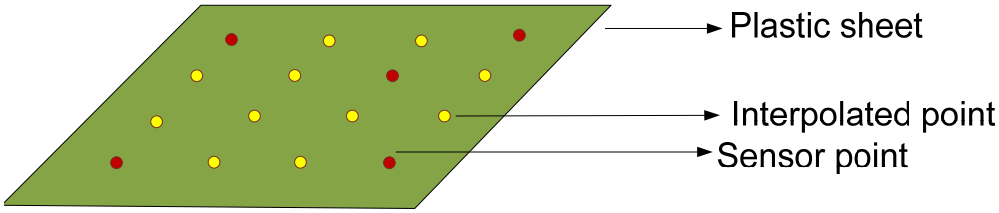


(b)

Fig.5.4: Sensor position arrangement used in simulation results

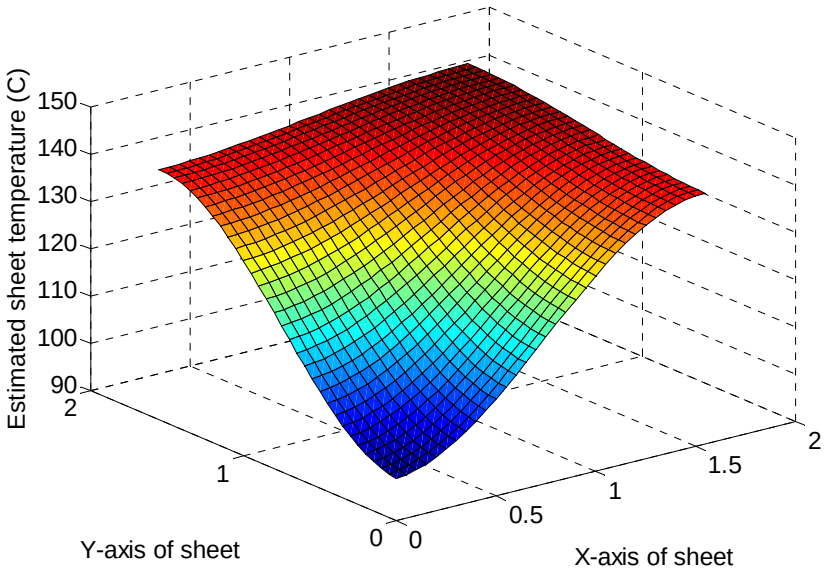


Fig.5.5 (a): The estimated temperature profile using the proposed technique in Chapter 4 with 9 equidistant sensors

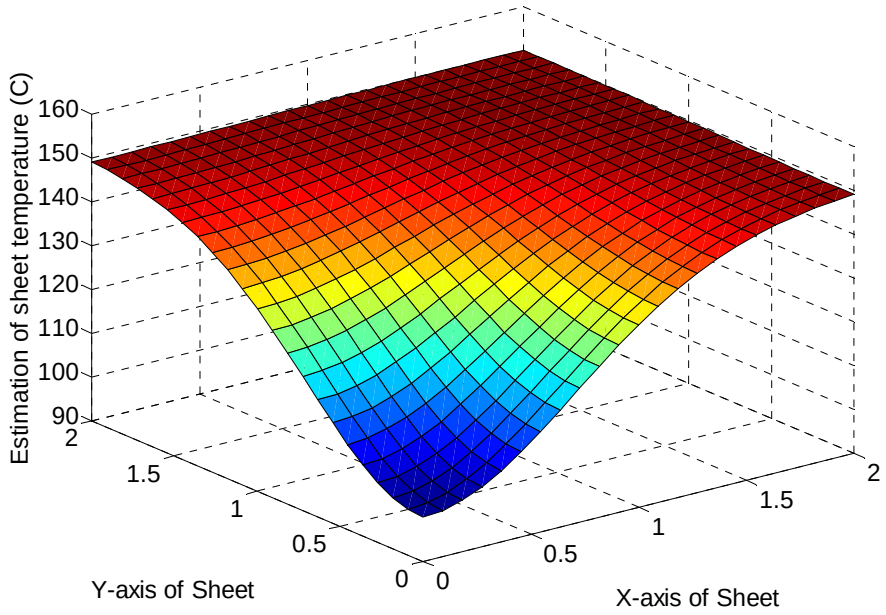


Fig.5.5 (b): The estimated temperature profile using proposed Lagrange interpolation technique with 5 sensors at the locations shown in Fig. 5.4(a)

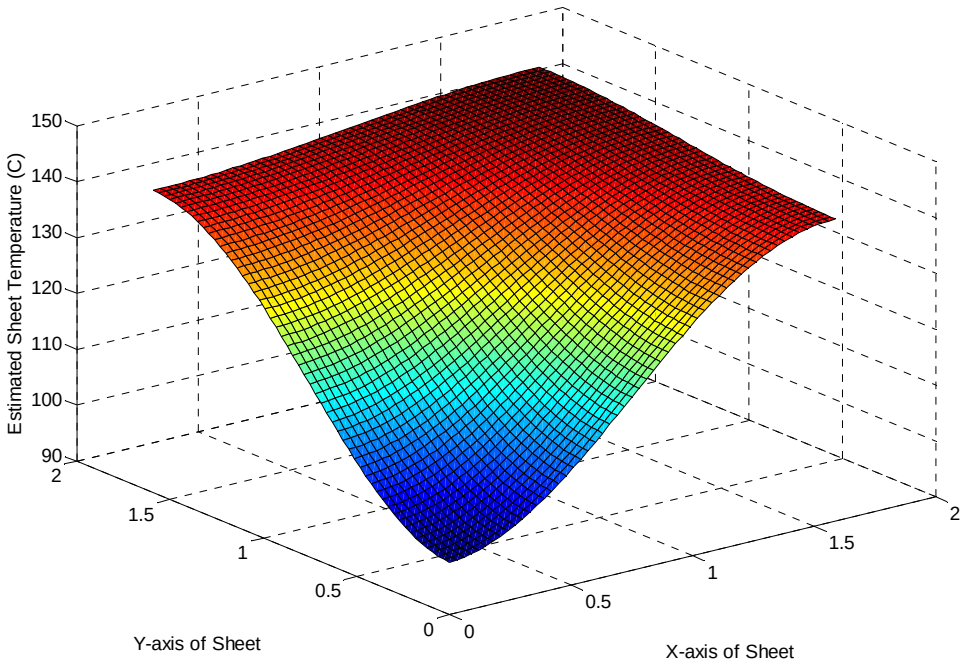


Fig.5.5(c): The estimated temperature profile using proposed harmonic predictor technique with 5 sensors at the locations shown in Fig. 5.4(a)

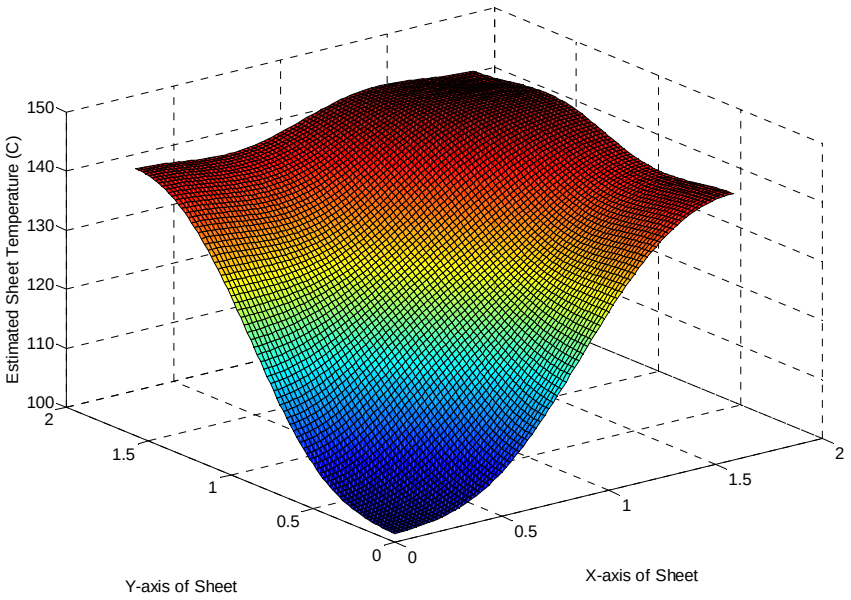


Fig.5.5 (d): The estimated temperature profile using proposed Lagrange interpolation technique with 5 sensors at the locations shown in Fig. 5.4(b)

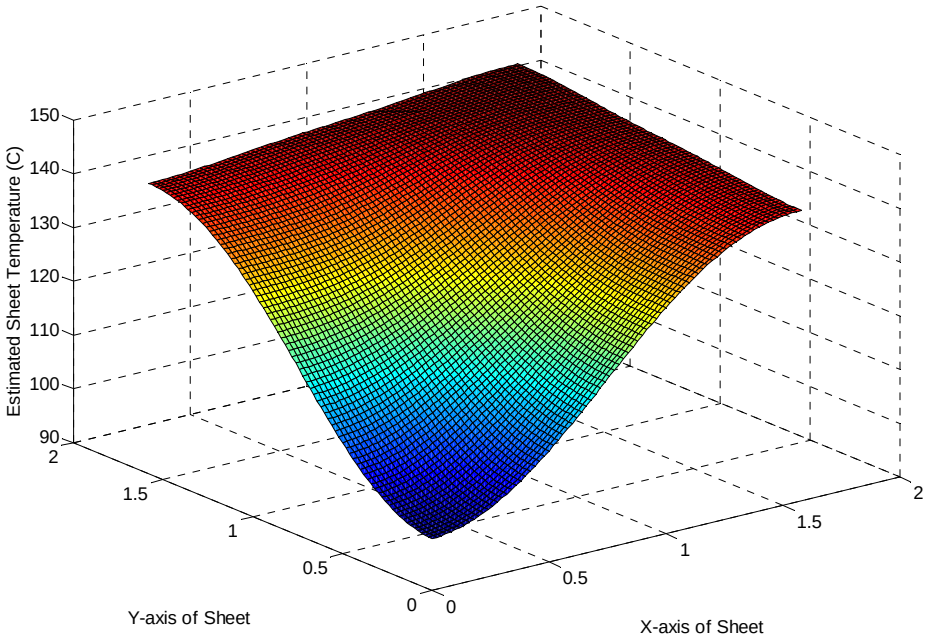


Fig.5.5 (e): The estimated temperature profile using proposed harmonic predictor technique with 5 sensors at the locations shown in Fig. 5.4(b)

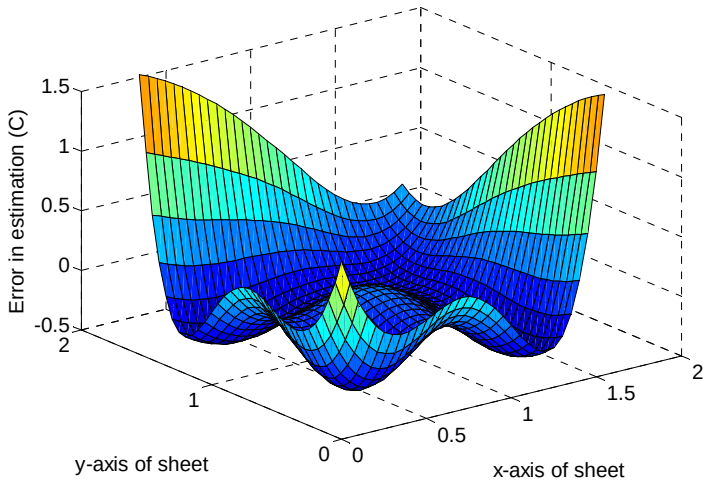


Fig.5.6 (a): The error in estimated temperature profile using the proposed technique in Chapter 4 with 9 equidistant sensors

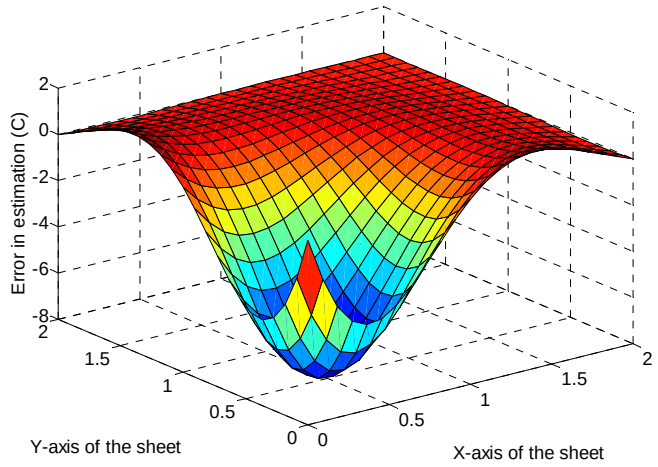


Fig.5.6 (b): The error between the actual temperature and estimated temperature using modified technique with 5 sensors (as shown in Fig. 5.4(a)) using Lagrange interpolation

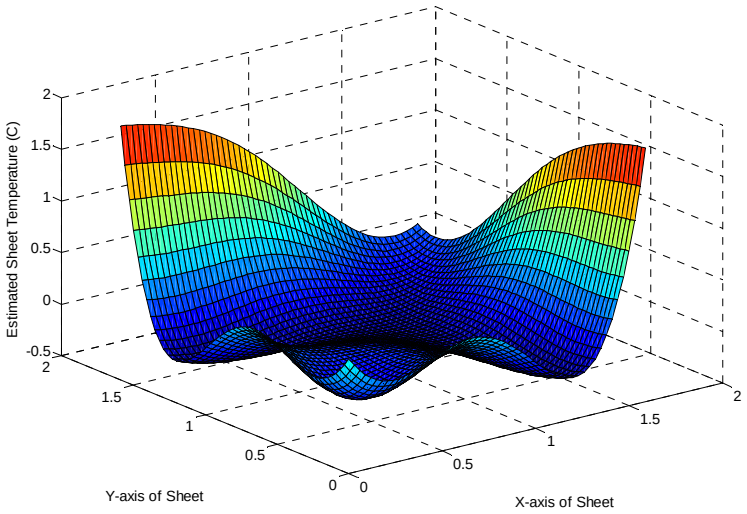


Fig.5.6 (c): The error between the actual temperature and estimated temperature using harmonic predictor technique with 5 sensors (as shown in Fig. 5.4(a))

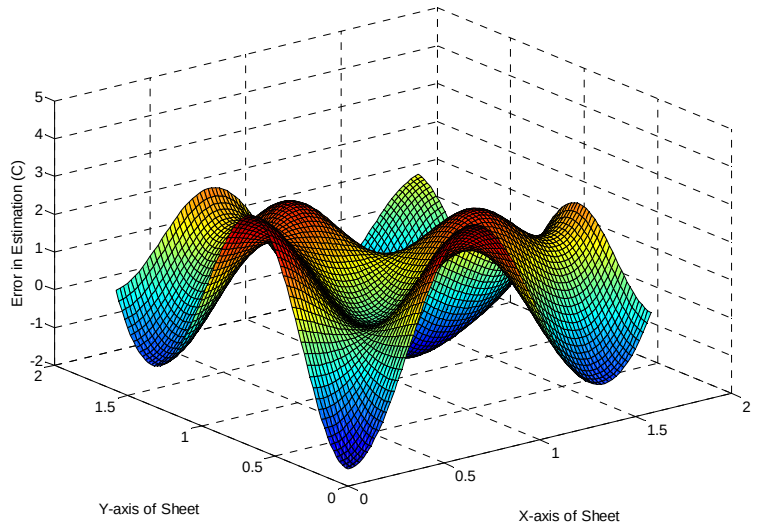


Fig.5.6 (d): The error between the actual temperature and estimated temperature using modified technique with 5 sensors (as shown in Fig. 5.4(b)) using Lagrange interpolation

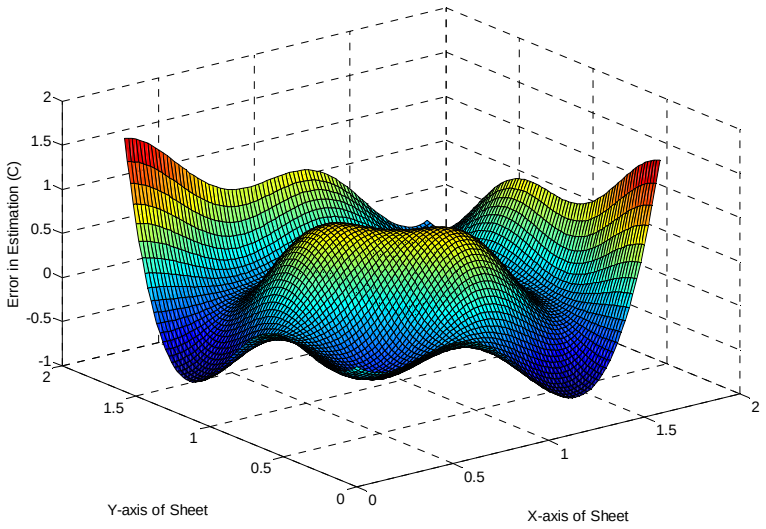


Fig.5.6 (e): The error between the actual temperature and estimated temperature using harmonic predictor technique with 5 sensors (as shown in Fig. 5.4(b))

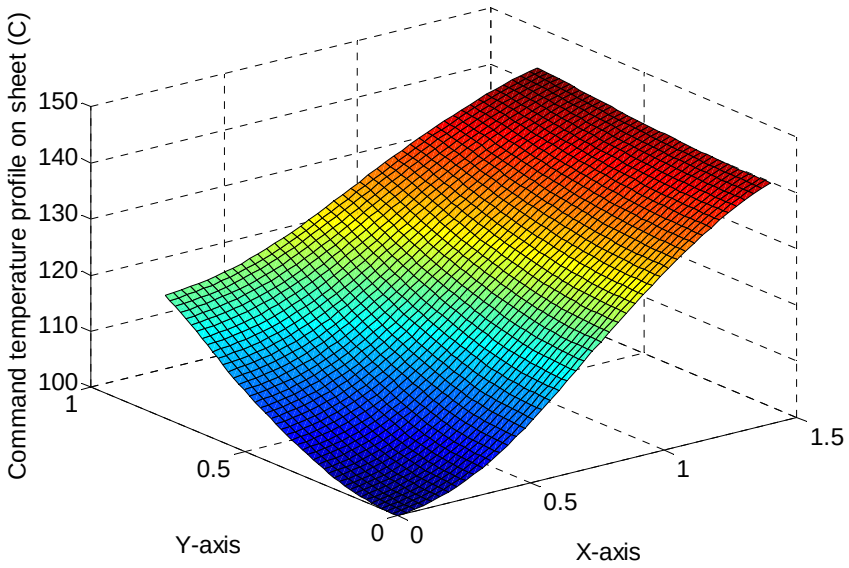


(a)

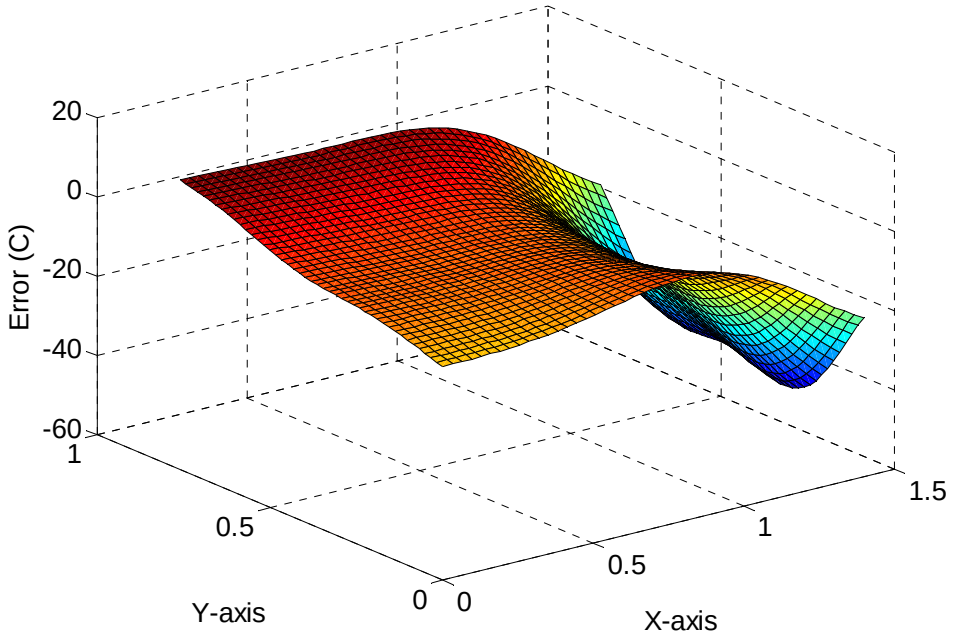


(b)

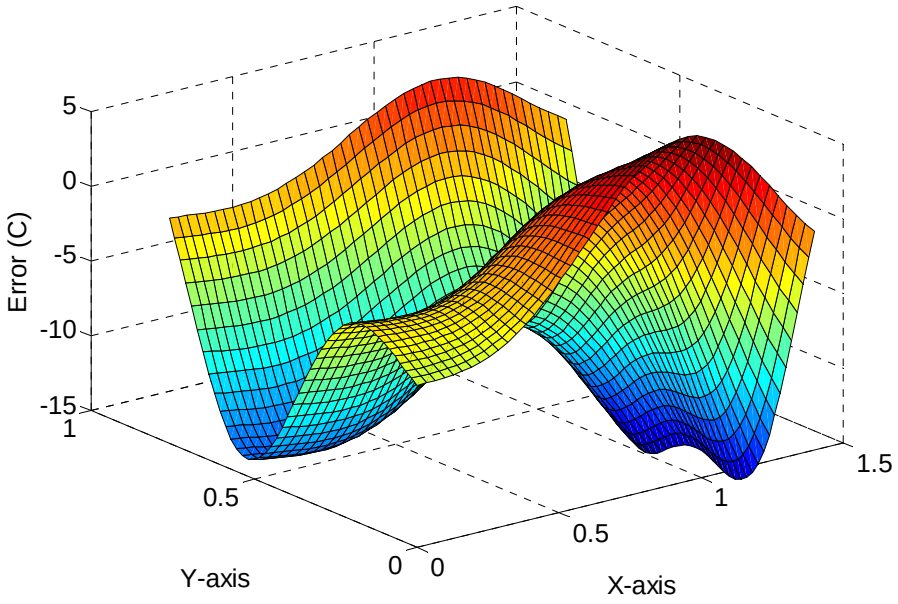


(c)

Fig.5.7: (a) Desired temperature profile (b) Error between desired and obtained temperature profiles using conventional controller (c) Error between desired and obtained temperature profiles using harmonic predictive controller.

## 5.6 Conclusion

This chapter proposed two different techniques to expand the application of the proposed estimation and control technique for the estimation of the temperature profile over a sheet in the last chapter in case of non-equidistant sensors. These two different techniques: one based on Lagrange interpolation and other based on spatial harmonic prediction method are proposed for two different scenarios to achieve better performance in estimation and control. Typically, the optimum placement of the sensors over the sheet is organized in such a way that yields a lot of missing sensor data to achieve the equidistant pattern of the sheet temperature. Therefore, we have shown through simulations that the proposed harmonic predictive controller is likely to give better performance than the modified harmonic controller based on Lagrange interpolation in that case.

# Chapter 6

# Model Predictive Control of Heating Phase

## 6.1 Introduction

In Chapters 4 and 5, we presented a new method to sense plastic sheet temperature. This chapter presents a method to control the surface temperature of a plastic sheet that not only gives an optimal performance but also takes into consideration the process constraints in calculating the control input. Although control techniques have been developed for the heating phase of the thermoforming process, oven heater temperatures in the thermoforming industry are still largely adjusted by trial and error based on the experience of the operator.

This process is a multi-input, multi-output (MIMO) system with a high degree of coupling between inputs and outputs which introduces additional complexity. With the continuous growth of the thermoforming industry and ever-expanding applications of plastic parts, the demand for rapid production of complex parts with tighter tolerances, superior finish and lower cost is increasing rapidly. These requirements cannot be met without a sophisticated process control system providing accurate control of key process variables that are inherently nonlinear and time-varying. Adaptive control does not give good performance for nonlinear systems with parameter uncertainty and it is sensitive to unmodelled dynamics and disturbances. It may have poor transient that affect the performance of the thermoforming process. It also requires a lot of computation for a large and complex system like the thermoforming process. Model Predictive Control (MPC) is one of the advanced and popular methods for process control that has been used on different plants since the 1980s [119]. Even though the MPC controller can handle a multi-input multi-output (MIMO) process, a large number of computations make it difficult to apply to large systems such as multi-zone temperature control in a

temperatures in the thermoforming industry are still largely adjusted by trial and error based on the experience of the operator.

This process is a multi-input, multi-output (MIMO) system with a high degree of coupling between inputs and outputs which introduces additional complexity. With the continuous growth of the thermoforming industry and ever-expanding applications of plastic parts, the demand for rapid production of complex parts with tighter tolerances, superior finish and lower cost is increasing rapidly. These requirements cannot be met without a sophisticated process control system providing accurate control of key process variables that are inherently nonlinear and time-varying. Adaptive control does not give good performance for nonlinear systems with parameter uncertainty and it is sensitive to unmodelled dynamics and disturbances. It may have poor transient that affect the performance of the thermoforming process. It also requires a lot of computation for a large and complex system like the thermoforming process. Model Predictive Control (MPC) is one of the advanced and popular methods for process control that has been used on different plants since the 1980s [119]. Even though the MPC controller can handle a multi-input multi-output (MIMO) process, a large number of computations make it difficult to apply to large systems such as multi-zone temperature control in a thermoforming machine. In this chapter, the design of a model predictive controller is presented and implemented on a complex thermoforming oven with a large number of inputs and outputs for precise control of sheet temperatures under hard constraints on heater temperatures and their heating/cooling rates. Multi-parametric programming is used to reduce computational complexity.

MPC has some interesting features. As an example, it can automatically compensate for process interaction and measure the disturbances as well as handle difficult process dynamics such as dead-time dominant dynamics. Another important advantage of this type of control is its ability to cope with hard constraints on controls, outputs and states. So MPC can optimize the performance by allowing for operation close to the system constraints. MPC is also able to handle structural changes and it is easy to tune. Details of MPC control can be found in [117,118].

An MPC predicts future control inputs by solving the optimization problem over an output horizon involving the minimization of a cost function using the model of the plant at each sampling instant. The computation of the optimization problem at every sampling instant may require complex calculations that demand a high speed processor [119]. Due to the online optimization at every sampling instant, MPC has not been an effective technique to deal with large multivariable constrained systems that increase computational complexity in solving the optimization problem. Moreover, although several issues like stability, feasibly and performances of linear MPC control are well developed and understood [117,118,119], much work needs to be done in the field of nonlinear MPC to make it popular in industry. Thus, the large system size and the presence of nonlinearities in the heating phase of thermoforming seem to have discouraged control engineers from using optimal control techniques for this kind of system. Recently, some works [120,121] have developed explicit solutions of the optimization problem and proposed a new framework to deal with a nonlinear system as a combination of piecewise affine hybrid systems. These results extend the applicability of the MPC controller to low-cost, slow processors and improve software adaptability and ratability in real-time implementation. These open a new door to the possibility of real-time implementation of optimal control techniques for large multivariable constrained systems such as the thermoforming process.

Multi-parametric quadratic programming helps in solving the model predictive optimization problem offline which reduces the real-time computational burden of the controller. Thus, in this chapter, we explore model predictive control using the explicit solution of the optimization problem (with the help of multi-parametric quadratic programming) for temperature control of a thermoforming machine. In this chapter, we introduce MPC for controlling the process in the first Section 6.2 whereas in the following Section 6.3 and Section 6.4, we discuss the multi-parametric quadratic programming used to solve the online optimization with an offline strategy in the development of MPC for the heating phase of thermoforming process. In Section 6.5, the design procedure of multi-parametric MPC is developed for the heating phase of the thermoforming process. The performance of the controller is investigated in Section 6.6.

## 6.2 Model predictive controller

The main concept behind MPC is using the information from the mathematical model of a system to predict future control inputs to optimize an objective function such that the desired performance of the system can be obtained. So, an optimization problem needs to be solved to predict the optimal control input over a future time horizon such that it minimizes or maximizes a predefined performance objective satisfying the process constraints. MPC does not only compute the optimal control input, it also considers the physical and operational constraints of the system as well as the current and past history of the plant to predict future corrective actions. MPC is basically an optimization problem which involves a performance objective function of the form:

$$J = \min_{\Delta u} \sum_{i=1}^{N_p} [\hat{y}(t+i) - y_r(t+i)]^T Q_i [\hat{y}(t+i) - y_r(t+i)] + \sum_{i=0}^{N_u-1} [\Delta u(t+i)^T R_i \Delta u(t+i)] \tag{6.1}$$

Subject to the inequality constraints for $t \in [0, T]$

$$\begin{aligned} u_{\min} &\le u(t) \le u_{\max} \\ y_{\min} &\le y(t) \le y_{\max} \\ g(x(t), u(t)) &\le 0 \end{aligned} \tag{6.2}$$

and the process dynamics;

$$\begin{aligned} x(t+1) &= f(x(t), u(t)) \\ y(t) &= h(x(t)) \end{aligned} \tag{6.3}$$

where the state is $x(t) \in \mathbb{R}^n$, the input is $u(t) \in \mathbb{R}^m$, the output is $y(t) \in \mathbb{R}^m$ and its prediction is $\hat{y}(t) \in \mathbb{R}^m$. In this control technique, at every sampling time instant the control move is predicted from the current time along the finite fixed horizon. However, only the first input is adopted as the control move and the whole procedure is repeated at the next sampling time. The control technique is shown in Fig. 6.1. At any time sample $k$, the optimization problem is solved to predict the optimal control input over the control horizon (four samples in this figure) such that it minimizes or maximizes the performance

objective over the output horizon

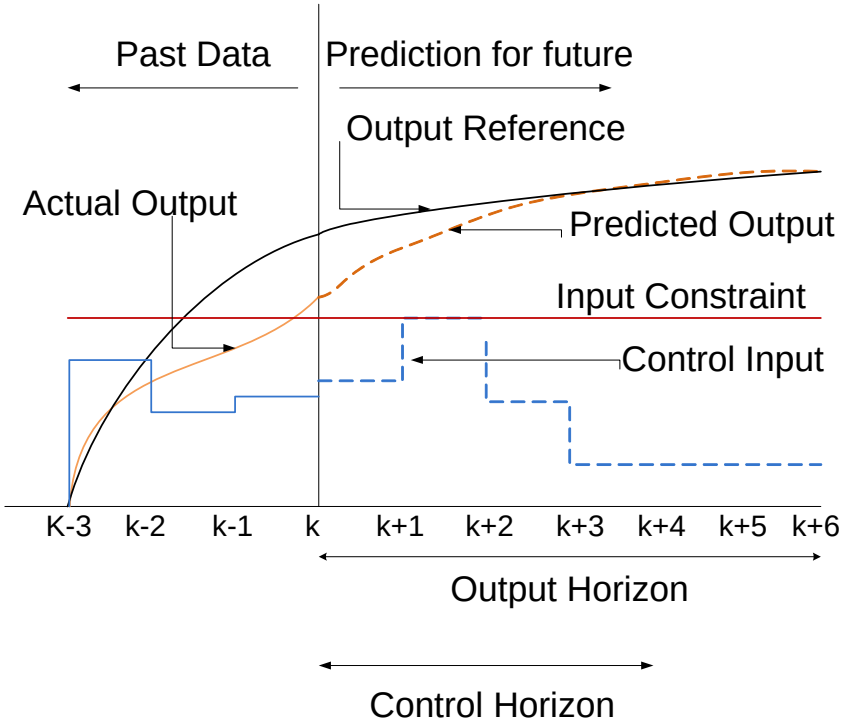


Fig. 6.1: Model Predictive Control

(six samples in this figure) taking into consideration the process constraints. The first term in equation (6.1) corresponds to the minimization of the predicted error over future time horizon, whereas the second term in the equation corresponds to the minimization of the control input over the control horizon. The $Q$ and $R$ are the weight matrices for tracking and control input of the system respectively. The main challenge in applying MPC is the computational burden of online optimization.

## 6.3 Multi-parametric quadratic MPC

The computation of the optimization problem online is a problem for complex MIMO process. So researchers have been working to come up with a technique to compute the optimization offline. Pistikopoulos, Georgiadis and Dua [123] proposed a new concept to compute the online optimization offline by parametric optimization

techniques named as Multi-Parametric Programming and express the solution of the optimization as a combination of affine functions of states and inputs. Hence, they succeed to overcome the implementation problem due to computational burden of the conventional MPC controller [123]. The solution is computed offline and the controller obtains its control move based on the value of the state using some affine function through which the computational burden for online optimization disappears. Using this offline parametric computation technique instead of a numerical optimization technique to solve the optimization problem is starting a new era for the implementation of MPC for large, fast multivariable plants using simple hardware. In this technique, the state space is divided into partitions or critical regions based on the system equations and objective function to be optimized. In each partition, an explicit affine function of the optimization variables and parameters makes up a complete map of look-up functions to optimize the performance objective function as shown in Fig. 6.2. The MPC controller computes future control input sequence at every sampling instant using the look up functions of state as an explicit control law. The procedure of multi-parametric quadratic MPC is as follows: at first, the current value of the state of the system is measured and then the partition to which the current value of the state belongs to is identified. The next step is to retrieve the corresponding affine function belonging to the region and calculate the control move by evaluating the explicit function using the value of the current state.

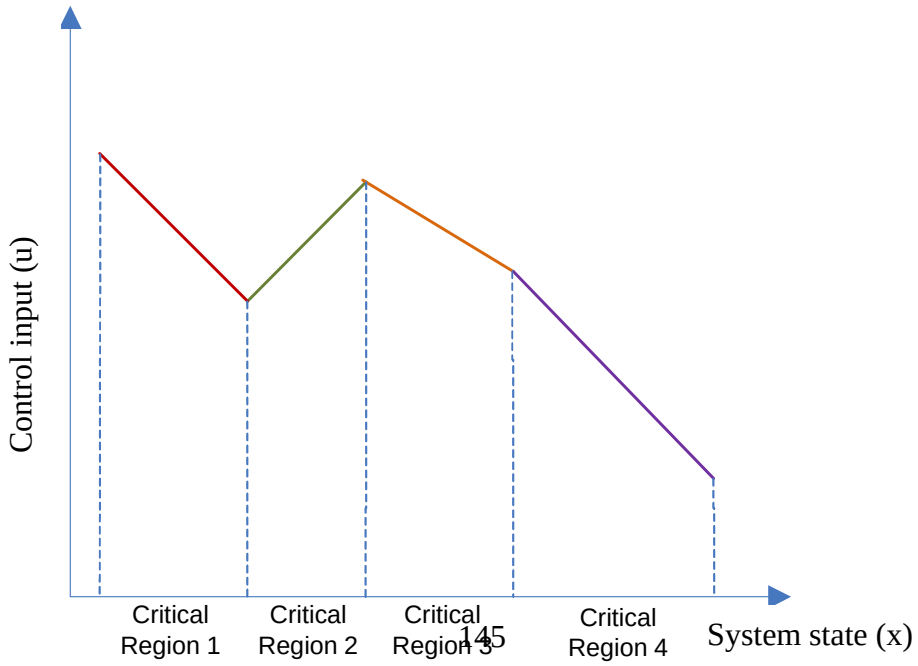

Fig. 6.2: Solution of control input as a look up function of state in different partition or critical region in 2D space

## 6.4 Multi-parametric quadratic MPC for heating phase of thermoforming

The thermoforming process is a complex multi-input multi-output system linking heater temperatures to infrared sensors outputs. Thus, employing a simple PI or PID controller cannot ensure satisfactory performance because it does not take the process constraints into consideration. A model predictive controller may be a better choice for controlling the heating phase. Although the heating phase of thermoforming machines is a slow process (which will give more time for computation), the number of system equations is high when multiple sensors are used (it will increase the amount of computation). Thus, much computation and expensive hardware is required to implement MPC for the system due to the online minimization of the cost function. Even though an advanced nonlinear programming algorithm for optimization is used, the speed and accuracy of the solution is not guaranteed. In this chapter, multi-parametric quadratic MPC for heating phase of the thermoforming machine is proposed. The model developed for the heating phase of the thermoforming machine (in Chapter 2) is nonlinear. So the model equations should be linearized around the operating point $(x^*, u^*)$ to control the system using multi-parametric quadratic MPC.

$$A = \left.\frac{\partial f(x,u)}{\partial x}\right|_{\substack{x=x^* \\ u=u^*}} \qquad B = \left.\frac{\partial f(x,u)}{\partial u}\right|_{\substack{x=x^* \\ u=u^*}} \qquad C = \left.\frac{\partial h(x)}{\partial x}\right|_{x=x^*} \tag{6.4}$$

In the rest of the chapter, we use $t$ as the present value and $t+k$ for $k^{th}$ future value predicted at $t$ time. The linear state space equations for the system are,

$$x(t+1) = Ax(t) + Bu(t)$$
$$y(t) = Cx(t) \tag{6.5}$$

where $A \in \mathbb{R}^{n\times n}, B \in \mathbb{R}^{n\times m}$. With the linearized system equation, by substituting $x(t+k)|_t = A^k x(t) + \sum_{j=0}^{k-1} A^j B u_{t+k-1-j}$, the optimization problem of MPC can be reformulated in the following form with some algebraic manipulation as in [123],

$$V(x(t)) = \frac{1}{2} x^T(t) Y x(t) + \min_U \left\{ \frac{1}{2} U^T H U + x^T(t) F U \right\} \tag{6.6}$$

$$\text{Such that } GU \le W + Ex(t) \tag{6.7}$$

Where, $U \triangleq [u_t, \ldots\ldots u_{t+N_U-1}]^T$ is the optimization vector and $H, F, Y, G, W, E$ are obtained from $Q, R$. By defining a new vector $z \triangleq U + H^{-1}F^T x(t)$, the optimization problem can be transformed into,

$$V_z(x(t)) = \min_z \frac{1}{2} z^T H z \tag{6.8}$$

$$\text{Such that } Gz \le W + Sx(t) \tag{6.9}$$

Where $S \triangleq E + GH^{-1}F^T$, $V_z(x(t)) = V(x(t)) - \frac{1}{2} x(t)^T \left(Y - FH^{-1}F^T\right) x(t)$, the current state $x(t) = x_o$ can be taken as a vector of parameters, and if there are $q$ number of inequalities exist, then $z \in \mathbb{R}^{m.N}$, $H \in \mathbb{R}^{m.N\times m.N}$, $G \in \mathbb{R}^{q\times m.N}$, $W \in \mathbb{R}^{q\times 1}$, $S \in \mathbb{R}^{q\times n}$ and $F \in \mathbb{R}^{n\times q}$. In [123], it was shown that the explicit solution of the equation is a continuous piecewise affine function defined over the partition of the parameter space. Based on the result of that paper, we propose an algorithm for the offline computation of the optimization problem for heating phase of thermoforming process and hence

implement it in MPC control of the process. The whole algorithm is described by the flow chart in Fig. 6.3 and Fig. 6.4.

## 6.5 Design of multi-parametric quadratic MPC for heating phase of thermoforming machine

The design of the MPC controller is discussed in this section. At first, the system equation is linearized to obtain a linear system of equations so that multi-parametric MPC can be developed. The next step is to incorporate the constraint into the controller. The thermoforming oven heaters have maximum and minimum temperature constraints. The heating and cooling rate of the heaters also have some limitations. The conventional MPC requires an online solution of the optimization problem within a sampling period. As the size of the model of heating phase of the thermoforming process is large, it is difficult to use online optimization to

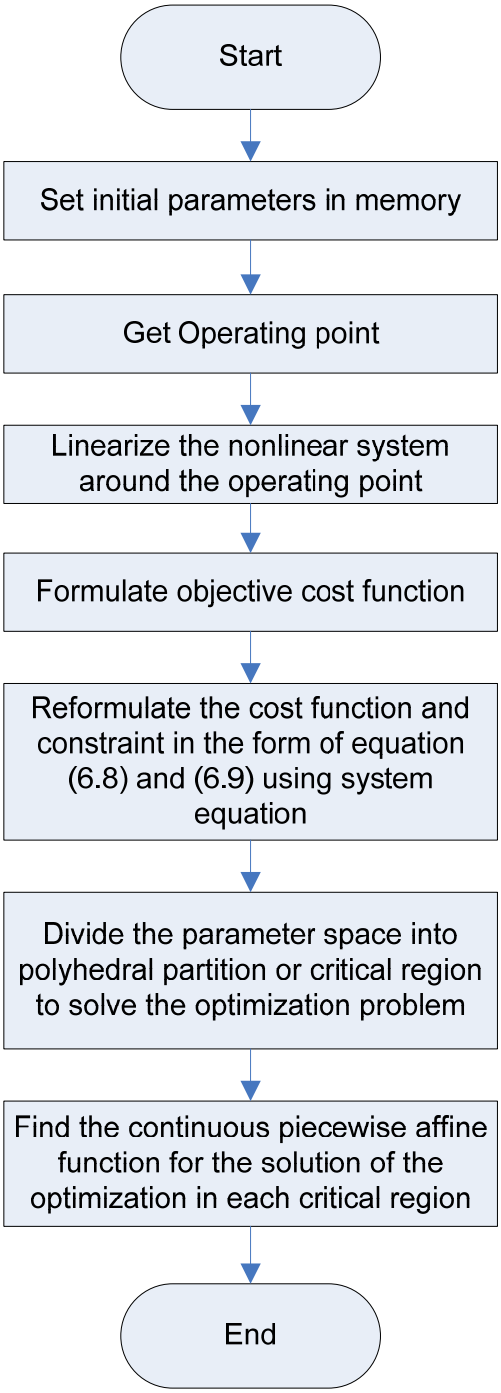


Fig. 6.3: Algorithm for offline optimization of the objective function for MPC

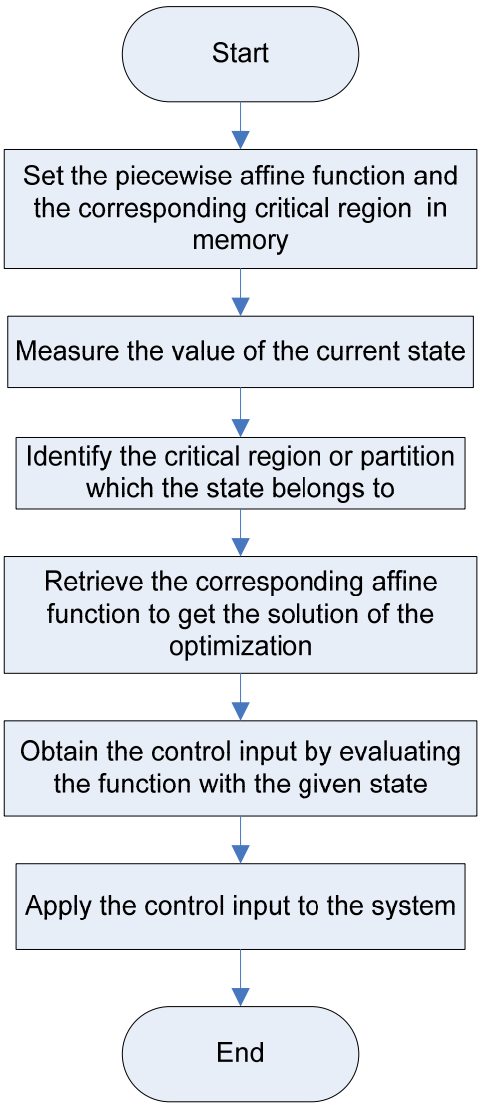


Fig. 6.4: Algorithm for incorporating the solution of offline optimization into the controller

implement MPC. So, the next step is to compute the optimization offline using multi-parametric programming. This recently developed technique allows solving an optimization problem offline for a constrained system within a certain range of the parameters. With the increase of parameter and complexity of the system, the number of polyhedral partition and hence the number of affine function increases. The solution of the optimization problem will be provided by a piecewise affine function by analyzing several properties of the geometry of the polyhedral partition and its relation to the combination of the active constraints for different polyhedral region. Then, the MPC

controller based on the model is tuned in such a way that the desired performance of the process is achieved.

### 6.5.1 Linearization of the system

The nonlinear system equations of the thermoforming process need to be linearized at an operating point of the system to incorporate the model in the design of the MPC controller. On the other hand, because of the nonlinear property of the system, the equation obtained by linearizing the system at a particular operating point may not properly sustain the properties of the actual system at another operating point far from the linearization point. Thus, the system is linearized at different operating point and different controllers are developed for each linear system. Based on the operating point, the control input will switch among different controllers.

### 6.5.2 Incorporating constraints

There are some input-constraints in sheet heating of the thermoforming process such as the maximum and minimum heater temperatures as well as maximum heating and cooling rates. The heaters are usually made of ceramic that could be damaged if heated more than 500C, which results in a constraint in the input heater temperature. On the other hand, the heater cannot be cooled less than the environment temperature. Ajersch performed some experiments to determine the maximum rate of heating and cooling to develop a model of the heater bank [11]. Although it can give some primary idea about the maximum heating and cooling rate, these rates depend on the operating condition of the system like the input power, heat consumed by the sheet, heat consumed by oven air and oven wall (that largely depend on sheet, oven air and oven wall temperature). As the maximum electrical power input to the heater is bounded, it is quite understandable that the maximum heating rate is bounded too. The boundary of the maximum heating and cooling rates of the heater depend on the amount of heat transfer to plastic sheet, oven wall by radiation and to oven air by convection. With the increase of the heater temperature, the maximum cooling rate increases as the heater can lose heat faster to the sheet, oven wall and to the environment. As the heat loss increases at higher temperature, the maximum heating rate will be reduced. On the contrary, at lower temperature of the

heater the maximum heating rate increases and maximum cooling rate decreases. So the input constraints about heating and cooling rate are function of the current heater temperature. Unfortunately, MPC cannot handle this kind of input-constraints that depend on present value of the input heater temperature. But the whole operating range of the heater can be divided into different sub-range and different maximum heating and cooling rate constraints could be incorporated in the design of the controller. So the input constraints can be given according to present value of the input heater temperature for different operating range which will be more accurate.

### 6.5.3 Reduction of the number of partitions in offline solution of multi-parametric quadratic MPC

The number of polyhedral regions depends on the number of parameters which include system state, previous control input, reference output, measured disturbance and prediction horizon as well as the number of input and output constraint. The number of polyhedral regions also depends on the range of the parameters for which multi-parametric quadratic programming is used to solve the optimization problem. Because of the large number of inputs, states and constraints in the thermoforming, multi-parametric quadratic programming (mp-QP) results in a large number of polyhedral regions with piecewise affine function for each region that is practically not possible to implement. So the next challenge in implementing MPC for this process is to reduce the number of regions in the offline solution. One of the possible ways to reduce the number of regions is to reduce the size of the system input and hence reduce the number of parameters as well as number of input constraints. The model of the heating phase of the thermoforming process has all of the constraints in its inputs. It can be proven that as the rank of the $S$ matrix in the constraint of equation (6.9) is less than or equal to the number of constraints, the number of regions for the piecewise affine solution will remain the same for any number of parameters that is higher than the number of constraints. In the case of the heating phase of this process, the number of parameters is much higher than the number of constraints. Therefore, the number of partitions of the parameter space defining the optimal controller is insensitive to the dimension of the parameter vector or the number of parameters involved in the mp-QP. So if we can reduce the number of input constraints,

the number of partitions will be reduced. In the case of the MPC design of the thermoforming machine, only a couple of heaters (top heater and its opposite bottom heater) are used at a time to control the temperature of the sheet and all other heater temperatures are considered to stay constant. As the temperature of a heater can change at most 1K per second (where the actual heater temperature is within the range 350K~700K), it is reasonable to consider heater temperature constant within a sample time (which is 1 second). For each pair of heaters a different MPC will be designed whereas other heater temperatures will be considered constant at the starting temperature of the sample. If there are $2M$ heaters in the thermoforming oven, then there will be $M$ numbers of MPC that have just 2 inputs with the constraint applicable for those inputs. It is observed that the number of partitions is significantly reduced for every MPC controller with this technique.

### 6.5.4 Choosing the weighting matrices of the controller

There are $M$ controllers for the process and each controller computes reference heater temperatures for a pair of heaters. If the same weights are given for output tracking at every point's temperature of the sheet, then the controller will try to force the heater temperature in such a way that it tries to optimize error between reference and actual temperature at every point of the sheet to achieve the desired temperature. But some parts of the sheet are so far from the heater that the heater has very little influence on that part of the sheet i.e. the sensitivity of the part of the sheet is very low with the change of heater temperature. This will force the heater to attain very high temperature to heat the point of the sheet far from the heater to the desired temperature even at the cost of a higher temperature at the nearest point of the sheet from the heater. This could even burn some parts of the sheet. As the heaters are well distributed all over the oven, every heater can be used more to heat those point of the sheet that are closer to them. This could be attained by using appropriate weight matrix for reference outputs. The elements of the weight matrix are chosen to be inversely proportional to the distance between the sheet points and the heater.

### 6.5.5 Tuning parameters of the controller

The parameters of the controller like output prediction horizon, control horizon and constraint horizon length are tuned in such that the controller gives its desired performance within significant amount of computation to implement in real-time. With the increase of the horizon length (both prediction and control), the performance improves at the cost of an increase in the number of constraints that will increase the number of polyhedral regions. As a result, the complexity of the final piecewise affine functions for the MPC controller increases dramatically. So the resolution of this problem is a compromise between performance and computational complexity. The lengths of the output prediction horizon, control horizon and constraints horizon are chosen such that they give convenient number of polyhedral regions as well as it will ensure desired performance.

After the computation of the optimization problem using multi-parametric programming, the optimal control input to the system will be obtained as an affine function of system state, previous control input, reference output and measured disturbance. The diagram of the proposed Multi-parametric MPC for heating phase is shown in Fig. 6.5.

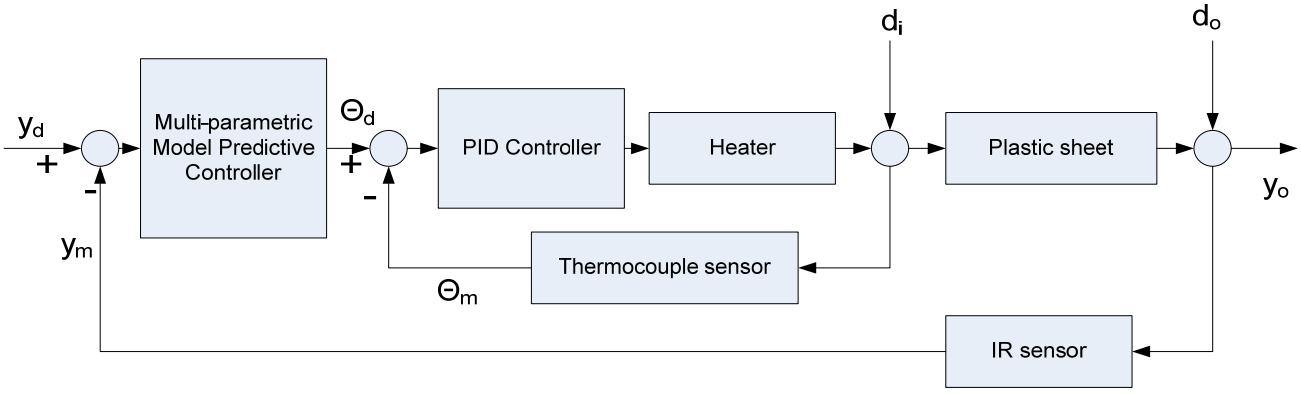


Fig. 6.5: Multi-parametric MPC for heating phase of thermoforming process.

## 6.6 Simulation results

The effectiveness of the proposed MPC controller is investigated extensively in simulation. The performance of the proposed controller is compared to other commonly used controllers (like PI) as well as state-of-the-art controllers (ILC, TILC) for this system. First, a simulation model is developed using Matlab/Simulink. Then the performance of the proposed method and conventional methods are compared using the developed model. The oven consists of top and bottom heaters. Each heater consists of 6 (3x2) heater banks. There are 9 equidistant sensors (3x3) considered on each side of the sheet. The positions of the sensors are as mentioned in Chapter 3. The conventional PI controller, cycle-to-cycle iterative learning controller (ILC) and terminal iterative learning controller (TILC) are used to compare the performance with the proposed MPC controller. After the design and development of the MPC controller, each pair of control inputs will be formulated in an explicit expression of 30 system states (18 outputs, 2 air temperature and 10 other inputs), 2 previous control inputs and 18 reference outputs. The sheet output temperature at the sensor points for the first 11 cycles with cycle duration of 600s are shown in Fig. 6.6 for the PI, ILC and MPC controllers respectively. The reference temperature input is chosen as an exponential function with starting temperature value 30C and final value at the end of the cycle period of 130C so that the plastic sheet will be heated very fast at the beginning of the cycle to give enough time for the heat to propagate throughout the thickness of the plastic sheet by conduction (conduction is a very slow process of heating as compared to radiation). Moreover, we should give enough time for the energy to propagate so that it will not burn any parts of the sheet. The fast production rate of plastic products forces us to have a high heating rate. On the other hand, enough time should be allowed so that the sheet will be heated properly throughout its thickness. Although uneven temperature distributions are required in some applications, we only consider an even distribution of 130C at the end of the cycle for simplicity. The performance of PI, ILC, TILC and MPC controllers are presented in Fig. 6.6 and Fig. 6.7. We can observe that the PI controller cannot follow the reference input as it does not consider the actuator (heater) constraint during the heating process.

Actually, the PI controller is working very much the same way as a bang-bang controller as evidenced by the heater temperature error plot in Fig. 6.8. The control inputs generated by the PI and ILC controllers do not consider the cooling limitation of the actuators. As a result, the performance degrades with the progress of time in a cycle. The use of a changing input in the case of TILC is irrelevant as its only focus is on the terminal output of the repetitive process. Hence, it can be considered that a constant temperature is used for TILC to heat the sheet to a uniform temperature of 130 C at the end of the cycle. TILC performs well to achieve the final output but it cannot follow the temperature profile over the cycle that will ensure enough heat propagation throughout the thickness of the sheet so that the surface as well as the inner layer of the sheet will be heated properly. It is observed that the PI controller results in a large deviation of 8C while ILC yields error of as much as 40C. The TILC controller gives bad performance at the beginning that is getting better with time whereas the proposed controller gives a better performance as the sheet temperature obtained at the end of the cycle remains pretty close to the desired temperature. On the other hand, the MPC controller shows good performance that can follow the reference input reasonably. In Fig. 6.8, it is observed that the heater temperature of the PI controller cannot follow the command heater temperature from the controller output as the controller did not consider the constraint of the heater in calculating the control input. So the error between the heater temperature command and actual heater temperature is as high as 800C. In the ILC case, the error is very high in the first few cycles as it does not have much information from previous cycles. But with the advance of cycle number, the ILC controller is generating a control input that does not consider the actuator constraint. As a result, the deviation between control input and heater output increases. In the case of TILC, the error in the first few cycles is high but it gets better with time, even though the controller does consider the constraint of the heater in calculating the control input. But it takes one full cycle time to attain the command heater temperature. In the case of MPC, the heater can follow the heater temperature command from the controller and the error is as low as 3C. In the next two figures (Fig. 6.9, Fig. 6.10) we observe the performance of these controllers in the presence of large disturbances (between -4C to 4C) that may come due to model mismatch, noise, ambient temperature fluctuations, sensor errors etc. As PI, ILC, TILC techniques are sensitive to

these non-periodic random disturbances, they do not achieve good performances as expected. The proposed MPC controller gives better performance and lower error as compared to other controllers. The proposed MPC tries to estimate the disturbances from last few samples and incorporate the information into the controller.

Now, we investigate the performance of PI, ILC, TILC, MPC controllers in the presence of repetitive fixed disturbances of 10C that affect the output at every cycle of the

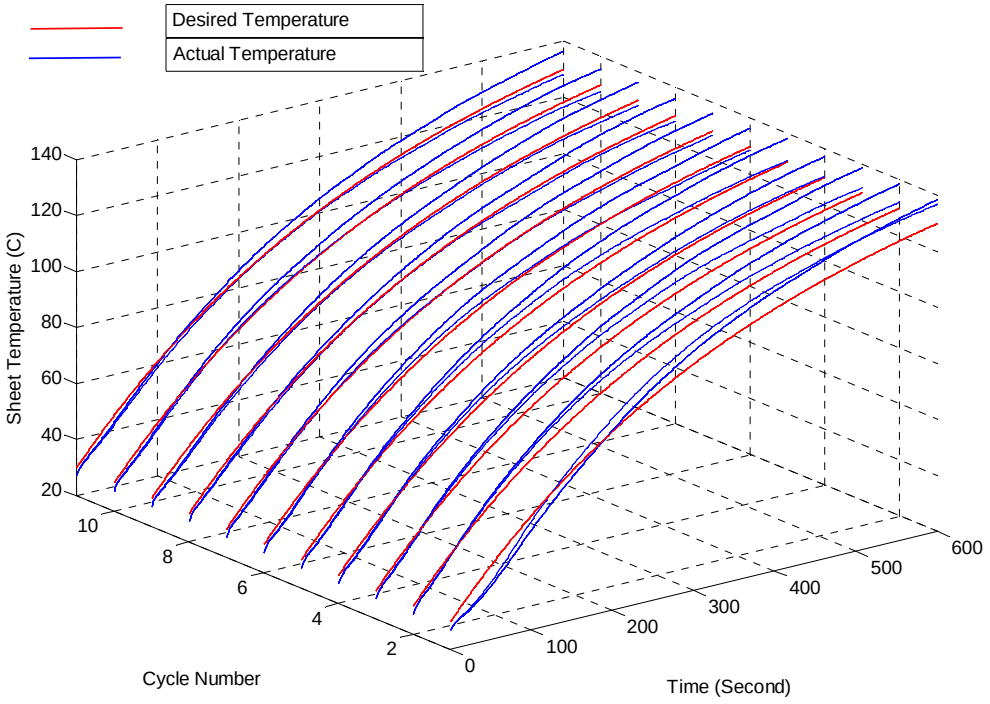


(a) PI

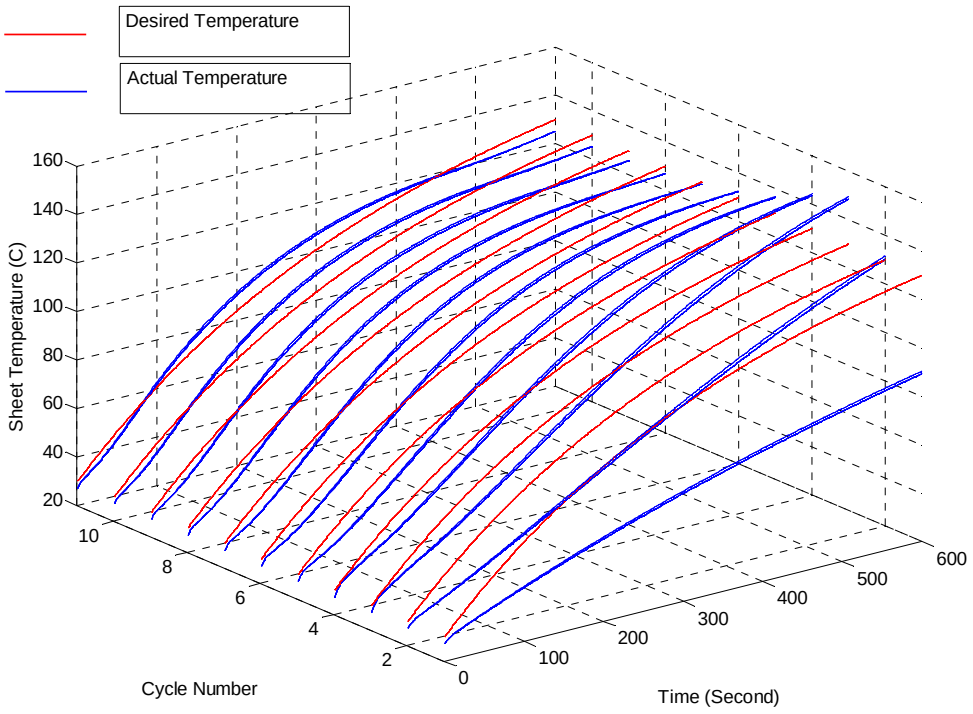
Desired Temperature
Actual Temperature
Sheet Temperature (C)
160
140
120
100
80
60
40
20
10
8
6
4
2
Cycle Number
0
100
200
300
400
500
600
Time (Second)

(b) ILC

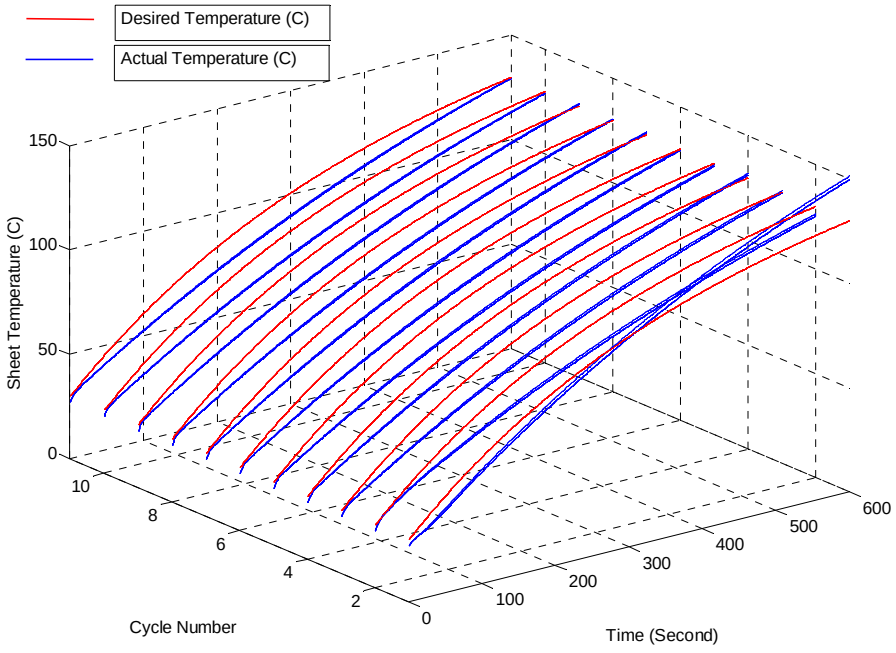
Desired Temperature (C)
Actual Temperature (C)
Sheet Temperature (C)
150
100
50
0
10
8
6
4
2
Cycle Number
0
100
200
300
400
500
600
Time (Second)

(c) TILC

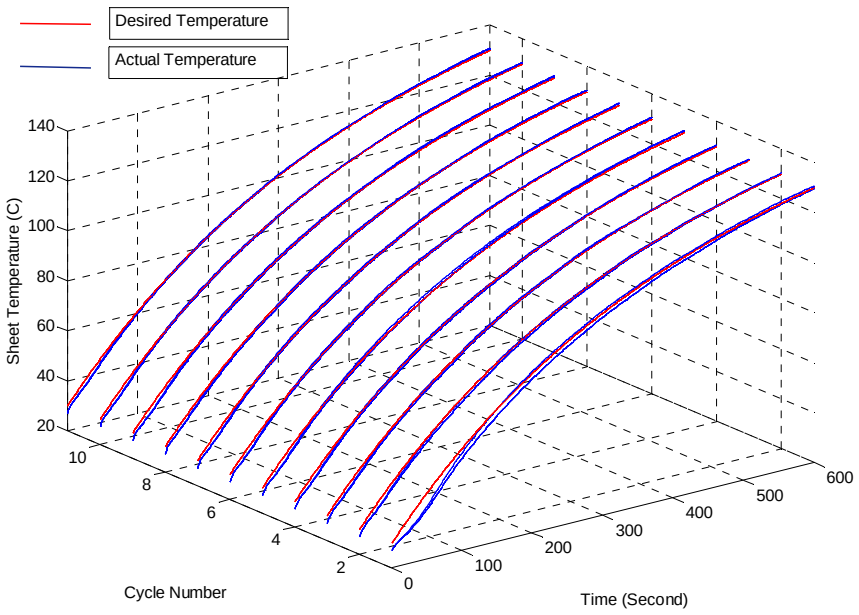


(d) MPC

Fig. 6.6: the sheet temperature at sensor point of the sheet for (a) PI (b) ILC (c) TILC (d) MPC

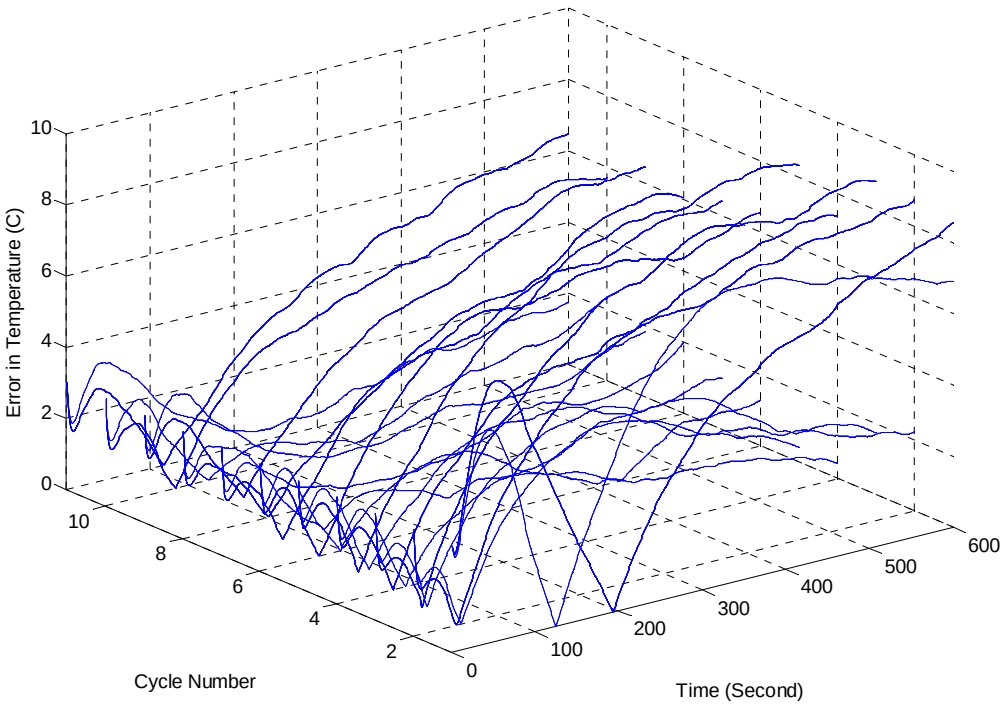


(a) PI

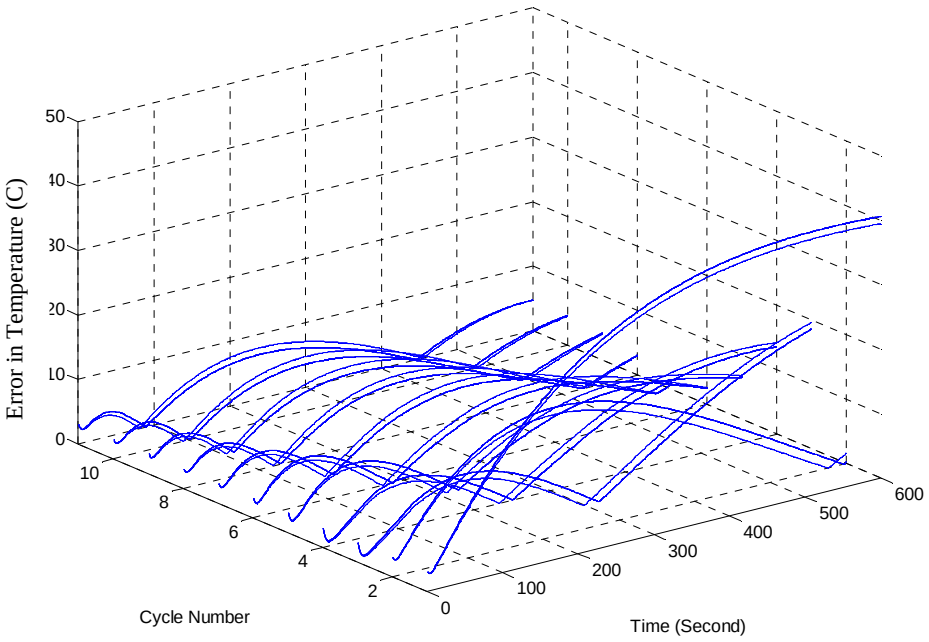
Error in Temperature (C)
50
40
30
20
10
0
10
8
6
4
2
Cycle Number
0
100
200
300
400
500
600
Time (Second)

(b) ILC

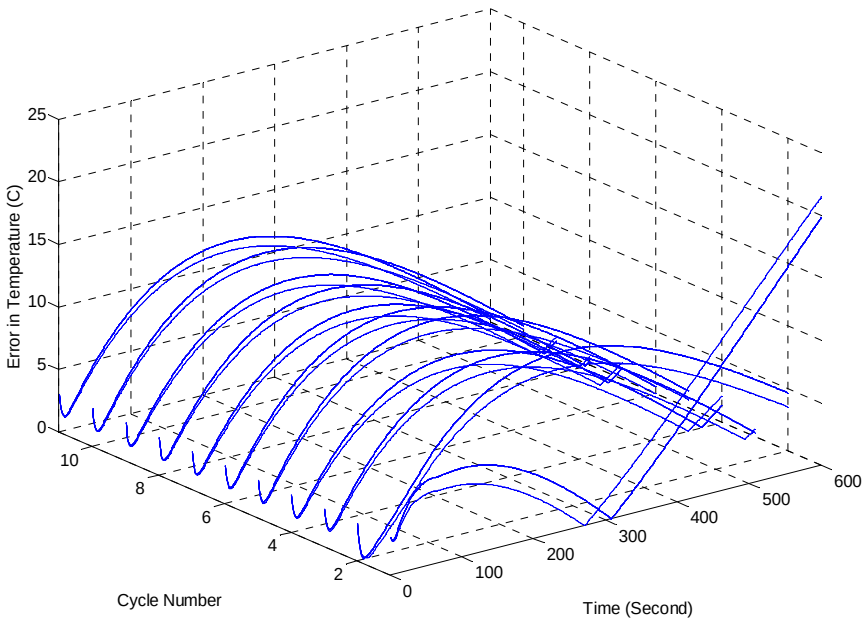
Error in Temperature (C)
25
20
15
10
5
0
10
8
6
4
2
Cycle Number
0
100
200
300
400
500
600
Time (Second)

(c) TILC

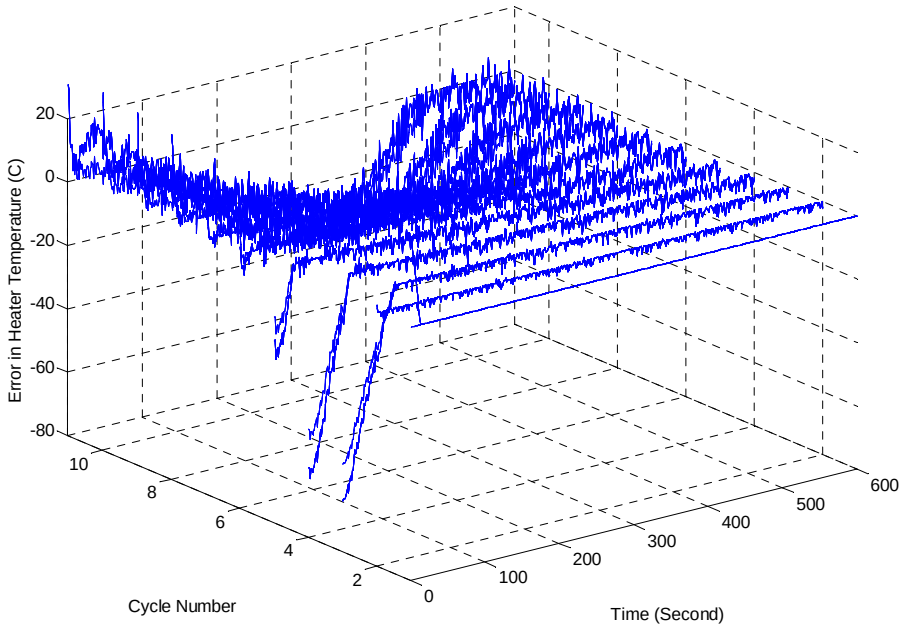
Error in Heater Temperature (C)
20
0
-20
-40
-60
-80
10
8
6
4
2
Cycle Number
0
100
200
300
400
500
600
Time (Second)

(b) ILC

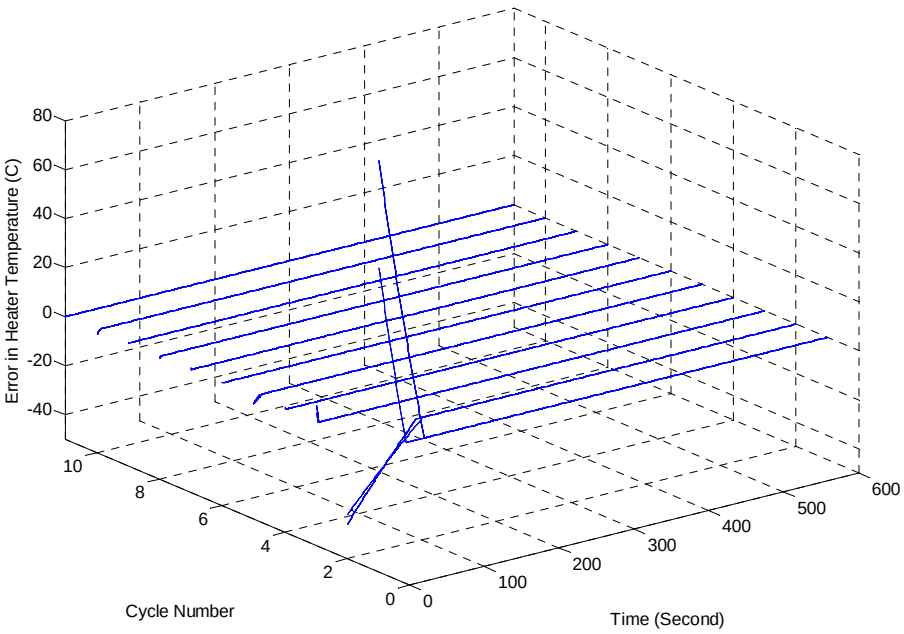
Error in Heater Temperature (C)
80
60
40
20
0
-20
-40
10
8
6
4
2
0
Cycle Number
0
100
200
300
400
500
600
Time (Second)

(c) TILC

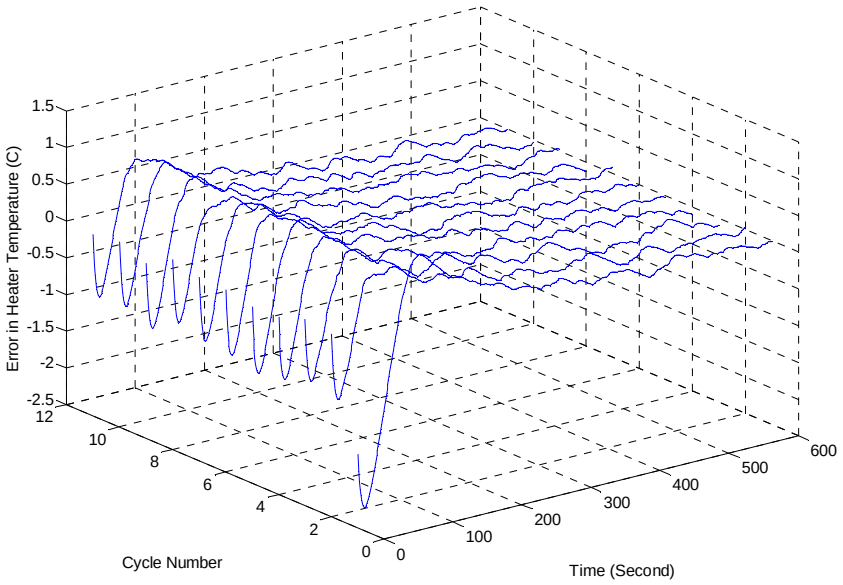


(d) MPC

Fig. 6.8: Error between command input temperature and actual heater temperature for (a) PI (b) ILC (c) TILC (d) MPC

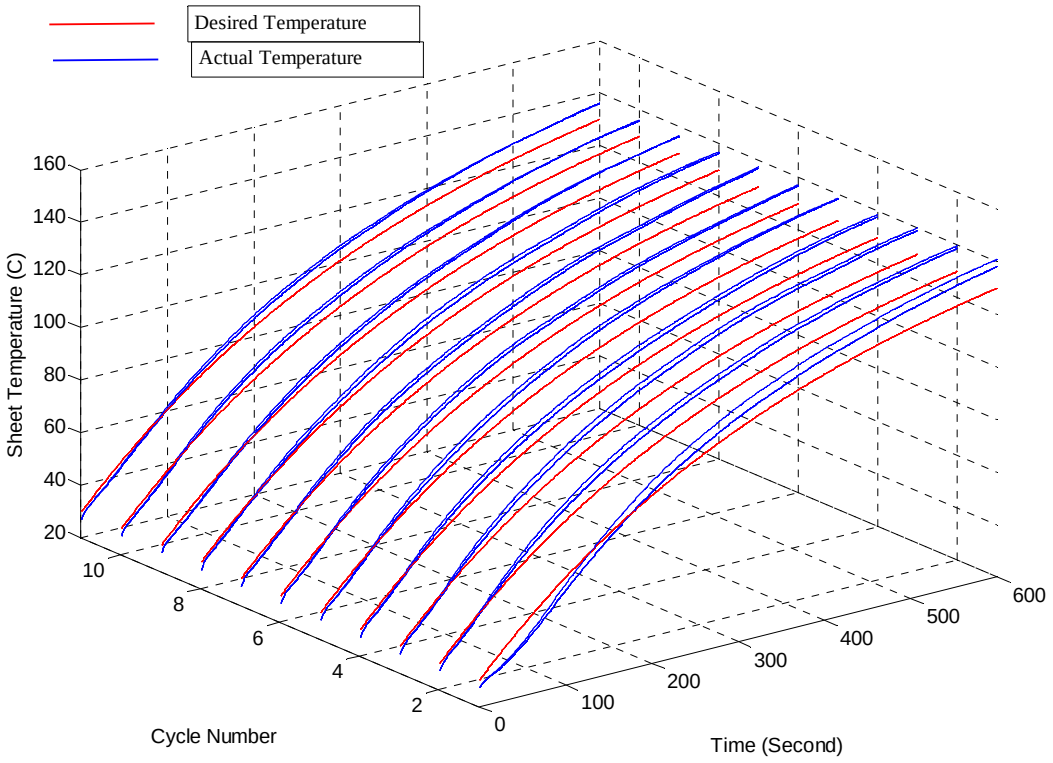
Desired Temperature
Actual Temperature
Sheet Temperature (C)
160
140
120
100
80
60
40
20
10
8
6
4
2
Cycle Number
0
100
200
300
400
500
600
Time (Second)

(a) PI

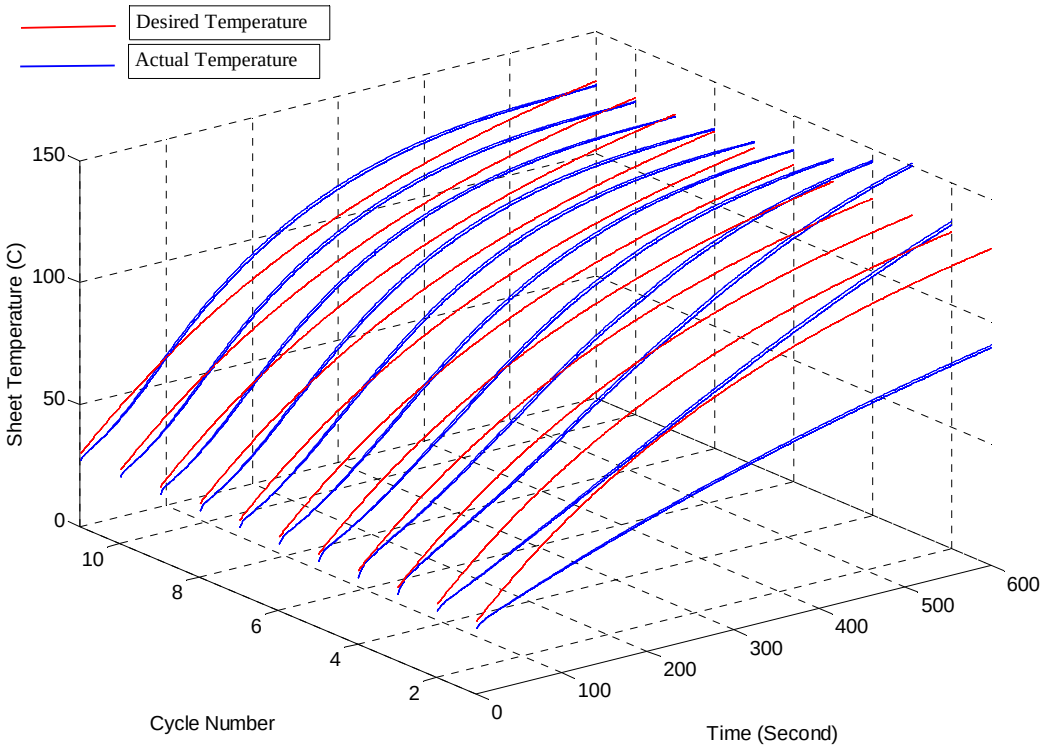
Desired Temperature
Actual Temperature
Sheet Temperature (C)
150
100
50
0
10
8
6
4
2
Cycle Number
0
100
200
300
400
500
600
Time (Second)

(b) ILC

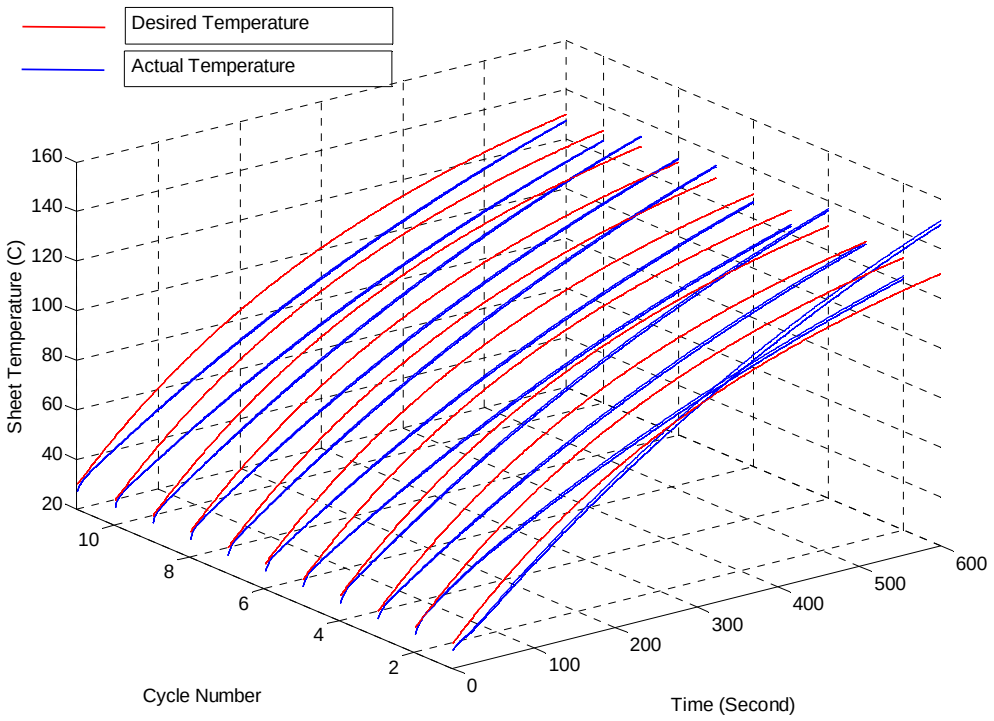


(c) TILC

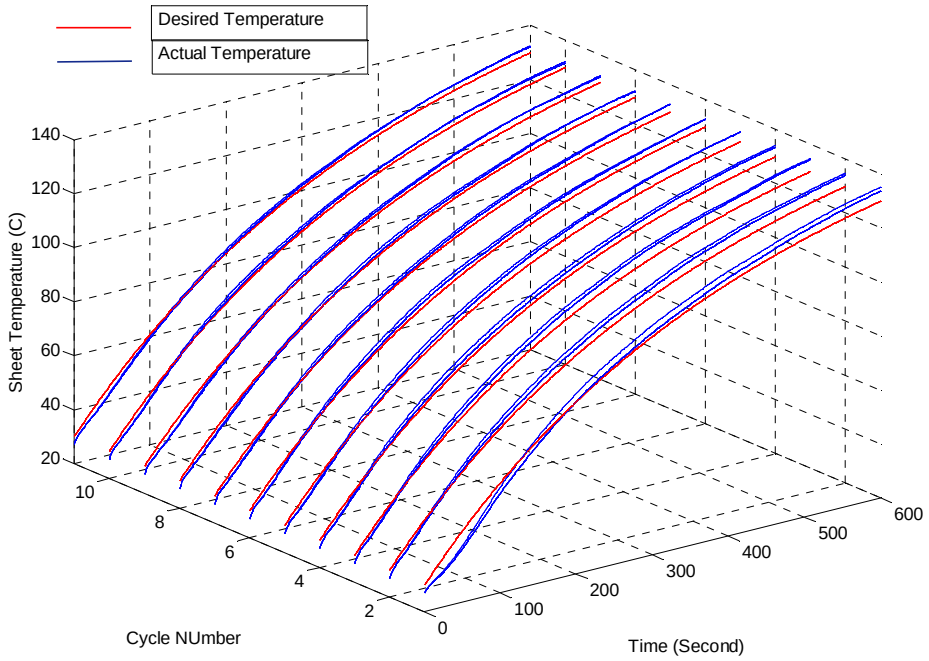


(d) MPC

Fig. 6.9: Sheet temperature at sensor point of the sheet at the presence of large non-repetitive disturbances for (a) PI (b) ILC (c) TILC (d) MPC

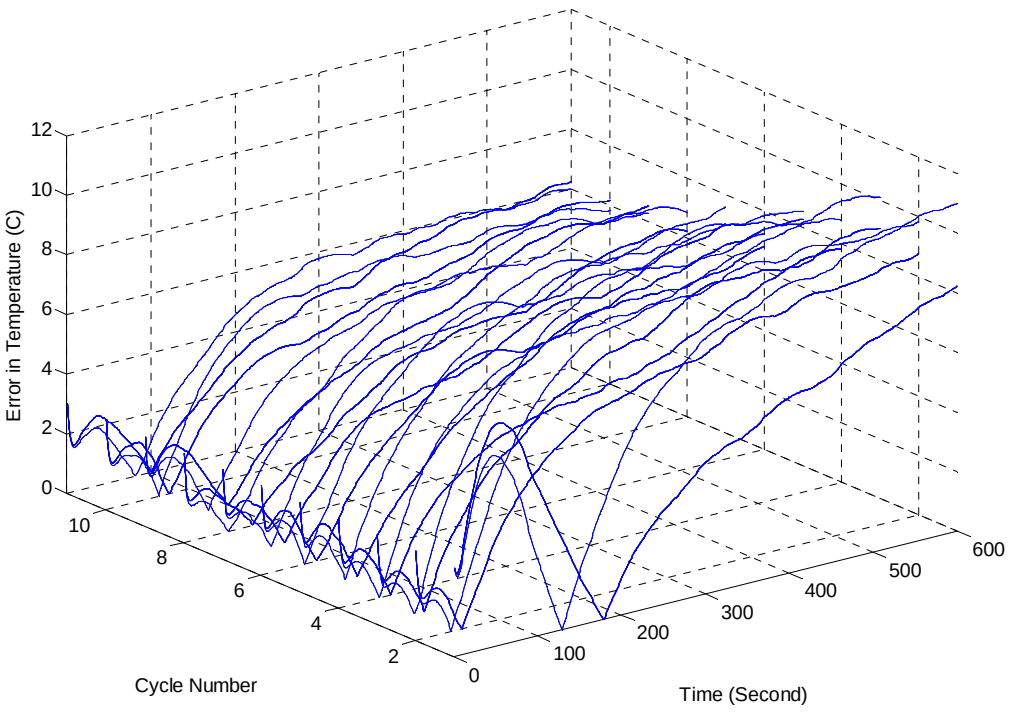
Error in Temperature (C)
0
2
4
6
8
10
12
Cycle Number
10
8
6
4
2
Time (Second)
0
100
200
300
400
500
600

(a) PI

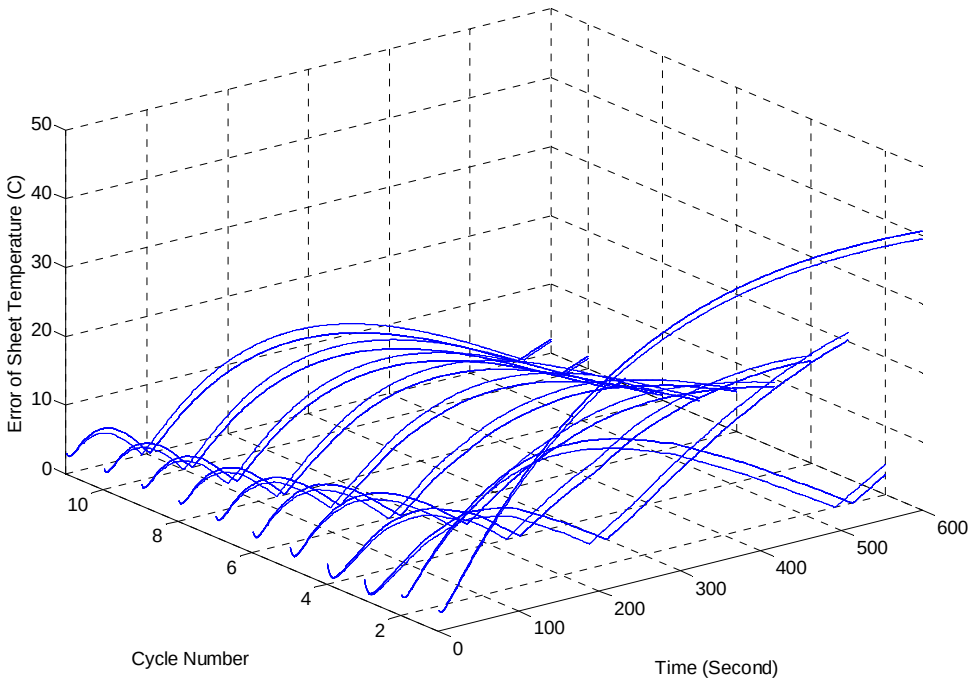
Error of Sheet Temperature (C)
0
10
20
30
40
50
Cycle Number
10
8
6
4
2
Time (Second)
0
100
200
300
400
500
600

(b) ILC

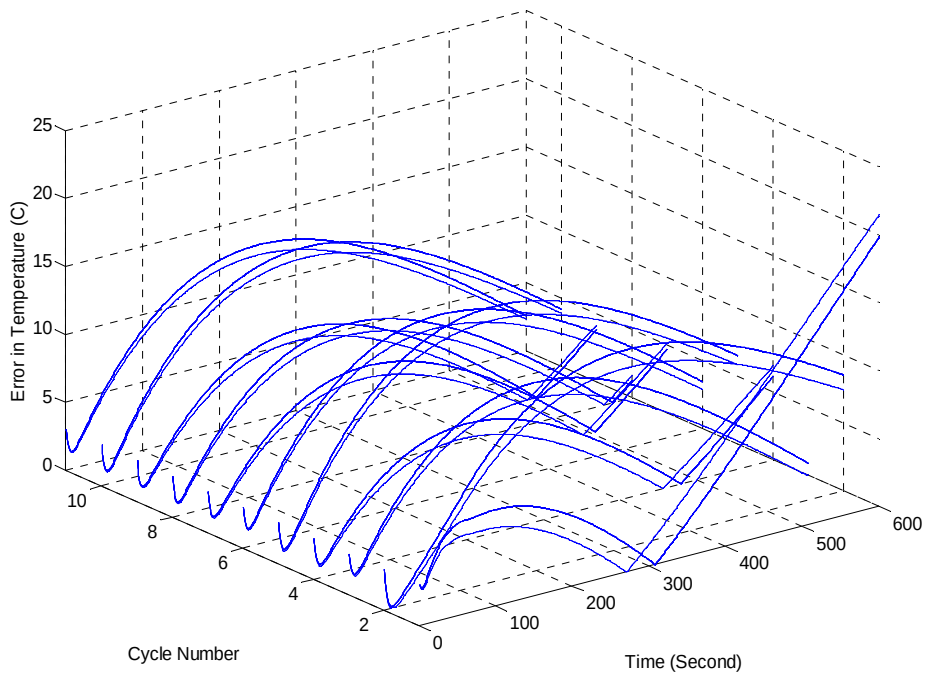


(c) TILC

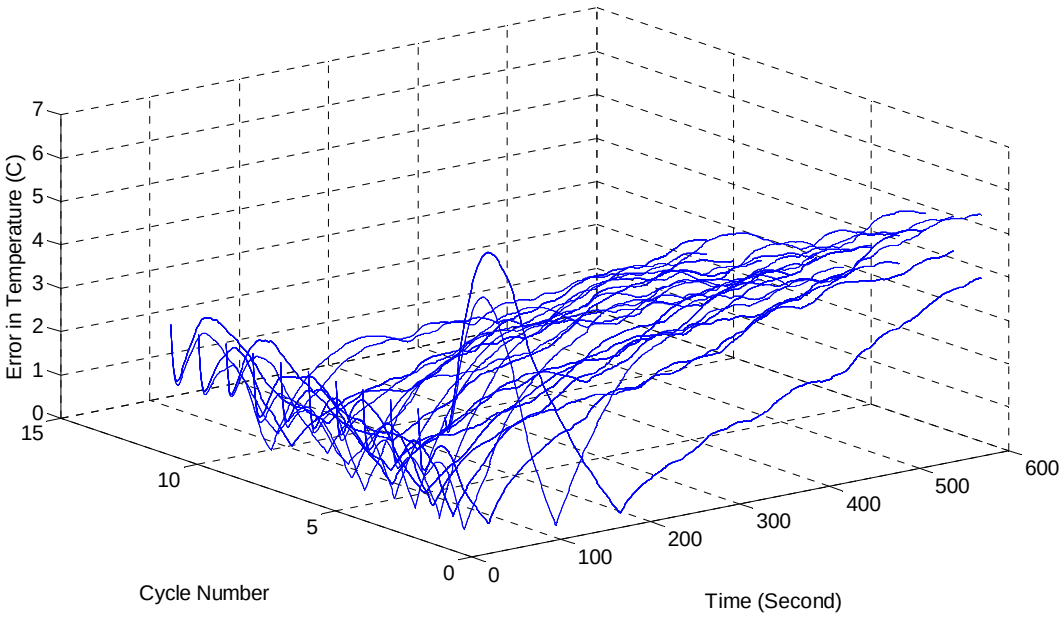


(d) MPC

Fig. 6.10: Error in sheet temperature at sensor point of the sheet at the presence of large non-repetitive disturbances for (a) PI (b) ILC (c) TILC (d) MPC

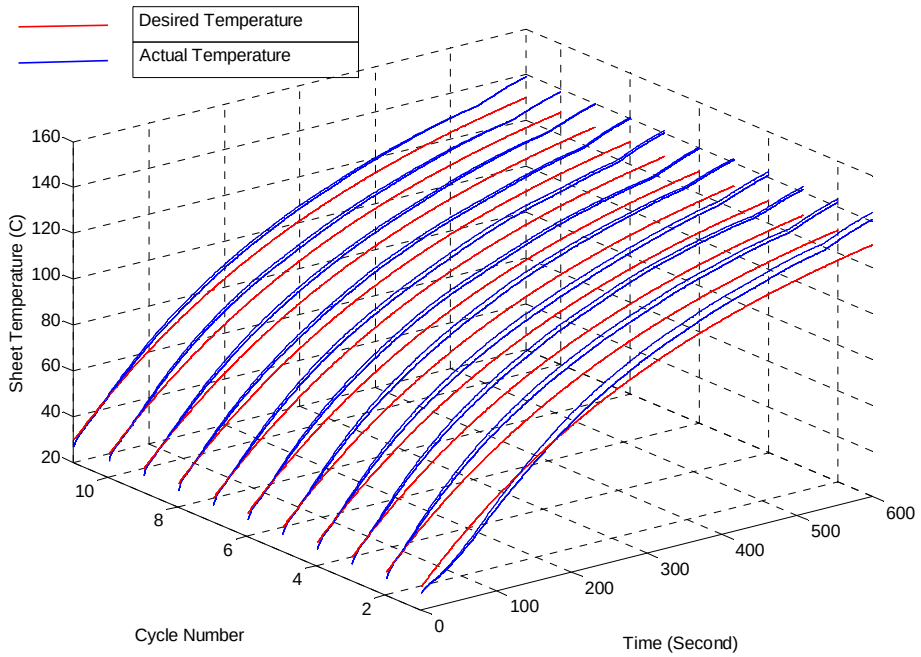
Desired Temperature
Actual Temperature
Sheet Temperature (C)
160
140
120
100
80
60
40
20
10
8
6
4
2
Cycle Number
0
100
200
300
400
500
600
Time (Second)

(a) PI

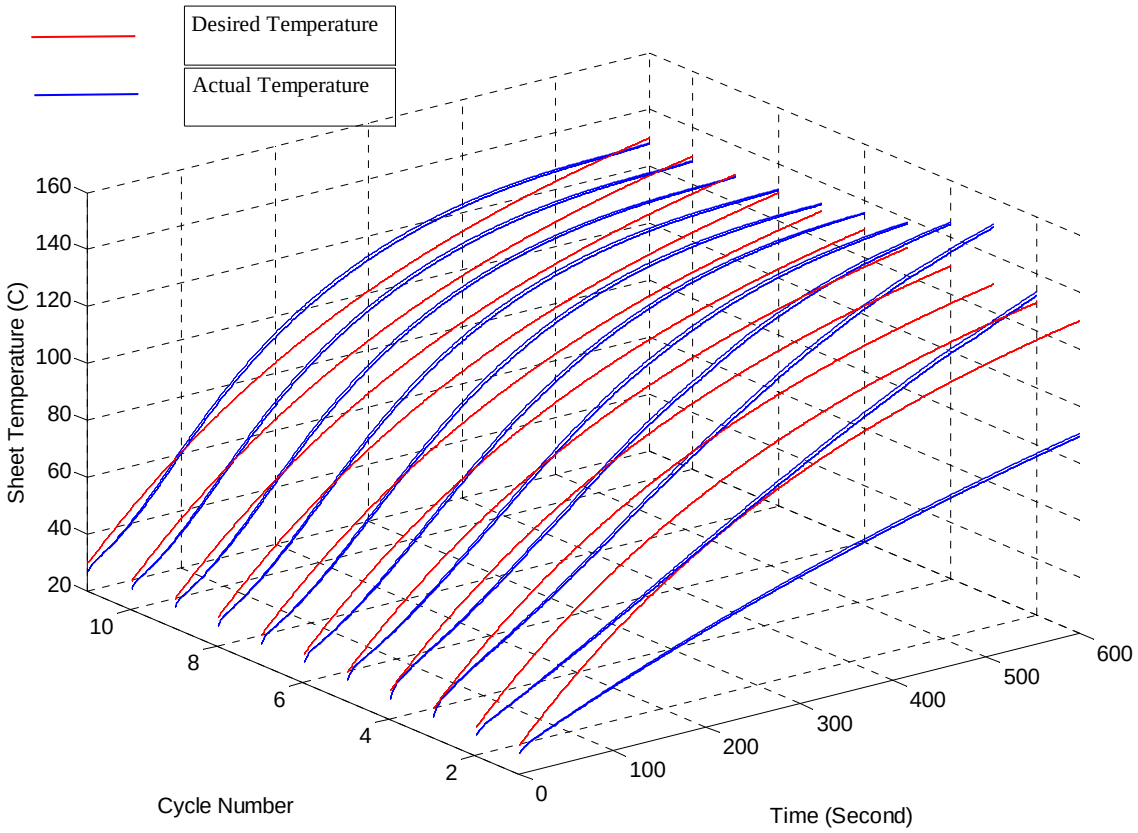
Desired Temperature
Actual Temperature
Sheet Temperature (C)
160
140
120
100
80
60
40
20
10
8
6
4
2
Cycle Number
0
100
200
300
400
500
600
Time (Second)

(b) ILC

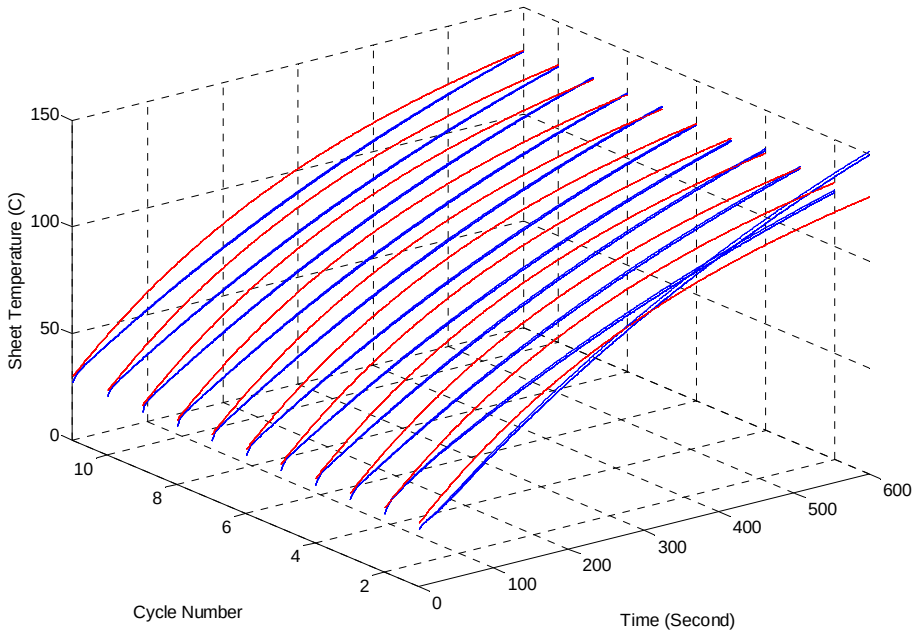


(c) TILC

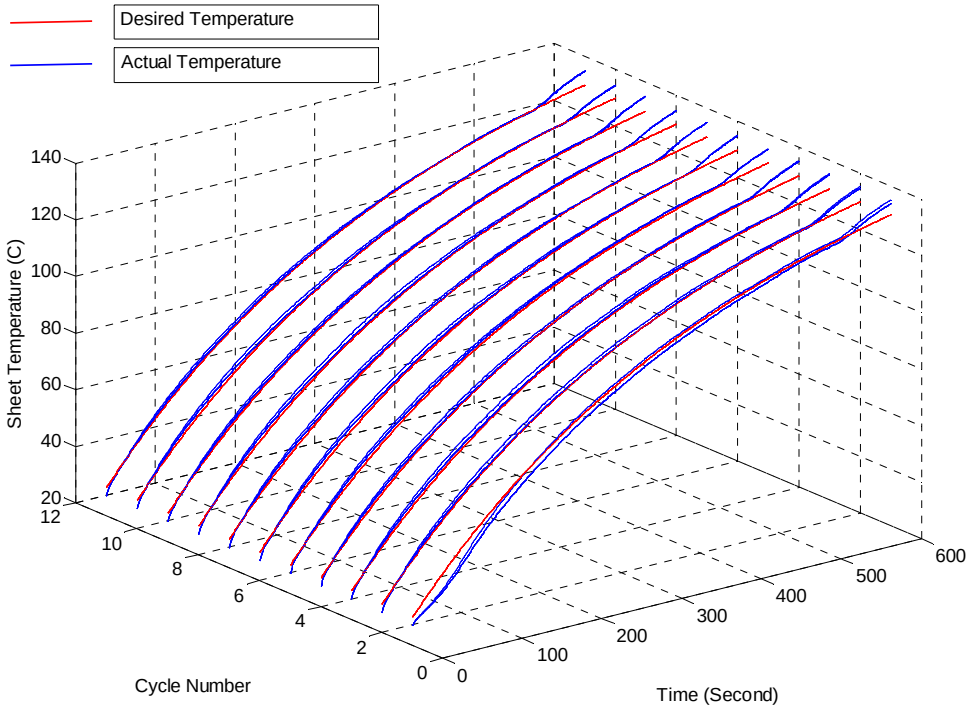


(d) MPC

Fig. 6.11: Sheet temperature at sensor point of the sheet at the presence of repetitive disturbances for (a) PI (b) ILC (c) TILC (d) MPC

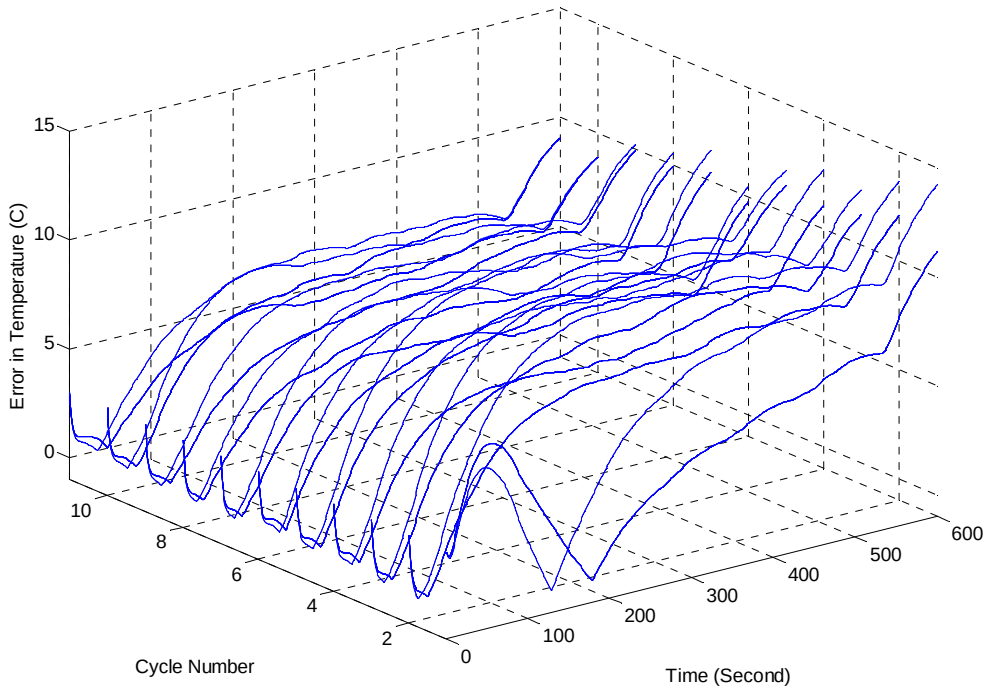
Error in Temperature (C)
15
10
5
0
10
8
6
4
2
Cycle Number
0
100
200
300
400
500
600
Time (Second)

(a) PI

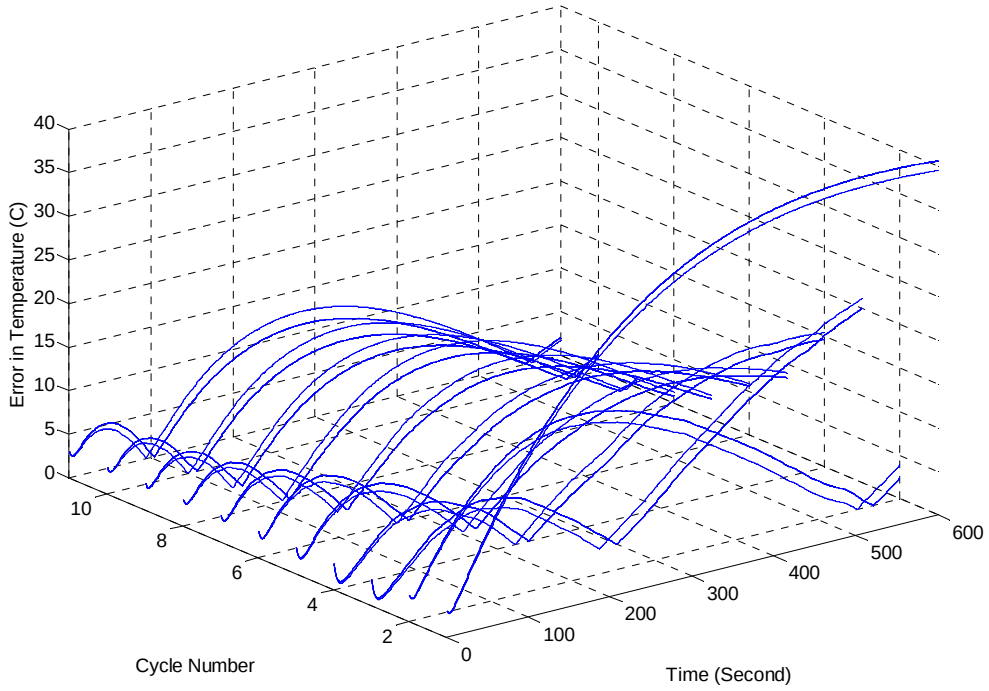
Error in Temperature (C)
40
35
30
25
20
15
10
5
0
10
8
6
4
2
Cycle Number
0
100
200
300
400
500
600
Time (Second)

(b) ILC

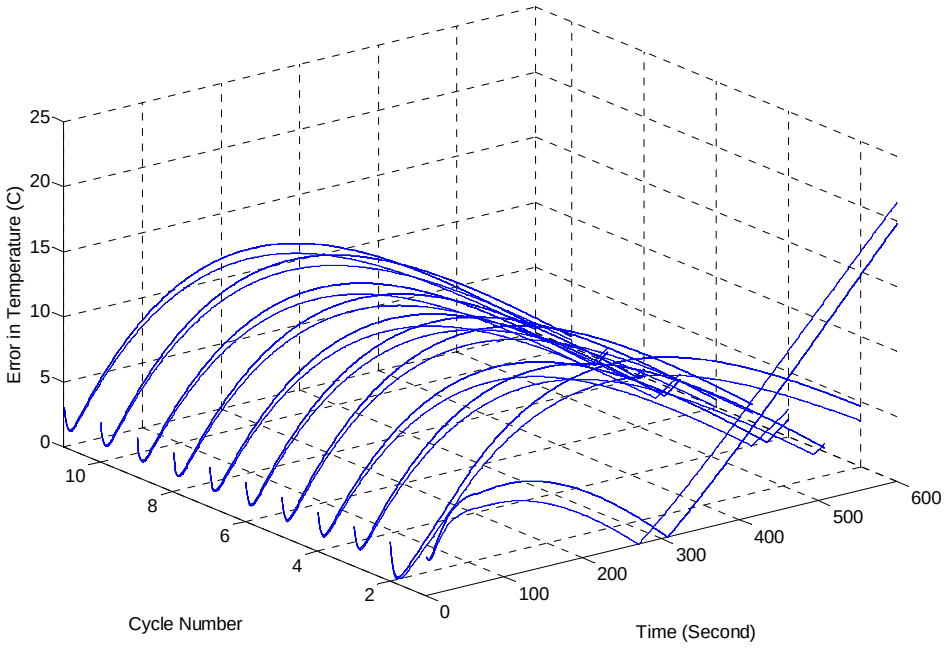


(c) TILC

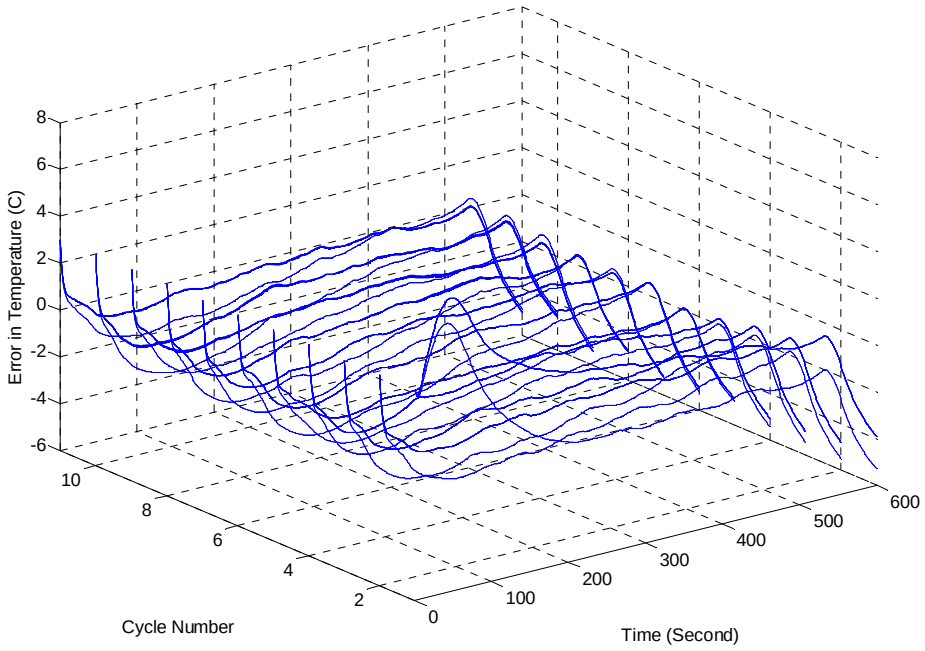


(d) MPC

Fig. 6.12: Error in sheet temperature at sensor point of the sheet at the presence of repetitive disturbances for (a) PI (b) ILC (c) TILC (d) MPC

process after 500 seconds and until the end of the cycle. This kind of disturbance may come from sagging of the plastic sheet after a certain time of heating and that disturbance exists until the end of the cycle. In Fig. 6.11 and Fig. 6.12, it is observed that the PI controller and MPC cannot perform very well in the presence of repetitive disturbances although MPC can perform well in the presence of non-repetitive disturbances. Both PI and MPC only use the information that it achieved from previous samples throughout the present cycle, but the information from previous cycles of the batch process are not used in calculating control input. So these two types of controller cannot achieve the desired performance. In case of ILC, even though it uses the information of the previous cycles, it does not consider the actuator constraints of the process. This controller may have good performance in the presence of repetitive disturbances if the heater can follow the control input of the controller. On the other hand, TILC can achieve the desired temperature at the end of the cycle although it cannot follow the reference input along the cycle.

## 6.7 Conclusion

In this chapter, a step-by-step approach is proposed for the development of the multi-parametric MPC of the thermoforming process. The main challenges in the deployment of the MPC controller for the process is discussed and solved in this chapter. The explicit implementation of the MPC controller, in the form of a piecewise affine control law computed offline, obviates the need for online optimization. Although the proposed MPC can handle non-repetitive disturbances better than the conventional controller, it does not perform very well in the presence of periodic disturbances. We propose a new method in next chapter that can handle both kinds of disturbances.

# Chapter 7

# Iterative Learning Model Predictive Control of Heating Phase

## 7.1 Introduction

The heating phase of the thermoforming process is a repetitive process. At the start of the cycle, the plastic sheet is entered into the oven and gets heated throughout the cycle time. The heated sheet is then transferred to the molding section as a new sheet enters the oven to be heated. Model predictive control (MPC) has been adopted in the last chapter to handle the control problems. MPC has some nice features. For example, it can automatically compensate for process interaction and measure the disturbances as well as handle difficult process dynamics. Another important advantage of this type of control is its ability to cope with constraints on controls and states. So MPC can optimize the performance by allowing for operation close to the system constraints. MPC is also able to handle structural changes. However, the computation of MPC for the optimization problem at every sampling instant may require complex calculations that were solved in last chapter.

This MPC control strategy as well as other model based control, however, focuses on single-cycle performance improvement. The heating phase of the thermoforming process is characterized by repetitive dynamics over a fixed cycle period [60]. Some researchers have developed cycle-to-cycle control techniques to control the repetitive process [124,125,126,127,128,129,130,131,132,133,134,135,136,137,138,139]. The idea is to use information from past cycles to help the closed-loop system track the desired trajectory across cycles. By using the repetitive nature of the process, Terminal Iterative Learning Controller (TILC) improves the control accuracy along the cycle index $k$ from cycle to cycle [60]. On the other hand, TILC may not perform well in the presence of

non-periodic disturbances. Control during sheet reheat is also complicated by the fact that there is a high level of uncertainty surrounding the process, particularly with the material properties. Moreover, environmental conditions may change around a machine causing a cycle-to-cycle controller to converge very slowly, resulting in lots of rejected parts.

The thermoforming process can be described in terms of two distinct time scales, namely, the finite period of continuous time within each repeating cycle, and the cycle index. Conventional control formulations do not explicitly incorporate or exploit this 2D representation of cyclic systems. Additionally, conventional one-dimensional control formulations have been shown to have limited success in controlling repetitive systems [60]. Two-dimensional learning controller results in advantages over the conventional feedback control techniques where only one input action is made in-cycle. For this reason, a real-time feedback control combining in-cycle and cycle-to-cycle strategies can improve control performance. Therefore, a 2D control technique combining iterative control technique with MPC can perform better in the presence of repetitive and non-repetitive disturbances. This approach utilizes not only the incoming information from the ongoing cycle, but also the information stored from the past cycles. The MPC technique can be incorporated to update the control law within the cycle to deal with non-repetitive disturbances considering the constraints of the process and the repetitive nature of the heating phase of the process can be exploited using a cycle-to-cycle iterative learning control technique. The iterative learning strategy is useful for achieving desired temperature despite model mismatch and disturbances. Even though the large number of computations makes it difficult to apply to large systems such as a thermoforming machine, multi-parametric programming can be used to compute optimization offline as in Chapter 6.

## 7.2 Iterative Learning Control

Iterative learning control (ILC) is a control technique that can be used to improve tracking performance of a batch process. It works based on improving the control signal for the current cycle using the information from previous cycles. Therefore, ILC does not require much information about the process dynamics prior to the controller design. It

basically concentrates on learning from the past performance with the objective of attaining the desired tracking performance even with model uncertainty and periodic disturbances.

The main purpose of ILC is to have better performance using a mechanism of trial and error with the help of previous experience. *Learning* usually means gaining knowledge and *iterative* corresponds to an action that requires the same dynamic process be repeated. Hence, the expression “iterative learning” indicates gaining knowledge from the same repeated dynamics over a finite tracking period. This knowledge can be learned from experience when a control task is performed repeatedly, providing the opportunity of refining the tracking control performance. If we refine our controller based on our knowledge, we can eventually get perfect tracking if the system dynamics stay exactly the same. Without learning, a control system can only give the same performance, even if the system dynamics repeats consecutively. But in real applications, the process dynamics may change a bit in two consecutive cycles or there might be some disturbances that might not repeat in the same way in every cycle. ILC cannot perform perfectly in those situations. Moreover, it does not consider the process constraints in calculating the control input.

## 7.3 Model Predictive Control Based Iterative Learning Controller

ILC cannot handle various disturbances that may affect the process in a non-periodic way. In the design of this controller, MPC will be employed with ILC to handle this kind of uncertainty and disturbances. At first, we formulate the problem in the next subsection.

### 7.3.1 Problem Formulation

Let us consider a repetitive process that is described in a particular $k^{th}$ cycle as follows:

The linear state space equations for the system are,

$$x_k(t+1) = Ax_k(t) + Bu_k(t)$$
$$y_k(t) = Cx_k(t) \tag{7.1}$$

where $A \in \mathbb{R}^{n\times n}$, $B \in \mathbb{R}^{n\times m}$ and $C \in \mathbb{R}^{p\times n}$ . In the rest of the chapter, we use $t$ as the present value and $t+i$ for $i^{th}$ future value predicted at $t$ time. With the linearized system equation, by using the response, $x_k(t+i) = A^i x_k(t) + \sum_{j=0}^{i-1} A^j B u_k(t+i-1-j)$,

$$y_k(1) = CAx_k(0) + CBu_k(0)$$

$$y_k(2) = CA^2 x_k(0) + CABu_k(0) + CBu_k(1)$$

$$y_k(3) = CA^3 x_k(0) + CA^2 Bu_k(0) + CABu_k(1) + CBu_k(2)$$

.

.

.

$$y_k(N) = CA^N x_k(0) + CA^{N-1} Bu_k(0) + CA^{N-2} Bu_k(1) + \ldots + CABu_k(N-2) + CBu_k(N-1) \tag{7.2}$$

this equation can be written in matrix form as follows:

$$y_k = Gu_k + Hx_k(0) \tag{7.3}$$

where the matrices for the $k^{th}$ cycle can be defined as,

$$y_k{}^T = \begin{bmatrix} y_k(1)^T & y_k(2)^T & y_k(3)^T & \ldots & y_k(N-2)^T & y_k(N-1)^T & y_k(N)^T \end{bmatrix}$$

$$u_k{}^T = \begin{bmatrix} u_k(0)^T & u_k(1)^T & u_k(2)^T & \ldots & u_k(N-3)^T & u_k(N-2)^T & u_k(N-1)^T \end{bmatrix}$$

$$G = \begin{bmatrix} CB & 0 & 0 & ... & 0 \\ CAB & CB & 0 & ... & 0 \\ . & . & . & ... & . \\ . & . & . & ... & . \\ CA^{N-1}B & CA^{N-2}B & CA^{N-3}B & ... & CB \end{bmatrix}$$

$$H^T = \begin{bmatrix} (CA)^T & (CA^2)^T & (CA^3)^T & ... & (CA^N)^T \end{bmatrix}$$

Including the non-periodic disturbances, the model can be written as:

$$y_k = Gu_k + Hx_k(0) + d \tag{7.4}$$

Let us consider that $y_r(t)$ is the reference output and the output $y_k(t)$ will converge to the reference output. $\lim_{k\to\infty} y_k(t) \to y_r(t)$ and the control input needed to obtain the desired output is $\lim_{k\to\infty} u_k(t) \to u_r(t)$

Let us define the error as the difference between the reference output and actual output.

$$e_k := y_r - y_k = G(u_r - u_k) + d \tag{7.5}$$

At the start of the batch process, the reference control input to achieve the reference output cannot be known and the reference control input may be changed in the presence of non-periodic disturbances. Let us consider a new variable that is the estimation of the reference control input as, $\hat{u}_r$, then we can reformulate equation (7.5) as,

$$e_k = G(\hat{u}_r - u_k) + G(u_r - \hat{u}_r) + d \tag{7.6}$$

The second part of the equation can be defined as a new variable,

$$e_k^{\,e} = G(u_r - \hat{u}_r) + d \tag{7.7}$$

It includes both deterministic part $G(u_r - \hat{u}_r)$ and stochastic part $d$. It will be more convenient to model the error in state space form of a linear stochastic system.

$$x_{k+1}{}^{e} = A^{e} x_{k}{}^{e} + B^{e} w_{k}$$
$$e_{k}{}^{e} = C^{e} x_{k}{}^{e} + D^{e} v_{k} \tag{7.8}$$

Where both $w_k$, $v_k$ are zero-mean independent and identically distributed sequences at $k^{th}$ cycle. For simplicity, we can consider that the system matrices $A^e, B^e, C^e, D^e$ are identity matrices. It is reasonable to consider the error state in one cycle mostly depend on the same error state of previous cycles and this assumption will make the problem simpler. So the system state space equation becomes,

$$x_{k+1}{}^{e} = x_{k}{}^{e} + w_{k}$$
$$e_{k}{}^{e} = x_{k}{}^{e} + v_{k} \tag{7.9}$$

From the system state space equation $x_k^e$ includes the cyclic part of $e_k^e$ and $v_k$ is completely random part that interacts instantaneously for that particular cycle only. If we define a new variable that composes only the cyclic part of the tracking error $e$ as $e_d$,

$$e_d = G(\hat{u}_r - u_k) + x^e \tag{7.10}$$

Now, we can get this for two successive cycles as follows:

$$e_{d_{k+1}} = G(\hat{u}_r - u_{k+1}) + x^e{}_{k+1} \tag{7.11}$$

$$e_{d_k} = G(\hat{u}_r - u_k) + x^e{}_k \tag{7.12}$$

Using equations (7.9),(7.11),(7.12) ,

$$e_{d_{k+1}} = e_{d_k} - G\Delta u_{k+1} + w_k \tag{7.13}$$

$$e_k = e_{d_k} + v_k \tag{7.14}$$

From this model equation it is observed that the error can be estimated not only using

the information of current cycle but also using the information from the previous cycles. Hence model predictive controller will use current cycle information to handle non-periodic uncertainties and disturbances and ILC will take care of periodic disturbances.

### 7.3.2 Controller development

A model predictive controller is a good choice to eliminate non-repetitive disturbances for controlling the heating phase as we see in Chapter 6. Although the heating phase of thermoforming machines is a slow process, the number of system equations is high when multiple sensors are used. So multi-parametric programming will be used for this system to eliminate computational burden and cost of hardware. As we already discussed the design procedure of multi-parametric MPC in Chapter 6, we will not repeat it here.

Iterative Learning Control will work on the cyclic disturbances as feed-forward. Hence, the output of the ILC for $k^{th}$ cycle will be,

$$u_k{}^{ILC}(t) = u_{k-1}(t) + Le_{k-1}(t) \tag{7.15}$$

Where $L$ is the ILC learning gain. So the control input $u_k(t)$ is composed of two terms: control input from MPC $u_k{}^{MPC}(t)$ and the control input from ILC, $u_k{}^{ILC}(t)$. Final control input is,

$$u_k(t) = u_k{}^{ILC}(t) + u_k{}^{MPC}(t) = u_{k-1}(t) + Le_{k-1}(t) + u_k{}^{MPC}(t) \tag{7.16}$$

The diagram of the proposed MPC based ILC is shown in Fig.7.1.

But the proposed controller raised another problem. One of the advantages of MPC was its ability to cope with hard constraints on control inputs by allowing for operation close to the system constraints. However, the addition of an ILC controller to the MPC in the proposed controller does not ensure control inputs that can be produced by the actuator considering the system constraint. To eliminate this problem, we propose

a new iterative learning model predictive controller (ILMPC) in the next section.

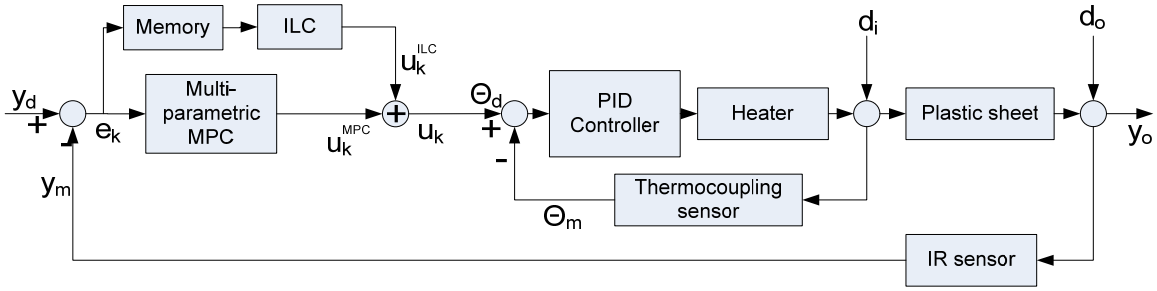


Fig. 7.1: MPC based ILC for heating phase of thermoforming process.

## 7.4 Iterative Learning Model predictive controller (ILMPC)

As we discussed before, an MPC predicts future control inputs by solving the optimization problem over an output horizon involving the minimization of a cost function using the model of the system at each sampling instant. MPC does not only compute the optimal control input, it also considers the physical and operational constraints of the system as well as the current and past history of the plant to predict future corrective actions. MPC is basically an optimization problem which involves a performance objective function of the form:

$$\min_{\substack{u_{k+1}(t+i|t) \\ i=0,\ldots,N_p}} \sum_{i=1}^{N_p} [\hat{y}(t+i\,|\,t) - y_r(t+i)]^T Q_i [\hat{y}(t+i\,|\,t) - y_r(t+i)]$$

$$+ \sum_{i=0}^{N_u-1} [\Delta u(t+i\,|\,t)^T R_i \Delta u(t+i\,|\,t)] \qquad (7.17)$$

Where $Q_i$ is weighting matrix with element those reflecting relative importance of the element of output vector and $R_i$ $Q_i$ is weighting matrix with element those penalizing for relative big change of input.

Subject to the inequality constraints

$$u_{\min} \le u(t) \le u_{\max}; y_{\min} \le y(t) \le y_{\max}; g(x(t), u(t)) \le 0 \tag{7.18}$$

Where $g(x(t), u(t))$ is the vector of system constraints and the linearized process dynamics of the non-linear system are given by,

$$\begin{aligned} x(t+1) &= Ax(t) + Bu(t) \\ y(t) &= Cx(t) + Du(t) \end{aligned} \tag{7.19}$$

where the state is $x(t) \in \mathbb{R}^n$, the input is $u(t) \in \mathbb{R}^m$, the output is $y(t) \in \mathbb{R}^p$, $N_p$ and $N_u$ are the output and control prediction horizons, $\hat{y}(t+i \mid t)$ is the predicted value of $y(t+i)$ at time $t+i$ based on information at the current discrete time $t$ using the process model. In this section, we propose an iterative learning model predictive control (ILMPC) framework that can be applied to 2D systems and that performs well while incorporating input and output constraints.

*A. Control Objective*

The thermoforming process is a periodic nonlinear system that must track a particular output profile repeatedly over each cycle while staying within process actuator constraints. In this section, we develop ILMPC for a linear periodic system. In the next section, it will be explained how this could be applied to the nonlinear thermoforming process. We require that the proposed control scheme tracks a repeating reference trajectory while satisfying all the constraints by specifically exploiting the 2D nature of the system. Mathematically such a control objective within a cycle $k+1$ can be defined as:

$$\min_{\substack{u_{k+1}(t+i|t) \\ i=0,\ldots,N_p}} \sum_{i=1}^{N_p} [\hat{y}_{k+1}(t+i \mid t) - y_r(t+i)]^T Q_i [\hat{y}_{k+1}(t+i \mid t) - y_r(t+i)]$$

$$+ \sum_{i=0}^{N_u - 1} [\Delta u_{k+1}(t+i \mid t)^T R_i \Delta u_{k+1}(t+i \mid t)] \tag{7.20}$$

Where, the subscript $k$+1 refer to the cycle index. The output reference trajectory $y_r$ $(t+i)$ is the same for all cycles. Note that the objective of MPC is to minimize the output error over the current cycle. It is also important to note that the control and prediction horizons are finite.

*B. Augmented error model with integral information*

The system is required to track the output reference trajectory or, in other words, the process output profile must converge in the cycle-to-cycle direction to a limit profile $y_r$. To achieve this goal, we "integrate" the error information propagating across the cycles. This integral information can be defined with the help of a new variable:

$$es_k(t) = \sum_{j=1}^{k} [y_j(t) - y_r(t)] \tag{7.21}$$

at discrete time $t$ within cycle $k$. $es_k$ sums the error across all the cycles at the same discrete time $t$ within each cycle. Next, we define an extended output vector $z_k(t) = [y_k^T \quad es_k^T]^T$. We now see that:

$$es_{k+1}(t) = Cx_{k+1}(t) + Du_{k+1}(t) + \begin{bmatrix} 0 & I \end{bmatrix} z_k(t) - y_r(t) \tag{7.22}$$

Thus the extended output vector can be represented as:

$$z_{k+1}(t) = \begin{bmatrix} C \\ C \end{bmatrix} x_{k+1}(t) + \begin{bmatrix} D \\ D \end{bmatrix} u_{k+1}(t) + \begin{bmatrix} 0 & 0 \\ 0 & I \end{bmatrix} z_k(t) + \begin{bmatrix} 0 \\ -1 \end{bmatrix} y_r(t) \tag{7.23}$$

The target trajectory for each cycle remains the same. We assume that $\lim_{k\to\infty} x_k(t) \to x_r(t)$, $\lim_{k\to\infty} y_k(t) \to y_r(t)$, $\lim_{k\to\infty} u_k(t) \to u_r(t)$, $\lim_{k\to\infty} z_k(t) \to z_r(t)$. To define the error model, let:

$$\begin{aligned}
\overline{x}_{k+1}(t) &:= x_{k+1}(t) - x_r(t) \\
\overline{y}_{k+1}(t) &:= y_{k+1}(t) - y_r(t) \\
\overline{u}_{k+1}(t) &:= u_{k+1}(t) - u_r(t) \\
\overline{z}_{k+1}(t) &:= z_{k+1}(t) - z_r(t)
\end{aligned} \tag{7.24}$$

Following [62], the error model can then be defined using these error variables as:

$$\begin{aligned}
\overline{x}_{k+1}(t+1) &= A\overline{x}_{k+1}(t) + B\overline{u}_{k+1}(t) \\
\overline{z}_{k+1}(t) &= \overline{C}\overline{x}_{k+1}(t) + \overline{D}\overline{u}_{k+1}(t) + \overline{D}_0\overline{z}_k(t)
\end{aligned} \tag{7.25}$$

where,

$$\overline{C} = \begin{bmatrix} C \\ C \end{bmatrix}, \overline{D} = \begin{bmatrix} D \\ D \end{bmatrix}, \overline{D}_0 = \begin{bmatrix} 0 & 0 \\ 0 & I \end{bmatrix}$$

The optimization problem can be rewritten within a cycle $k$+1 as:

$$\min_{\substack{\overline{u}_{k+1}(t+i|t) \\ i=0,\ldots,N_p}} \sum_{i=1}^{N_p} [\hat{z}_{k+1}(t+i \mid t) - z_r(t+i)]^T Q_i [\hat{z}_{k+1}(t+i \mid t) - z_r(t+i)] + \sum_{i=0}^{N_u-1} [\overline{u}_{k+1}(t+i \mid t)^T R_i \overline{u}_{k+1}(t+i \mid t)] \tag{7.26}$$

where, $z_r(t) = [y_r^T \quad es_r^T]^T$ and $es_r^T$ is a null vector, subject to the inequality constraints for $t \in [0, T]$ due to the constraints in the actual process

$$\begin{aligned}
\overline{u}_{\min} &\le \overline{u}(t) \le \overline{u}_{\max} \\
\overline{z}_{\min} &\le \overline{z}(t) \le \overline{z}_{\max}
\end{aligned}$$

### 7.4.1 Design of multi-parametric quadratic ILMPC

The thermoforming process is a complex MIMO system linking heater temperatures to infrared sensors outputs. Although the heating phase of thermoforming machines is a slow process, the number of system equations is high when multiple sensors are used. Thus, much computation and expensive hardware is required to

implement the online minimization of the cost function. Even though an advanced nonlinear programming algorithm for optimization is used, the speed and accuracy of the solution is not guaranteed. In this section, mp-ILMPC for heating phase of the thermoforming machine is proposed. The model developed for the heating phase of the thermoforming machine is nonlinear. So the model equations are linearized around the operating point $(x^*, u^*)$ to control the system using mp-MPC.

$$A = \left.\frac{\partial f(x,u)}{\partial x}\right|_{\substack{x=x^* \\ u=u^*}} \qquad B = \left.\frac{\partial f(x,u)}{\partial u}\right|_{\substack{x=x^* \\ u=u^*}} \qquad C = \left.\frac{\partial h(x)}{\partial x}\right|_{x=x^*} \tag{7.27}$$

The linear state-space equations for the process are:

$$\begin{aligned} x(t+1) &= Ax(t) + Bu(t) \\ y(t) &= Cx(t) \end{aligned} \tag{7.28}$$

where $A \in \mathbb{R}^{n\times n}, B \in \mathbb{R}^{n\times m}$, $C \in \mathbb{R}^{p\times n}$. With the linearized system equations, using equations (7.28) and substituting $\bar{x}(t+i)|_t = A^i \bar{x}(t) + \sum_{j=0}^{i-1} A^j B \bar{u}_{t+i-1-j}$, the optimization problem of MPC in equation (7.26) can be reformulated following some algebraic manipulation (see [62]) to get the minimum value,

$$V(\bar{x}(t)) = \frac{1}{2}\bar{x}^T(t) Y \bar{x}(t) + \min_U \left\{ \frac{1}{2} U^T H U + \bar{x}^T(t) F U \right\} \tag{7.29}$$

$$\text{Such that } GU \le W + E\bar{x}(t)$$

where, $U = [\bar{u}_t{}^T, \ldots\ldots \bar{u}_{t+N_U-1}{}^T]^T$ is the optimization vector and $H, F, Y, G, W, E$ are obtained from $Q, R$. By defining a new vector $w := U + H^{-1}F^T\bar{x}(t)$, the optimization problem can be transformed into,

$$V_w(\bar{x}(t)) = \min_w \frac{1}{2} w^T H w \tag{7.30}$$

$$\text{Such that } Gw \leq W + S\bar{x}(t)$$

Where $S = E + GH^{-1}F^T$ and $V_w(\bar{x}(t)) = V(\bar{x}(t)) - \frac{1}{2}\bar{x}(t)^T \left(Y - FH^{-1}F^T\right)\bar{x}(t)$, the current state $\bar{x}(t) = x_o$ can be taken as a vector of parameters. If there are $q$ inequalities, then $w \in \mathbb{R}^{2m.N}$, $H \in \mathbb{R}^{m.N \times m.N}$, $G \in \mathbb{R}^{q \times 2m.N}$, $W \in \mathbb{R}^{q \times 1}$, $S \in \mathbb{R}^{q \times n}$ and $F \in \mathbb{R}^{n \times q}$. In [61], it is shown that the explicit solution of the equation is a continuous piecewise affine function defined over the partition of the parameter space. Based on these results, we propose the same algorithm as in the previous chapter for the offline computation of the optimization problem for the heating phase and hence implement it in ILMPC control of the process. The algorithm is described by the flow charts in Fig.7.2.

### 7.4.2 Design steps of multi-parametric quadratic ILMPC

The steps in the design of the ILMPC controller will not be discussed in details as they are very similar to the previous chapter. The steps are as follows:

(1) Linearization of the system
(2) Incorporating constraints
(3) Reducing the number of partitions in offline solution
(4) Choosing the weight matrix of the controller
(5) Tuning the parameters of the controller

After the computation of the controller using mp-QP, the optimal heater control input to the system will be obtained as an affine function of system state, previous control input, reference output, previous cycle error and measured disturbance. The algorithm for incorporating the solution of offline optimization into the controller is shown in Fig. 7.3.

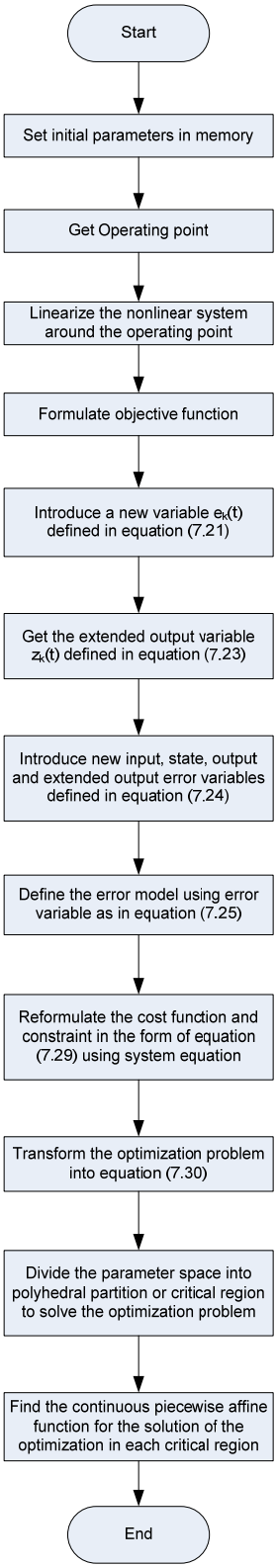


Fig.7.2: Algorithm for offline optimization of the objective function for ILMPC

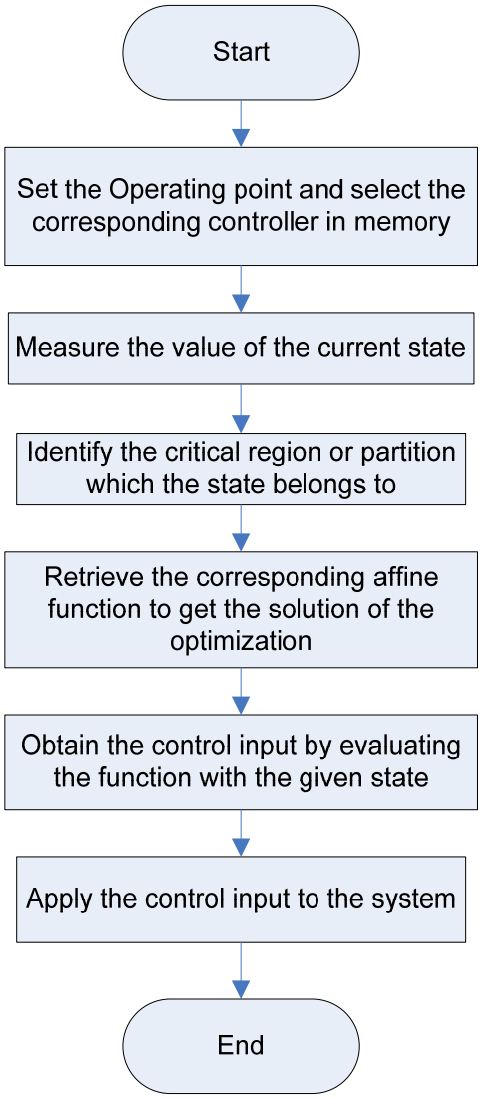


Fig.7.3: Algorithm for incorporating the solution of offline optimization into the controller

## 7.5 Simulation results

The effectiveness of the proposed ILMPC controller is investigated using same simulation model that was developed using Matlab/Simulink. The performance of the proposed method and conventional method is compared using the developed model. The oven configuration with 9 equidistant infrared sheet temperature sensors (3x3) location on each side of the sheet is discussed in details in Chapter 3. The performance of a

conventional PI controller and some state-of-the-art controllers like ILC, TILC and MPC are used from Chapter 6 to compare with the MPC based iterative learning controller and ILMPC controller. In the design and development of the MPC based iterative learning controller, MPC part of the controller is designed using exactly the same procedure as in the last chapter, and the iterative learning controller part used information from the last 5 cycles to generate the control inputs. Final control inputs are the summation of MPC part and iterative learning part of the controller. On the other hand, ILMPC controller is designed and developed using the extended output variables. Each pair of control inputs is formulated in an explicit expression of 48 system states (36 outputs, 2 air temperatures and 10 other inputs), 2 previous control inputs and 36 reference outputs.

The output sheet temperature at the sensor locations for the first 11 cycles with a cycle length of 600s are shown in Fig.7.4 and 7.5 for MPC based ILC and ILMPC controller. At the start of each cycle, a sheet enters the oven and comes out of it after a cycle period of 600s, as a new sheet enters the oven. An exponential input profile (same as last chapter) is chosen such that the heat has enough time to propagate to the inner layers of the sheet. The sheet temperature should follow as closely as possible the desired profile so that it will not melt down or burn but will be heated across its thickness. We observed in last chapter that the PI controller and ILC have weak control over the temperature because of the long time constant of the process. The TILC controller cannot follow the profile even though it can get close to the target temperature at the end of the cycle as the output measurement occurs only once at the end of the cycle. Therefore, TILC is mono-dimensional. The MPC controller performs well but there is a steady-state error passing through the cycle-to-cycle direction as it does not use any information from the previous cycle. In Fig.7.4 and 7.5, the MPC based ILC does not perform very well. Although MPC is incorporated with ILC, the controller output does not ensure to be followed by the actuator. So it does not really have the advantages of the MPC. On the other side, the performance of ILMPC controller is quite satisfactory even though there was a small error in the first cycle. The controller tunes itself to achieve the desired profile. In Fig. 7.6, it is observed that the heater temperature of the MPC based ILC controller cannot follow the command heater temperature from the controller output as the ILC part of the controller output is an extra term that is added with the MPC part of

the controller which is calculated considering system constraints. So the heater cannot follow the control input generated by the controller. But in case of ILMPC, the heaters can follow the control input as it was calculated considering the system constraint. If we compare these two controller with all other controllers in the last chapter, we see that MPC and ILMPC can follow the control input whereas PI, ILC, TILC and MPC based ILC cannot follow it. The performance of the proposed MPC based ILC controller and ILMPC controller in presence of non-repetitive disturbances are shown in Fig.7.7 and Fig.7.8. The performance of ILMPC looks better than MPC based ILC controller. ILMPC and MPC controller performs better than other controller in the presence of non-repetitive disturbances. The tracking error of ILMPC and MPC is much less than other conventional controllers. At last, the performances of the proposed controllers are shown in Fig, 7.9 and Fig. 7.10. It is observed that ILMPC can perform much better than MPC controller as it combines cycle to cycle control technique with in cycle control. Now, we will present a comparison table (Table 7.1) based on the results of the previous and current chapters.

*Table 7.1: Comparison of different control technique for heater in terms of error*

| Name of the control Technique | Maximum error among $6^{th}$ to $11^{th}$ cycle under normal operation | | Maximum sheet temperature error among $6^{th}$ to $11^{th}$ cycle under disturbances | |
|---|---|---|---|---|
| | Sheet temperature error (Celsius) | Heater temperature error (Celsius) | Non-repetitive disturbances (Celsius) | Repetitive disturbances (Celsius) |
| PI | 8 | 800 | 10 | 12 |
| ILC | 10 | 50 | 13 | 13 |
| TILC | 13 | 5 | 14 | 12 |
| MPC | 3 | 1.5 | 4.5 | 6 |
| MPC based ILC | 6 | 15 | 17 | 8 |
| ILMPC | 3 | 1.5 | 5 | 3 |

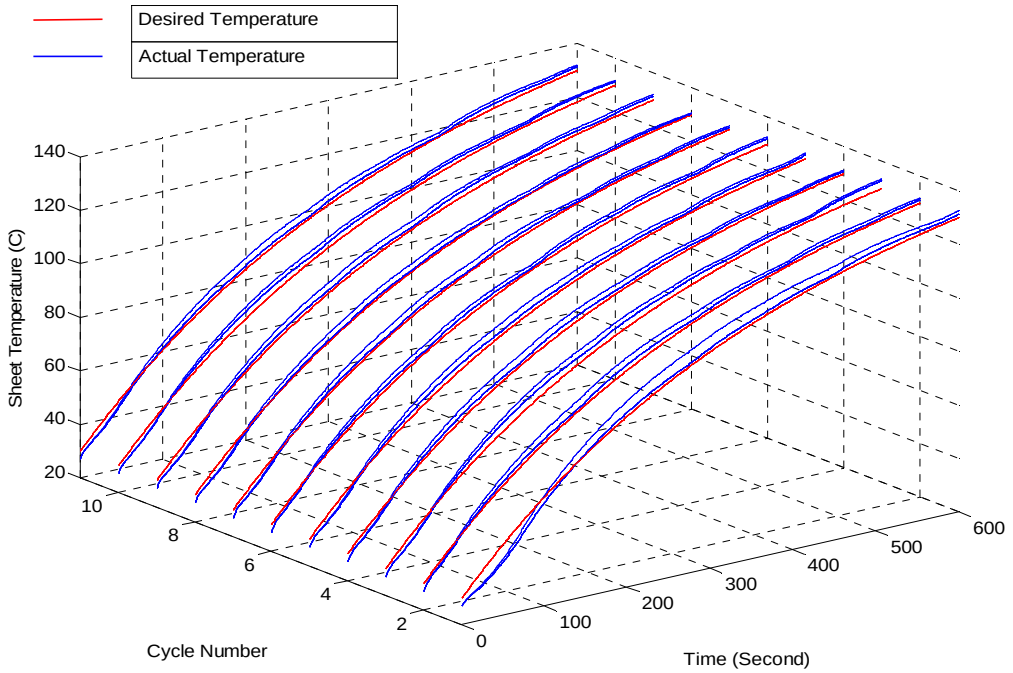


(a) MPC based ILC

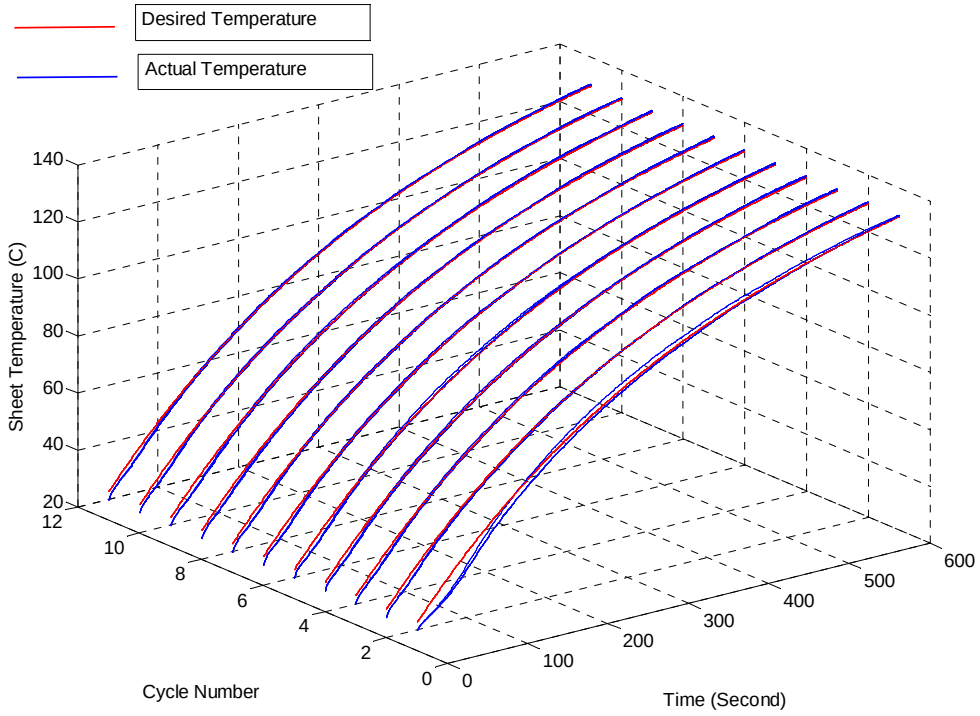


(b) ILMPC

Fig. 7.4: the sheet temperature at sensor point of the sheet for (a) MPC based ILC (b) ILMPC

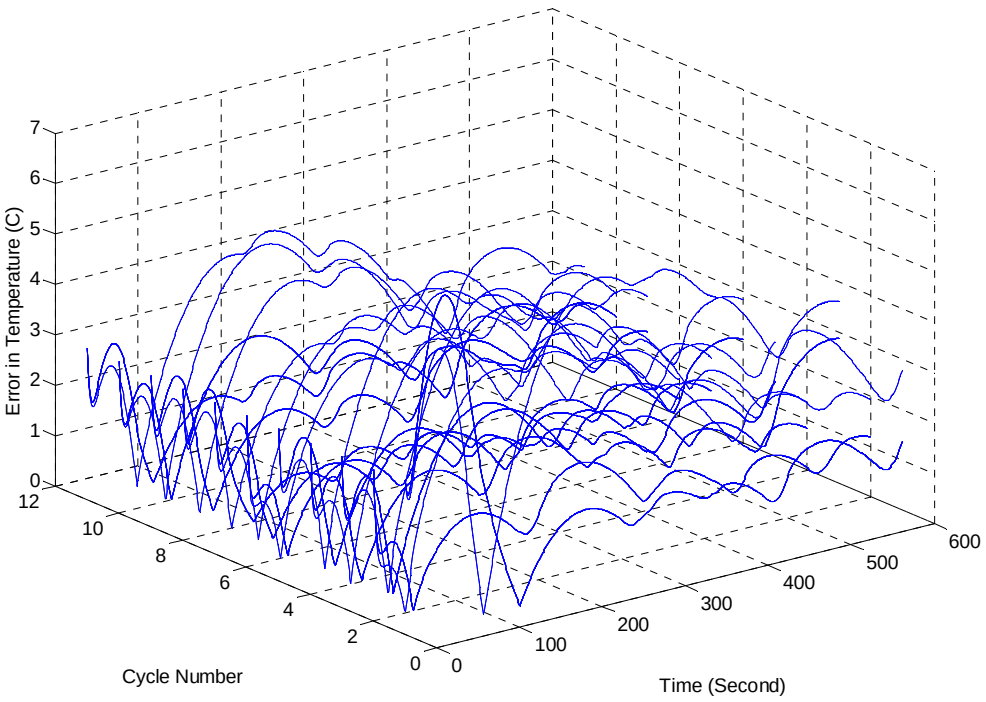


(a) MPC based ILC

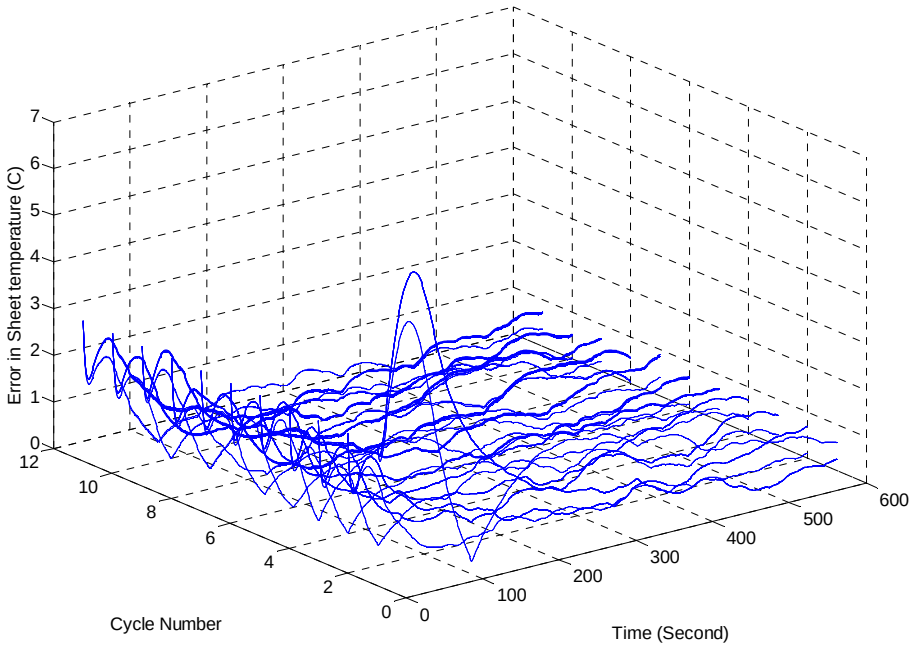


(b) ILMPC

Fig. 7.5: Error in sheet temperature at sensor point of the sheet for (a) MPC based ILC (b) ILMPC

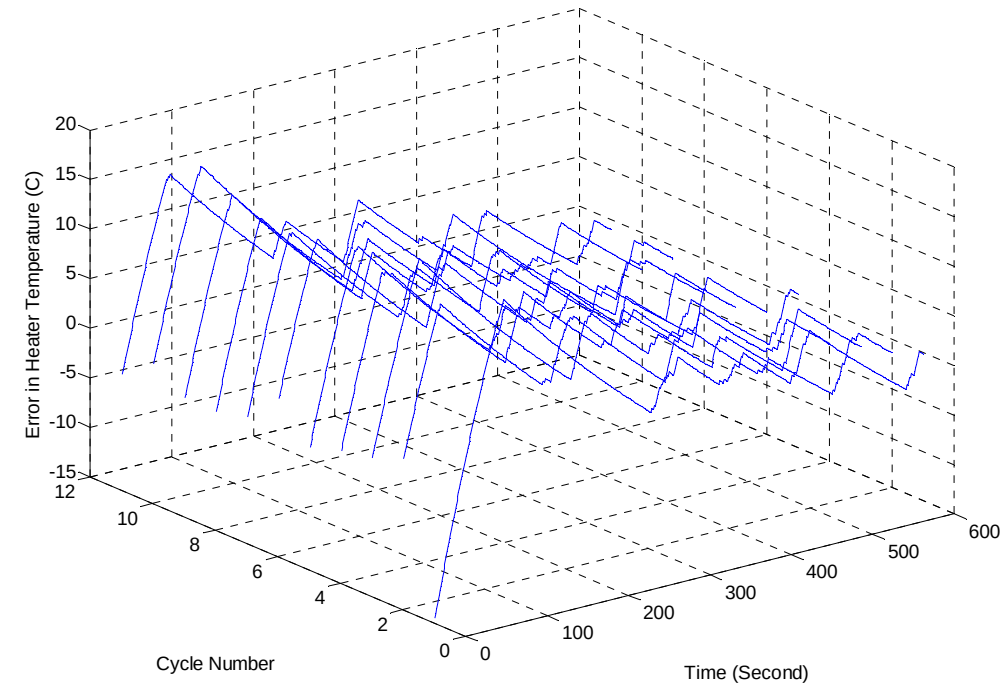


(a) MPC based ILC

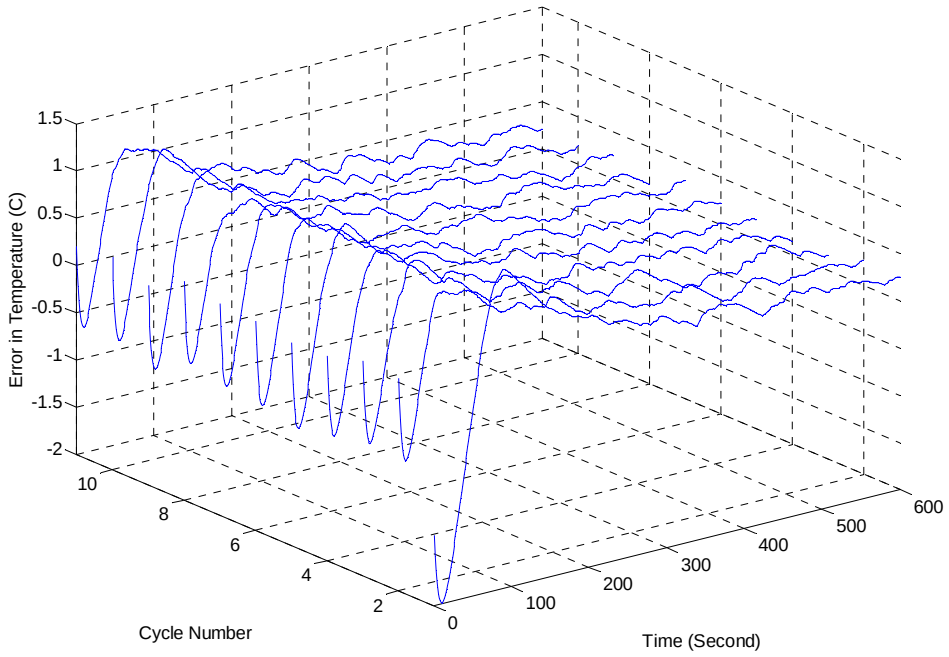


(b) ILMPC

Fig. 7.6: Error between command input temperature and actual heater temperature

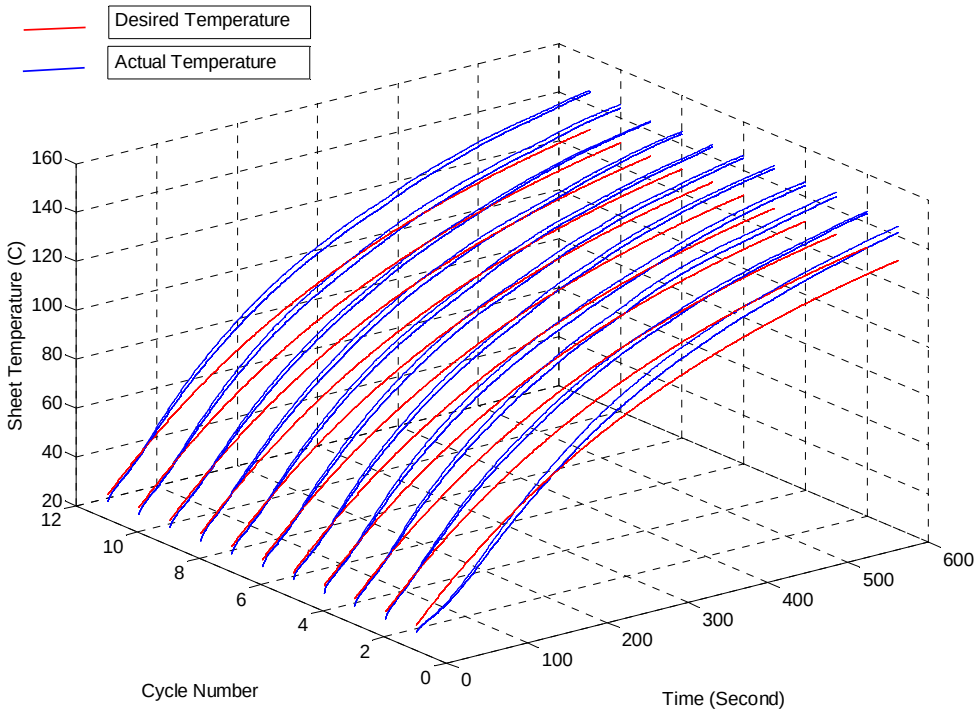


(a) MPC based ILC

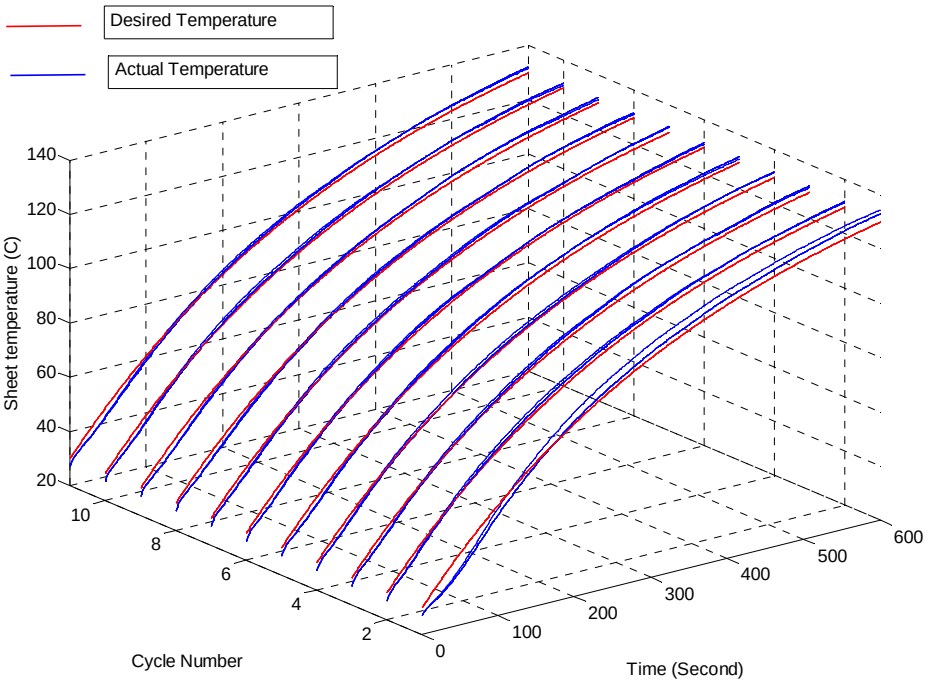


(b)

Fig. 7.7: Temperature at sensor point of the sheet with presence of large non-repetitive disturbances

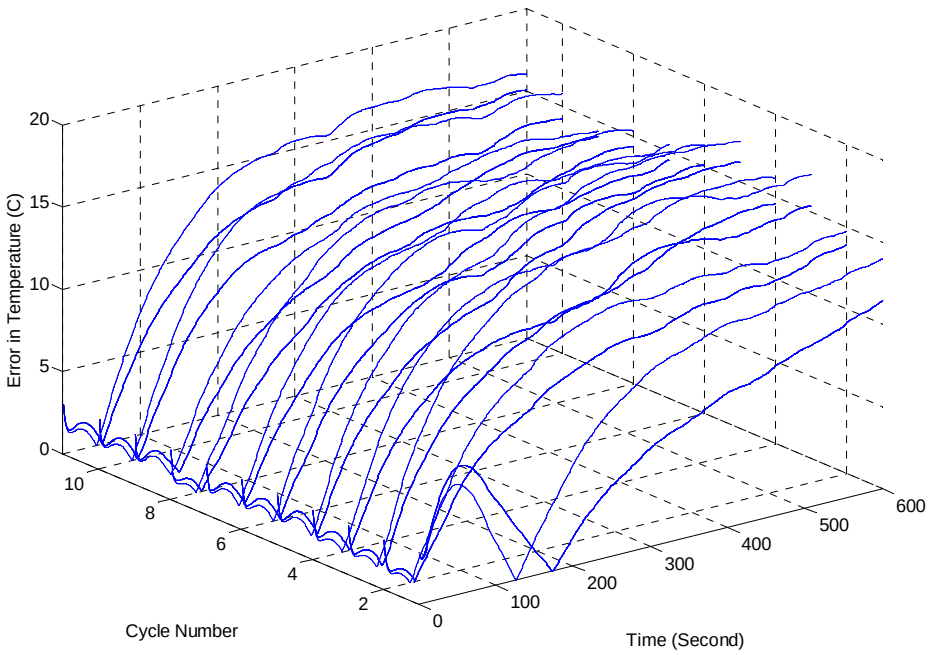


(a) MPC based ILC

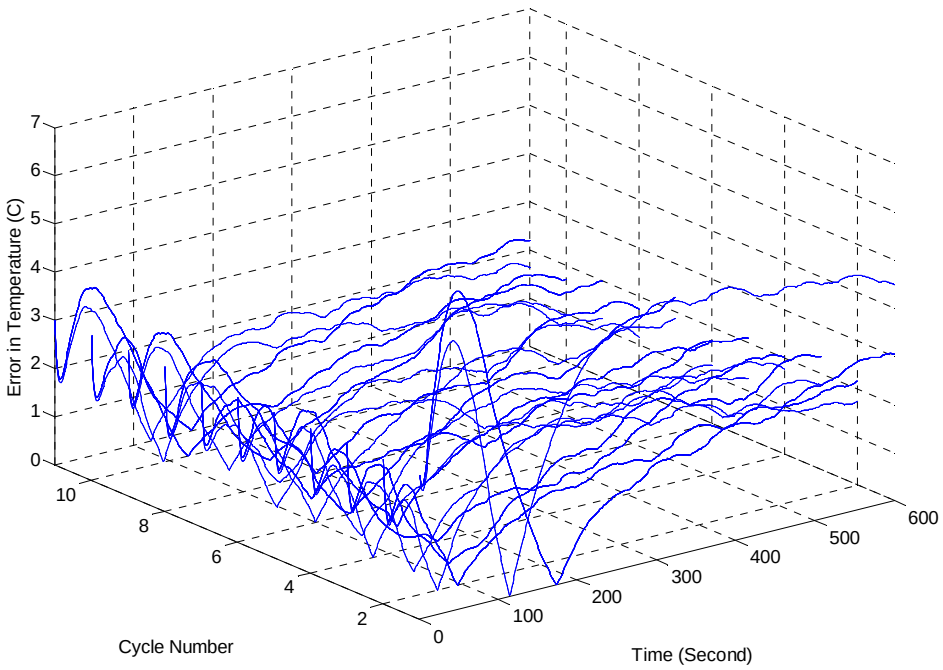


(b) ILMPC

Fig.7.8: Error in temperature at sensor point of the sheet with presence of non-repetitive disturbances

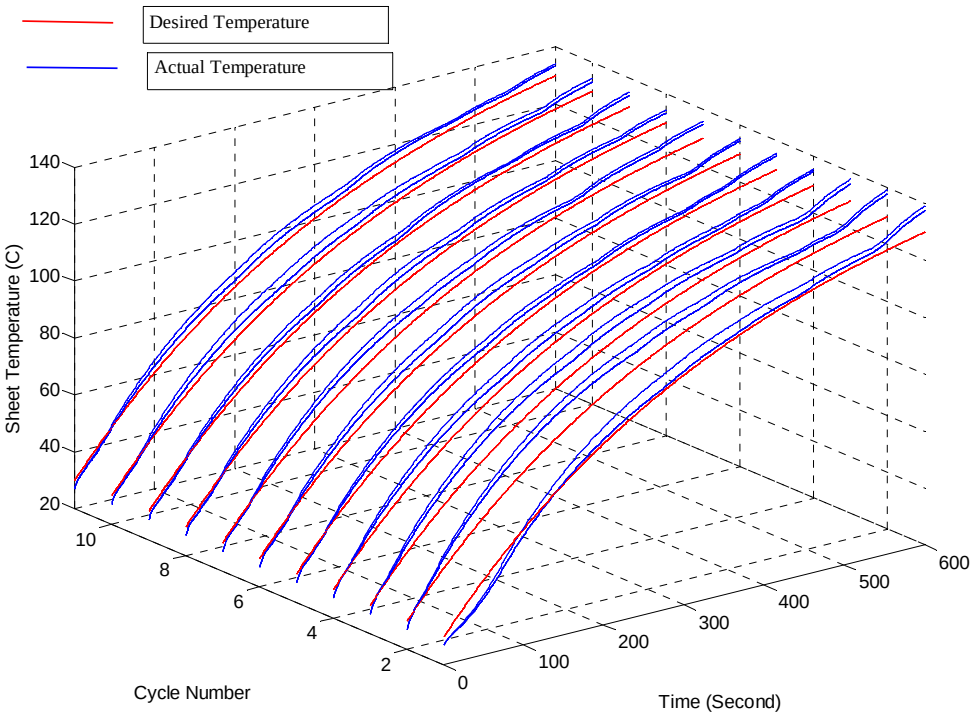


(a) MPC based ILC

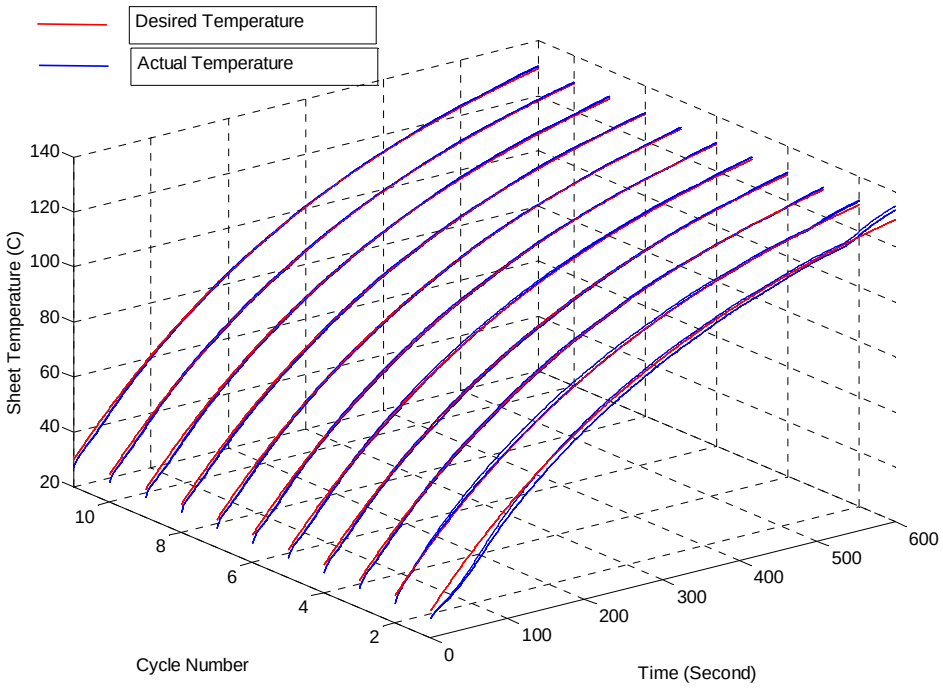


(b) ILMPC

Fig. 7.9: Sheet temperature at sensor point of the sheet at the presence of repetitive disturbances

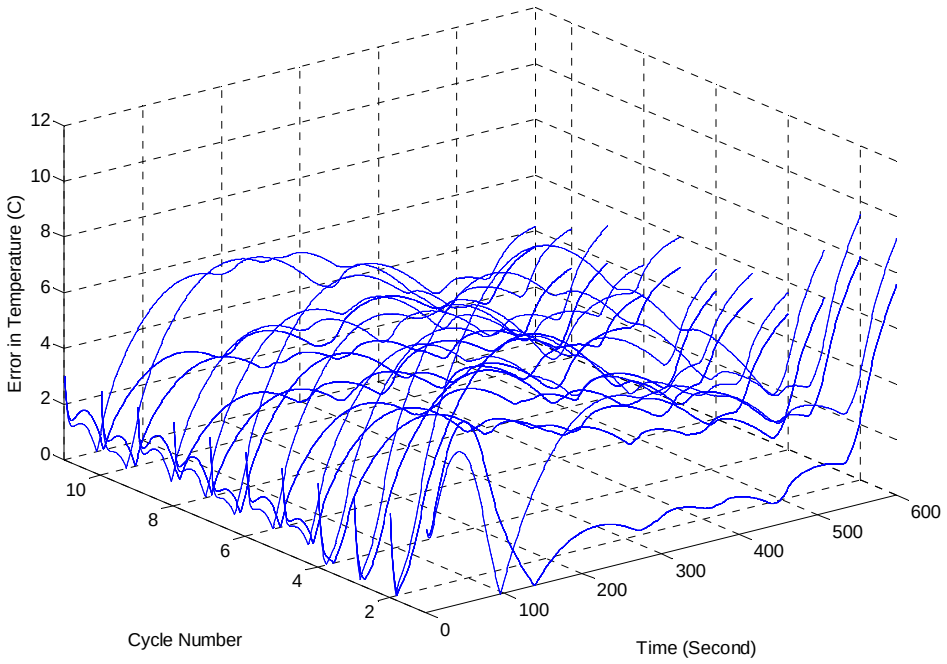


(a) MPC based ILC

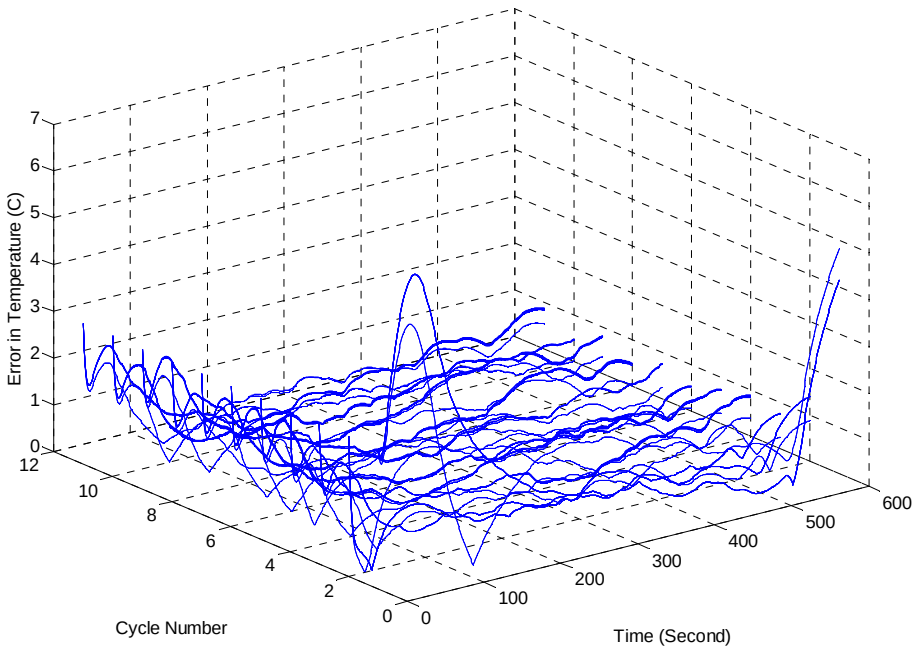


(b) ILMPC

Fig. 7.10: Error in temperature at sensor point of the sheet at the presence of repetitive disturbances

## 7.6 Conclusion

In this chapter, a step-by-step approach is proposed for the development of 2D controller that uses the information from input and output samples within the cycle and the information from cycle to cycle. Iterative control technique along with model predictive control is presented in this chapter on 2D control of the thermoforming process. Two controllers are developed for the purpose of achieving better performances in presence of non-repetitive and repetitive disturbances. To deal with constraints as well as non-repetitive disturbances in the process, the MPC technique is incorporated in ILMPC to update the control law within the cycle. To exploit the repetitive nature of the heating phase of the process, a cycle-to-cycle iterative learning control technique direction is proposed. To reduce the computational burden, the control laws are computed offline using multi-parametric programming. The main feature of the ILMPC controller for the process is that it can handle model mismatch and periodic and non-periodic disturbances very well as compared to other techniques. But the MPC based ILC controller has poor performances as compared to ILMPC.

# Chapter 8
# Conclusion

In the control of a complex industrial process, we face typical challenges such as building a mathematical model that represents the behavior of the system, arranging to collect process variable information, knowing the constraints of the actuator, developing a technique to overcome the process constraints and designing a suitable controller that performs the objective satisfactorily. In this thesis, we tried to focus on these issues one by one, then proposed solutions to these issues and developed an appropriate control technique step by step for sheet temperature control of the thermoforming process. In this development process, the advantages and drawbacks are identified for the proposed controllers. In the last part of the thesis, a new control technique is introduced to achieve the desired performance.

## 8.1 Content of this thesis

In Chapter 2, some possible ways to improve the model is presented. In next Chapter 3, another challenging problem in controlling the thermoforming process, known as IHP, is discussed. Thus, in Chapter 3, a method based on the conjugate gradient method is proposed such that it can provide setpoint temperature values for the heaters resulting in a specific temperature distribution in the plastic sheet after a predefined cycle time. In Chapter 4, a new method is proposed for the estimation of the whole sheet temperature profile based on spatial harmonics. Then, a new controller is designed to control these spatial harmonics, which has the effect of controlling the temperature over the whole sheet instead of just controlling temperatures at certain locations. In Chapter 5, the proposed method of Chapter 4 is modified to overcome some of the discrepancies. In the following chapter, we explore model predictive control using the explicit solution of the optimization problem for temperature control of a thermoforming machine. In this chapter, I discuss the multi-parametric quadratic programming used to solve the online

optimization with an offline strategy in the development of MPC for the heating phase of thermoforming process, and a multi-parametric MPC is developed for it. Chapter 7 introduces a 2D control combining MPC and ILC to control the heater temperature.

## 8.2 Future work

This thesis presents some new sensing and controlling techniques for sheet temperature of heating phase in thermoforming process. These techniques can also be used in other repetitive slow processes. But more research can be conducted to sense the temperature signal from plastic sheet and control the sheet temperature of the heating phase. Some of them are proposed in this thesis as follows:

### 8.2.1 Temperature Sensing

A new temperature sensing technique is proposed in this thesis. It has satisfactory performance. But we can make this sensing technique more effective by locating the sensors of the plastic sheet at optimal positions. This arrangement of the sensors depends on the expected temperature profile on the sheet. Therefore, more research can be done in this area to find optimal arrangement of the sensors. This would ensure the best estimation of temperature from the least number of sensors.

### 8.2.2 Nonlinear Model Predictive Controller

Even though the dynamics of the thermoforming process is nonlinear due to the radiation heat transfer between heater and sheet, nonlinear behavior of the heater actuator and presence of constraints; linear MPC approaches have been found successful in controlling sheet temperature. In this thesis, linear MPC technique is used to control the system as important issues of MPC such as online computation can be solved using well developed multi-parametric programming. The thermoforming system is, however, in general inherently nonlinear. Linear models are often inadequate to describe the process dynamics and nonlinear models have to be used. This motivation can lead researchers to use nonlinear model predictive control in sheet temperature control in the future. Solving the

optimization problem will be the main challenge in implementing this nonlinear control technique as it requires a lot of computation within a sampling period to solve online.

### 8.2.3 Linear Model Predictive Controller with time varying linear model

The nonlinear model of the thermoforming process can be linearized at different operating points. The system matrices of the linear system will be changing with a change of operating point of the process. So the model of the thermoforming process can be expressed as a linear system with time varying system matrices that depend on system states and system inputs to capture nonlinear behaviors of the thermoforming process more accurately. In future work, one could also work to develop a model predictive control for a time-varying multivariable process model.

The linear state space model equations for the system can be expressed as,

$$\begin{aligned} x(t+1) &= A(t)x(t) + B(t)u(t) \\ y(t) &= C(t)x(t) \end{aligned} \tag{8.1}$$

Where the system matrices are,

$$A(t) = \left.\frac{\partial f(x(t),u(t))}{\partial x(t)}\right|_{\substack{x(t)=x^*(t) \\ u(t)=u^*(t)}} \qquad B(t) = \left.\frac{\partial f(x(t),u(t))}{\partial u(t)}\right|_{\substack{x(t)=x^*(t) \\ u(t)=u^*(t)}}$$

$$C(t) = \left.\frac{\partial h(x(t))}{\partial x(t)}\right|_{x(t)=x^*(t)}$$

$$A(t) = g_1(x(t),u(t)) \in \mathbb{R}^{n\times n}, B(t) = g_2(x(t),u(t)) \in \mathbb{R}^{n\times m},$$
$$C(t) = g_3(x(t),u(t)) \in \mathbb{R}^{p\times n}$$

The MPC uses the information from the mathematical model of a system to

calculate future control inputs that optimize an objective function to have desired performance of the system. The performance objective function is of the form:

$$J = \min_{\Delta u} \sum_{i=1}^{N_p} [\hat{y}(t+i) - y_r(t+i)]^T Q_i [\hat{y}(t+i) - y_r(t+i)] + \sum_{i=0}^{N_u - 1} [\Delta u(t+i)^T R_i \Delta u(t+i)] \tag{8.2}$$

Subject to the inequality constraints for $t \in [0, T]$

$$\begin{aligned} u_{\min} &\le u(t) \le u_{\max} \\ y_{\min} &\le y(t) \le y_{\max} \\ g(x(t), u(t)) &\le 0 \end{aligned} \tag{8.3}$$

and the process dynamics;

$$\begin{aligned} x(t+1) &= f(t, x(t), u(t)) \\ y(t) &= h(t, x(t)) \end{aligned} \tag{8.4}$$

where the state is $x(t) \in \mathbb{R}^n$, the input is $u(t) \in \mathbb{R}^m$, the output is $y(t) \in \mathbb{R}^m$. The control move is calculated from the current time along the horizon at every sampling time instant using the model information. But the nonlinear model information can be simplified using linearization of the model at that current operating point of the thermoforming process to provide the system information as accurate as nonlinear model around the operating point. The thermoforming process can be represented as linear system where the system matrices depend on the arbitrary system states $x^*(t)$ and inputs $u^*(t)$.

The system equation for the system at time *t* can be written as:

$$x(t+1) = A_t(x^*(t), u^*(t))x(t) + B_t(x^*(t), u^*(t))u(t)$$
$$y(t) = C_t(x^*(t), u^*(t))x(t)$$

Where, $A_t, B_t, C_t$ are system matrices at system operating point $(x^*(t), u^*(t))$. The system equation for the same system at time *t+1* can be written as:

$$x(t+2) = A_{t+1}(x^*(t+1), u^*(t+1))x(t+1) + B_{t+1}(x^*(t+1), u^*(t+1))u(t+1)$$
$$y(t+1) = C_{t+1}(x^*(t+1), u^*(t+1))x(t+1)$$

Where, $A_{t+1}, B_{t+1}, C_{t+1}$ are system matrices at system operating point $(x^*(t+1), u^*(t+1))$. In general, the system equation can be written as,

$$x(t+k+1) = A_{t+k}(x^*(t+k), u^*(t+k))x(t+k) + B_{t+k}(x^*(t+k), u^*(t+k))u(t+k)$$
$$y(t+k) = C_{t+k}(x^*(t+k), u^*(t+k))x(t+k)$$

(8.5)

Where, $A_{t+k}, B_{t+k}, C_{t+k}$ are system matrices at system operating point $(x^*(t+k), u^*(t+k))$.

A new objective function can be developed in the form of (8.2) to obtain the desired performance of the system.

$$J = \min_{\Delta u} \sum_{i=1}^{N_p} [\hat{y}(t+i) - y_r(t+i)]^T Q_i [\hat{y}(t+i) - y_r(t+i)] + \sum_{i=0}^{N_u - 1} [\Delta u(t+i)^T R_i \Delta u(t+i)]$$

The estimated output of the system using the model equations can be found as,

$$\hat{y}(t+1) = C_t(x^*(t), u^*(t))A_t(x^*(t), u^*(t))x(t) + C_t(x^*(t), u^*(t))B_t(x^*(t), u^*(t))u(t)$$

$$\hat{y}(t+2) = C_{t+1}(x^*(t+1),u^*(t+1))A_{t+1}(x^*(t+1),u^*(t+1))A_t(x^*(t),u^*(t))x(t)$$
$$+ C_{t+1}(x^*(t+1),u^*(t+1))A_{t+1}(x^*(t+1),u^*(t+1))B_t(x^*(t),u^*(t))u(t)$$
$$+ C_{t+1}(x^*(t+1),u^*(t+1))B_{t+1}(x^*(t+1),u^*(t+1))u(t+1)$$

$$\hat{y}(t+3) = C_{t+2}(x^*(t+2),u^*(t+2))A_{t+2}(x^*(t+2),u^*(t+2))$$
$$A_{t+1}(x^*(t+1),u^*(t+1))A_t(x^*(t),u^*(t))x(t)$$
$$+ C_{t+2}(x^*(t+2),u^*(t+2))A_{t+2}(x^*(t+2),u^*(t+2))$$
$$A_{t+1}(x^*(t+1),u^*(t+1))B_t(x^*(t),u^*(t))u(t)$$
$$+ C_{t+2}(x^*(t+2),u^*(t+2))A_{t+2}(x^*(t+2),u^*(t+2))$$
$$B_{t+1}(x^*(t+1),u^*(t+1))u(t+1)$$
$$+ C_{t+2}(x^*(t+2),u^*(t+2))B_{t+2}(x^*(t+2),u^*(t+2))u(t+2)$$

. . .

$$\hat{y}(t+N_p) = C_{t+N_p-1}(x^*(t+N_p-1),u^*(t+N_p-1))A_{t+N_p-1}(x^*(t+N_p-1),u^*(t+N_p-1))$$
$$A_{t+N_p-2}(x^*(t+N_p-2),u^*(t+N_p-2))...A_t(x^*(t),u^*(t))x(t)$$
$$+ C_{t+N_p-1}(x^*(t+N_p-1),u^*(t+N_p-1))A_{t+N_p-1}(x^*(t+N_p-1),u^*(t+N_p-1))$$
$$A_{t+N_p-2}(x^*(t+N_p-2),u^*(t+N_p-2))...A_{t+1}(x^*(t+1),u^*(t+1))B_t(x^*(t),u^*(t))u(t)$$
$$+ C_{t+N_p-1}(x^*(t+N_p-1),u^*(t+N_p-1))A_{t+N_p-1}(x^*(t+N_p-1),u^*(t+N_p-1))$$
$$A_{t+N_p-2}(x^*(t+N_p-2),u^*(t+N_p-2))...A_{t+2}(x^*(t+2),u^*(t+2))$$
$$B_{t+1}(x^*(t+1),u^*(t+1))u(t+1)+...+C_{t+N_p-1}(x^*(t+N_p-1),u^*(t+N_p-1))$$
$$A_{t+N_p-1}(x^*(t+N_p-1),u^*(t+N_p-1))A_{t+N_p-2}(x^*(t+N_p-2),u^*(t+N_p-2))$$
$$B_{t+N_p-3}(x^*(t+N_p-3),u^*(t+N_p-3))u(t+N_p-3)$$
$$+ C_{t+N_p-1}(x^*(t+N_p-1),u^*(t+N_p-1))A_{t+N_p-1}(x^*(t+N_p-1),u^*(t+N_p-1))$$
$$B_{t+N_p-2}(x^*(t+N_p-2),u^*(t+N_p-2))u(t+N_p-2)+...$$
$$+ C_{t+N_p-1}(x^*(t+N_p-1),u^*(t+N_p-1))B_{t+N_p-1}(x^*(t+N_p-1),u^*(t+N_p-1))u(t+N_p-1)$$

These predicted outputs can be substituted into the objective function of (8.2) to get a form to be used in multi-parametric programming. The objective function will be as follows:

$$
\begin{aligned}
J = \min_{\Delta u}\{&[C_t(x^*(t),u^*(t))A_t(x^*(t),u^*(t))x(t) + C_t(x^*(t),u^*(t))B_t(x^*(t),u^*(t))u(t) - \\
&y_r(t+1)]^T Q_1[C_t(x^*(t),u^*(t))A_t(x^*(t),u^*(t))x(t) + C_t(x^*(t),u^*(t))B_t(x^*(t),u^*(t))u(t) \\
&- y_r(t+1)] + [C_{t+1}(x^*(t+1),u^*(t+1))A_{t+1}(x^*(t+1),u^*(t+1))A_t(x^*(t),u^*(t))x(t) \\
&+ C_{t+1}(x^*(t+1),u^*(t+1))A_{t+1}(x^*(t+1),u^*(t+1))B_t(x^*(t),u^*(t))u(t) \\
&+ C_{t+1}(x^*(t+1),u^*(t+1))B_{t+1}(x^*(t+1),u^*(t+1))u(t+1) - \\
&y_r(t+2)]^T Q_2[C_{t+1}(x^*(t+1),u^*(t+1))A_{t+1}(x^*(t+1),u^*(t+1))A_t(x^*(t),u^*(t))x(t) \\
&+ C_{t+1}(x^*(t+1),u^*(t+1))A_{t+1}(x^*(t+1),u^*(t+1))B_t(x^*(t),u^*(t))u(t) \\
&+ C_{t+1}(x^*(t+1),u^*(t+1))B_{t+1}(x^*(t+1),u^*(t+1))u(t+1) - y_r(t+2)]... \\
&+ [C_{t+N_p-1}(x^*(t+N_p-1),u^*(t+N_p-1))A_{t+N_p-1}(x^*(t+N_p-1),u^*(t+N_p-1)) \\
&A_{t+N_p-2}(x^*(t+N_p-2),u^*(t+N_p-2))...A_t(x^*(t),u^*(t))x(t) \\
&+ C_{t+N_p-1}(x^*(t+N_p-1),u^*(t+N_p-1))A_{t+N_p-1}(x^*(t+N_p-1),u^*(t+N_p-1)) \\
&A_{t+N_p-2}(x^*(t+N_p-2),u^*(t+N_p-2))...A_{t+1}(x^*(t+1),u^*(t+1))B_t(x^*(t),u^*(t))u(t) \\
&+ C_{t+N_p-1}(x^*(t+N_p-1),u^*(t+N_p-1))A_{t+N_p-1}(x^*(t+N_p-1),u^*(t+N_p-1)) \\
&A_{t+N_p-2}(x^*(t+N_p-2),u^*(t+N_p-2))...A_{t+2}(x^*(t+2),u^*(t+2)) \\
&B_{t+1}(x^*(t+1),u^*(t+1))u(t+1) + ... + C_{t+N_p-1}(x^*(t+N_p-1),u^*(t+N_p-1)) \\
&A_{t+N_p-1}(x^*(t+N_p-1),u^*(t+N_p-1))A_{t+N_p-2}(x^*(t+N_p-2),u^*(t+N_p-2)) \\
&B_{t+N_p-3}(x^*(t+N_p-3),u^*(t+N_p-3))u(t+N_p-3) \\
&+ C_{t+N_p-1}(x^*(t+N_p-1),u^*(t+N_p-1))A_{t+N_p-1}(x^*(t+N_p-1),u^*(t+N_p-1)) \\
&B_{t+N_p-2}(x^*(t+N_p-2),u^*(t+N_p-2))u(t+N_p-2) + ... \\
&+ C_{t+N_p-1}(x^*(t+N_p-1),u^*(t+N_p-1))B_{t+N_p-1}(x^*(t+N_p-1),u^*(t+N_p-1))u(t+N_p-1) \\
&- y_r(t+N_p)]^T Q_{N_p}[C_{t+N_p-1}(x^*(t+N_p-1),u^*(t+N_p-1))A_{t+N_p-1}(x^*(t+N_p-1),u^*(t+N_p-1)) \\
&A_{t+N_p-2}(x^*(t+N_p-2),u^*(t+N_p-2))...A_t(x^*(t),u^*(t))x(t) \\
&+ C_{t+N_p-1}(x^*(t+N_p-1),u^*(t+N_p-1))A_{t+N_p-1}(x^*(t+N_p-1),u^*(t+N_p-1)) \\
&A_{t+N_p-2}(x^*(t+N_p-2),u^*(t+N_p-2))...A_{t+1}(x^*(t+1),u^*(t+1))B_t(x^*(t),u^*(t))u(t) \\
&+ C_{t+N_p-1}(x^*(t+N_p-1),u^*(t+N_p-1))A_{t+N_p-1}(x^*(t+N_p-1),u^*(t+N_p-1)) \\
&A_{t+N_p-2}(x^*(t+N_p-2),u^*(t+N_p-2))...A_{t+2}(x^*(t+2),u^*(t+2)) \\
&B_{t+1}(x^*(t+1),u^*(t+1))u(t+1) + ... + C_{t+N_p-1}(x^*(t+N_p-1),u^*(t+N_p-1)) \\
&A_{t+N_p-1}(x^*(t+N_p-1),u^*(t+N_p-1))A_{t+N_p-2}(x^*(t+N_p-2),u^*(t+N_p-2)) \\
&B_{t+N_p-3}(x^*(t+N_p-3),u^*(t+N_p-3))u(t+N_p-3) \\
&+ C_{t+N_p-1}(x^*(t+N_p-1),u^*(t+N_p-1))A_{t+N_p-1}(x^*(t+N_p-1),u^*(t+N_p-1)) \\
&B_{t+N_p-2}(x^*(t+N_p-2),u^*(t+N_p-2))u(t+N_p-2) + ... \\
&+ C_{t+N_p-1}(x^*(t+N_p-1),u^*(t+N_p-1))B_{t+N_p-1}(x^*(t+N_p-1),u^*(t+N_p-1))u(t+N_p-1) \\
&- y_r(t+N_p)]\} + \sum_{i=0}^{N_u-1}[\Delta u(t+i)^T R_i \Delta u(t+i)]
\end{aligned}
$$

Where, $A_t(x^*(t),u^*(t)), B_t(x^*(t)u^*(t)), C_t(x^*(t),u^*(t))$ are system matrices of the linear model of thermoforming process at linearization point $(x^*(t),u^*(t))$. At any time sample $k$, the optimization problem can be solved to predict the optimal control input over the control horizon such that it minimizes or maximizes the performance objective over the output horizon taking into consideration the process constraints. But it should be ensured that the computational burden of online optimization will be low enough to implement MPC in industry using existing hardware. So the optimization problem can be solved offline using multi-parametric programming. It will be a challenge for researchers to develop multi-parametric programming for a system with variable system matrices to solve the optimization problem.

### 8.2.4 Robust Model Predictive Controller

MPC has very good performance in controlling sheet temperature due to its capability to deal with multivariable constraints. Despite the widely acknowledged capabilities of MPC, it has three drawbacks for repetitive processes like thermoforming. The first drawback is that real time implementation demands huge computation effort for solving the online optimal control problem. This drawback limits the use of MPC to only simple slowly varying processes. This problem is solved in this thesis by using multi-parametric programming. The second drawback is that the control technique cannot use the information from previous cycles to tackle repetitive disturbances. In this thesis, two-dimensional control technique was proposed to have a better performance in presence of both repetitive and non-repetitive disturbances. The last drawback is that even though MPC has inherent robustness due to the implicit feedback, it relies on nominal models for the prediction of control input. If there were no disturbance and no model-plant mismatch, and if the optimization problem could be solved for infinite horizons, then one could apply the input function found at time zero to the system for all times. However, this is not possible in general. Due to disturbances and model-plant mismatch, the true system behavior is different from the predicted behavior. So it cannot guarantee the satisfaction of constraints and optimal performance in presence of uncertainties and

disturbance. The presence of uncertainties and disturbances should thus be taken into consideration. The optimization problem for robust MPC can be modified as:

$$J = \min_{\Delta u} \sum_{i=1}^{N_p} [\hat{y}(t+i) - y_r(t+i)]^T Q_i [\hat{y}(t+i) - y_r(t+i)] + \sum_{i=0}^{N_u - 1} [\Delta u(t+i)^T R_i \Delta u(t+i)]$$

Such that,

$$x(t+1) = (A + \Delta A)x(t) + (B + \Delta B)u(t) + W\theta(t)$$
$$y(t) = (C + \Delta C)x(t) + F\theta(t)$$

Subject to the inequality constraints for $t \in [0, T]$

$$u_{\min} \le u(t) \le u_{\max}$$
$$y_{\min} \le y(t) \le y_{\max}$$
$$g(x(t), u(t)) \le 0$$

Where, $x \in \mathbb{R}^n$, $u \in \mathbb{R}^m$, $y \in \mathbb{R}^q$ and $\theta \in \mathbb{R}^w$ are state, input, output and disturbance vector respectively. $\Delta A, \Delta B, \Delta C$ are modeling uncertainties in system matrices $A, B, C$ respectively. $A, B, C, W, F, \Delta A, \Delta B, \Delta C$ are matrices with appropriate dimensions. The disturbance vector includes input disturbances and noises. This disturbances and uncertainties degrade the performance of the controller. Future prediction of the states contains the information about the past uncertainty values. This implies that the future control action can be re-adjusted to compensate the past uncertainty and disturbance realization by deriving a closed loop MPC problem. The main idea of this control technique will be to introduce constraint into control optimization problem that preserve feasibility and performance for all disturbance realization. These constraints can be incorporated into the system equation and give rise to a new optimization problem. In this optimization, at every time instant the future control input is readily adjusted to offset effect of past uncertainty to satisfy the constraint.

## 8.3 Concluding Remarks

In this thesis a survey on the state-of-the-art work on plastic sheet temperature control of thermoforming process is presented at the beginning. The detail modeling of the heating phase of the thermoforming process is presented. A new method for estimating sheet temperature for both uniform and non-uniform sensor location is developed and hence implemented through harmonic controller of the process. In order to get better performance, MPC is developed for sheet temperature control through heater control of the thermoforming process. The proposed controller is found to have better performance as compared to conventional controller with some drawbacks. To improve the performance of the control, iterative learning control technique is incorporated with MPC.

# Reference


[1] Throne, James, *Technology of thermoforming,* Hanser Gardner Publications, 1996.

[2] G. J. Nam and J. W. Lee, "Numerical and Experimental Studies of 3-Dimensional Thermoforming Process" *Journal of Reinforced Plastics and Composites,* vol. 20, no. 14-15, pp.1182-1190, 2001.

[3] O. Rozant, P. E. Bourban and J. A. E. Manson, "Pre-Heating of Thermoplastic Sandwich Materials for Rapid Thermoforming" *Journal of Thermoplastic Composite Materials*, vol. 13, no. 6, pp. 510-523, 2000.

[4] H. Gross, *Advances in PolymerTechnology*, 1984.

[5] B. Moore, In-Cycle Control of the Thermoforming Reheat Process, M.Eng. thesis, Department of Electrical and Computer Engineering. McGill University, Montreal, Canada, 2002.

[6] J. L. Throne, "Heating Semitransparent Polymers in Thermoforming" *Thermoforming Quarterly,* vol. 7, 1996.

[7] Vijay Kumar, Estimation of absorptivity and heat flux at the reheat phase of thermoforming process, M.Eng. thesis, Department of Mechanical Engineering. McGill University, Montreal, Canada, 2005.

[8] F. M. Schmidt, Y. Le Maoult and S. Monteix, "Modelling of infrared heating of thermoplastic sheet used in Thermoforming process" *Journal of Materials Processing Technology*, vol. 143–144, pp. 225–231, 2003.

[9] A. Yousefi, A. Bendada, R. Diraddo, "Improved modeling for the reheat phase in thermoforming through an uncertainty treatment of the key parameters", *Polymer Engineering and Science,* vol. 42, no. 5, pp. 1115 – 1129, 2004.

[10] S. Monteix, R. Diraddo, F. Schmidt, "Profiles infrared radiative heating in blow molding and thermoforming." *PPS'98 North American Meeting, Toronto*, August 17–19, 1998.

[11] M. Ajersch, Modeling and Real-Time Control of Sheet Reheat Phase in Thermoforming, M.Eng. thesis, Department of Electrical and Computer Engineering, McGill University, 2004.

[12] G. Gauthier, Terminal iterative learning for cycle-to-cycle control of industrial processes, PhD thesis, Department of Electrical and Computer Engineering. McGill University, Montreal, Canada, 2008.

[13] Y. Hao, Infrared sensor placement optimization and monitoring in *thermoforming* ovens, Master's thesis, Department of Electrical and Computer Engineering. McGill University, Montreal, Canada, 2008.

[14] P. Girard, V. Thomson and B. Boulet, "Advanced In-cycle and Cycle-to cycle On-line adaptive Control for Thermoforming of large Thermoplastic Sheets." *SAE Advances in Plastic Components, Processes and Technologies*, 2005.

[15] B. Boulet, V. Thomson, P. Girard, R. di. Raddo and A. Haurani, "On-Line Adaptive Control For Thermoforming Of Large Thermoplastic Sheets", *Intelligent Processing and Manufacturing of Materials*. 2005, Monterey, CA.

[16] F. M. Duarte and J. A. Covas, "IR sheet heating in roll fed thermoforming: Part 1 - Solving direct and inverse heating problems." *Plastics, Rubber and Composites*. vol.31, no.7,pp. 307-317, 2002

[17] K. H. Lee, S. W. Baek and K. W. Kim "Inverse radiation analysis using repulsive particle swarm optimization algorithm." *International Journal of Heat and Mass Transfer,* vol. 51, no. 11, pp. 2772-2783 , June 2008.

[18] F. M. Duarte and J. A. Covas, "Heating thermoplastic sheets for thermoforming solution to direct and inverse problems." *Plastics rubber and composites processing and app.*, vol. 26, no.5, pp. 213-221,1997.

[19] F. M. Duarte and J. A. Covas, "Infrared sheet heating in roll fed thermoforming: Part 2 - Factors influencing inverse heating solution." *Plastics, Rubber and Composites*. vol. 32, no. 1, pp. 32-39, 2003.

[20] J. R. Burggraf, "An exact solution of the inverse problem in Heat conduction theory and application." *Journal of Heat transfer*, vol. 86, pp. 373-382, 1964.

[21] G. Mulholland, B. P. Gupta, R. L. San Martin "lnverse Problem of Heat Conduction in Composite Media." *AMSE paper 75-WA/HT-83*, 1975.

[22] R. G. Arledge and A. Haji-Sheikh, "An Iterative Approach to the Solution of lnverse Heat Conduction Problems," *Numer. Hear Transfer*, vol. 1, pp. 365-376. 1978.

[23] G. Stolz, “Numerical Solutions to an lnverse Problem of Heat Conduction for Simple Shapes.” *Trans. ASME, J. Hear Transfer*, vol. 82C, pp. 20-26, 1960.

[24] E. M. Sparrow, A. Haji-Sheikh, and T. S. Lundgren, “The Inverse Problem in Transient Heat Conduction.” *Trans. ASME, J. Appl. Mech*., vol. 86E, pp. 369-375, 1964.

[25] J. V. Beck, “Surface Heat Flux Determination Using an Integral Method”, *Nucl. Eng. Des.,* vol. 7, pp. 170- 178, 1968.

[26] M. lmber and J. Khan, “Prediction of Transient Temperature Distributions with Embed- ded Thermocouples”, *AlAA J.,* vol. 10, pp. 784-789, 1972.

[27] K. C. Woo and L. C. Chow, “lnverse Heat Conduction by Direct Inverse Laplace Transform”, *Numerical Heat Tran.*, vol. 4, pp. 499-504, 1981.

[28] E. Apiñaniz, A. Mendioroz, A. Salazar, and R. Celorrio, “Analysis of the Tikhonov regularization to retrieve thermal conductivity depth-profiles from infrared thermography data” *Journal of Appl. Phys*. vol. 108, no.06, 2010.

[29] O. Cortes, G. Urquiza, J. A. Hernandez and M.A. Cruz, “Artificial Neural Networks for Inverse Heat Transfer Problems” *Electronics, Robotics and Automotive Mechanics Conference,* 2007. Sept. 2007, pp. 198-201.

[30] K. Kudo, A. Kuroda, A. Eid, T. Saito and M. Oguma, "Solution of the Inverse Radiative Heat Source Problems by the Singular Value Decomposition," *Radiative Transfer I: Proc. First Int. Symp. on Radiative Heat Transfer,* M. Pinar Menguç, ed., Begell House, New York, 1996, pp. 568–578.

[31] F. França, J. C. Morales, M. Oguma and J. Howell, "Inverse Radiation Heat Transfer Within Enclosures With Nonisothermal Participating Media," *Proc. of the 11th Int. Heat Transfer Conference*, Korea, vol. 1, 1998, pp. 433–438.

[32] F. França, M. Oguma, J. R. Howell, "Inverse Radiation Heat Transfer Within Enclosures With Non-Isothermal, Non-Gray Participating Media," *Proc. of the ASME International Mechanical Engineering Congress and Exposition, Anaheim,* CA, vol.5, 1998, pp. 145–151.

[33] F. França, O. A. Ezekoye and J. R. Howell, "Inverse Determination of Heat Source Distribution in Radiative Systems With Participating Media," *Proc. of National Heat Transfer Conference,* Albuquerque, New Mexico,1999.

[34] F. França, O. Ezekoye and J. Howell, "Inverse Heat Source Design Combining Radiation and Conduction Heat Transfer," *Proc. of the ASME 1999 International Mechanical Engineering Congress and Exposition*, Nashville, vol. 1, 1999, pp. 45–52.

[35] S. Haykin, *Adaptive Filter Theory.* , Prentice-Hall, Englewoods Cliffs, NJ (1996).

[36] M. Janicki, J. Soraghan, A. Napieralski and M. Zubert, "Application of adaptive filters to integrated circuit temperature estimation from noisy temperature sensor measurements", *Proceedings of MIXDES'98—Fifth International Conference on Mixed Design of Integrated Circuits and Systems, Lódz ,* Poland, 18–20 June 1998, pp. 183–188.

[37] J. V. Beck and H. Wolf, "The Non Linear Inverse Heat Conduction Problem", *ASME paper 65-HT-40.* 1965.

[38] J. V. Beck, "Non-linear Estimation Applied to the Non-Linear lnverse Heat Conduction Problem", *Inr. J. Heat Mass Transfer,* vol. 13, pp. 703-716, 1970.

[39] 0 . M. Alifanov, "Numerical Solution of a Non Linear Reverse Problem of Heat Conduction," *J. Eng. Phys. (USSR),* vol. 25, no. 2. pp. 1070-1076, 1975.

[40] L. Gnrifo, V. E. Schrock, and E. Spcdicato, "On the Solution of the lnverse Heat Conduction Problem by Finite Differences", *Energ. Nucl.,* vol. 22, pp. 452-464, 1975.

[41] N. D'Souza, "Numerical Solution of One-dimensional Inverse Transient Heat Conduction by Finite Difference Method", *ASME paper* 75-WA/HT-81, 1975.

[42] S. D. Williams and D. M. Curry, "An Analytical and Experimental Study for Surface Heat Flux Determination," *J. of spacecraft and rockets,* vol. 14, no. 10, pp. 632-637, 1977.

[43] B. F. Blackwell. "Efficient Technique for the Numerical Solution of the One-dimensional lnverse Problem of Heat Conduction", *Numer. Heat Transfer,* vol. 4, pp. 229-238, 1981

[44] X. Pham, P. Bates and A. Chesney, "Modeling of Thermoforming of Low-density Glass Mat Thermoplastic" *J. Reinforced Plastics and Composites,* vol. 24, no. 3, pp. 287-298, 2005.

[45] O. M. Alifanov, J. Antonenko, V. V. Mikchailov, A. V. Nenarokomov, H. Ritter, A. Santovincenzo, D. M. Titov and V. M. Tdin, "A study of spacecraft structures materials thermal properties based on inverse problem technique" *Thermal Protection Systems and Hot Structures, Proceedings of the 5th European Workshop* ,17-19 May, 2006, ESTEC, Noordwijk, The Netherlands.Published on CDROM, p.32.1

[46] O. M. Alifanov, A. V. Nenarokomov, S.A. Budnik, V. V. Michailov, V. M. Ydin, "Identification of thermal properties of materials with applications for spacecraft structures" *Inverse Problem in Science and Engineering*, vol. 12, no. 5, pp. 579-594, 2004.

[47] C. Huang and S. Wang, "A three-dimensional inverse heat conduction problem in estimating surface heat flux by conjugate gradient method" *International Journal of Heat and Mass Transfer*, vol. 42, no. 18, pp. 3387–3403, 1999.

[48] C. H. Huang and M. N. Özisik, "Inverse problem of determining unknown wall heat flux in laminar flow through a parallel plate duct" *Numerical Heat Transfer, Part A: Applications: An International Journal of Computation and Methodology*, vol. 21, no. 1, pp: 55-70, 1992.

[49] C. Huang and Y. Jan-Yuan, "An inverse problem in simultaneously measuring temperature-dependent thermal conductivity and heat capacity" *International Journal of Heat and Mass Transfer*, vol. 38, no. 18, pp. 3433–3441, 1995.

[50] J. Su and G. F. Hewitt, "Inverse heat conduction problem of estimating time-varying heat transfer coefficient" *Numerical Heat Transfer, Part A: Applications: An International Journal of Computation and Methodology*, vol. 45, no.8, pp. 777-789, 2004.

[51] B. Sulikowski, K. Galkowski, E. Rogers, and D. Owens, "PI control of discrete linear repititive processes," *Automatica*, vol. 42, pp. 877–880, 2006.

[52] B. Boulet, V. Thomson, P. Girard, R. di. Raddo and A. Haurani, "On-Line Adaptive Control for Thermoforming of Large Thermoplastic Sheets", *Intelligent Processing and Manufacturing of Materials*. 2005, Monterey, CA.

[53] M. I. Chy. and B. Boulet “A New Method for Estimation and Control of Temperature Profile Over a Sheet in Thermoforming Process" *Industry Application Society meeting*, Houston, Texas, USA, Oct, 2010.

[54] M. I. Chy. and B. Boulet “A Conjugate Gradient Method for The Solution of the Inverse Heating Problem in Thermoforming Process" *Industry Application Society meeting*, Houston, Texas, USA, 2010.

[55] M. I. Chy., B. Boulet and A. Haidar “A Model Predictive Controller of Plastic Sheet Temperature for a Thermoforming Process" *ACC*, San Francisco, California, USA, June-July, 2011.

[56] G. J. Nam and J. W. Lee, “Numerical and Experimental Studies of 3-Dimensional Thermoforming Process” *Journal of Reinforced Plastics and Composites*, vol. 20, no. 14-15, pp-1182-1190, 2001.

[57] Y. Yang and F. Gao, “Adaptive control of the filling velocity of thermoplastics injection molding” *Control Engineering Practice*, vol. 8, no. 11, pp. 1285-1296, 2000.

[58] M. V. Kothare, V. Balakrishnan, and M. Morari, “Robust constrained model predictive control using linear matrix inequalities,” *Automatica*, vol. 32, no. 10, pp. 1361–1379, Oct. 1996.

[59] H.-S. Ahn, Y. Chen, and K. L. Moore, “Iterative Learning Control: Brief survey and categorization,” *IEEE Transactions on Systems, Man and Cybernetics – Part C: Applications and Reviews*, vol. 37, no. 6, pp. 1099–1121, November 2007.

[60] M. Pandit and K. Buchheit, “Optimizing iterative learning control of cyclic production processes with application to extruders,” *IEEE Transactions on control systems technology*, vol. 7, no. 3, pp. 382–390, May,1999.

[61] A. Bemporad, M. Morari, V. Dua and E.N. Pistikopoulos, “The explicit linear quadratic regulator for constrained systems”, *Automatica*, vol. 38, pp. 3-20, 2002.

[62] V. Dua, K.P. Papalexandri and E.N. Pistikopoulos, “Global optimization issues in multiparametric continuous and mixed-integer optimization problems” *Journal of Global Optimization* , vol. 30, no. 1, pp. 59-89, 2004.

[63] A. Bemporad, F. Borrelli, and M. Morari, "Optimal controllers for hybrid systems: Stability and piecewise linear explicit form," *Proc. Conference on Decision and Control*, Sydney, 2000.

[64] KL. L. Moore, "Iterative Learning Control: An Expository Overview", *Applied and Computational Control, Signals, and Circuits, Birkhauser*. pp. 151-214, 1999.

[65] R.W. Longman, "On the Interaction Between Theory, Experiments, and Simulation in Developing Practical Learning Control Algorithms". *International Journal of Applied Computational Science*, vol. 13, no.1,pp. 101-111. 2003.

[66] R.W. Longman, "Iterative learning control and repetitive control for engineering practice". *International Journal of Control*, vol. 73, no. 10, pp. 930-954. 2000.

[67] R.W. Longman, "Designing Iterative Learning and Repetitive Controllers", *Iterative Learning Control - Analysis, Design, Integration and Applications*, Kluwer Pulisher. pp. 107-134, 1998.

[68] Y. Chen, and J.-X. Xu, "High-order Terminal Iterative Learning Control with an Application to a Rapid Thermal Process for Chemical Vapor Deposition," *Iterative Learning Control – Convergence Robustness and Applications*. 1999, Springer Verlag: New York.

[69] C. Zhang, H. Deng, and J.S. Baras, *Comparison of Run-to-Run Control Methods in Semiconductor Manufacturing Processes*. 2000, Institute for System Research.

[70] J. Moyne, E. del Castillo, and A. M. Hurwitz, *Run-to-Run Control in Semiconductor Manufacturing*. 2001: CRC Press.

[71] S. Adivikolanu and E. Zafiriou. "Robust Run-to-Run Control for Semiconductor Manufacturing: An Internal Model Control Approach" American Control Conference. 1998. Philadelphia, Pennsylvania.

[72] R. Murray-Smith, T. A. Johansen, and R. Shorten, "On transient dynamics, off-equilibrium behavior and identification in blended multiple model structures." 5th European Control Conference, 31 August - 3 September 1999, Karlsruhe, Germany.

[73] J. M. Strauss; V. Shikoana; "Online estimation of synchronous generator parameters using PRBS perturbations" *IEEE Transactions on Power Systems*, vol. 17 , no. 3, pp. 694 – 700.

[74] R. Bhaskar; M. L. Crow; E. Ludwig; K. T. Erickson ; K. S. Shah; "Nonlinear parameter estimation of excitation systems" *IEEE Transactions on Power Systems*, vol. 15, no. 4 , pp. 1225 – 1231.

[75] G. W. Krutz. R. J. Schoendals, and P. S. Hore, "Application of the Finite-Element to the lnvcrsc Hcat Conduction Problem", *Numer. Heat Transfer*, vol. 1 , pp. 489-498, 1978.

[76] M. K. Warby, J. R. Whitemen, W. G. Jiang, P. Warwick, and T. Wright, "Finite element simulation of thermoforming processes for polymer sheets" *Mathematics and Computers in Simulation*, vol. 61, no. 3–6, pp: 209–218, 2003.

[77] J. R. Ehlert and T.F. Smith, "View Factors for Perpendicular and Parallel, Rectangular Plates." *Journal of Thermo-physics and Heat Transfer*, vol. 7, no. 1, pp. 173-174, 1993.

[78] J.R. Lloyd and W. R. Moran, "Natural Convection Adjacent to Horizontal Surfaces of Various Platforms" *ASME paper* 74-WA/HT-66, 1974.

[79] W.H. McAdams, *Heat Transmission*, 3rd ed. McGraw-Hill, New York, 1954.

[80] S. W. Churchill and H. H. S. Chu, "Correlating Equations For Laminar and Turbulence Free Convection From Vertical Plate." *International Journal of Heat Mass Transfer*, vol. 18, pp. 1323, 1975.

[81] S. Yang, "Cycle-to-cycle control of plastic sheet heating on the AAA thermoforming machine", M.Eng. thesis, Department of Electrical and Computer Engineering, McGill University, 2008.

[82] J. R. Howell; R. Siegel; M. P. Menguc; *Thermal radiation heat transfer*, Boca Raton, Fla. : CRC Press, 2011

[83] L. Zhang and W. Zhou, "Spectral gradient projection method for solving nonlinear monotone equations." *Journal of Computational and Applied Mathematics*. vol. 196 , no. 2, pp. 478 – 484, 2006.

[84] G. V. Savinov, "Conjugate gradient method for systems of nonlinear equations", *Computational methods and algorithms*, vol. 70, pp. 178–183, 1977.

[85] Y. H. Dai and Y. Yuan, "A Nonlinear Conjugate Gradient Method with a Strong Global Convergence Property", *SIAM J. Optim*. vol. 10, no. 1, pp. 177-182 , 1999.

[86] R. Fletcher, C. M. Reeves, “Function minimization by conjugate gradients”, *Computation Journal*, pp. 149-154, 1964

[87] R. Fletcher, *Practical Methods of Optimization*, John Wiley, New York,

[88] M. F. Møller. "A scaled conjugate gradient algorithm for fast supervised learning." *Neural networks* vol. 6, no. 4, pp. 525-533, 1993.

[89] R. Magnus, *Hestenes* and E. *Stiefel*, “Methods of Conjugate Gradients for Solving*”, Journal of research of the national bureau of standards*, vol. 49, no. 6, pp. 409-436, 1952.

[90] P. E. Gill, W. Murray, M. H. Wright, *Practical optimization*, Academic Press Inc. Harcourt Brace Jovanovich Publishers, London, 1981

[91] P. Wolfe, Convergence conditions for ascent methods, *SIAM Rev*., vol. 11, pp. 226–235, 1963.

[92] G. Zoutendijk, J. Abadie, *Nonlinear programming, computational methods: Integer and nonlinear programming*, North-Holland, Amsterdam, 1970, pp. 37–86

[93] P. Wolfe, *Convergence conditions for ascent methods. II. Some correction*s, SIAM Rev., 13 , pp. 185–188, 1971.

[94] E. Polak, G. Ribière, Note sur la convergence de méthodes de directions conjuguées, *Rev. Française Informat. Recherche Opérationnelle*, vol. 3,1969, pp. 35–43.

[95] M. Al-Baali, “Descent property and global convergence of the Fletcher-Reeves method with inexact line search”, I*MA J. Numer. Anal*., vol. 5, pp. 121–124, 1985.

[96] M. J. D. Powell, “Nonconvex minimization calculations and the conjugate gradient method Numerical analysis (Dundee, 1983)”, *Lecture Notes in Math*., *Springer, Berlin*, vol. 1066, pp. 122–141, 1984

[97] M. J. D. Powell, “Convergence properties of algorithms for nonlinear optimization”, *SIAM Rev*., vol. 28, pp. 487–500, 1986.

[98] D. Touati-Ahmed, C. Storey, “Efficient hybrid conjugate gradient techniques”, *Journal Optim. Theory Appl.*, vol. 64, pp. 379–397, 1990.

[99] J. C. Gilbert and J. Nocedal, “Global Convergence Properties of Conjugate Gradient Methods for Optimization”, *SIAM J. Optim*. vol. 2, pp. 21-42.

[100] C. Lemaréchal, A. Auslander, W. Oettli, J. Stoer, “A view of line-searchesOptimization and optimal control (Proc. Conf., Math. Res. Inst., Oberwolfach, 1980)”, *Lecture Notes in Control and Information Sci.*, vol. 30, Springer, Berlin, 1981, pp. 59–78

[101] J. J. Moré, D. J. Thuente, “On line search algorithms with guaranteed sufficient decrease”, *Mathematics and Computer Science Division Preprint MCS-P153-0590*, Argonne National Laboratory, Argonne, IL, 1990.

[102] A. Jain, *Fundamentals of Digital Image Processing*, Prentice-Hall, 1989, pp. 15 - 20.

[103] A. Marion *An Introduction to Image Processing*, Chapman and Hall, 1991, Chap. 9.

[104] N. Beaudoin and S. S. Beauchemin, “An accurate discrete Fourier transform for image processing” *Proceedings of 16th International conference on pattern recognition*, vol. 3, 2002, pp. 935-939.

[105] G. Michael and M. Porat, “Image reconstruction from localized Fourier magnitude” *Proceedings of international conference on image processing*, vol.-1, 2001, pp. 213-216.

[106] J. R. Fienup, “Reconstruction of an object from the modulus of its Fourier transforms.” *Optics Letters*, vol. 3, no. 1, pp. 27-29, 1978.

[107] M. D. Sacchi, T. J. Ulrych and C. J. Walker, “Interpolation and extrapolation using a high-resolution discrete Fourier transform” *IEEE Transactions on signal Processing*, vol. 46, no. 1 pp. 31-38, 1998.

[108] A. E. Yagle, “Closed-form reconstruction of images from irregular 2-D discrete Fourier samples using the Good_Thomas FFT.” *International Conference on Image Processing*, vol. 1, 2000, pp.117-119.

[109] S. Jean-Luc, E.J. Candes and D.L. Donoho, “The curvelet transform for image denoising” *IEEE Transacetion on Image Processing*, vol. 11, no. 6, pp. 670-684, 2002.

[110] S. MartíNez and F. Bullo. "Optimal sensor placement and motion coordination for target tracking." *Automatica*, vol. 42, no.4, pp. 661-668, 2006.

[111] M. M. Bronstein, A. M. Bronstein, M. Zibulevsky, H. Azhari, " Reconstruction in diffraction ultrasound tomography using nonuniform FFT" *IEEE Transaction of Medical Imaging.* vol. 21, no. 11, pp. 1395-1401, 2002.

[112] M. Numada, T. Nomura, K. Kamiya, H. Koshimizu, H. Tashiro, " Sharpening of CT images by cubic interpolation using B-spline" *Proceedings of the 17th International Conference on pattern recognition*, vol. 4, 2004, pp:23-26.

[113] C. Habermann and F. Kindermann, "Multidimensional Spline Interpolation: Theory and Applications" *Computational Economics*, vol. 30, no. 2, pp. 153-169, 2007.

[114] P. Marziliano and M. Vetterli, "Reconstruction of Irregularly Sampled Discrete-Time Bandlimited Signals with Unknown Sampling Locations" *IEEE Transactions On Signal Processing*, vol. 48, no. 12, pp. 3462-3471, 2000.

[115] C. V´azquez, E. Dubois_ and J. Konrad, "Reconstruction Of Irregularly-Sampled Images By Regularization In Spline Spaces" *Proceedings of International Conference on Image Processing*, vol. 3, 2002, pp: III-405- III-408.

[116] A. Björck and V. Pereyra, "Solution of Vandermonde Systems of Equations" *mathematics of computation*, vol. 24, no. 112, pp. 893-903, 1970.

[117] M. Morari and J. Lee, "Model predictive control: Past, present and future" *Computational Chemical Engineering*, vol 23, pp. 667, 1999.

[118] D.Q. Mayne, J.B. Rawlings, C.V. Rao and P.O.M. Scokaert, "Constrained model predictive control: Stability and optimality, *Automatica*, vol. 36, pp. 789, 2000.

[119] P. Dua, . Model based and parametric control for drug delivery systems. PhD thesis. Centre for Process Systems Engineering, Imperial College London. 2005.

[120] V. Dua, N.A. Bozinis and E.N. Pistikopoulos, "A multiparametric programming approach for mixed integer and quadratic engineering problems", *Computers & Chemical Engineering*, vol. 26, pp. 715, 2002.

[121] E. Pistikopoulos, M. Georgiadis and V. Dua, *Multi-Parametric Programming*, WILEY-VCH Verlag GmbH & Co. KGaA, 2007

[122] D. E. Hardt and T.-S. Siu, "Cycle to Cycle Manufacturing Process Control", *Innovation in Manufacturing Systems and Technology* 2002, Massachusetts Institute of Technology: Boston, Massachusetts.

[123] S. J. Qin, G.W. Scheid, and T.J. Riley, “Adaptive run-to-run control and monitoring for a rapid thermal processor”. *Journal of Vacuum Science Technology*, vol. 21, no. 1, pp. 301-310, 2003.

[124] C. Zhang, H. Deng, and J.S. Baras, “Run-to-Run control methods based on the DHOBE algorithm”. *Automatica*,. vol. 39: pp. 35-45, 2003.

[125] C. Kempf, et al., “Comparison of Four Discrete-Time Repetitive Control Algorithms”. *IEEE Control Systems*, pp. 48-54, 2003.

[126] S. Adivikolanu and E. Zafiriou, “Internal Model Control Approach to Run-to-Run Control for Semiconductor Manufacturing”, *American Control Conference*. 1997: Albuquerque, New Mexico.

[127] M. Sun and D. Wang, “Closed-loop iterative learning control for non-linear systems with initial shift”s. *International Journal of Adaptive Control and Signal Processing*, vol. 16, pp. 515-538, 2002.

[128] S. Kawamura, F. Miyazaki, and S. Arimoto, “Realization of Robot Motion Based on a Learning Method”. *IEEE Transactions on Systems, Man and Cybernetics,vol*. 18, no.1, pp. 126-134, 1988.

[129] Hsu, C.-T., C.-J. Chien, and C.-Y. Yao. “A new Algorithm of Adaptive Iterative Learning Control for Uncertain Robotic Systems.” International Conference on Robotics and Automation. 2003. Taipei, Taiwan: IEEE.

[130] Chen, Y., et al., *Iterative Learning Control and Repetitive Control in Hard Disk Drive Industry - A Tutorial.* 2006.

[131] Zheng, D. and A. Alleyne. Learning Control of an Electro-hydraulic Injection Molding Machine with Smoothed Fill-to-Pack Transition. American Control Conference. 2000. Chicago, Illinois.

[132] R. S. Guo, A. Chen, and J.-J. Chen, “Run-To-Run Control Schemes For CMP Process Subject to Deterministic Drifts,” Semiconductor Manufacturing Technology Workshop. 2000: Hsinchu, China.

[133] S. R. Oh, Z. Bien, and I.H. Suh, “An Iterative Learning Control Method with Application for the Robot Manipulator”. *IEEE Journal of Robotics and Automation*, vol. 4, no. 5, pp. 508-514, 1988.

[134] D. Zheng, *Iterative Learning Control of an Electro-Hydraulic Injection Molding Machine with Smoothed Fill-to-Pack Transition and Adaptive Filtering*. 2002, University of Illinois at Urban-Champaign, Illinois: Urban-Champaign, Illinois.

[135] F. Gao, Y. Yang, and C. Shao, "Robust iterative learning control with application to injection molding process". *Chemical Engineering Science*, vol. 56: pp. 7025-7034, 2001.

[136] K. K. Tan and J.C. Tang, "Learning-enhanced PI control of RAM velocity in injection molding machines". *Engineering Applications of Artificial Intelligence,*. vol. 15, pp. 65-74, 2002.

[137] S. Adivikolanu and E. Zafiriou, "Internal Model Control Approach to Run-to-Run Control for Semiconductor Manufacturing", in American Control Conference. 1997: Albuquerque, New Mexico.

[138] S. Adivikolanu and E. Zafiriou, "Extensions and Performance/Robustness Tradeoffs of the EWMA Run-to-Run Controller by Using the Internal Model Control Structure". *IEEE Transactions on Electronics Packaging Manufacturing*, vol. 23, no.1, pp. 56-68, 2000.

[139] S. Emanuel, A. Hu, and A. Ingolfsson. "Run by run process control: combining SPC and feedback control." *IEEE Transactions on Semiconductor Manufacturing, vol.* 8, no.1 pp. 26-43, 1995.

[140] C. C. Cheah and D. Wang, "A model reference learning control scheme for a class of nonlinear systems". *International Journal of Control*, vol. 66, no.2, pp. 271-287, 1997.

[141] K, Hamamoto and T. Sugie, "Iterative Learning Control for Robot Manipulators Using the Finite Dimensional Input Subspace." *IEEE Transactions on Robotics and Automation*, vol. 18, no. 4, pp. 632-6352002.

[142] D. Ballard and C. Brown, *Computer Vision*, Prentice-Hall, 1982, pp. 24 - 30.

[143] R. Gonzales, R. Woods, *Digital Image Processing*, Addison-Wesley Publishing Company, 1992, pp. 81 - 125.

[144] B. Horn *Robot Vision*, MIT Press, 1986, Chaps 6, 7.

[145] G. Gauthier and B. Boulet, “Terminal iterative learning control applied to thermoforming reheat phase,” *Proceedings of the IEEE International Symposium on Industrial Electronics (ISIE '06)*, Montreal, Canada, July 2006, pp. 353–357.

[146] Christopher J Zarowski, *An introduction to numerical analysis for electrical and computer engineers*, Hoboken, NJ : Wiley, 2004